FOREWORD

This report presents the results of a portion of the experimental program for the investigation of hypersonic flow separation and control characteristics being conducted by the Research Department of Grumman Aircraft Engineering Corporation, Bethpage, New York. Messrs. Donald E. Hoak and Wilfred J. Klotzback, of the Air Force Flight Dynamics Laboratory, Research and Technology Division, located at Wright-Patterson Air Force Base, Ohio, are the Air Force Project Engineers for the program, which is being supported partly under Contract AF 33(616)8130, Air Force Task 821902.

The authors wish to express their appreciation to the staff of the von Karman Facility for their helpfulness in conducting the tests and particularly to Messrs. Schueler and Donaldson for providing the machine plotted graphs of the experimental data included in this report. Ozalid reproducible copies of the tabulated data are available on loan from the Flight Control Division of the Air Force Flight Dynamics Laboratory.

ABSTRACT

Six-component force and moment data were obtained for Mach 5 and 8 flows over a blunt pyramidal configuration. The model had a triangular cross section and was composed of two dihedral surfaces and a 70-degree sweepback delta wing lower surface. Three-component force and moment data were obtained on a remotely controlled trailing edge flap at deflections up to 40 degrees. All three surfaces had trailing edge flaps and the model was tested with and without canards and a ventral fin. The model was pitched at angles of attack between ± 54 degrees and side-slip angles between -4 and +14 degrees. For both Mach numbers, the data were obtained for a nominal free stream Reynolds number, based on model length, of 4.5 million. Selected configurations were tested at other Reynolds numbers between 1.2 and 9.1 million.

This report has been reviewed and is approved.

W. A. SLOAN, Jr.
Colonel, USAF
Chief, Flight Control Division
Air Force Flight Dynamics Laboratory

TABLE OF CONTENTS

LIST OF ILLUSTRATIONS

LIST OF TABLES

LIST OF SYMBOLS

A	Instrumented flap reference area; $A = b\ c = 13.50$ sq. in.
b	Instrumented flap span; $b = 4.464$ in.
c	Instrumented flap chord; $c = 3.025$ in.
C_A	Axial force coefficient; $C_A \equiv$ axial force/$q_\infty S$.
C_{FN}	Flap normal force coefficient; $C_{FN} \equiv$ flap normal force/$q_\infty A$.
C_{hm}	Flap hinge moment** coefficient; $C_{hm} \equiv$ flap hinge moment/$q_\infty Ac$.
C_ℓ	Rolling moment* coefficient; $C_\ell \equiv$ rolling moment/$q_\infty SL$.
C_m	Pitching moment* coefficient; $C_m \equiv$ pitching moment/$q_\infty SL$.
C_n	Yawing moment* coefficient; $C_n \equiv$ yawing moment/$q_\infty SL$.
C_N	Normal force coefficient; $C_N \equiv$ normal force/$q_\infty S$
C_{pb}	Base pressure coefficient; $C_{pb} \equiv \frac{1}{3}\sum_{n=1}^{3}\frac{p_n - p_\infty}{q_\infty}$.
C_{tm}	Flap twisting moment** coefficient; $C_{tm} \equiv$ flap twisting moment/$q_\infty A\ b$.
C_Y	Side force coefficient; $C_Y \equiv$ side force/$q_\infty S$.
L	Reference length (planform virtual length of model); $L = 20.81$ in.
M_∞	Free stream Mach number.
p_o	Stagnation pressure (psia)

$p_{1,2,3}$	Base pressures (psia)
p_∞	Free stream static pressure (psia)
q_∞	Free stream dynamic pressure (psia)
Re_∞/ft	Reynolds number per foot; $Re_\infty/ft \equiv \rho_\infty U_\infty/\mu_\infty$.
S	Reference area (planform virtual area); $S = L^2 \tan 20° = 157.6$ sq. in.
T_o	Stagnation temperature (°R).
T_∞	Free stream static temperature (°R).
U_∞	Free stream velocity (ft/sec).
α	Angle of attack (degrees).
β	Sideslip angle (degrees).
δ	Flap deflection angle, used when both upper or both lower flaps are deflected (degrees).
δ_{fin}	Ventral fin (rudder) deflection angle (degrees).
δ_p	Flap deflection angle, used when only the port upper or lower flap is deflected (degrees).
μ_∞	Viscosity of air in the free stream (slugs/ft sec).
ρ_∞	Density of air in the free stream (slugs/ft^3).

---

*Moments are referenced to a point on the longitudinal axis of the balance at a distance 0.60L downstream of the planform virtual apex.

**Hinge and twisting moments are referenced to the instrumented-flap hinge line and mid-chord.

INTRODUCTION

The experimental data generated by an investigation of hypersonic flow separation and aerodynamic control characteristics are being presented in a series of reports, of which this is one. Pressure, heat transfer, and force data were obtained for hypersonic flows over "basic geometries," such as a wedge mounted on a flat plate, and for "typical" hypersonic flight configurations with aerodynamic control surfaces. The experimental portion of the program required a total of 11 models (see Fig. 1), 8 for tests in the von Karman Facility of the Arnold Engineering Development Center and 3 for tests in the Grumman Hypersonic Shock Tunnel (Refs. 1 and 2). Data obtained from AEDC tests in March and April 1963 on one of the models are presented herein. Analyses of the entire test program are to be presented in a forthcoming final report on the investigation of hypersonic flow separation and control characteristics.

This report presents force and moment data obtained in the AEDC 40-inch (Mach 5) and 50-inch (Mach 8) continuous flow wind tunnels (Ref. 3) on a blunt pyramidal configuration with aerodynamic controls. In addition to six-component force and moment data for the configuration, three-component force and moment data were obtained for a remotely controlled trailing edge flap. Pressure and aerodynamic heating distributions were obtained on a geometrically similar model tested in the AEDC 40-inch and 50-inch wind tunnels at the same model length Reynolds number (Refs. 4, 5 and 6). A third, geometrically similar model, with limited pressure and heat transfer instrumentation, is to be tested in the Grumman Hypersonic Shock Tunnel (Fig. 1).

DESCRIPTION OF MODEL

Photographs of the model are shown in Fig. 2. The model has a delta planform lower surface with cylindrical leading edges swept 70 degrees (Fig. 3). The planar portions of the upper surfaces are right triangles forming 35-degree dihedral angles, measured in a plane perpendicular to the lower surface. The dihedral surfaces are connected by a cylindrical segment which forms the "ridge line" of the model. The three cylindrical leading

---

Manuscript released by authors in June 1964 for publication as an RTD Technical Documentary Report.

edges and the spherical nose of the model all have the same radius. (The radius is also the same as for Configuration "C" shown in Fig. 1.)

The dihedral surfaces have trailing edge flaps that are remotely actuated with a range of deflection from 0 to -40 degrees, measured in planes normal to the flap hinge lines. The flaps have rectangular planforms and chords equal to 15 per cent of the projected model reference length (Fig. 3). Four pairs of wedge shaped flaps can be mounted on the lower surface trailing edge, namely, 10-, 20-, and 40- degree flaps having chords equal to 15 per cent of the model reference length, and a pair of 20- degree flaps with a chord equal to 25 per cent of the model reference length. All flap hinge lines are parallel to the base of the model (perpendicular to the model ridge line).

As indicated in Fig. 3, the model also has attachable canards and a ventral fin. The cylindrical leading edges of the delta planform canards are swept 45 degrees. The canards have a planform area equal to that of the portion of the basic model from the nose to the trailing edge of the canards. The ventral fin is attachable in either of two positions on the lower surface of the model between the trailing edge flaps. The fin is wedge shaped (total wedge angle of 30 degrees), has a cylindrical leading edge, and , is geometrically similar to the instrumented fin of Configuration "B" shown in Fig. 1. The fin can be set at fin (or rudder) deflection angles of 0 or +15 degrees (trailing edge left), and has a chord equal to 15 per cent of the model reference length.

The dihedral surface flaps are separately actuated by drive screws powered by 27-volt, dc electric motors. Flap settings are achieved through linear potentiometers and Leeds and Northrup Midget Model D indicators. The electric motors and potentiometers are encased in water cooling coils.

The port dihedral flap (shown deflected in Fig. 2.1), is supported by a force balance beam which is instrumented for flap normal force, hinge moment, and twisting moment (Fig. 3.2). The insulated and water cooled balance flexure is equipped with 3 pairs of strain gauges and a thermocouple for monitoring average flexure temperature.

TEST CONDITIONS

The 40-inch supersonic tunnel was operated at a nominal Mach number of 5 and free stream Reynolds number of 2.64 million per foot. In selected cases the Reynolds number per foot was varied from 0.67 million to 5.23 million. Tunnel static and stagnation conditions for the various Reynolds numbers are given in Table I.

The tunnel yaw actuator was used in the pitch plane to give an effective sector travel of 50 degrees for the pitch polars. Sideslip polars were obtained using the sector travel for sideslip angles with the yaw actuator set at the desired angles of attack.

The model was pitched from 30 degrees nose down to 45 degrees nose up at increments of 5 degrees (angles of attack referenced to the lower, delta wing, surface of the model). Sideslip polars, from -2 degrees to +14 degrees (nose left), were obtained for angles of attack of 0, +7, and +14.3 degrees. The significance of the +14.3 degree angle of attack is that the free stream direction is then parallel to the dihedral surfaces.

Oil film and schlieren flow photographs were obtained for several Mach 5 test conditions. The fluorescent oil film photographs were obtained in the following manner. Oil was sprayed on the model and the tunnel flow started. The oil flow pattern was photographed under ultra violet light once it had been established for the desired set of test conditions.

The 50-inch Mach 8 tunnel was operated at a nominal free stream Reynolds number per foot of 2.53 million. Corresponding static and stagnation tunnel conditions are given in Table I.

Split stings of 12- and 39-degree prebend angles were used to obtain pitch polars for angles of attack from -54 to +54 degrees.* As for the Mach 5 data, sideslip polars, from -4 to +14 degrees, were obtained for angles of attack of 0, +7, and +14.3 degrees. The tunnel shadowgraph system was used to obtain flow photographs for many sets of test conditions.

---

*In an attempt to attain higher angles of attack, a 48-degree prebend split sting was tried but the tunnel would not start with the model mounted on this sting.

DATA REDUCTION AND ACCURACY

Forces and moments were reduced to standard coefficient form and presented with respect to a body-fixed system of axes. Body axes were used in lieu of wind axes to facilitate determining control effectiveness. (Hypersonic control effectiveness is to be analyzed for the over-all program (see Fig. 1) and presented in a forthcoming final report.)

The normal, axial, and side force coefficients are:

$$C_N \equiv \frac{\text{normal force}}{q_\infty S}$$

$$C_A \equiv \frac{\text{axial force}}{q_\infty S}$$

and

$$C_Y \equiv \frac{\text{side force}}{q_\infty S}$$

where q_∞ (psia) is the free stream dynamic pressure and the reference planform area is $S = 157.6$ square inches. The pitching, yawing and rolling moment coefficients are:

$$C_m \equiv \frac{\text{pitching moment}}{q_\infty SL}$$

$$C_n \equiv \frac{\text{yawing moment}}{q_\infty SL}$$

and

$$C_\ell \equiv \frac{\text{rolling moment}}{q_\infty SL}$$

where the reference length $L = 20.81$ inches and moments are taken about a point $0.60L$ downstream of the planform virtual apex on the longitudinal axis of the balance (see Fig. 3). The coefficients presented herein are those due to the total forces and moments measured; they are not corrected for base pressure effects.

Pressures were measured in the balance cavity and at two locations on the base of the model. The corresponding three pressure coefficients were averaged to obtain base pressure coefficients:

$$C_{pb} \equiv \frac{1}{3}\sum_{n=1}^{3}\frac{p_n - p_\infty}{q_\infty}$$

where p_∞ is the free stream static pressure, and $p_{1,2,3}$ are measured base pressures. The reference body axis is not perpendicular to the base of the model; "corrections" to the forces and moments for base pressure effects should account for the slope of the model base.

The flap normal force coefficient is:

$$C_{FN} \equiv \frac{\text{flap normal force}}{q_\infty A}$$

where the flap reference area $A = 13.50$ square inches. The flap hinge moment and twisting moment coefficients are:

$$C_{hm} \equiv \frac{\text{flap hinge moment}}{q_\infty Ac}$$

and

$$C_{tm} \equiv \frac{\text{flap twisting moment}}{q_\infty Ab}$$

where the flap chord $c = 3.025$ inches, and the flap span $b = 4.464$ inches. The hinge moment, measured by the flap balance, is taken about the flap hinge line, and the twisting moment is taken about the flap balance center line.

Sign conventions are indicated in Fig. 3. Angle of attack is referenced to the flat-delta, lower surface of the model and is positive when this surface is windward. Positive sideslip angles are nose left, and positive rudder (fin) angles are fin trailing edge left (trimming at positive sideslip angle). Flap deflection angles are positive when flap trailing edges are deflected downward. Thus, the lower surface flaps are deflected at positive angles, whereas the upper, dihedral, surface flaps are deflected at negative angles. All flap angles are measured in planes normal to their hinge lines.

Positive force directions are: up (normal to model lower surface) for C_N, back (parallel to lower surface) for C_A, and to starboard for C_Y. Positive moments are nose up for C_m, nose right for C_n, and right hand roll (port side up) for C_ℓ. Positive force and moment directions for the instrumented (port) flap are down for C_{FN} and C_{hm} (in the positive δ direction, but tending to decrease $|\delta|$) and inboard side down (right hand roll) for C_{tm} (see Fig. 3).

The uncertainties in the force and moment coefficients obtained from the balance measurements are shown in Table II for the nominal values of the Mach 5 and Mach 8 free stream dynamic pressures. The uncertainties in the coefficients vary inversely with the q_∞ values, and can be calculated for the different Mach 5 free stream Reynolds numbers by dividing the tabulated uncertainties by the ratio of the q_∞ values for the different free streams. Base pressure coefficient uncertainties also vary inversely with the free stream dynamic pressures. For the Mach 5 tests the uncertainty in C_{pb} is ±0.004 for the nominal free stream Reynolds number of 2.64 million per foot. For the Mach 8 tests the uncertainty in C_{pb} is ±0.001.

Flap deflections, for the remotely controlled flaps, were set using Leeds and Northrup indicator readings of the potentiometers connected to the flap drive screws. The potentiometer readings were calibrated using hand held templates for 5-degree increments in the flap settings. The flap settings were estimated to be accurate to well within a quarter of a degree.

PRESENTATION OF RESULTS

Table III indicates the Mach 5 test conditions for the oil film and schlieren flow photographs presented in Fig. 4.

Table IV summarizes the Mach 5 test schedule and indicates the figure numbers for the corresponding force and moment data plots. The AEDC group numbers given in the table indicate the order in which the data were obtained, and are to be used when referring to the tabulated data (see the Foreword). The Mach 5 model balance data, three-component force and moment coefficients for symmetric configurations, and six-component force and moment coefficients for asymmetric configurations are plotted in Fig. 5. Three-component flap balance data are given in Fig. 6. Normal force, hinge moment, and twisting moment coefficients are plotted for the port upper (dihedral) surface flap. The flap center of pressure is readily calculable from the given moment coefficients.

Base pressure coefficients are tabulated for a wide range of the Mach 5 test conditions (Table V). Base pressure effects can be estimated using interpolated values of the coefficients for the desired test conditions.

Shadowgraph flow photographs are presented in Fig. 7 for the Mach 8 test conditions indicated in Table VI. The existing shadowgraph system employs a point light source and produces flow photographs covering half the test section window area (full coverage is obtained by rotating the camera from the upper to lower window halfs). Photographs of the upper half plane are shown in Fig. 7.1 and photographs of the lower half plane are shown in Fig. 7.2.

Table VII summarizes the Mach 8 test schedule; part A indicates the test conditions for the model balance data plotted in Fig. 8, and part B indicates the test conditions for the flap balance data plotted in Fig. 9. As for the Mach 5 test data, only longitudinal force and moment coefficients are presented for symmetric configurations.

Base pressure coefficients for sample Mach 8 test conditions are given in Table VIII. The sample test conditions include the limits of the ranges of α, β, and δ.

REFERENCES

1. Kaufman, Louis G. II, et al., A Review of Hypersonic Flow Separation and Control Characteristics, ASD-TDR-62-168, March 1962.

2. Evans, W. J., and Kaufman, L. G. II, Pretest Report on Hypersonic Flow Separation and Control Models for AEDC Tunnels A, B, Hotshot 2 and Grumman Hypersonic Shock Tunnel, Grumman Research Department Memorandum RM-209, July 1962.

3. Arnold Center, Test Facilities Handbook, Arnold Air Force Station, Tennessee, January 1961.

4. Kaufman, Louis G. II, Pressure Measurements for Mach Five Flows over a Blunt Pyramidal Configuration with Aerodynamic Controls, RTD-TDR 63-4239, January 1964.

5. Kaufman, Louis G. II, Pressure and Heat Transfer Measurements for Mach 8 Flows Over a Blunt Pyramidal Configuration with Aerodynamic Controls, FDL-TDR-64-2, Part I: Pressure Data for Delta Wing Surface, January 1964, Part II: Pressure Data for Dihedral Surfaces, Part III: Heat Transfer Data for Delta Wing Surface, and Part IV: Heat Transfer Data for Dihedral Surfaces, to be published.

6. Donaldson, Joseph C., Hypersonic Control Effectiveness Tests of a Blunted, Triangular-Pyramid Re-entry Configuration at Mach 5 and 8, AEDC-TDR-63-250, December 1963.

TABLE I

TUNNEL TEST CONDITIONS

$\frac{Re_\infty}{10^6 ft}$	0.67	1.32	2.64	5.23	2.53
M_∞	4.96	4.99	5.01	5.02	8.08
p_∞ (psia)	0.0275	0.0526	0.1031	0.2130	0.0560
q_∞ (psia)	0.474	0.918	1.812	3.750	2.559
p_o (psia)	13.9	27.6	55.2	115.3	584.0
T_o (°R)	597	600	602	621	1330

TABLE II

UNCERTAINTIES IN FORCE AND MOMENT COEFFICIENTS

Coefficients	Uncertainties in Coefficients*	
Model Balance	Mach 5 (q_∞ = 1.81 psia)	Mach 8 (q_∞ = 2.56 psia)
C_N	± 0.0080	± 0.0174
C_A	± 0.0020	± 0.0037
C_Y	± 0.0052	± 0.0087
C_m	± 0.0016	± 0.0043
C_n	± 0.0010	± 0.0021
C_ℓ	± 0.0002	± 0.0004
Flap Balance		
C_{FN}	± 0.018	± 0.032
C_{hm}	± 0.010	± 0.016
C_{tm}	± 0.002	± 0.007

*Due to error spread in balance readings and repeatability spread in data (Ref. 6).

TABLE III

MACH 5 FLOW PHOTOGRAPHS FOR BASIC CONFIGURATION

Oil Film Photographs of Lower Surface			
Figure Number	Flap Deflection Angle	Angle of Attack	A E D C Photo Number
4.1a	+20°	0	33299
b	+40°	0	33301
c	+20°	+12°	33300
d	+40°	+14.3°	33302

Profile Schlieren Photographs			
Figure Number	Flap Deflection Angle	Angle of Attack	A E D C Photo Number
4.2a	0	0	820
b	+40°	0	807
c	0	+14.3°	822
d	+40°	+14.3°	810

Note: Additional Mach 5 flow photographs are presented in Ref. 4.

TABLE IV

OUTLINE OF MACH 5 TESTS

A) MODEL BALANCE DATA

(sheet 1 of 2)

FIGURE NUMBER	CONFIGURATIONS AND FLAP SETTINGS	POLARS	DATA	A E D C GROUP NOS.
5.1a	Basic $(-40° \leq \delta \leq 0)$	pitch $(\beta=0)$	longi-tudinal	16-31, 34-37 and 40-49
b	Basic $(0 \leq \delta \leq +40°)$	pitch $(\beta=0)$	longi-tudinal	
5.2	Basic + longer chord flaps on lower surface $(\delta = 0$ and $+20°)$	pitch $(\beta=0)$	longi-tudinal	16-18, 32,33,48 and 49
5.3	Basic + canards $(-40° \leq \delta \leq 0)$	pitch $(\beta=0)$	longi-tudinal	1-15
5.4	Basic + port flap on lower surface $(\delta_p = 0$ and $+40°)$	pitch $(\beta=0)$	long., lat. and dir.	16, 17, and 48-50
5.5	Basic $(\delta = 0$ and $+40°)$	sideslip $(\alpha=0)$	long., lat. and dir.	51 and 61
5.6a	Basic + port flap $(-40° \leq \delta_p \leq 0)$ $(Re_\infty$ varied)	sideslip $(\alpha=0)$	long., lat. and dir.	61-75 and 77-79
b	Basic + port flap $(-40° \leq \delta_p \leq 0)$	sideslip $(\alpha=+7°)$	long., lat. and dir.	
c	Basic + port flap $(-40° \leq \delta_p \leq 0)$ $(Re_\infty$ varied)	sideslip $(\alpha=+14.3°)$	long., lat. and dir.	
5.7a	Basic + ventral fin (fin off and on with $\delta_{fin} = 0$ and $+15°)$	sideslip $(\alpha=0)$	long., lat. and dir.	53, 54, 57, 58, 61 and 63
b	Basic + ventral fin (fin off and on with $\delta_{fin} = 0$ and $+15°)$	sideslip $(\alpha=+14.3°)$	long., lat. and dir.	
5.8	Basic + ventral fin and port flap			54-60
a	$\delta_{fin} = 0$ $\delta_p = 0$ and $-20°$	sideslip $(\alpha=0)$	long., lat. and dir.	
b	$\delta_{fin} = +15°$ $\delta_p = 0$ and $-20°$	sideslip $(\alpha=0)$	long., lat. and dir.	
c	$\delta_{fin} = 0$ $\delta_p = 0$ and $-20°$	sideslip $(\alpha=+14.3°)$	long., lat. and dir.	
d	$\delta_{fin} = +15°$ $\delta_p = 0$ and $-20°$	sideslip $(\alpha=+14.3°)$	long., lat. and dir.	

TABLE IV

OUTLINE OF MACH 5 TESTS

A) MODEL BALANCE DATA

(sheet 2 of 2)

FIGURE NUMBER	CONFIGURATIONS AND FLAP SETTINGS	POLARS	DATA	A E D C GROUP NOS.
5.9	Basic + flare (all flaps deflected ± 40°)	pitch (β=0)	longi-tudinal	16-18, 38, 39, 48 and 49
5.10	Basic + port flap ($-40° \leq \delta_p \leq 0$)	port flap deflection (α=+14.3° and β=0)	long., lateral and directional	63, 64, 68, 69 and 74
5.11	Basic (δ = 0 and -40°)	Re_∞ varied (α=+14.3° and β=0)	longi-tudinal	20, 63, 76 and 78

Notes: The basic configuration is that without canards, without ventral fin, and with shorter chord (15% ref. length) flaps on lower surface.

+ longer chord flaps is the basic configuration with the longer chord (25% ref. length) flaps on the lower surface.

+ canards is the basic configuration with canards.

+ port flap indicates that only the port flap, on the upper or lower surface, was deflected.

+ ventral fin is the basic configuration with the ventral fin.

+ flare indicates that both lower and both upper flaps were deflected, lower flaps at δ = + 40° and upper flaps at δ = -40°.

δ, without a subscript, indicates both lower or both upper flaps deflected.

δ_p indicates deflections of the port flap only, on either the lower or upper surface.

$\delta > 0$ for lower surface flaps.

$\delta < 0$ for upper surface flaps.

δ_{fin} is the ventral fin (rudder) deflection angle, positive for fin trailing edge left.

All data are for $Re_\infty/10^6$ ft = 2.64 except where "Re_∞ varied" indicates data for additional values of Re_∞.

At α = + 14.3° the dihedral (upper) surfaces are parallel to the free stream flow.

TABLE IV

OUTLINE OF MACH 5 TESTS

B) FLAP BALANCE DATA*

FIGURE NUMBER	CONFIGURATIONS AND FLAP SETTINGS	ABSCISSA FOR DATA PLOTS	A E D C GROUP NOS.
6.1	Basic ($-40° \leq \delta \leq 0$)	angle of attack (β=0)	16-30 and 40-49
6.2	Basic + canards ($-40° \leq \delta \leq 0$)	angle of attack (β=0)	1-15
6.3a	Basic + port flap ($-40° \leq \delta_p \leq 0$) ($Re_\infty$ varied)	sideslip angle (α=0)	61-75 and 77-79
b	Basic + port flap ($-40° \leq \delta_p \leq 0$)	sideslip angle (α=+7°)	
c	Basic + port flap ($-40° \leq \delta_p \leq 0$) ($Re_\infty$ varied)	sideslip angle (α=+14.3°)	
6.4	Basic + port flap ($-40° \leq \delta_p \leq 0$)	port flap deflection (α=+14.3° and β=0)	63, 64, 68, 69 and 74
6.5	Basic (δ = 0 and -40°)	Re_∞ varied (α=+14.3° and β=0)	20, 63, 76 and 78

* Flap normal force, hinge moment and twisting moment coefficients obtained for flap on port dihedral surface of model.

Notes: $\delta < 0$ for upper (dihedral) surface flaps.

δ, without a subscript, indicates both upper flaps deflected.

δ_p indicates only port upper flap deflected.

All data are for $Re_\infty/10^6$ ft = 2.64 except where "Re_∞ varied" indicates data for additional values of Re_∞.

At α = + 14.3° the dihedral (upper) surfaces are parallel to the free stream flow and the hinge line of the instrumented flap is perpendicular to the free stream flow direction.

TABLE V

SAMPLE MACH 5 BASE PRESSURE COEFFICIENTS

Configuration and Flap Settings	$\frac{Re_\infty}{10^6 ft}$	α (deg) (β = 0)	C_{pb}
Basic, no flap deflections	2.64	-30	-0.038
	2.64	-15	-0.038
	2.64	0	-0.030
	2.64	+14.3	-0.030
	2.64	+30	-0.037
	2.64	+45	-0.035
	0.67	0	-0.038
	0.67	+14.3	-0.036
Basic + canards, no flap deflections	2.64	0	-0.020
	2.64	+14.3	-0.025
	2.64	+30	-0.036
	2.64	+45	-0.035
Basic, upper flaps deflected -40°	2.64	-30	-0.025
	2.64	0	-0.036
	2.64	+14.3	-0.035
	2.64	+45	-0.037
	0.67	+14.3	-0.030
	1.32	+14.3	-0.039
	5.23	+14.3	-0.047
Basic, lower flaps deflected +40°	2.64	-30	-0.034
	2.64	0	-0.030
	2.64	+30	-0.037

TABLE VI

MACH 8 PROFILE SHADOWGRAPH FLOW PHOTOGRAPHS

Flow Ahead of Upper Flaps (Both) Deflected -40°

Figure Number	Model Configuration	Angle of Attack	A E D C Photo No.
7.1a	Basic	+14.3°	12
b	Basic + Canards	+14.3°	9
c	Basic + Canards	0	1

Flow Ahead of Lower Flaps on Basic Configuration

Figure Number	Lower Surface Flap Settings Port	Lower Surface Flap Settings Starb'd	Angle of Attack	A E D C Photo Number
7.2a	+40°	+40°	+12°	70
b	+40°	+40°	+14.3°	73
c	+40°	0	+14.3°	76
d	+40°	0	0	77

TABLE VII

OUTLINE OF MACH 8 TESTS

A) MODEL BALANCE DATA

(sheet 1 of 2)

FIGURE NUMBER	CONFIGURATIONS AND FLAP SETTINGS	POLARS	DATA	A E D C GROUP NOS.
8.1a	Basic ($-40° \leq \delta \leq 0$)	pitch (β=0)	longi-tudinal	6-10, 42, 43, 45-48, and 51-55
b	Basic ($0 \leq \delta \leq +40°$)	pitch (β=0)	longi-tudinal	
8.2	Basic + longer chord flaps on lower surface (δ = 0 and + 20°)	pitch (β=0)	longi-tudinal	6, 42 and 49-52
8.3	Basic + canards ($-40° \leq \delta \leq 0$)	pitch (β=0)	longi-tudinal	1-5 and 56-59
8.4	Basic + port flap on lower surface (δ_p = 0 and + 40°)	pitch (β=0)	long., lat. and dir.	6,42, 51, 52 and 68
8.5a	Basic (δ = 0 and + 40°)	sideslip (α=0)	long., lat. and dir.	11-13, 60 and 67
b	Basic (δ = 0)	sideslip (α=+7°)	long., lat. and dir.	
c	Basic (δ = 0 and - 40°)	sideslip (α=+14.3°)	long., lat. and dir.	
8.6a	Basic + port flap ($-40° \leq \delta_p \leq 0$)	sideslip (α=0)	long., lat. and dir.	11-22, 24-29, and 33-41
b	Basic + port flap ($-40° \leq \delta_p \leq 0$)	sideslip (α=+7°)	long., lat. and dir.	
c	Basic + port flap ($-40° \leq \delta_p \leq 0$)	sideslip (α=+14.3°)	long., lat. and dir.	

TABLE VII

OUTLINE OF MACH 8 TESTS

A) MODEL BALANCE DATA

(sheet 2 of 2)

FIGURE NUMBER	CONFIGURATIONS AND FLAP SETTINGS	POLARS	DATA	A E D C GROUP NOS.
8.7	Basic + ventral fin			11-13 and 61-66
a	(fin off and on with δ_{fin} = 0 and + 15°)	sideslip (α=0)	long., lat., and dir.	
b	(fin off and on with δ_{fin} = 0 and + 15°)	sideslip (α =+7°)	long., lat., and dir.	
c	(fin off and on with δ_{fin} = 0 and + 15°)	sideslip (α =+14.3°)	long., lat., and dir.	

Notes: The basic configuration is that without canards, without ventral fin, and with shorter chord (15% ref. length) flaps on lower surface.

+ longer chord flaps is the basic configuration with the longer chord (25% ref. length) flaps on the lower surface.

+ canards is the basic configuration with canards.

+ port flap indicates that only the port flap, on the upper or lower surface, was deflected.

+ ventral fin is the basic configuration with the ventral fin.

δ, without a subscript, indicates both lower or both upper flaps deflected.

δ_p indicates deflections of the port flap only, on either the lower or upper surface.

$\delta > 0$ for lower surface flaps.

$\delta < 0$ for upper surface flaps.

δ_{fin} is the ventral fin (rudder) deflection angle, positive for fin trailing edge left.

All data are for $Re_\infty/10^6 ft = 2.53$.

At $\alpha = +14.3°$ the dihedral (upper) surfaces are parallel to the free stream flow.

TABLE VII

OUTLINE OF MACH 8 TESTS

B) FLAP BALANCE DATA*

FIGURE NUMBER	CONFIGURATIONS AND FLAP SETTINGS	ABSCISSA FOR DATA PLOTS	A E D C GROUP NOS.
9.1	Basic $(-40° \leq \delta \leq 0)$	angle of attack $(\beta=0)$	6-10, 42, 43, 45 and 51-55
9.2	Basic + canards $(-40° \leq \delta \leq 0)$	angle of attack $(\beta=0)$	1-5 and 56-59
9.3a	Basic + port flap $(-40° \leq \delta_p \leq 0)$	sideslip angle $(\alpha=0)$	11-22, 24-29, and 33-41
b	Basic + port flap $(-40° \leq \delta_p \leq 0)$	sideslip angle $(\alpha=+7°)$	
c	Basic + port flap $(-40° \leq \delta_p \leq 0)$	sideslip angle $(\alpha=+14.3°)$	

*Flap normal force, hinge moment and twisting moment coefficients obtained for flap on port dihedral surface of model.

Notes: $\delta < 0$ for upper (dihedral) surface flaps.

δ, without a subscript, indicates both upper flaps deflected.

δ_p indicates only port upper flap deflected.

All data are for $Re_\infty/10^6 ft = 2.53$.

At $\alpha = +14.3°$ the dihedral (upper) surfaces are parallel to the free stream flow and the hinge line of the instrumented flap is perpendicular to the free stream flow direction.

TABLE VIII

SAMPLE MACH 8 BASE PRESSURE COEFFICIENTS

Configuration and Flap Settings	β (deg)	α (deg)	C_{pb}
Basic, no flap deflections	0	-52	+0.053
	0	-47	+0.023
	0	-42	+0.006
	0	-30	-0.005
	0	-15	-0.015
	0	0	-0.015
	0	+14.3	-0.017
	0	+30	-0.008
	0	+54	+0.002
	+8	0	-0.016
	+14	+14.3	-0.016
Basic + canards, no flap deflections	0	0	-0.014
	0	+14.3	-0.014
	0	+30	-0.007
	0	+54	+0.006
Basic, upper flaps deflected -40°	0	-27	+0.002
	0	-15	-0.011
	0	0	-0.011
	0	+14.3	-0.015
	0	+30	-0.010
	0	+54	+0.001
	+14	+14.3	-0.010
Basic, lower flaps deflected +40°	0	-27	-0.012
	0	-15	-0.014
	0	0	-0.013

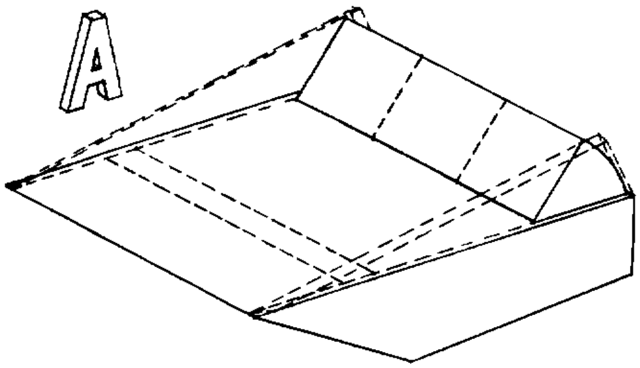

Separated Flows ahead of a Ramp
Fore and aft flaps, end plates
3 separate models:

1) Pressure and heat transfer, AEDC Tunnels A & B, M = 5 & 8

2) Controlled wall temperature, pressure, AEDC Tunnel B, M = 8

3) Pressure and heat transfer, Grumman Shock Tunnel, M $\approx$ 13 & 19

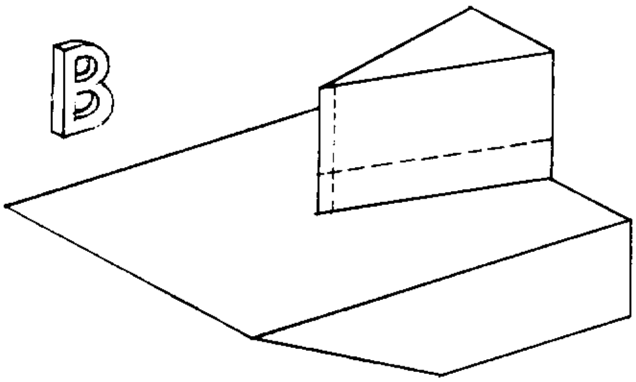

Wedge - Plate Interaction
Small and large fins with sharp and blunt leading edges
2 separate models:

1) Pressure and heat transfer, AEDC Tunnels A & B, M = 5 & 8

2) Pressure and heat transfer, Grumman Shock Tunnel, M $\approx$ 13 & 19

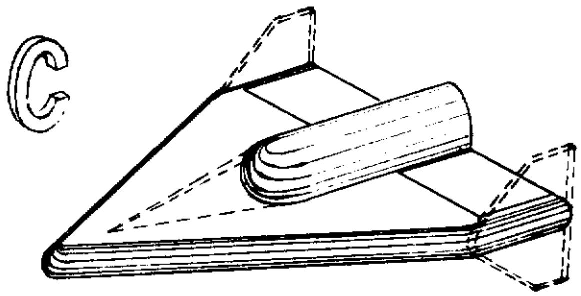

Clipped Delta, Blunt L.E.
Center body, T.E. flaps, drooped nose, spoiler, tip fins
3 separate models:

1) Pressure and heat transfer, AEDC Tunnels A & B, M = 5 & 8

2) Pressure, AEDC Hotshot 2, M $\approx$ 19

3) Six component force, AEDC Tunnels A & B, M = 5 & 8

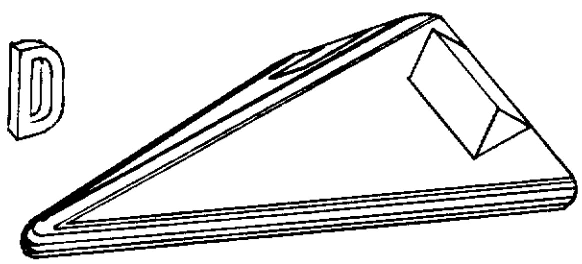

Delta, Blunt L.E., Dihedral
T.E. flaps, canard, ventral fin
3 separate models:

1) Pressure and heat transfer, AEDC Tunnels A & B, M = 5 & 8

2) Pressure and heat transfer, Grumman Shock Tunnel, M $\approx$ 19

3) Six component force, AEDC Tunnels A & B, M = 5 & 8

Fig. 1 General Outline of Models and Remarks for Over-all Program

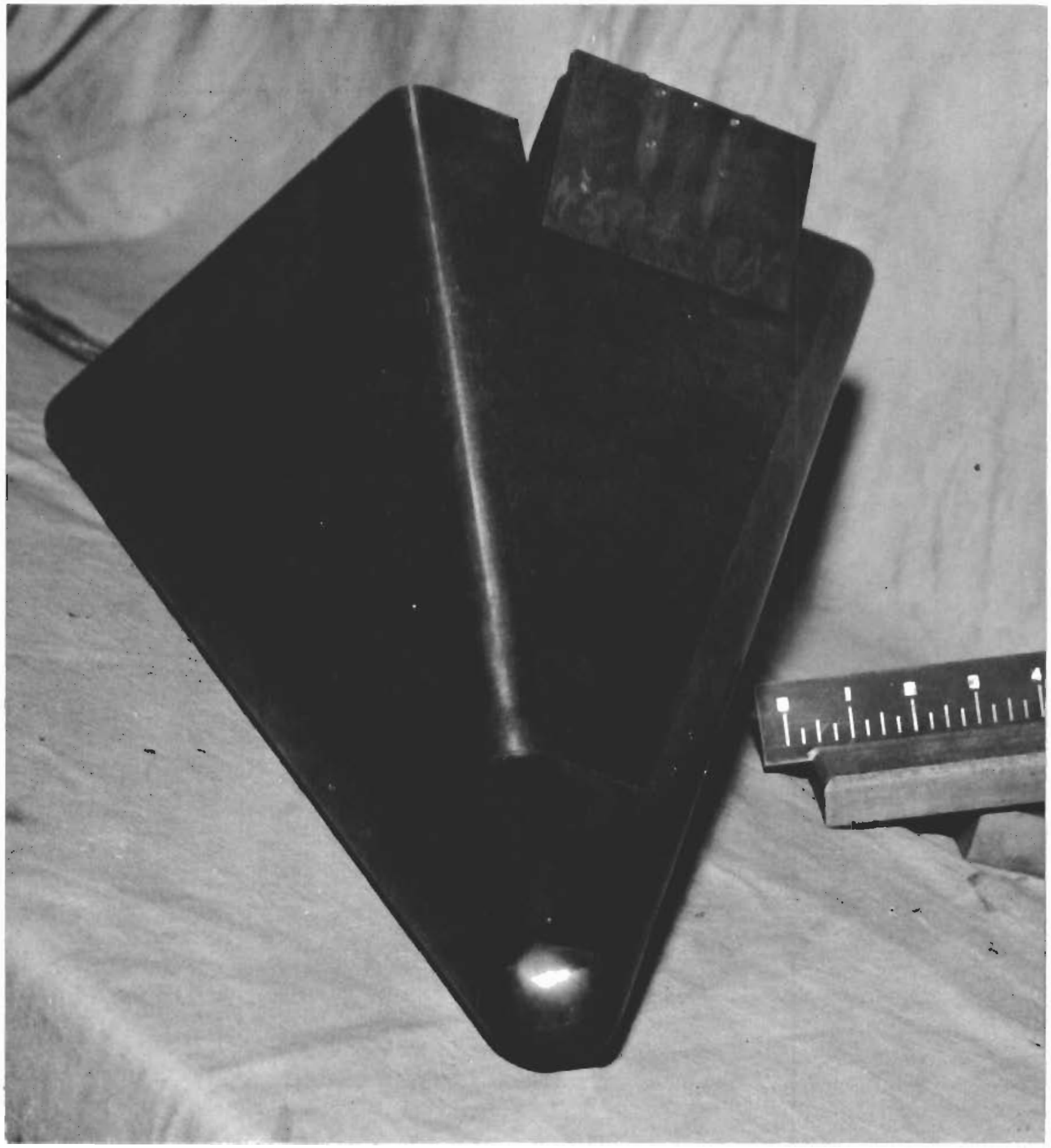

Fig. 2.1 Photograph of Model with Instrumented Flap Deflected

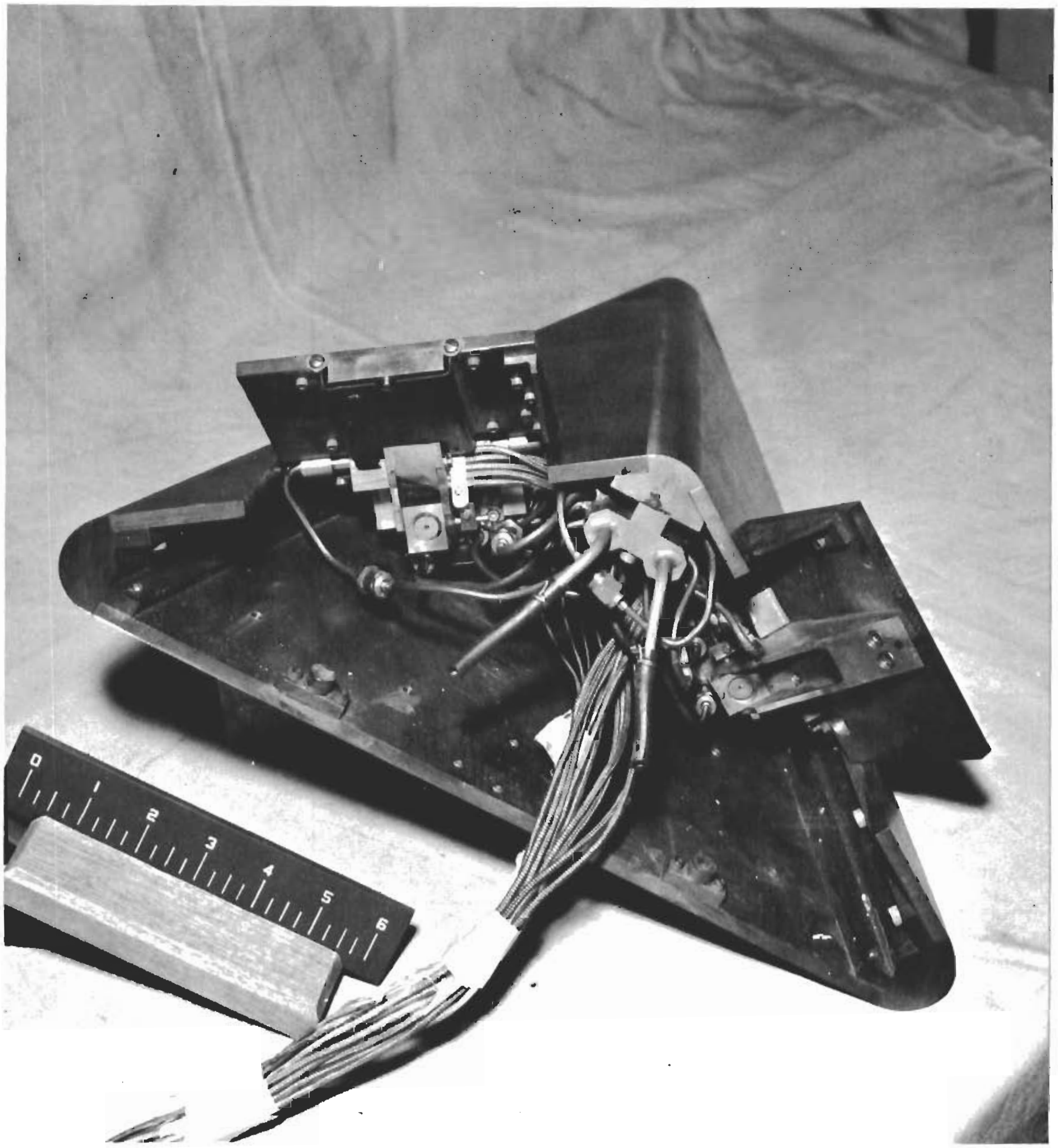

Fig. 2.2 Model Photograph Showing Port Dihedral Flap Balance

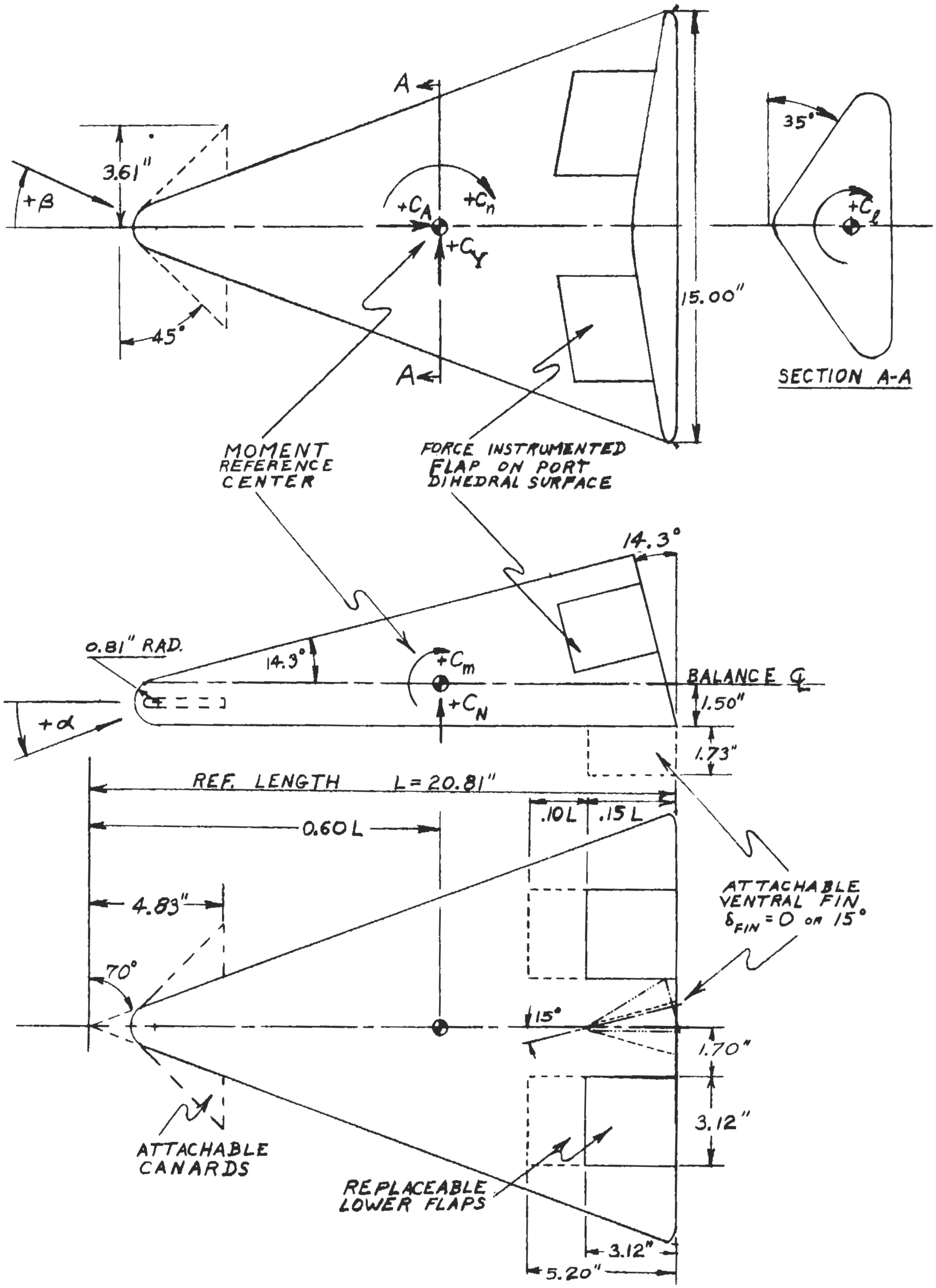

Fig. 3.1 Model Sketch

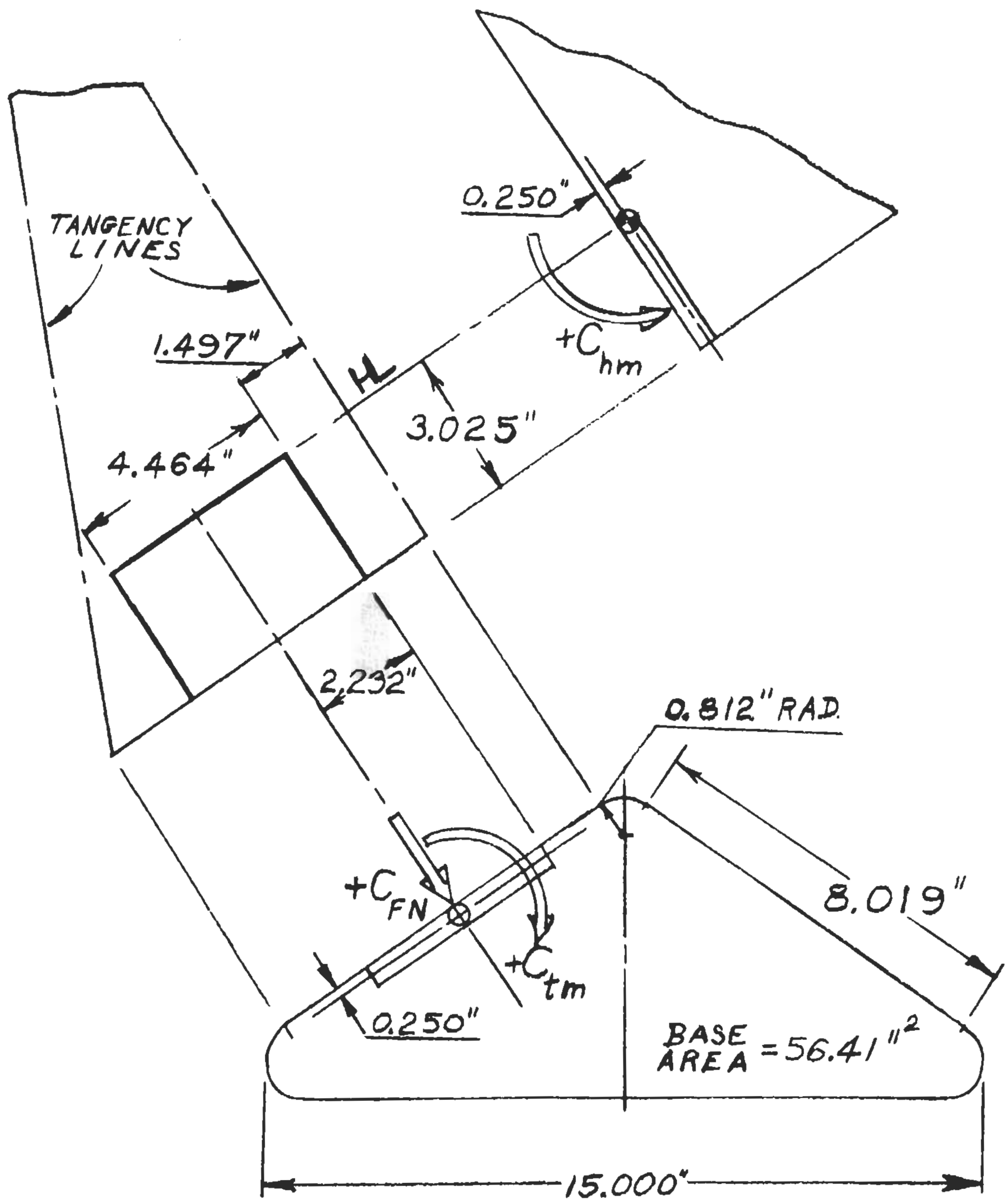

Fig. 3.2 Sketch of Force Instrumented Flap

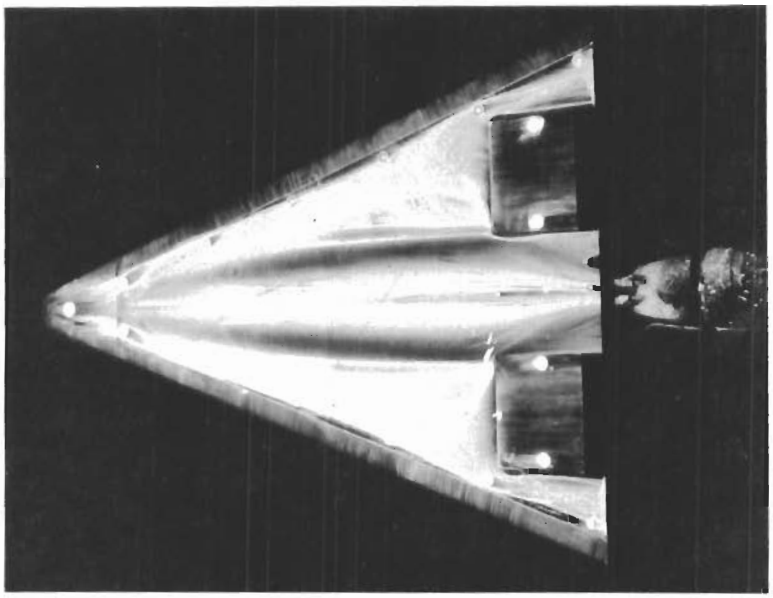

a) Flaps Deflected +20°, $\alpha = 0$

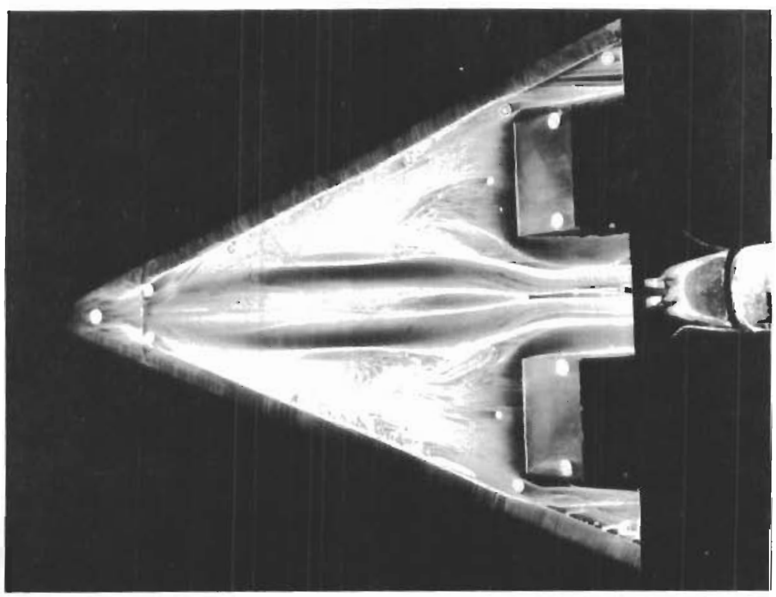

b) Flaps Deflected +40°, $\alpha = 0$

Fig. 4.1 Mach 5 Oil Film Flow Photographs of Lower Surface (sheet 1 of 2)

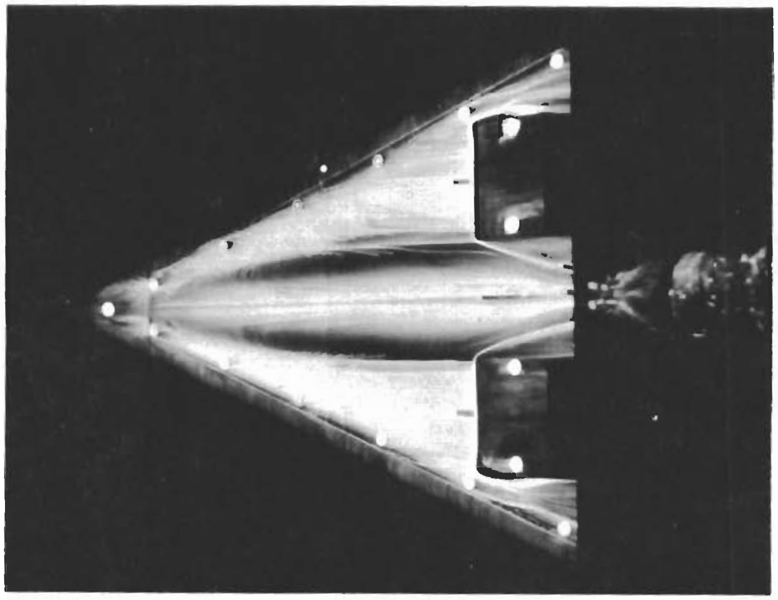

c) Flaps Deflected +20°, α = +12°

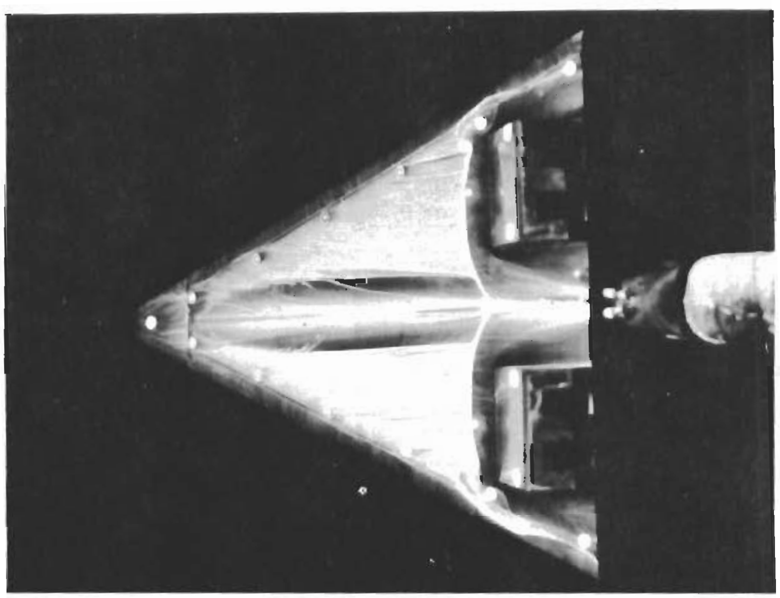

d) Flaps Deflected +40°, α = +14.3°

Fig. 4.1 Mach 5 Oil Film Flow Photographs of Lower Surface (sheet 2 of 2)

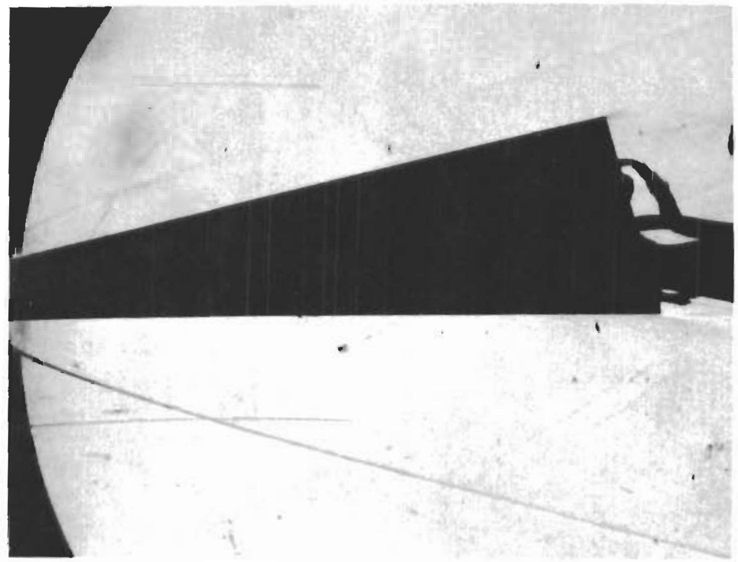

a) No Flap Deflections, $\alpha = 0$

b) Flaps Deflected +40°, $\alpha = 0$

Fig. 4.2 Mach 5 Schlieren Flow Photographs
(sheet 1 of 2)

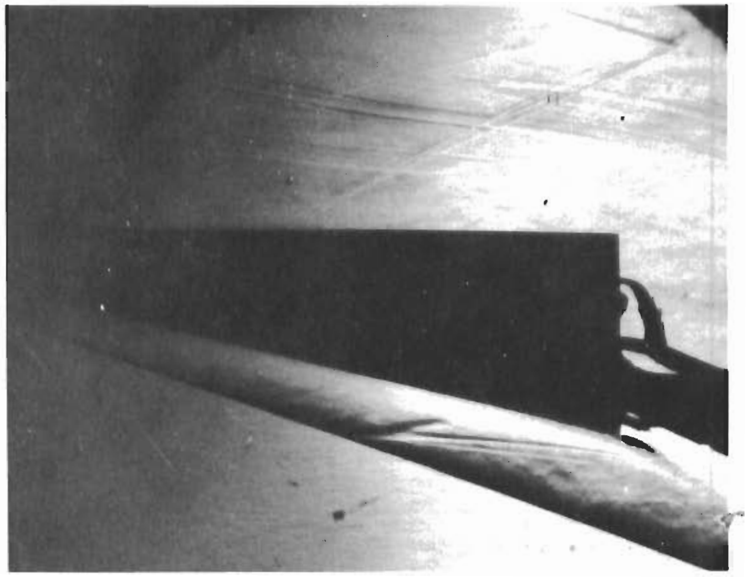

c) No Flap Deflections, $\alpha = +14.3°$

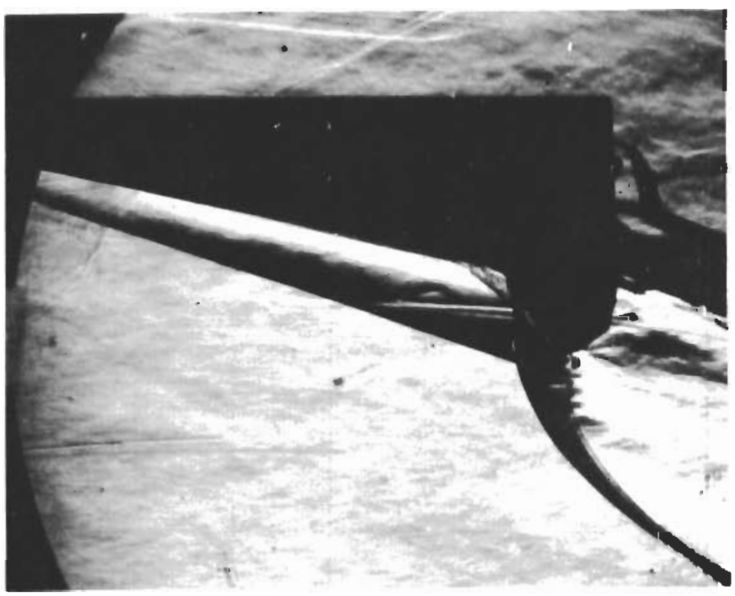

d) Flaps Deflected +40°, $\alpha = +14.3°$

Fig. 4.2 Mach 5 Schlieren Flow Photographs
(sheet 2 of 2)

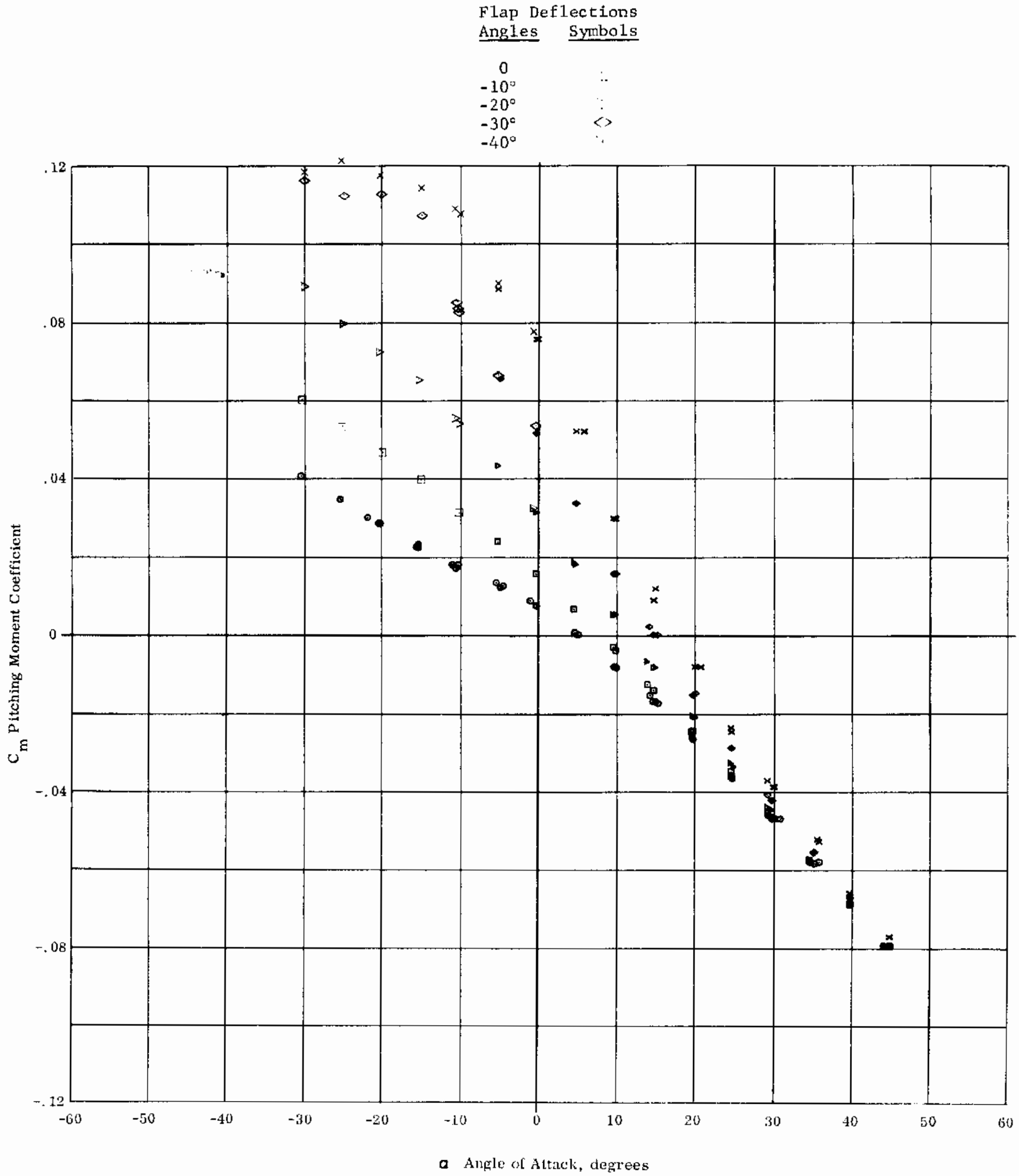

a) Upper Flaps Deflected

Fig. 5.1 Mach 5 Pitch Polars for Basic Configuration (sheet 1 of 4)

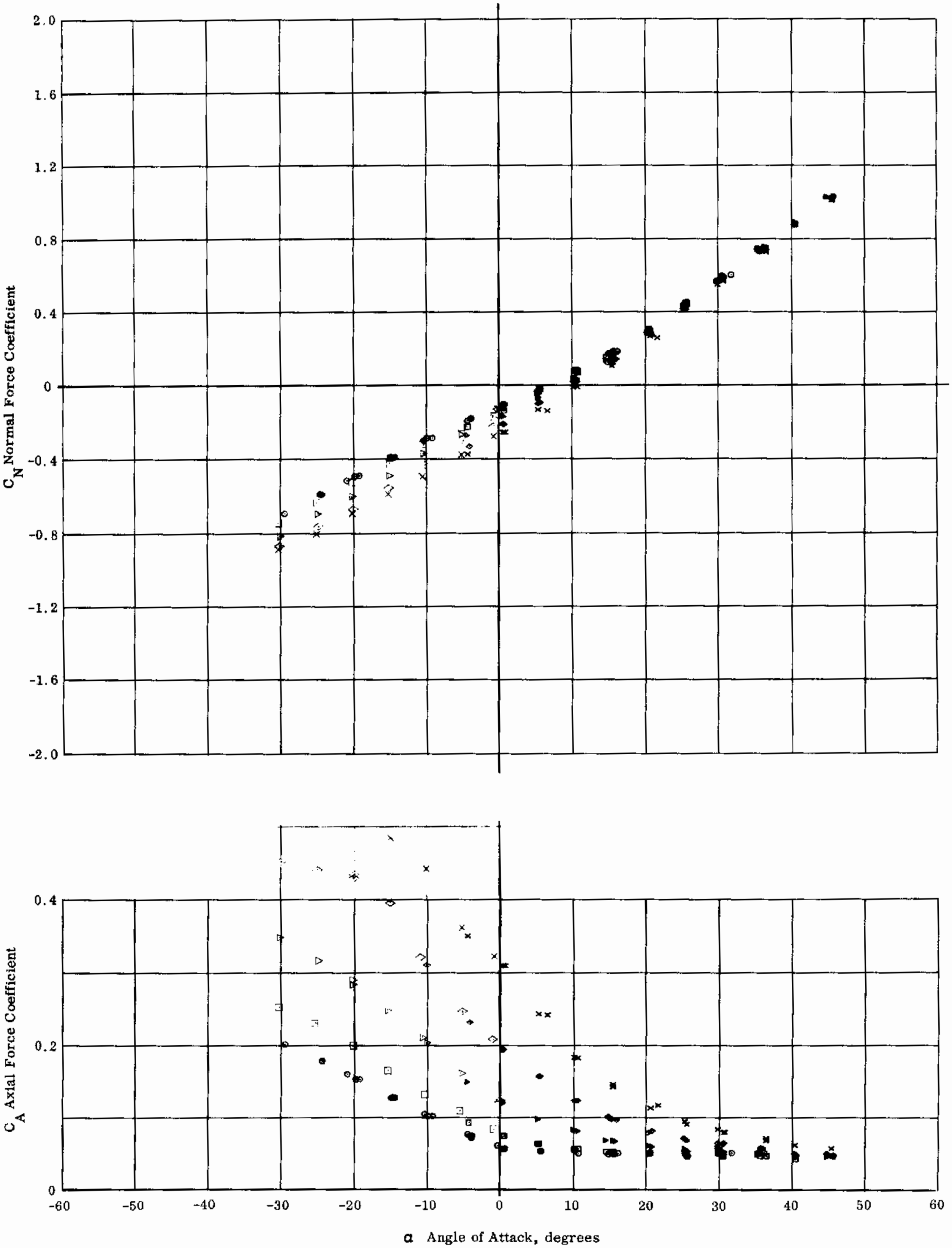

a) Upper Flaps Deflected

Fig. 5.1 Mach 5 Pitch Polars for Basic Configuration (sheet 2 of 4)

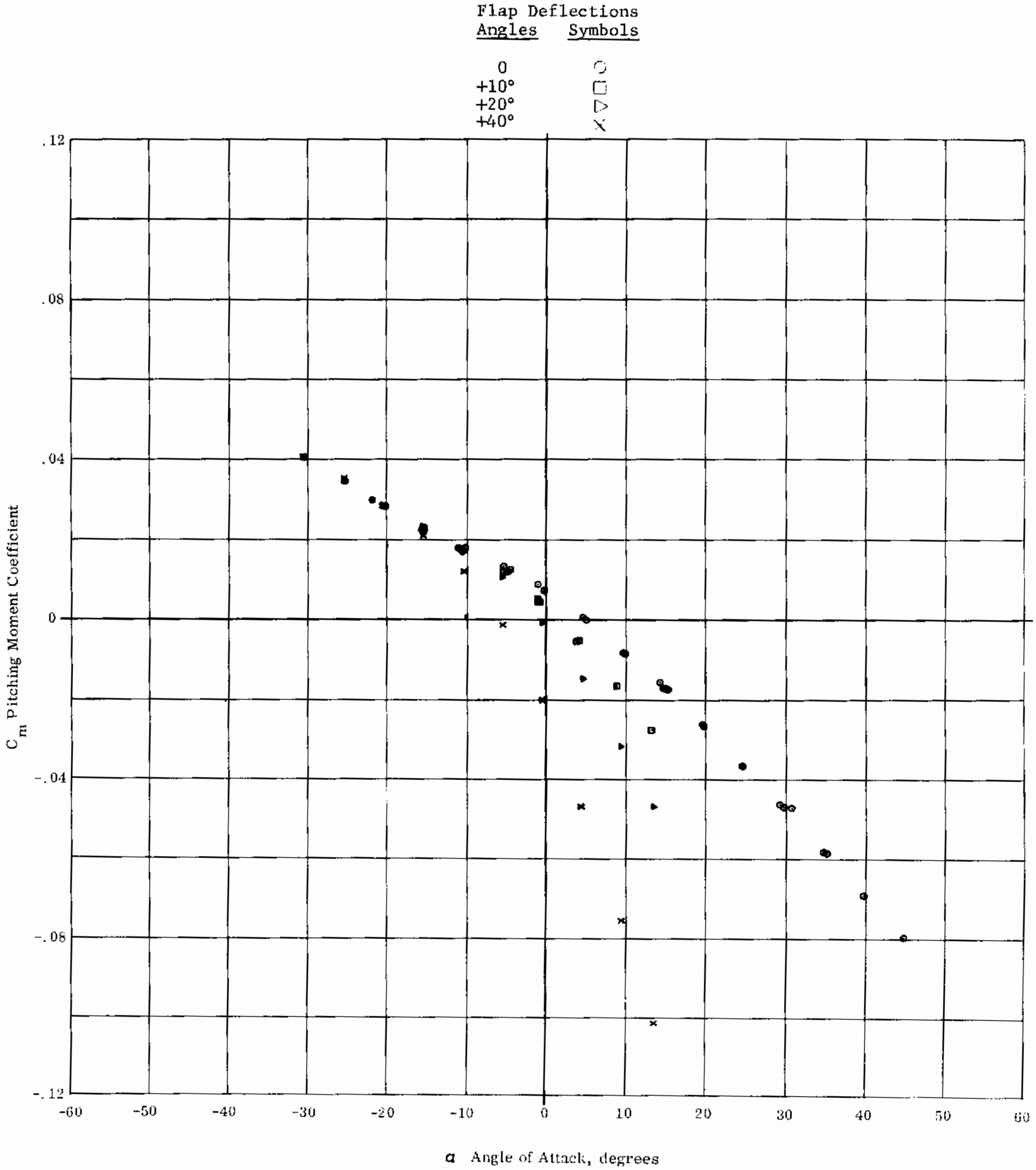

b) Lower Flaps Deflected

Fig. 5.1 Mach 5 Pitch Polars for Basic Configuration (sheet 3 of 4)

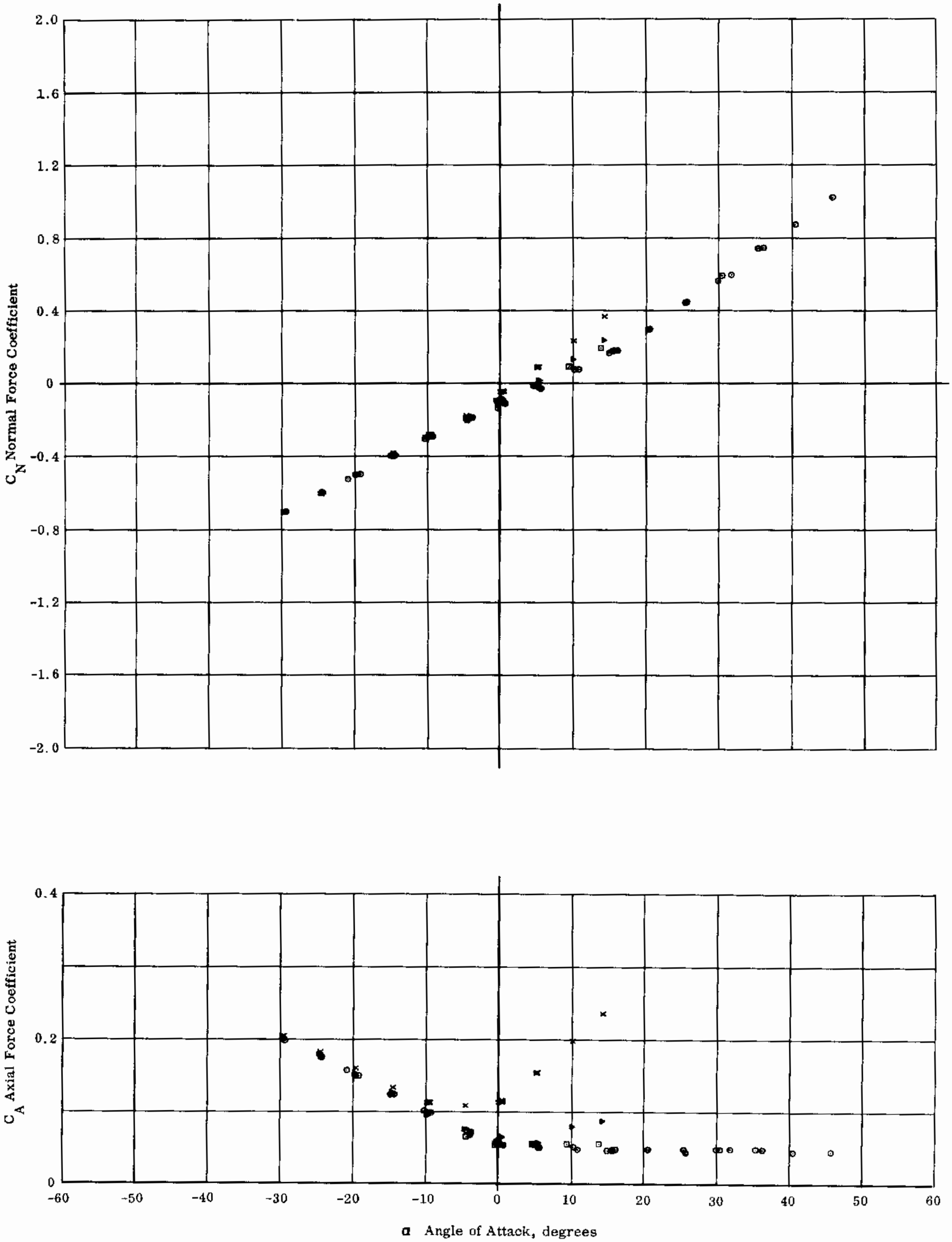

b) Lower Flaps Deflected

Fig. 5.1 Mach 5 Pitch Polars for Basic Configuration (sheet 4 of 4)

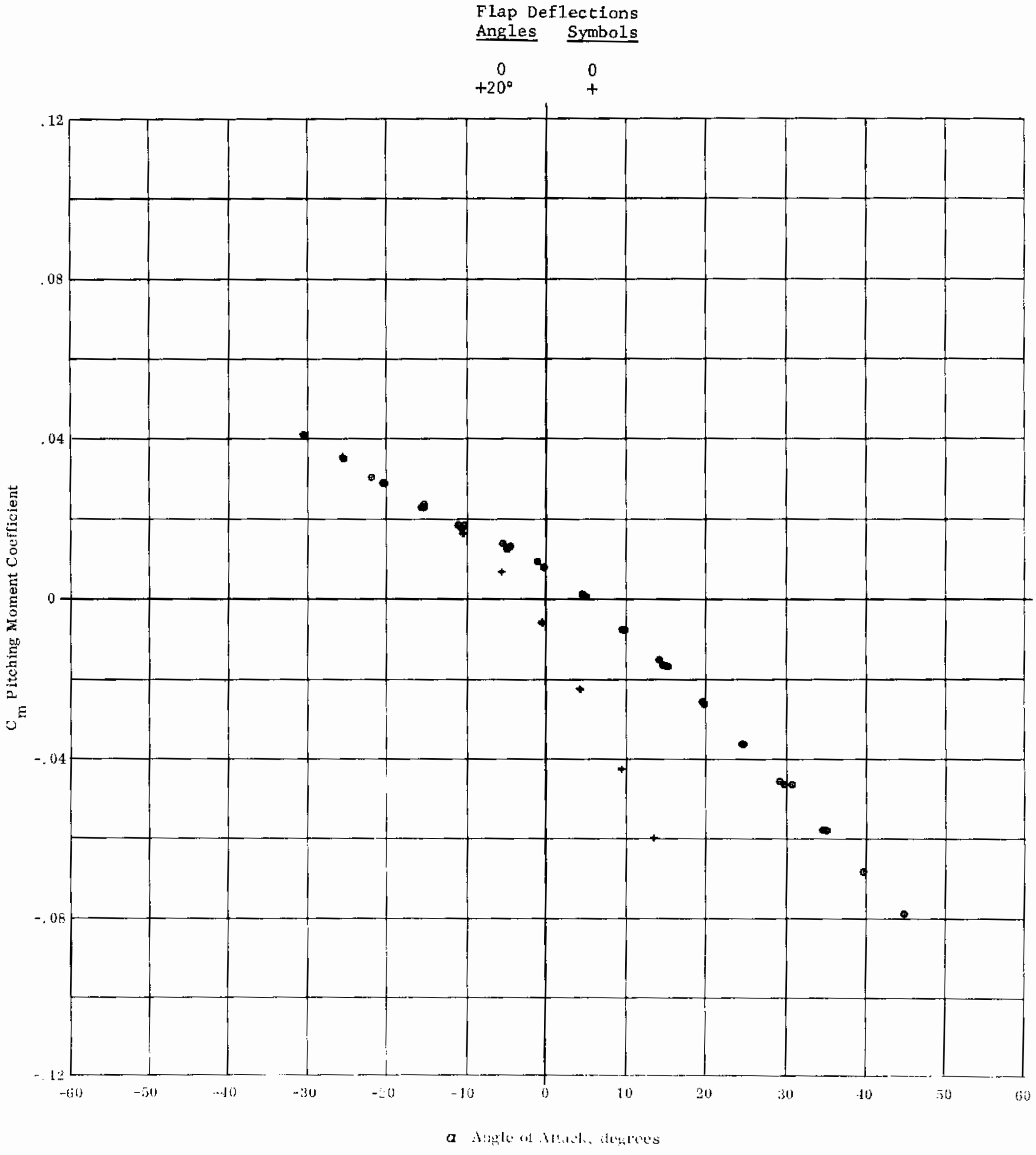

Fig. 5.2 Mach 5 Pitch Polars for Basic Configuration with Longer Chord Flaps on Lower Surface (sheet 1 of 2)

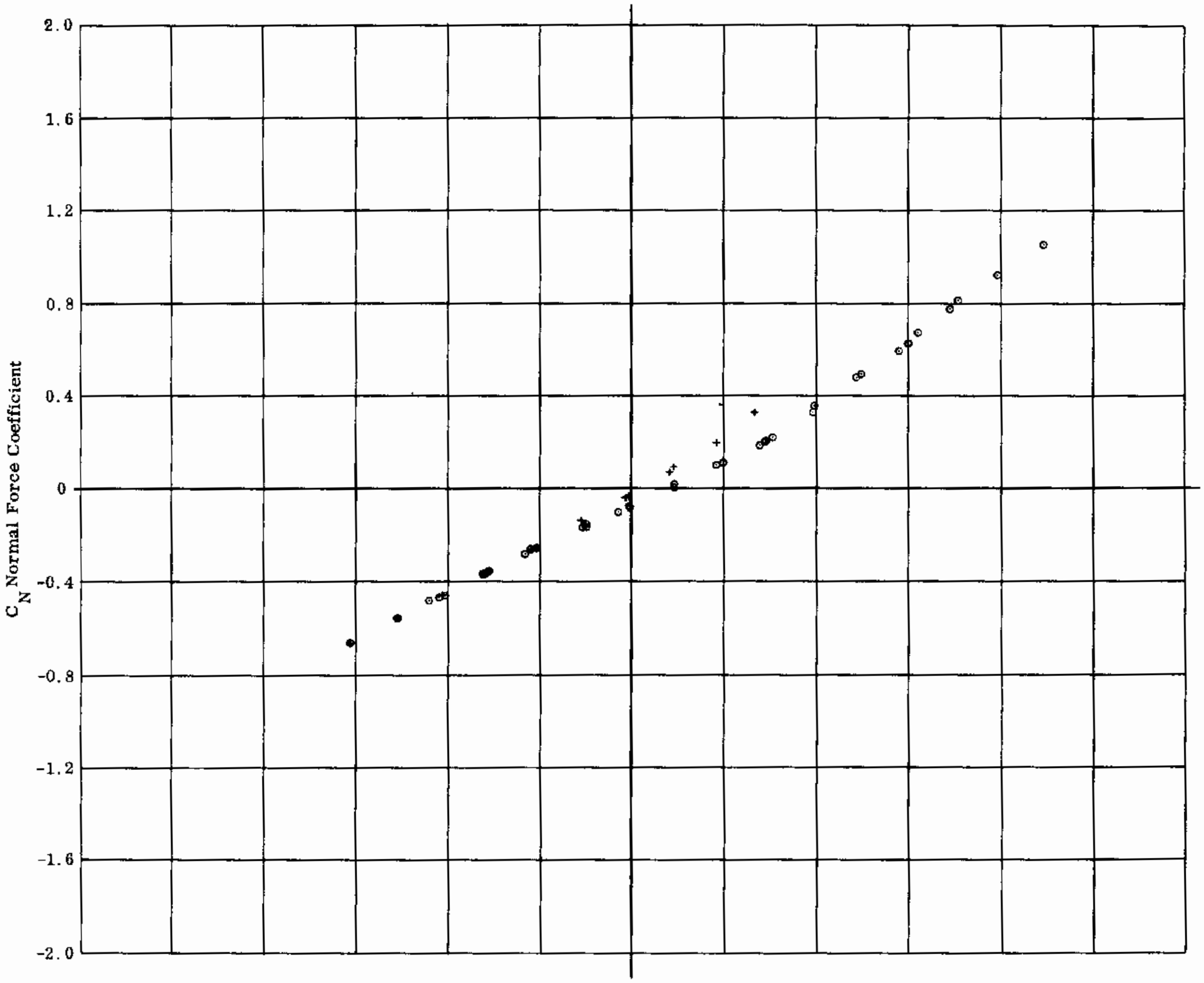

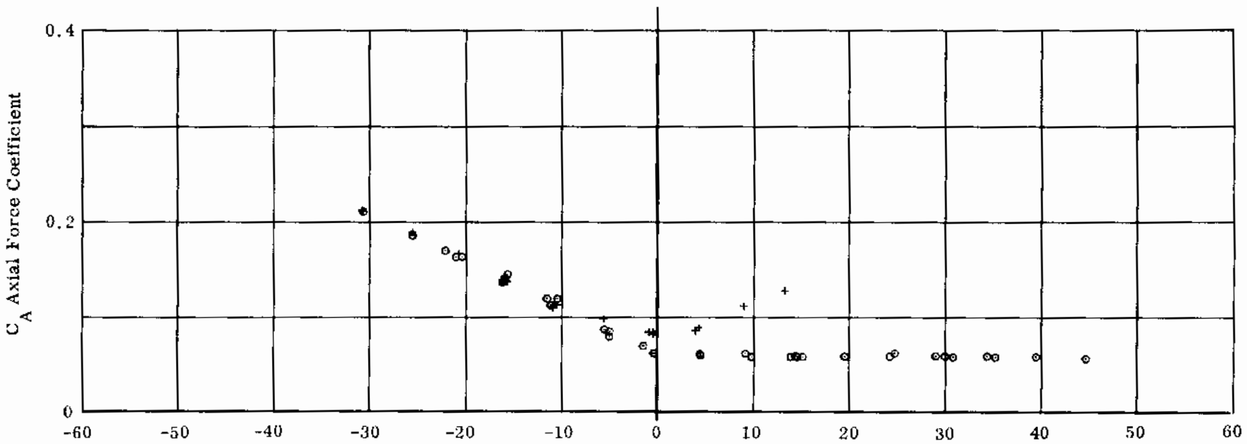

Fig. 5.2 Mach 5 Pitch Polars for Basic Configuration with Longer Chord Flaps on Lower Surface (sheet 2 of 2)

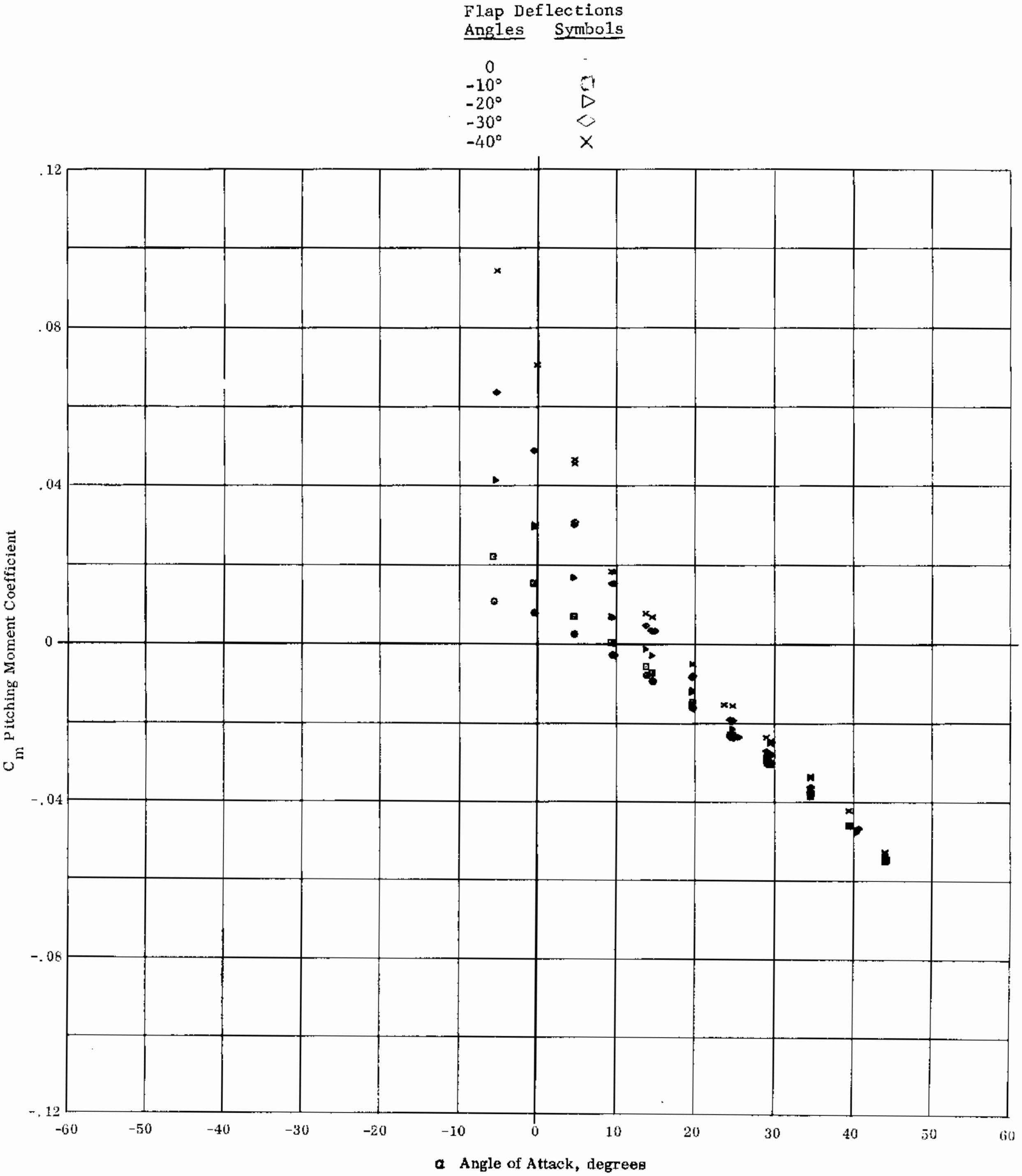

Fig. 5.3 Mach 5 Pitch Polars for Basic Configuration with Canards
(sheet 1 of 2)

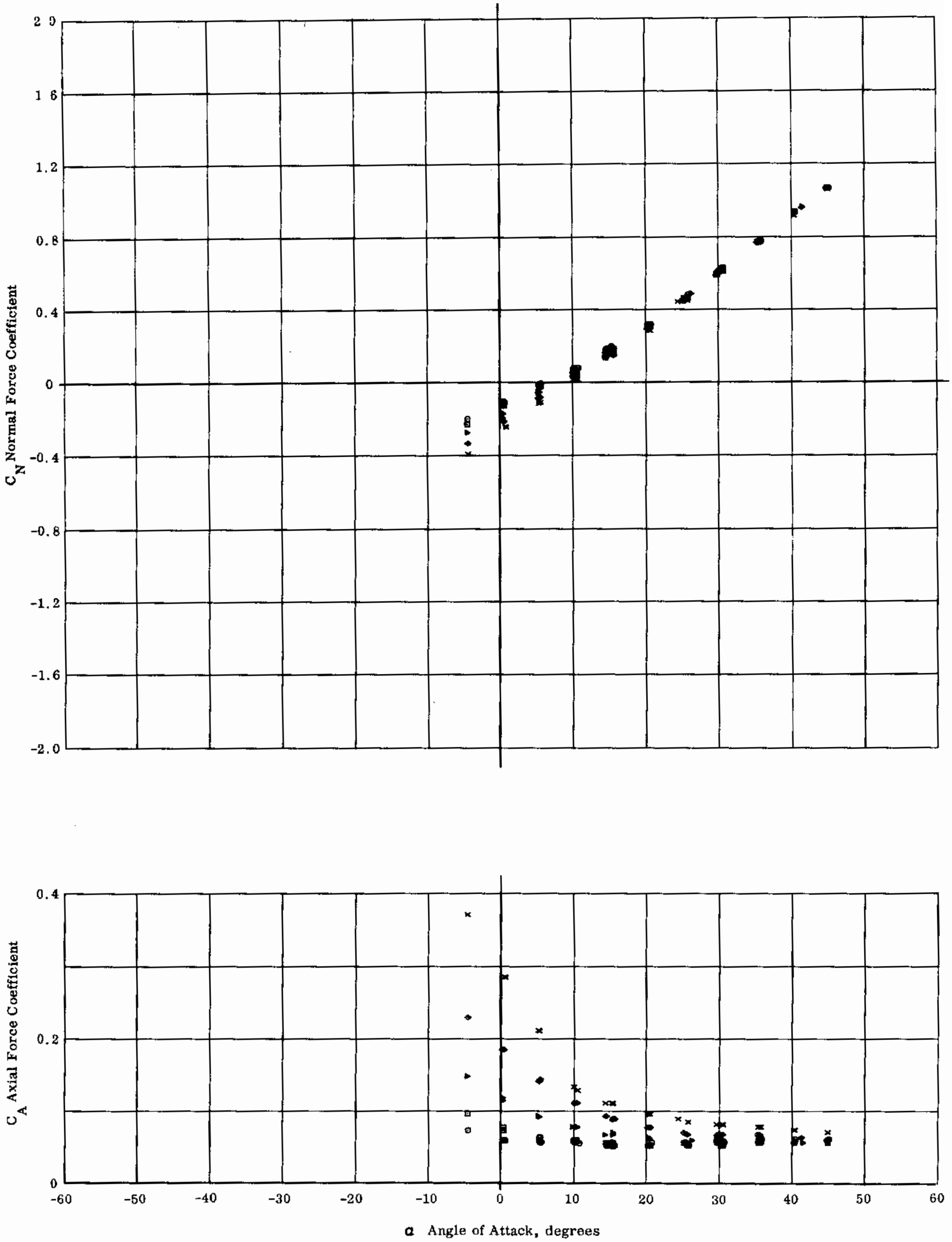

Fig. 5.3 Mach 5 Pitch Polars for Basic Configuration with Canards (sheet 2 of 2)

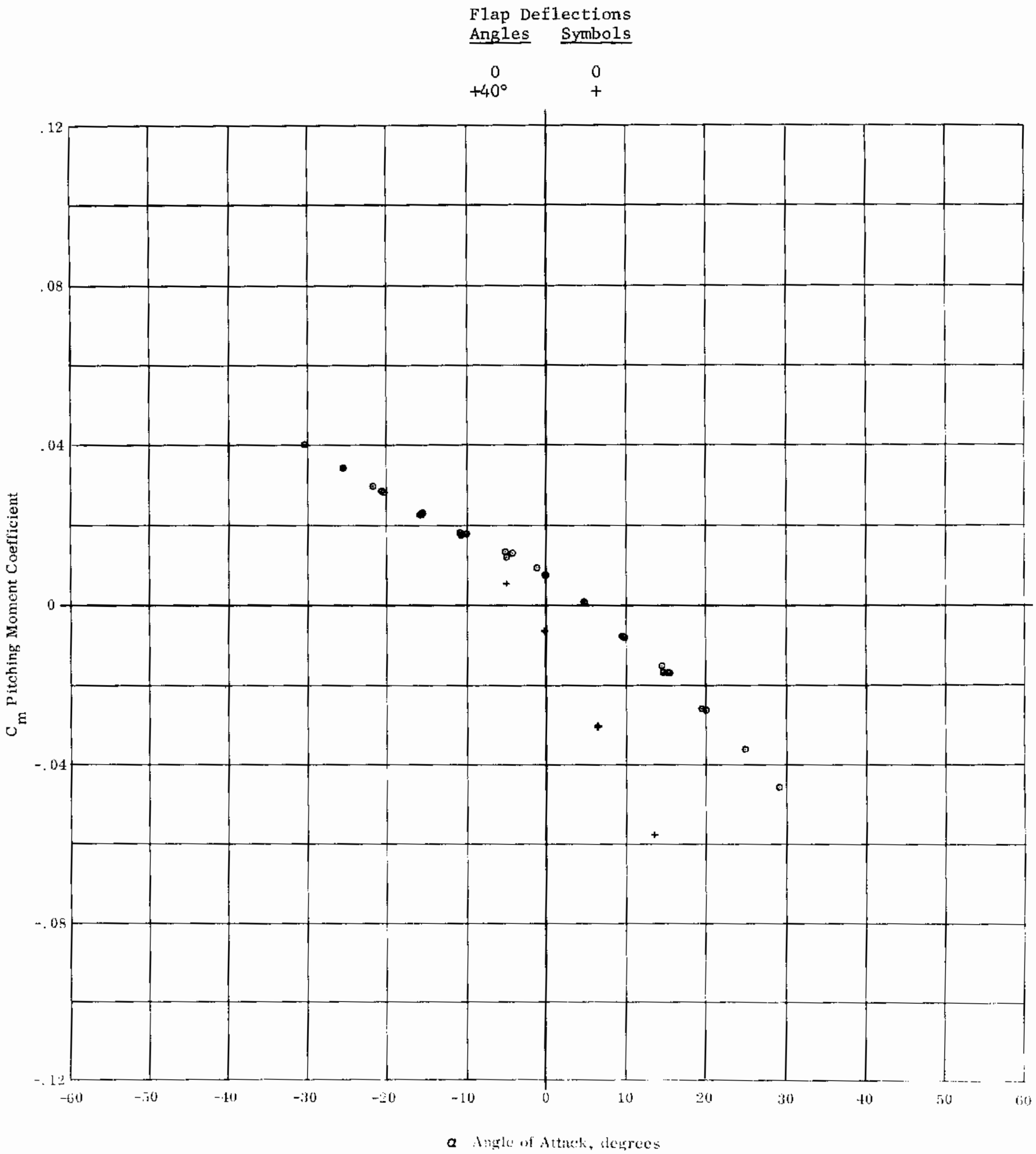

Fig. 5.4 Mach 5 Pitch Polars for Basic Configuration with Port Flap on Lower Surface (sheet 1 of 3)

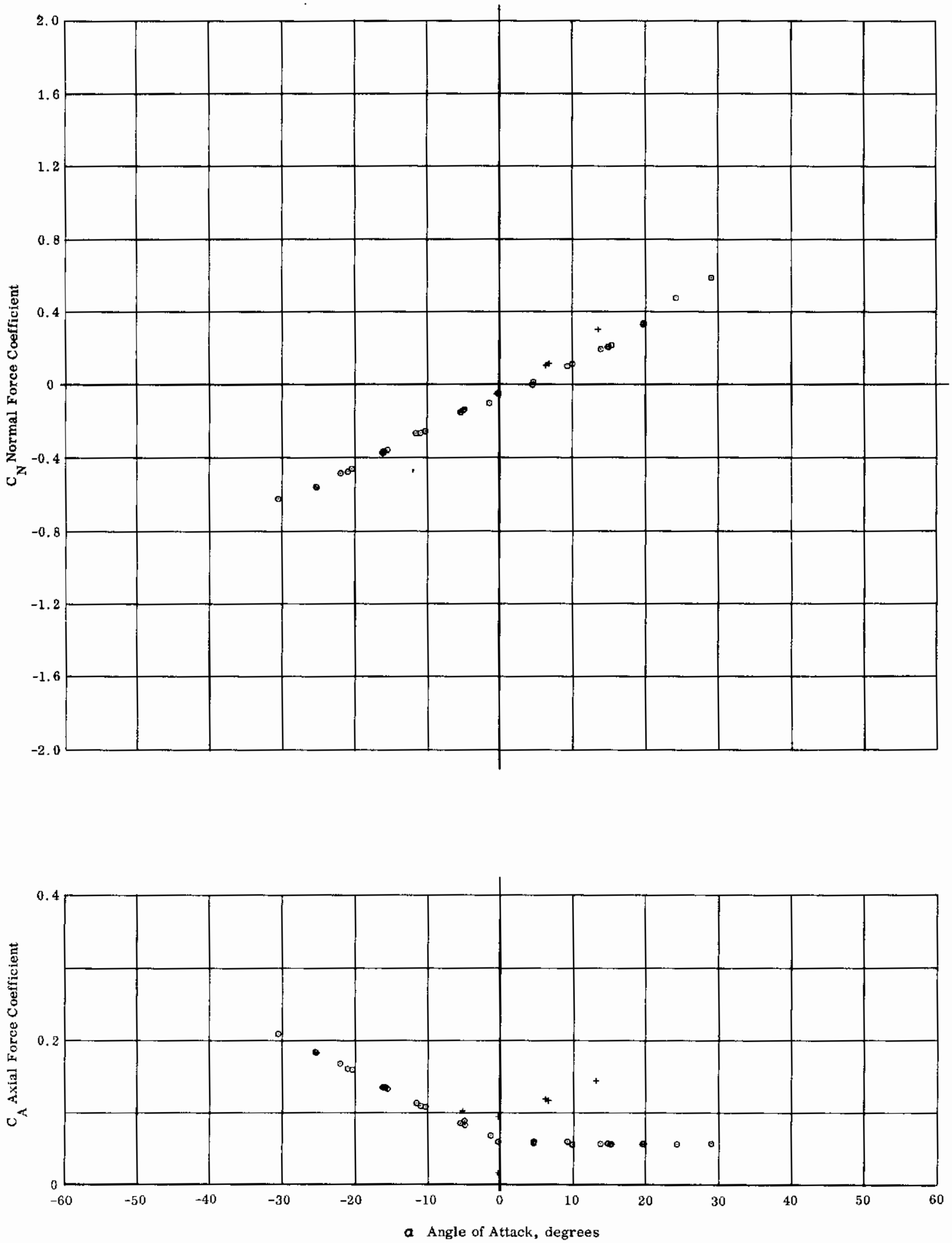

Fig. 5.4 Mach 5 Pitch Polars for Basic Configuration with Port Flap on Lower Surface (sheet 2 of 3)

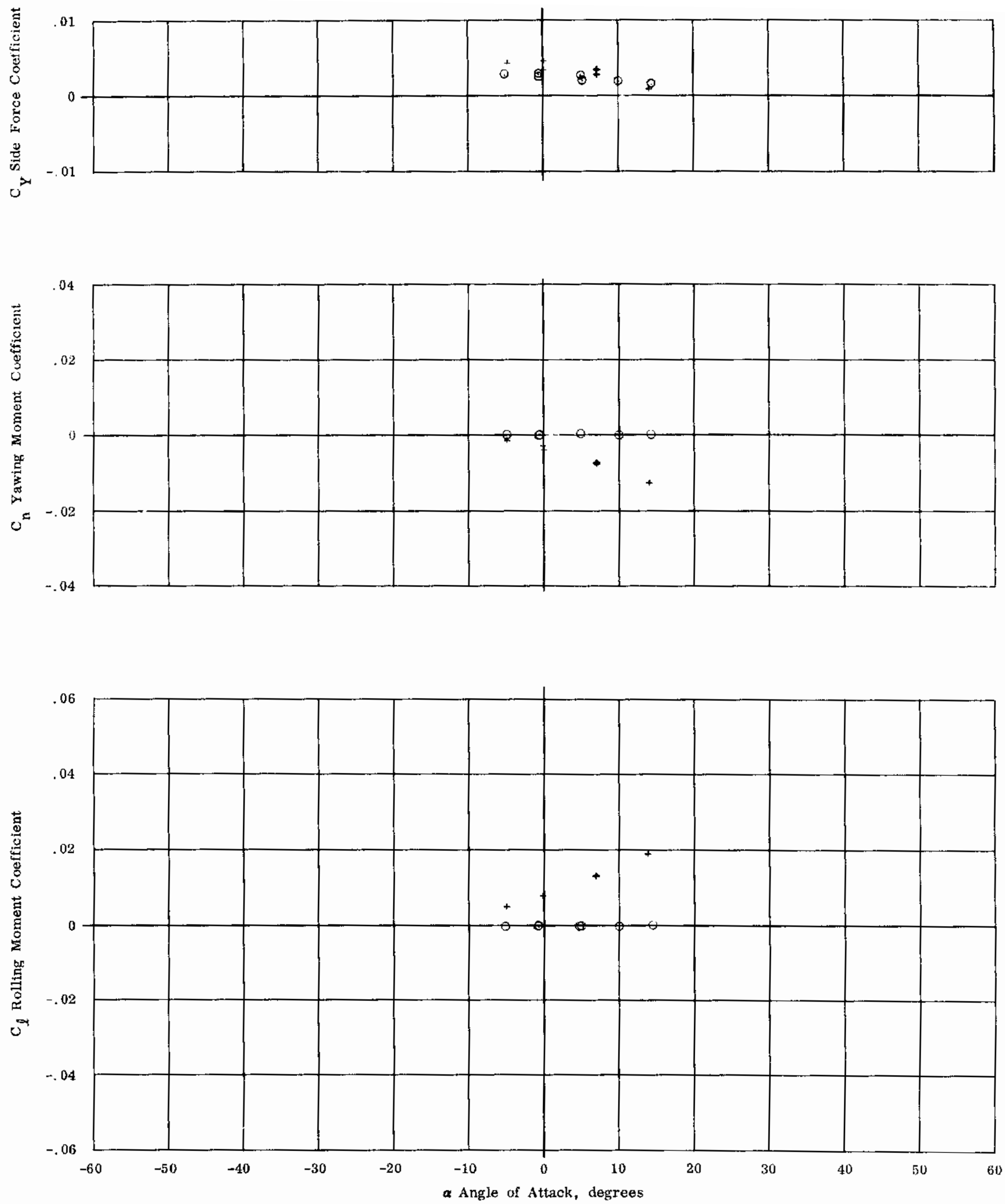

Fig. 5.4 Mach 5 Pitch Polars for Basic Configuration with Port Flap on Lower Surface (sheet 3 of 3)

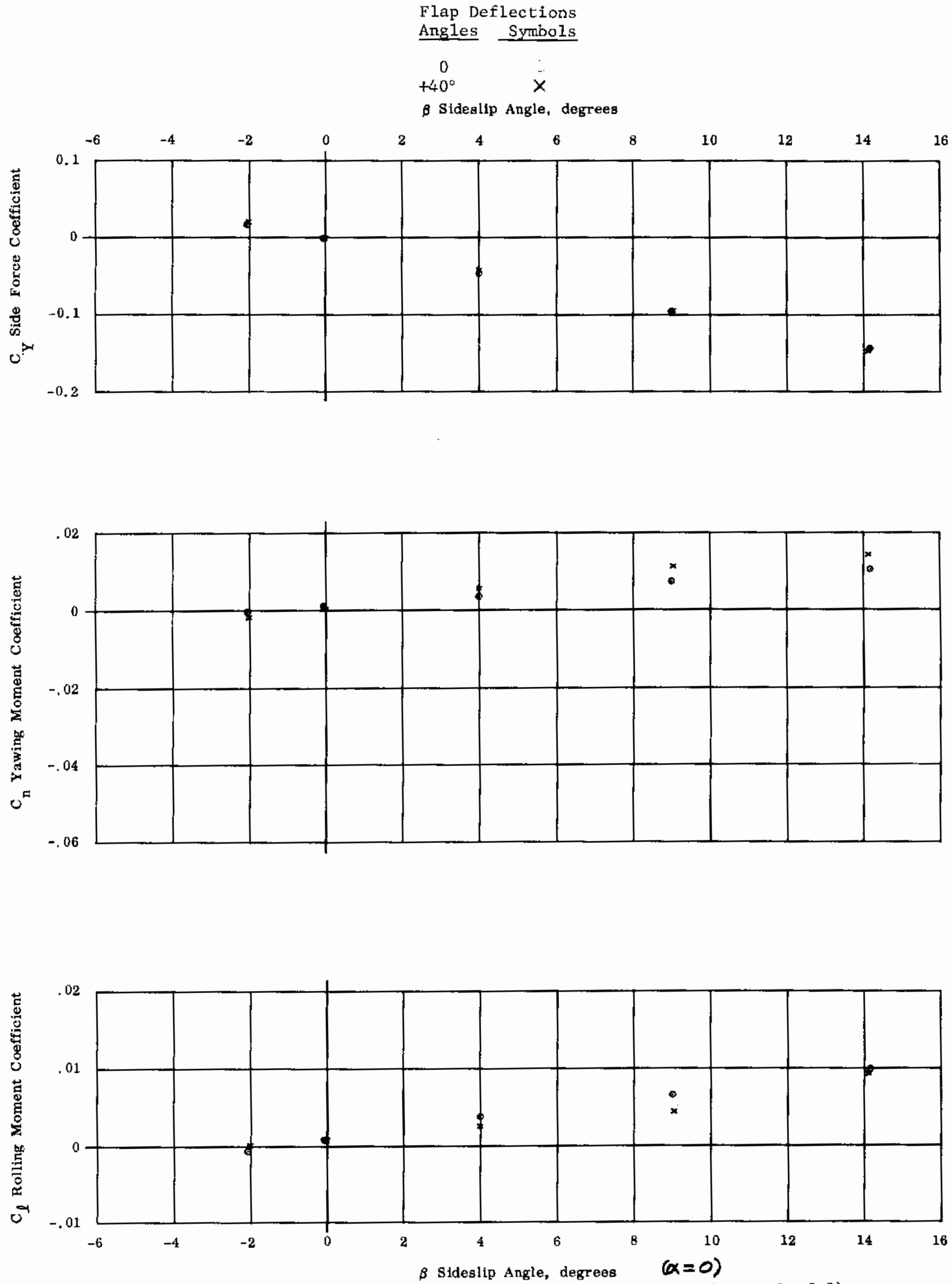

Fig. 5.5 Mach 5 Sideslip Polars for Basic Configuration (sheet 1 of 3)

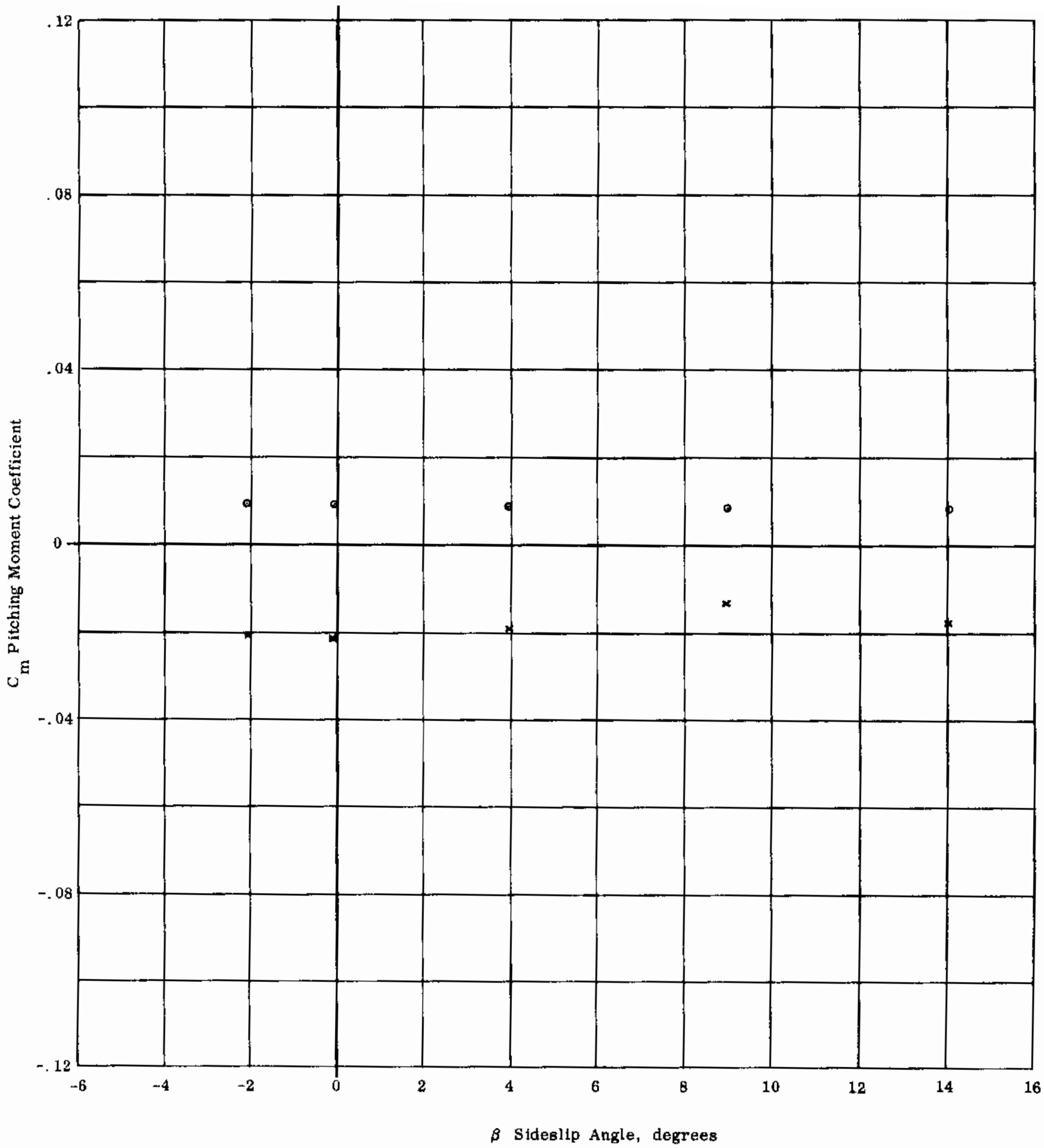

Fig. 5.5 Mach 5 Sideslip Polars for Basic Configuration (sheet 2 of 3)

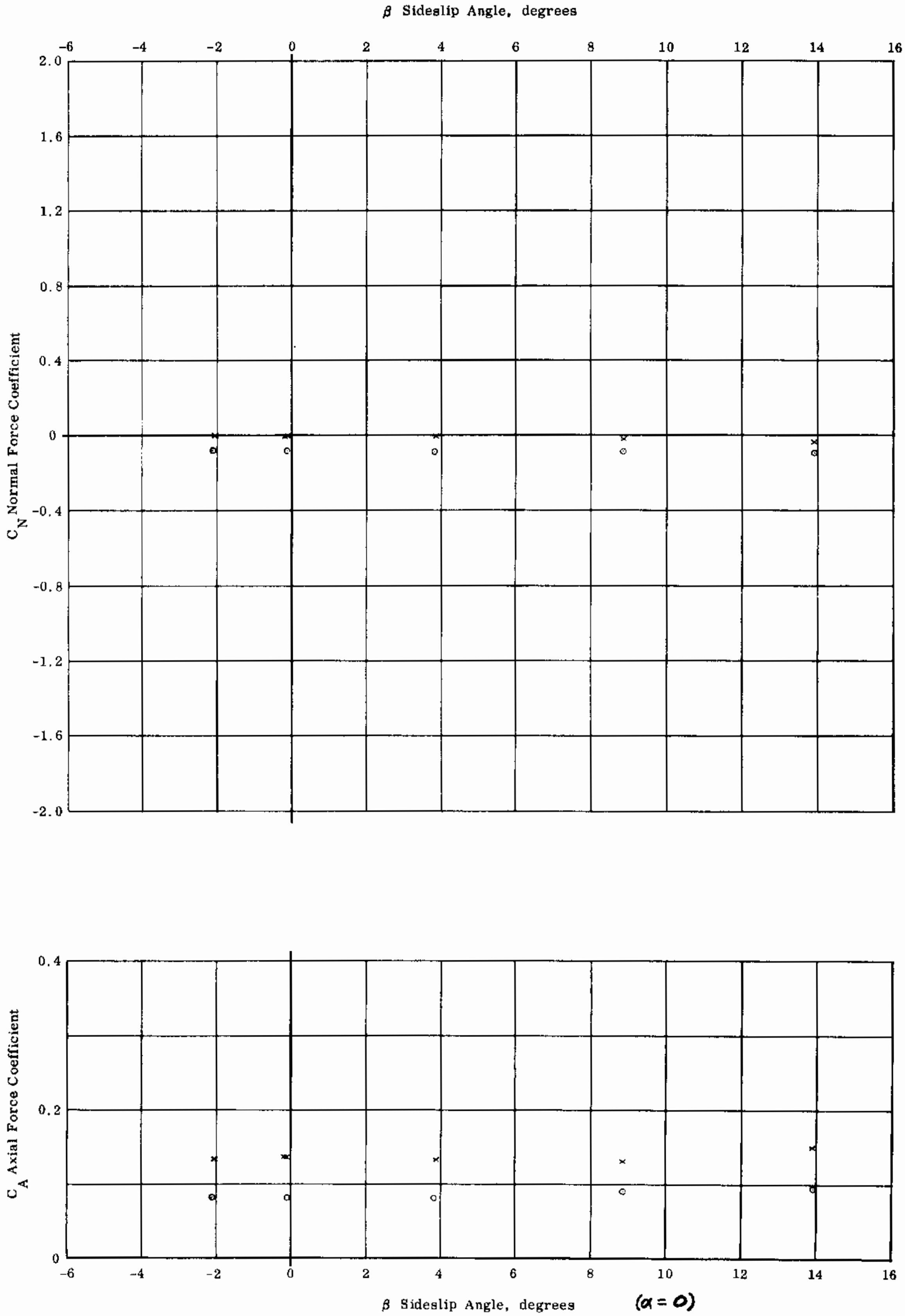

Fig. 5.5 Mach 5 Sideslip Polars for Basic Configuration (sheet 3 of 3)

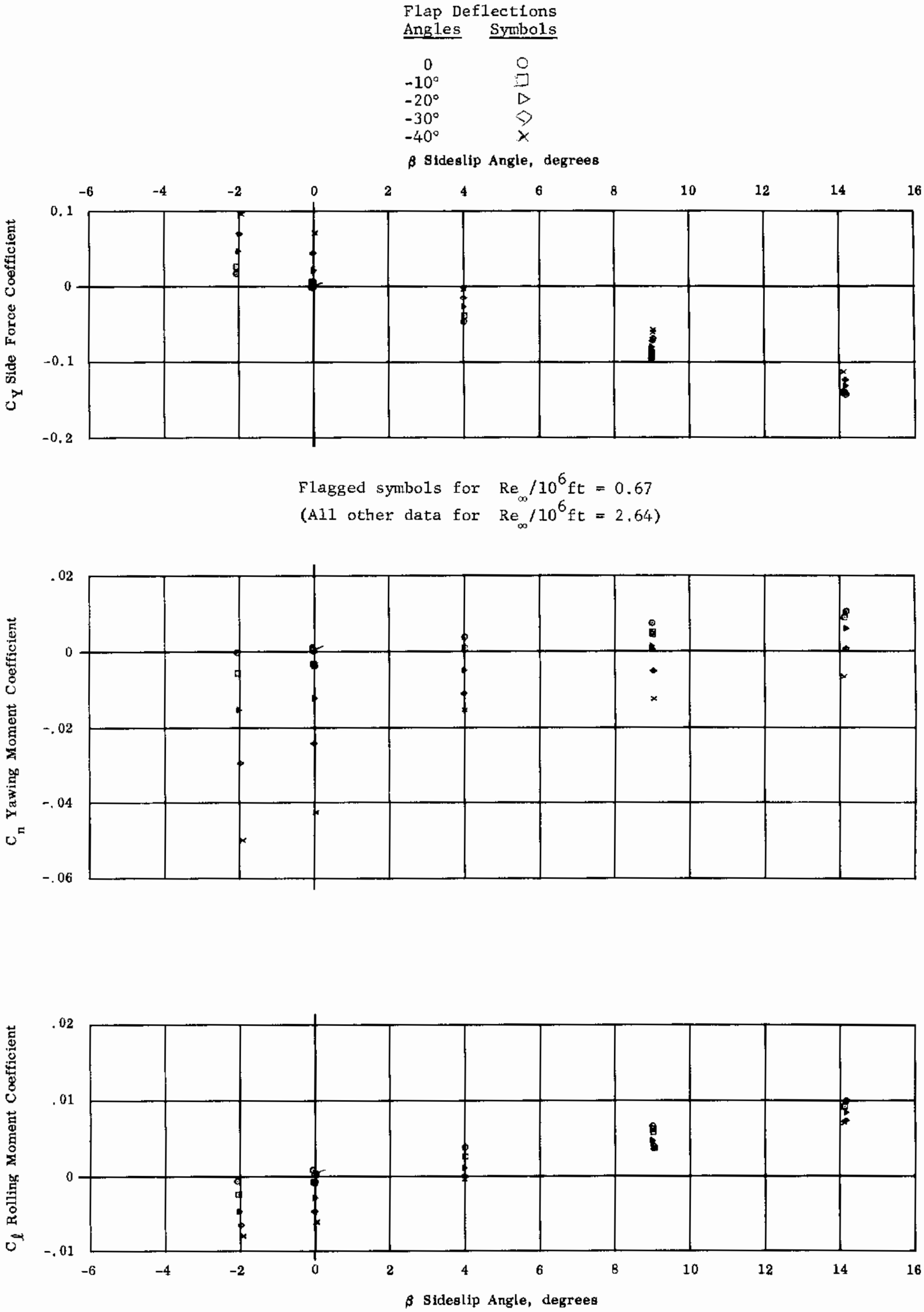

a) $\alpha = 0$

Fig. 5.6 Mach 5 Sideslip Polars for Basic Configuration with Upper Surface Port Flap Deflections (sheet 1 of 9)

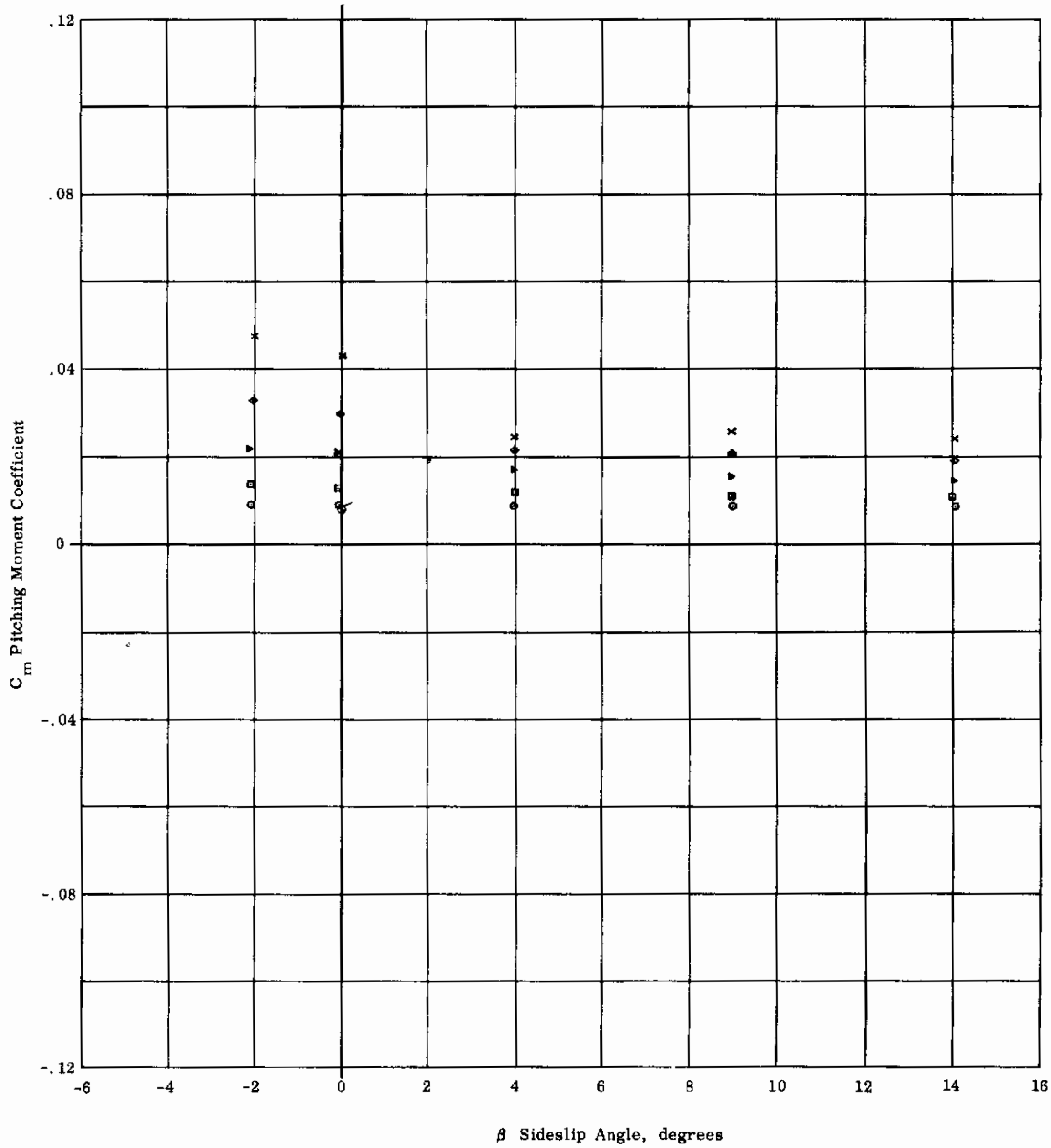

a) α = 0

Fig. 5.6 Mach 5 Sideslip Polars for Basic Configuration with Upper Surface Port Flap Deflections (sheet 2 of 9)

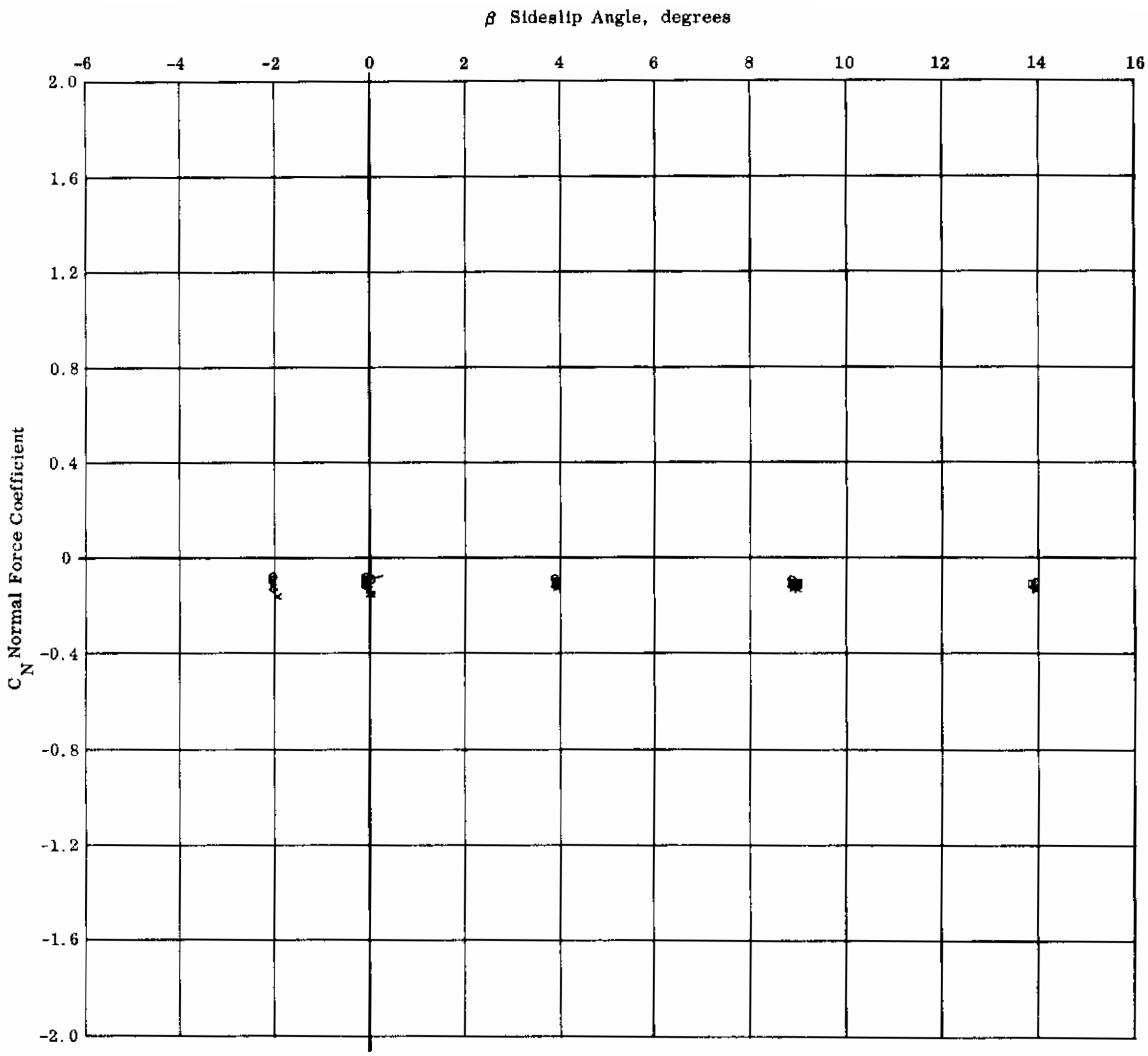

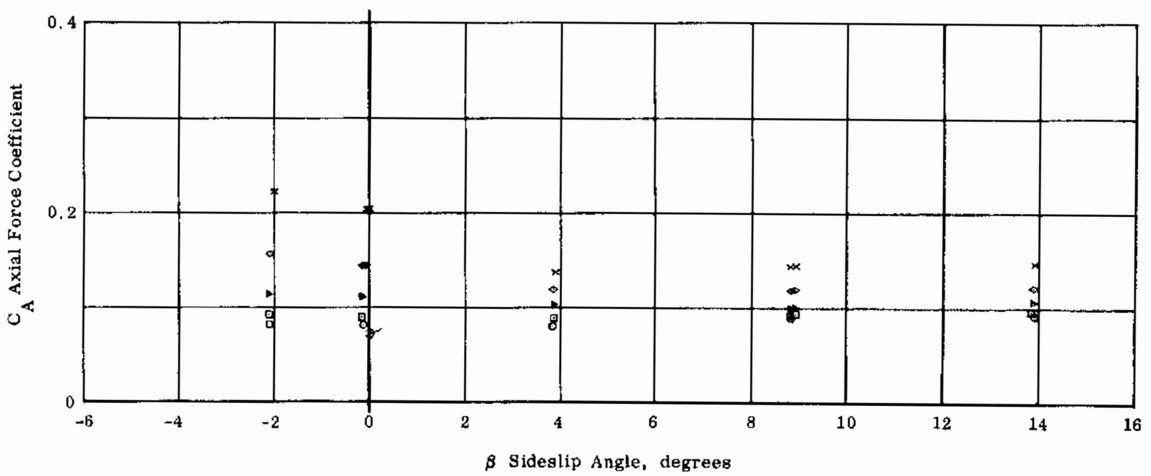

a) α = 0

Fig. 5.6 Mach 5 Sideslip Polars for Basic Configuration with Upper Surface Port Flap Deflections (sheet 3 of 9)

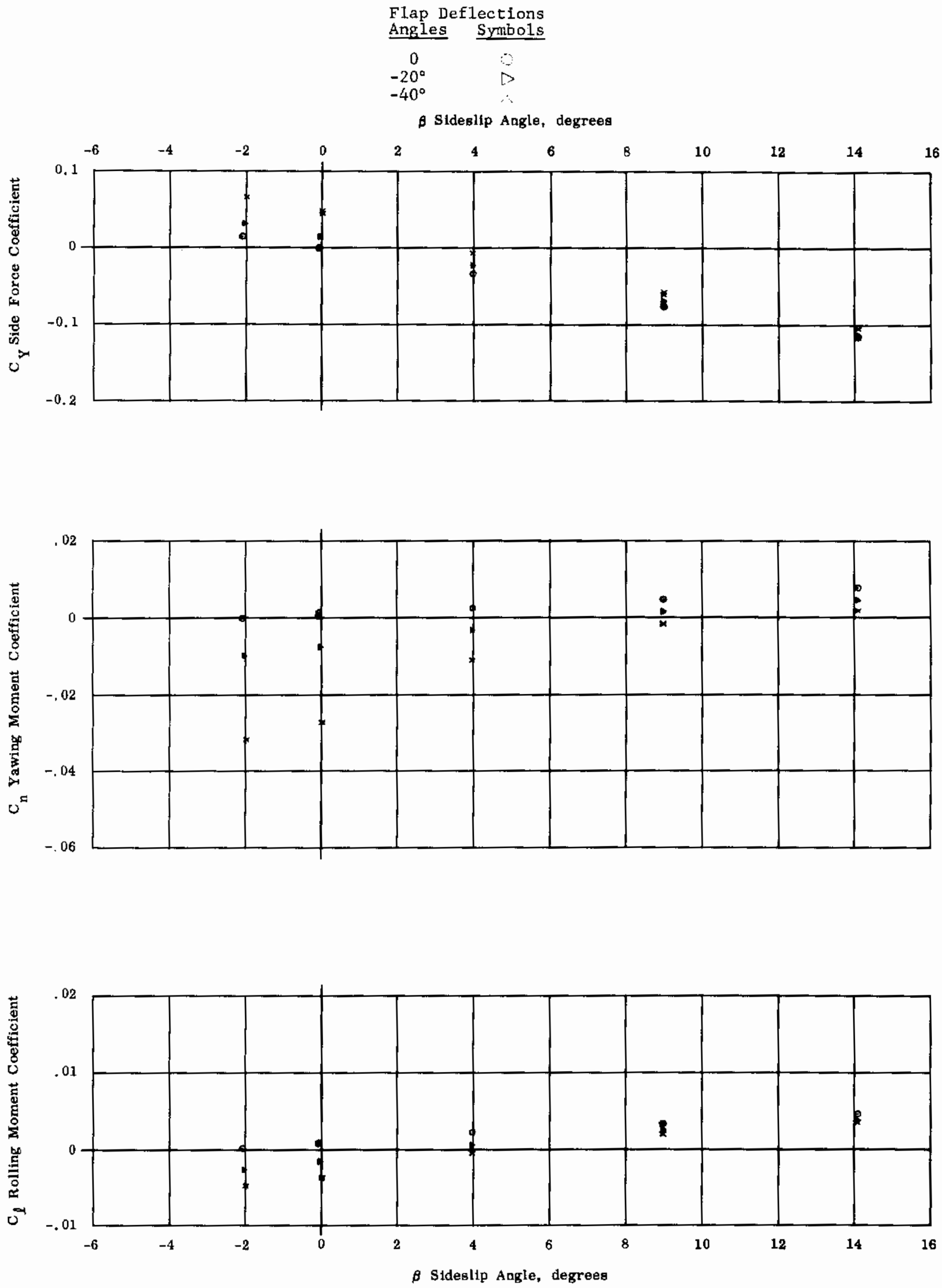

b) α = +7°

Fig. 5.6 Mach 5 Sideslip Polars for Basic Configuration with Upper Surface Port Flap Deflections (sheet 4 of 9)

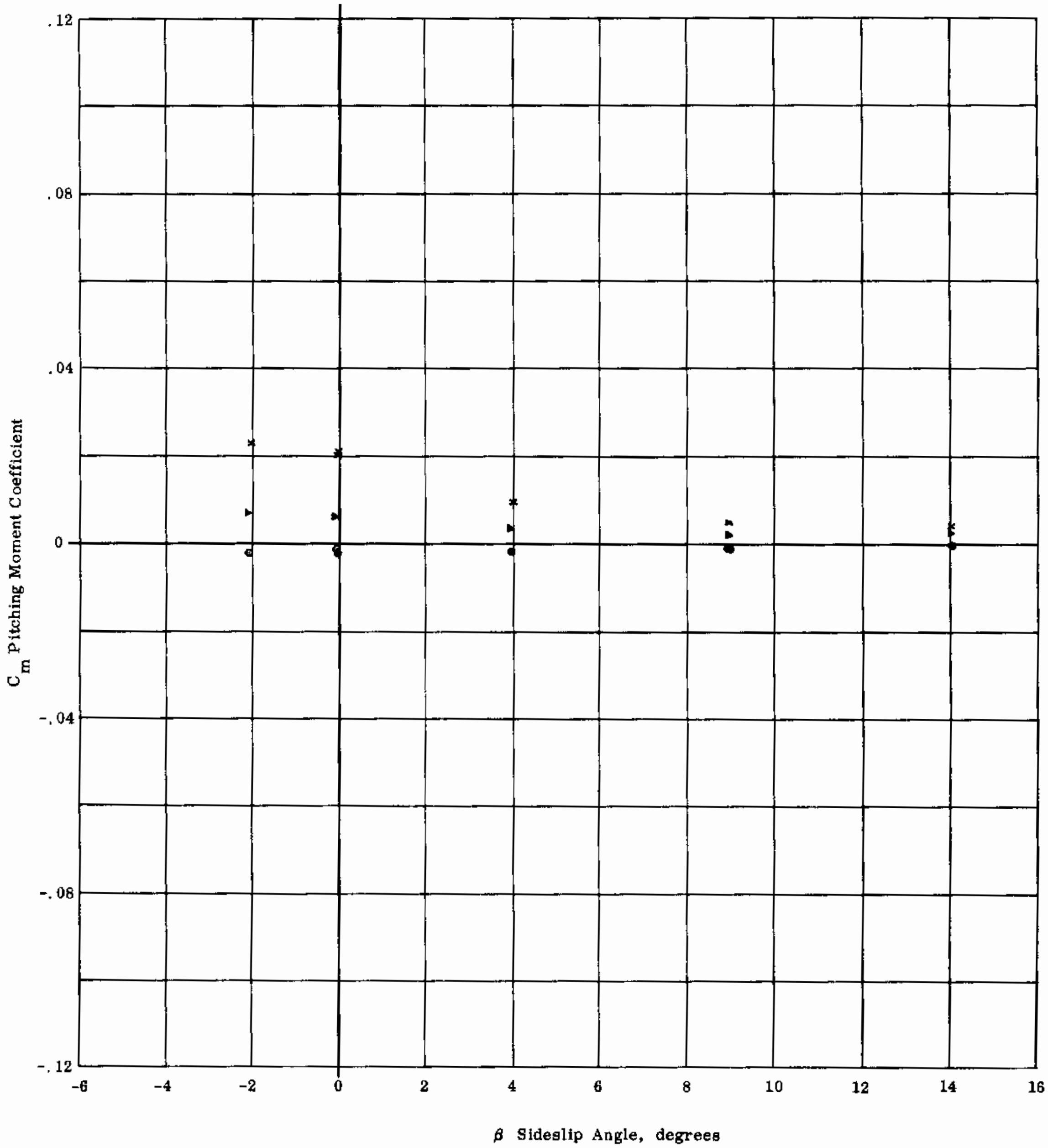

b) α = +7°

Fig. 5.6 Mach 5 Sideslip Polars for Basic Configuration with Upper Surface Port Flap Deflections (sheet 5 of 9)

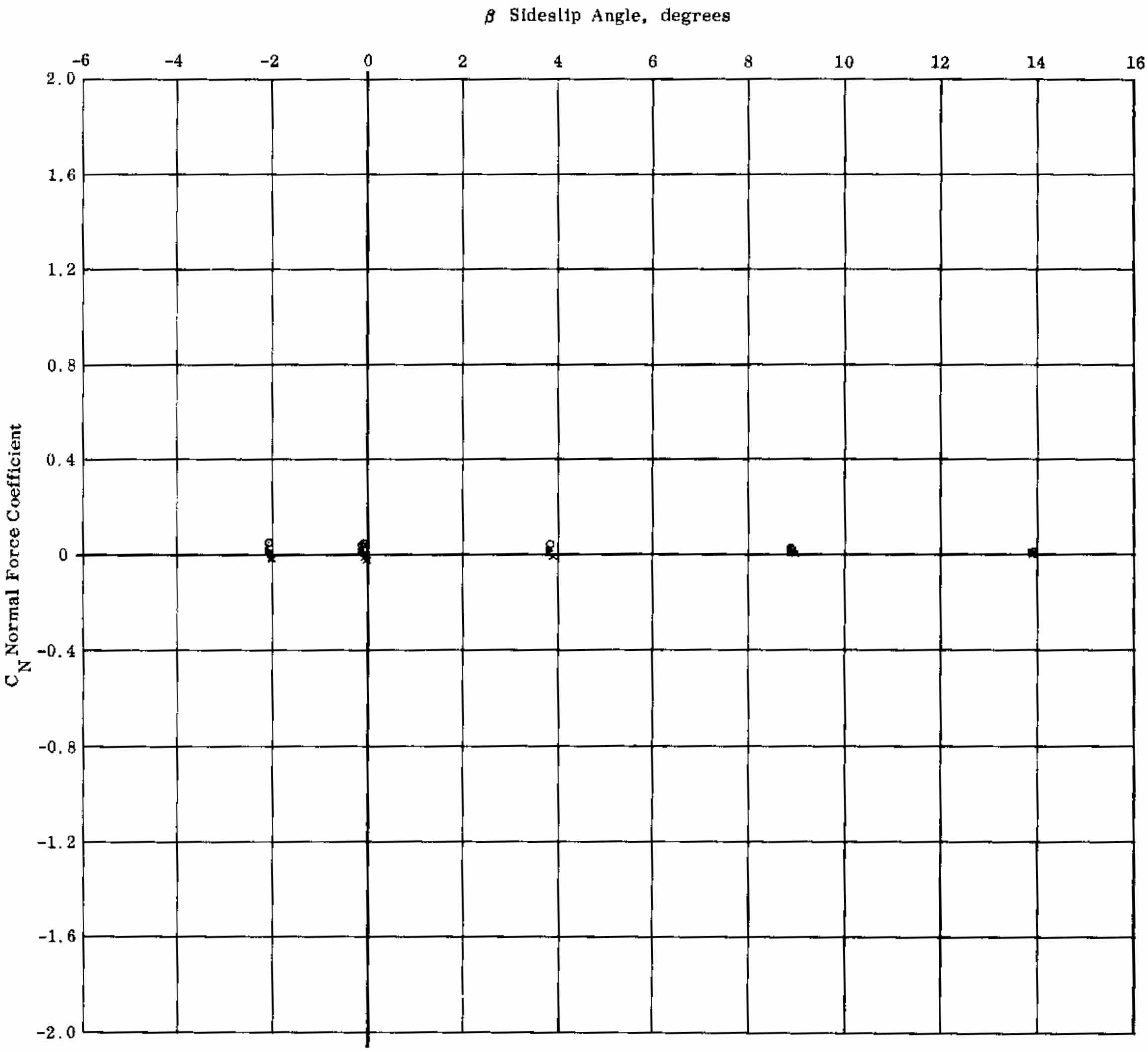

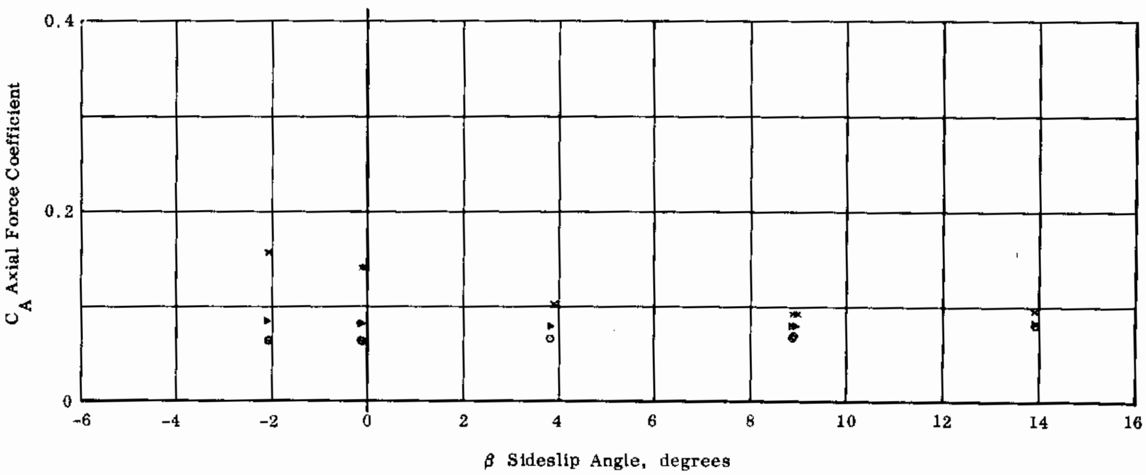

b) $\alpha = +7°$

Fig. 5.6 Mach 5 Sideslip Polars for Basic Configuration with Upper Surface Port Flap Deflections (sheet 6 of 9)

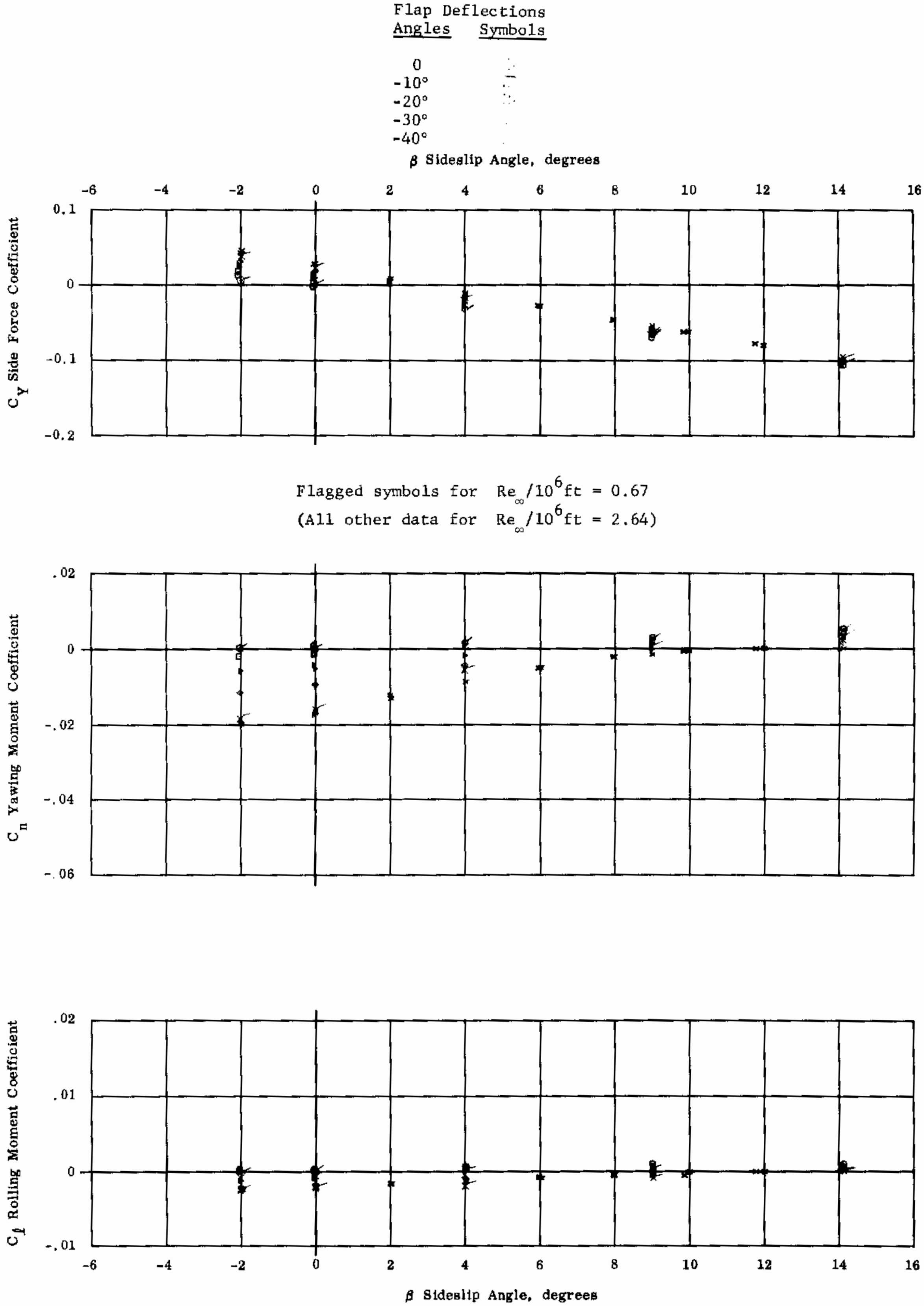

c) $\alpha = +14.3°$

Fig. 5.6 Mach 5 Sideslip Polars for Basic Configuration with Upper Surface Port Flap Deflections (sheet 7 of 9)

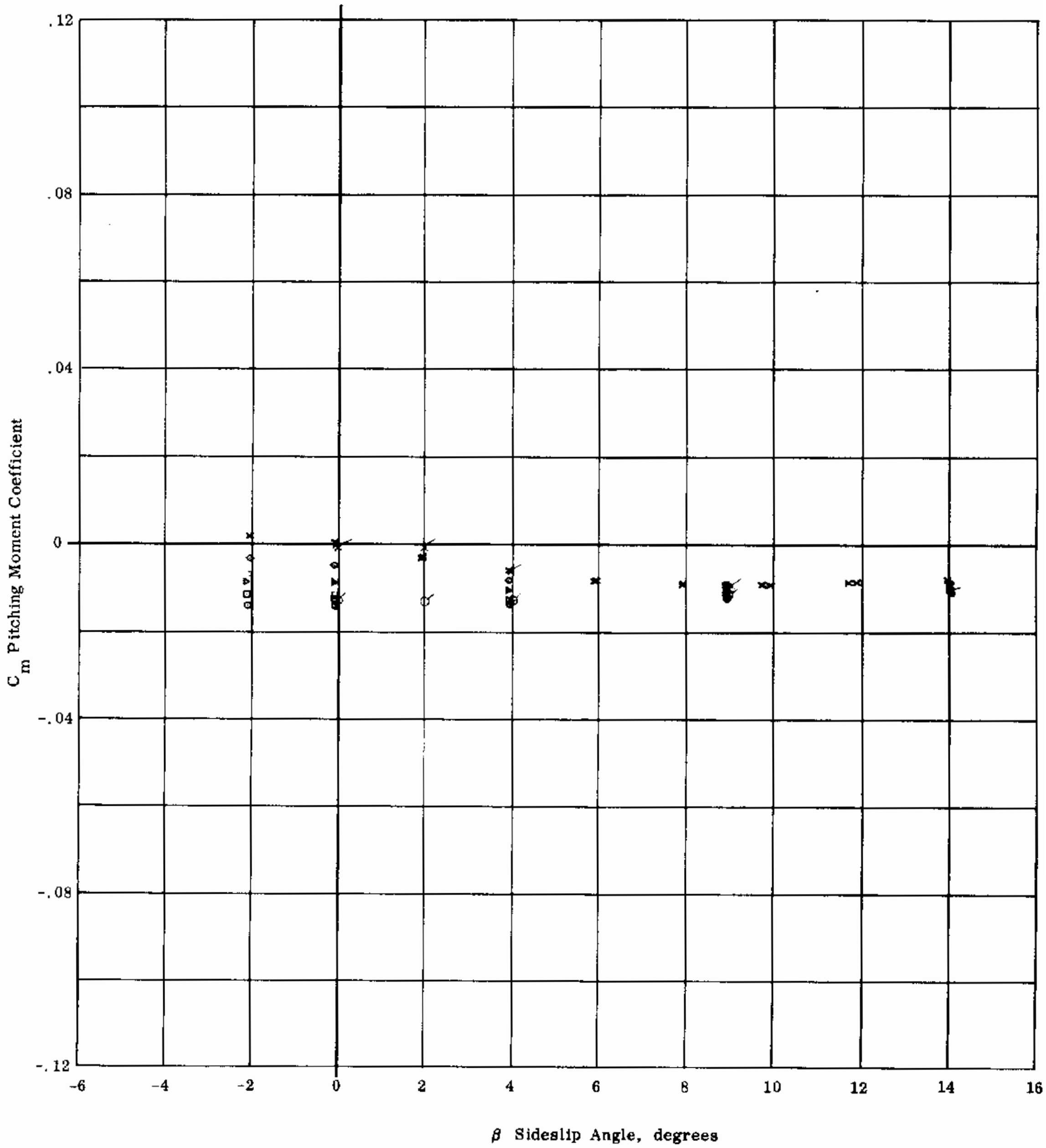

c) α = +14.3°

Fig. 5.6 Mach 5 Sideslip Polars for Basic Configuration with Upper Surface Port Flap Deflections (sheet 8 of 9)

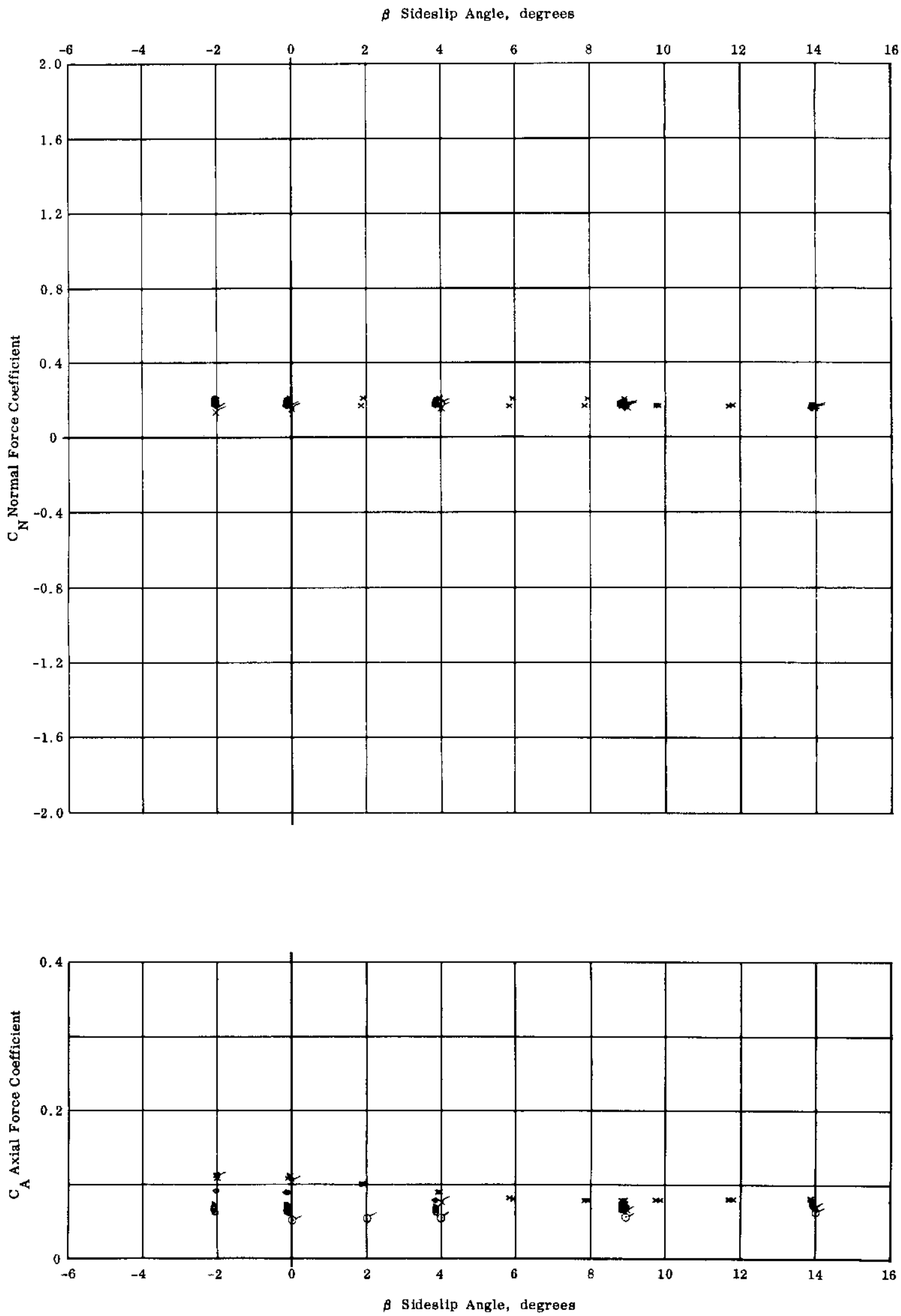

c) α = 14.3°

Fig. 5.6 Mach 5 Sideslip Polars for Basic Configuration with Upper Surface Port Flap Deflections (sheet 9 of 9)

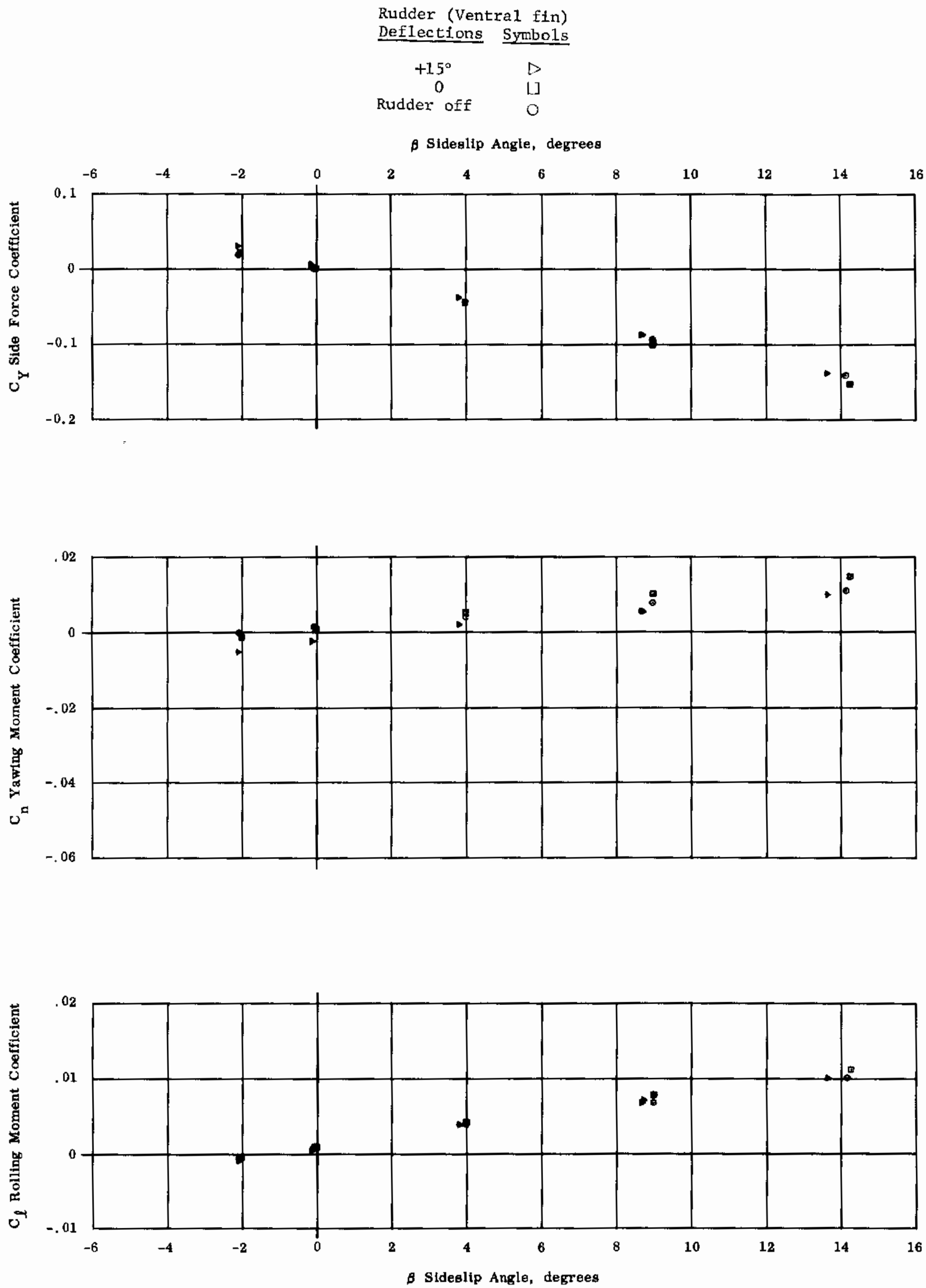

a) α = 0

Fig. 5.7 Mach 5 Sideslip Polars for Basic Configuration with Ventral Fin (sheet 1 of 6)

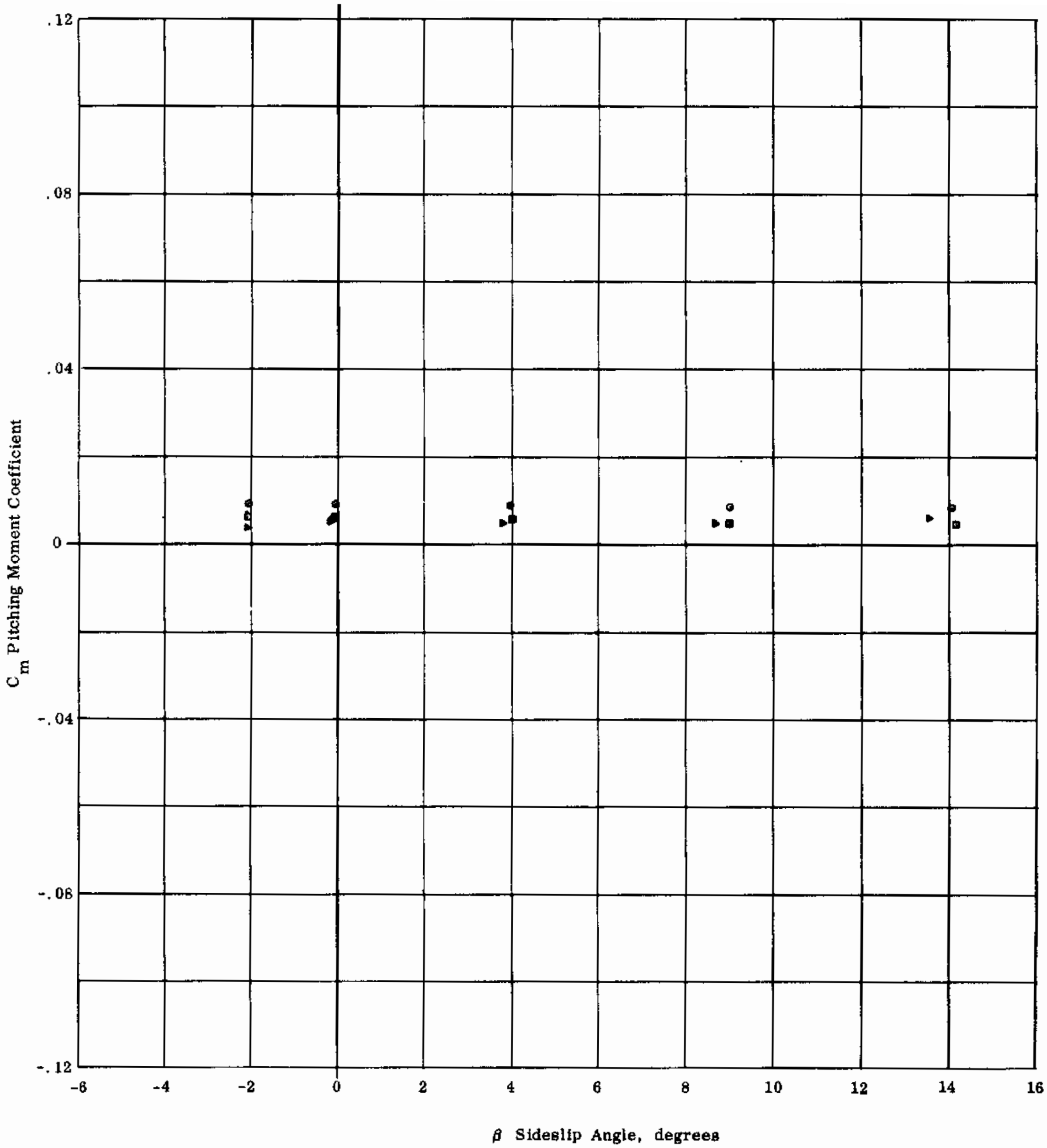

a) α = 0

Fig. 5.7 Mach 5 Sideslip Polars for Basic Configuration with Ventral Fin (sheet 2 of 6)

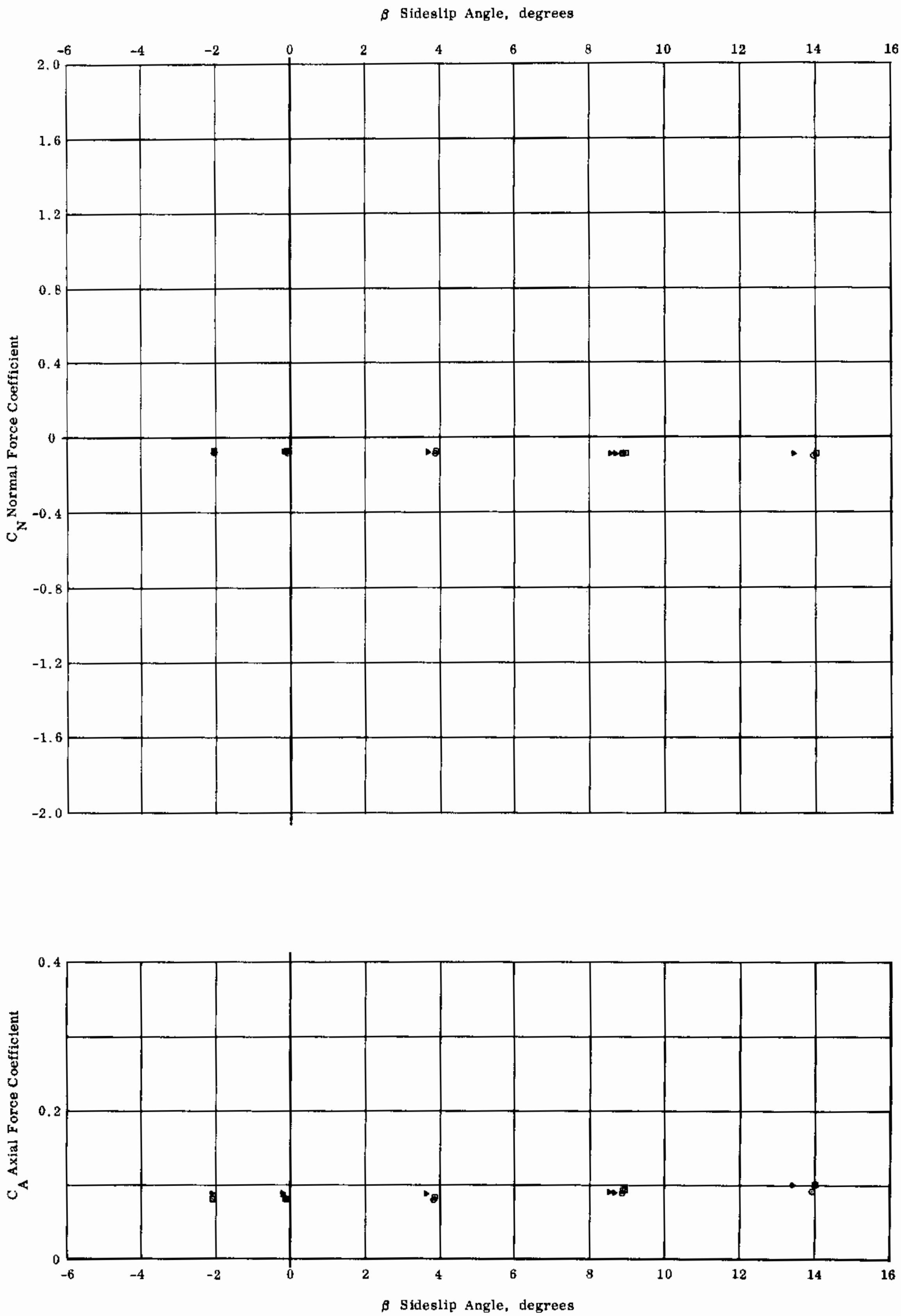

a) $\alpha = 0$

Fig. 5.7 Mach 5 Sideslip Polars for Basic Configuration with Ventral Fin (sheet 3 of 6)

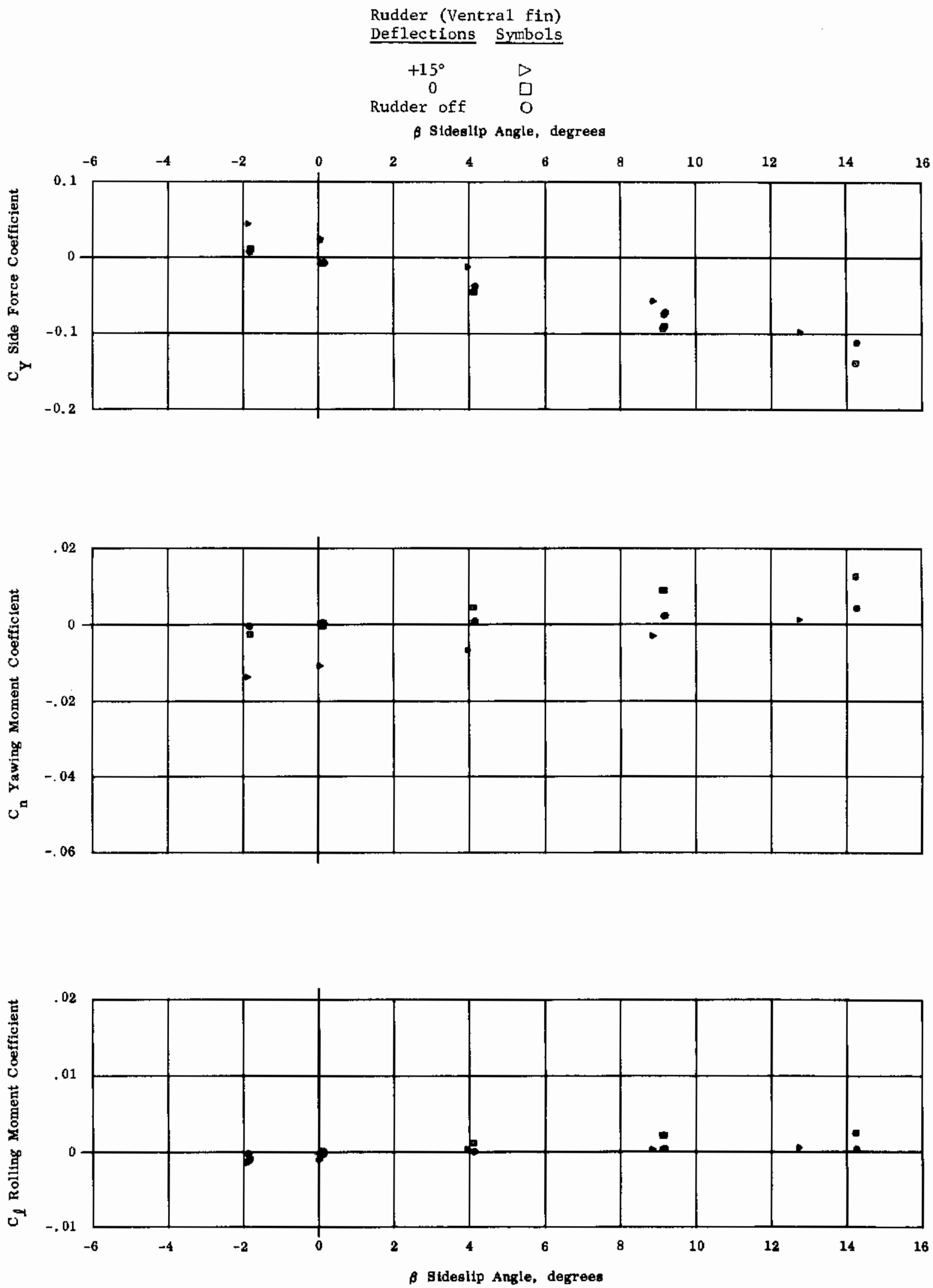

b) $\alpha = +14.3°$

Fig. 5.7 Mach 5 Sideslip Polars for Basic Configuration with Ventral Fin (sheet 4 of 6)

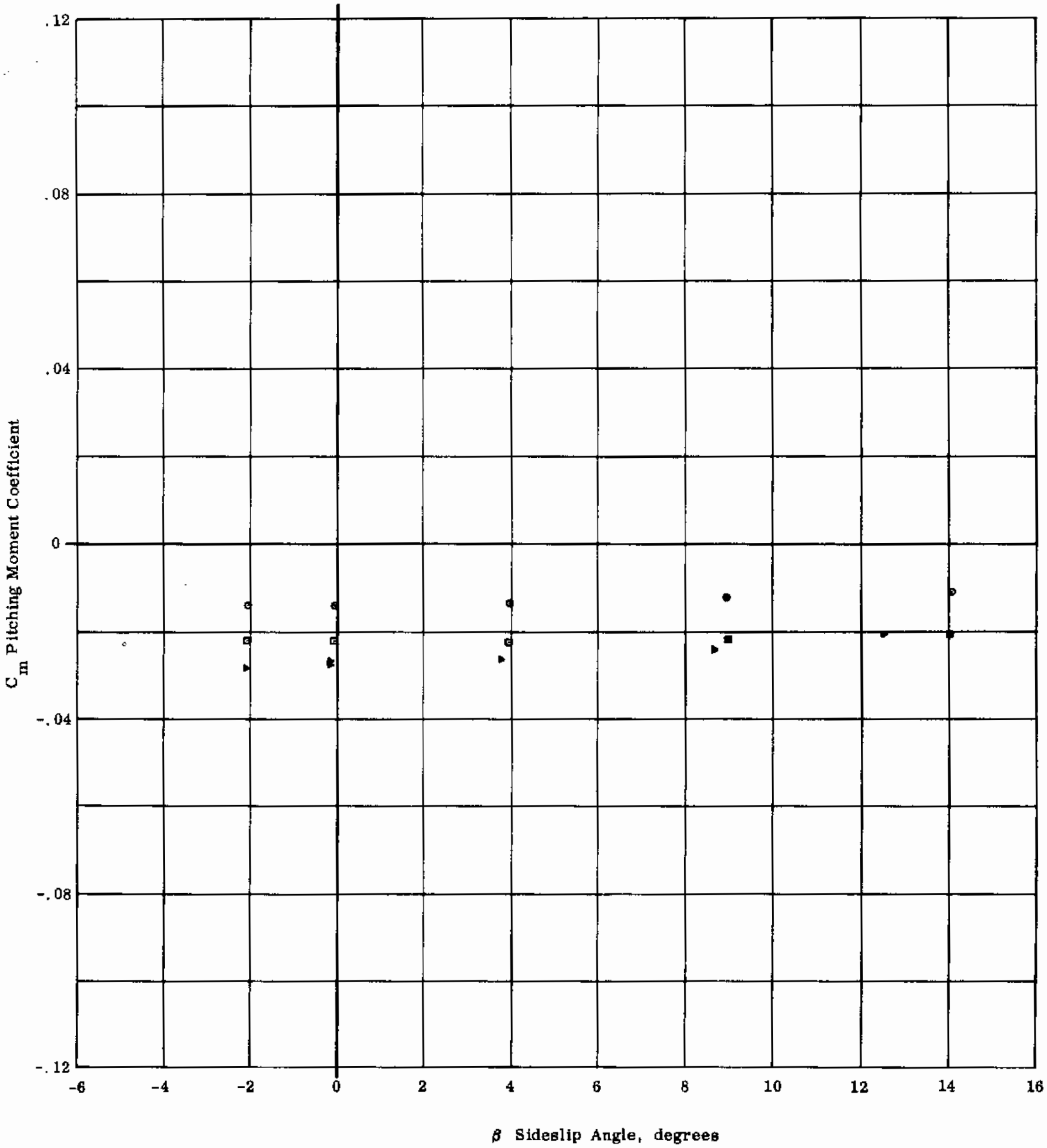

b) α = +14.3°

Fig. 5.7 Mach 5 Sideslip Polars for Basic Configuration with Ventral Fin (sheet 5 of 6)

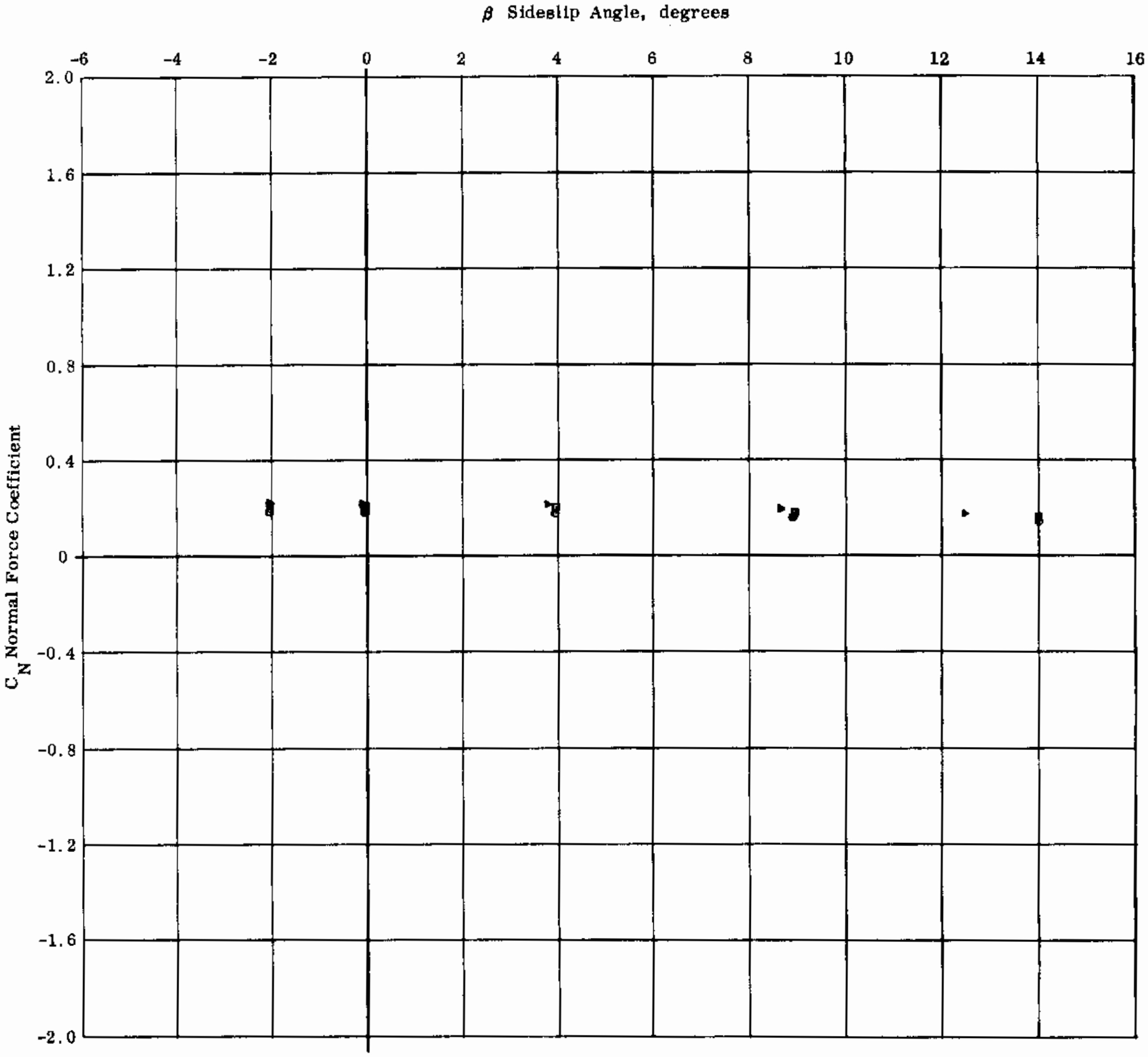

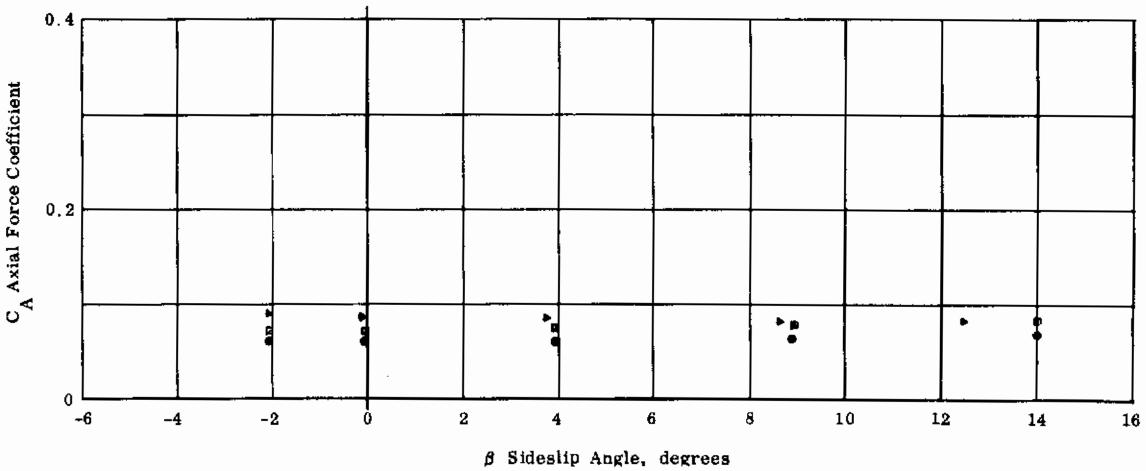

b) α = +14.3°

Fig. 5.7 Mach 5 Sideslip Polars for Basic Configuration with Ventral Fin (sheet 6 of 6)

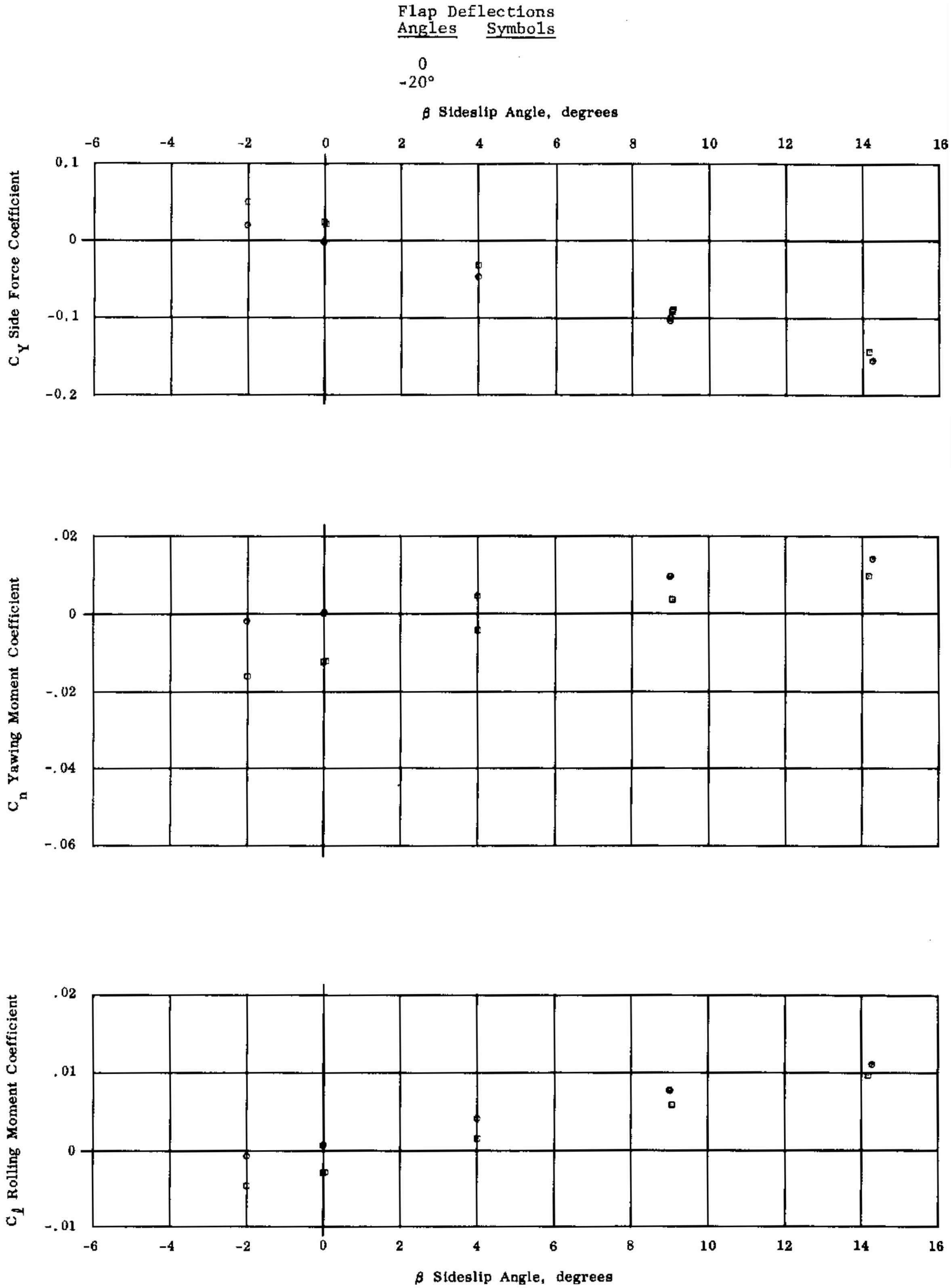

a) $\alpha = 0$ and $\delta_{fin} = 0$

Fig. 5.8 Mach 5 Sideslip Polars for Basic Configuration with Ventral Fin and Upper Surface Port Flap Deflections (sheet 1 of 12)

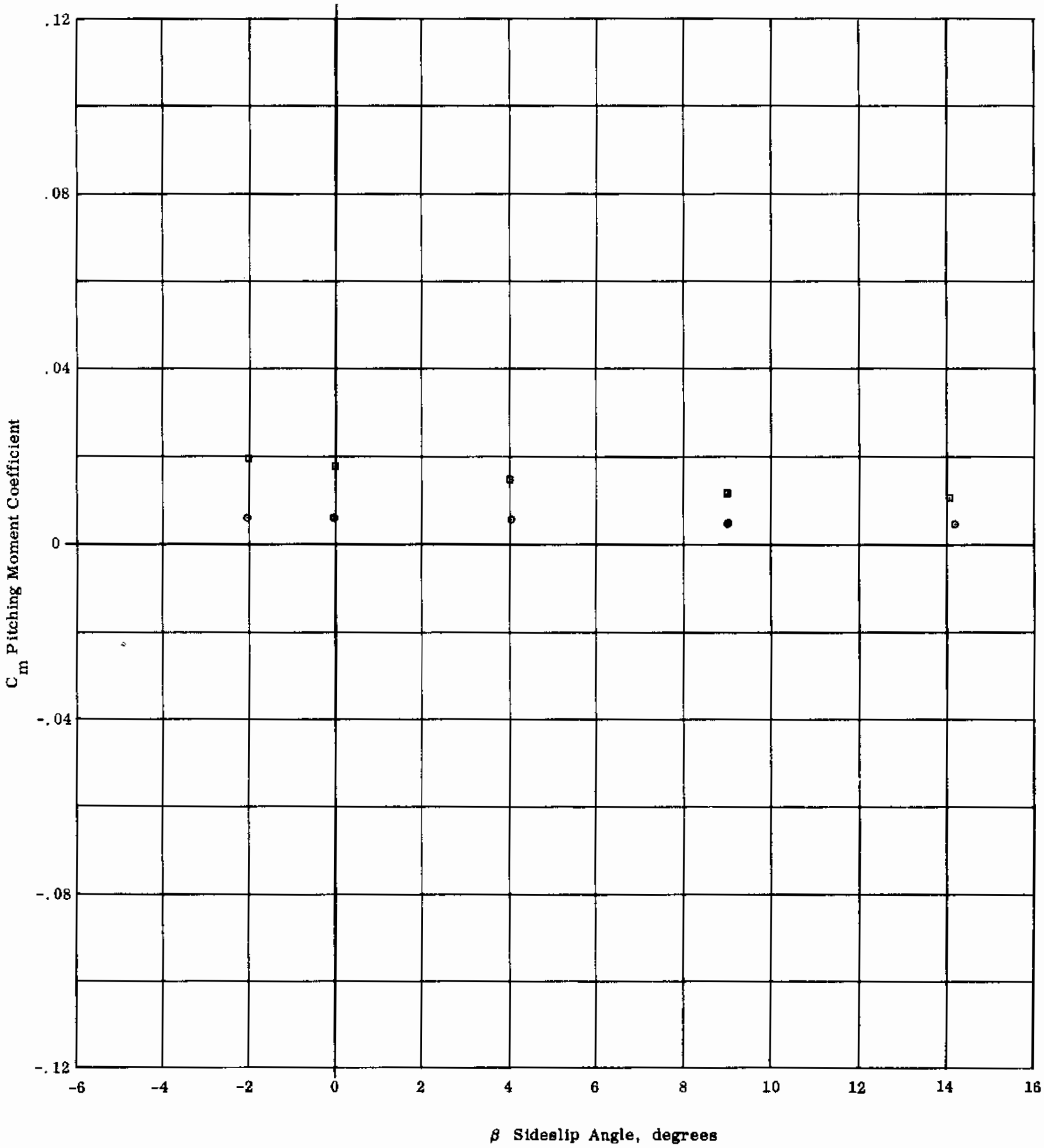

a) $\alpha = 0$ and $\delta_{fin} = 0$

Fig. 5.8 Mach 5 Sideslip Polars for Basic Configuration with Ventral Fin and Upper Surface Port Flap Deflections (sheet 2 of 12)

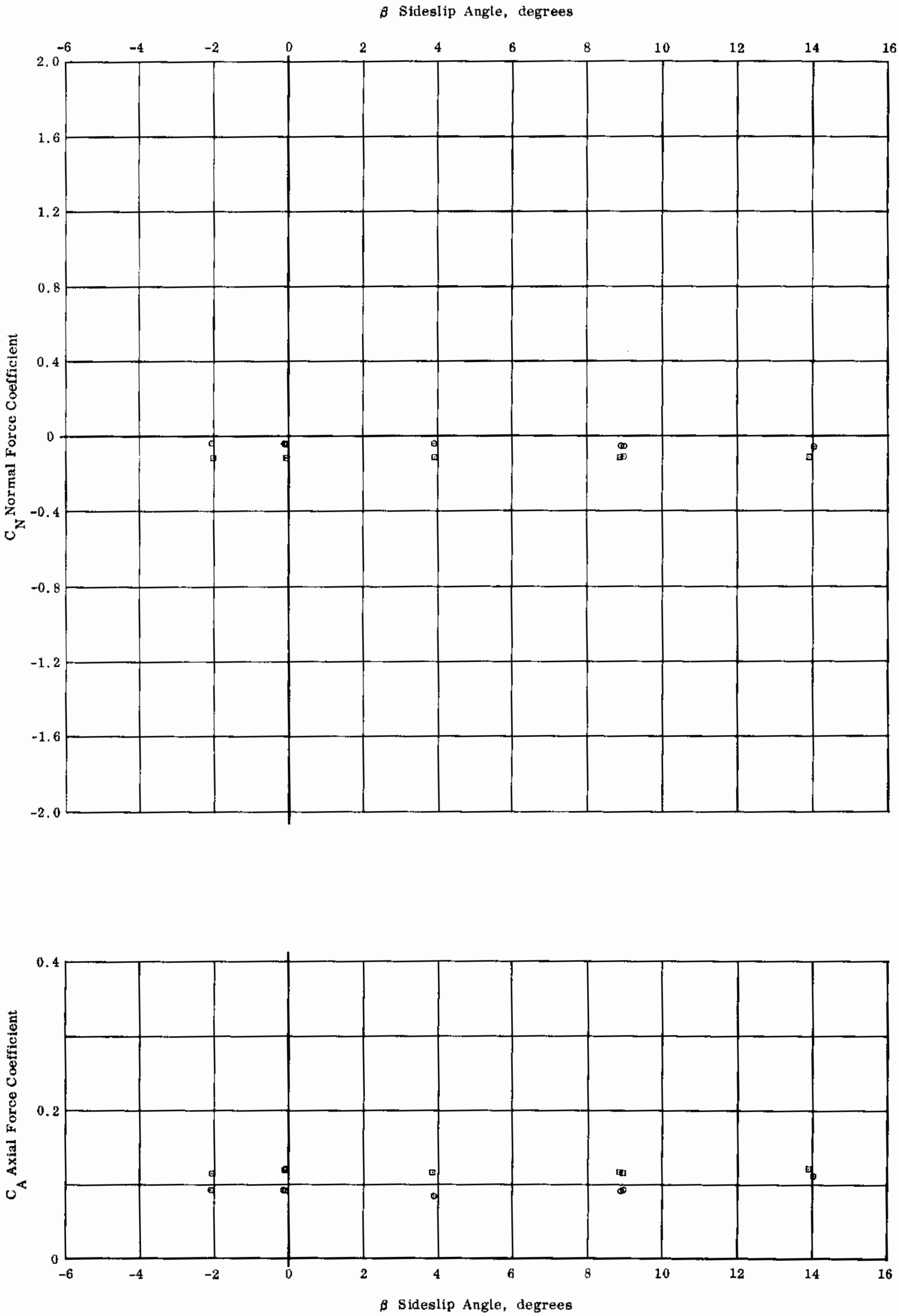

a) $\alpha = 0$ and $\delta_{fin} = 0$

Fig. 5.8 Mach 5 Sideslip Polars for Basic Configuration with Ventral Fin and Upper Surface Port Flap Deflections (sheet 3 of 12)

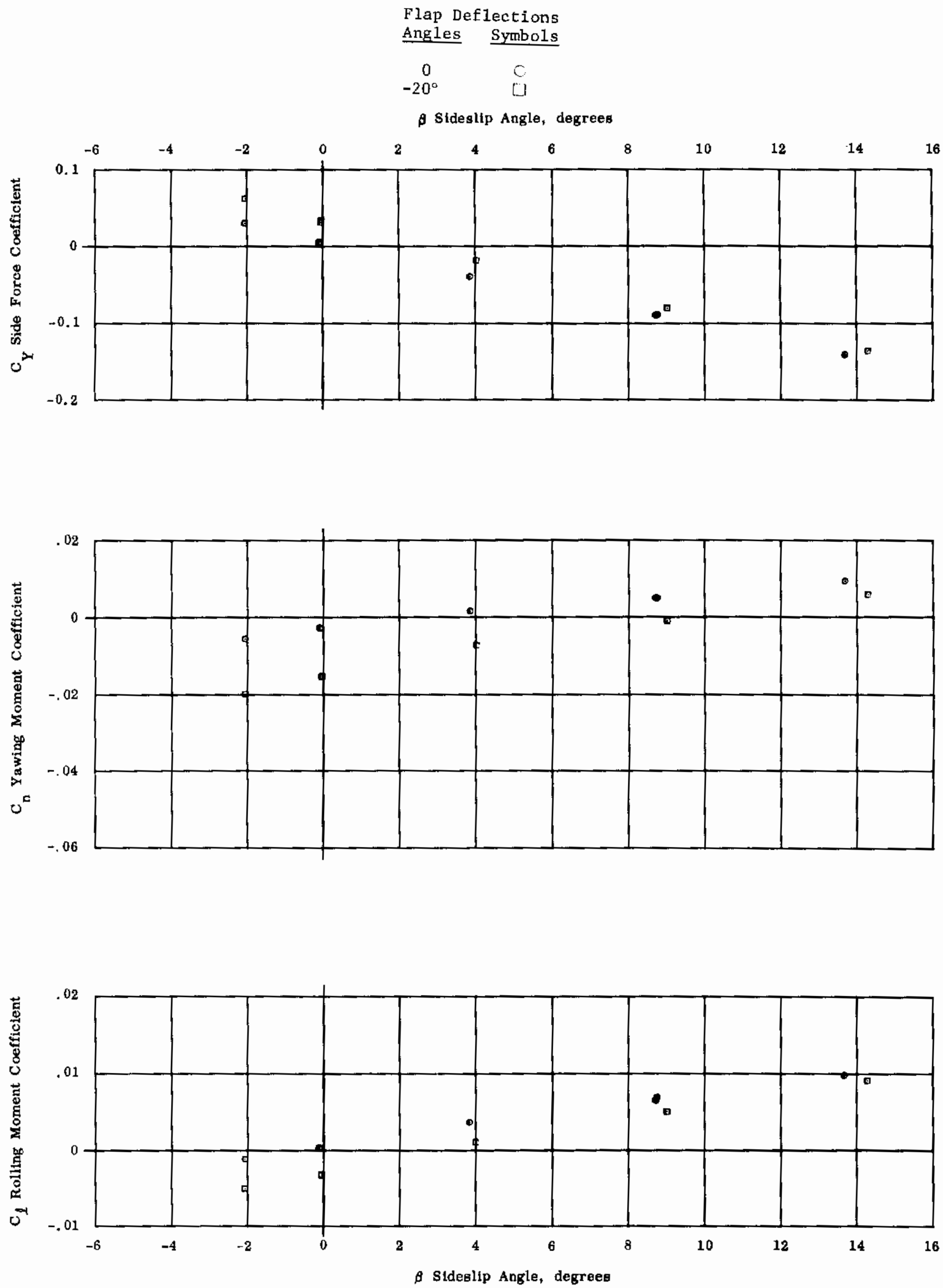

b) $\alpha = 0$ and $\delta_{fin} = +15°$

Fig. 5.8 Mach 5 Sideslip Polars for Basic Configuration with Ventral Fin and Upper Surface Port Flap Deflections (sheet 4 of 12)

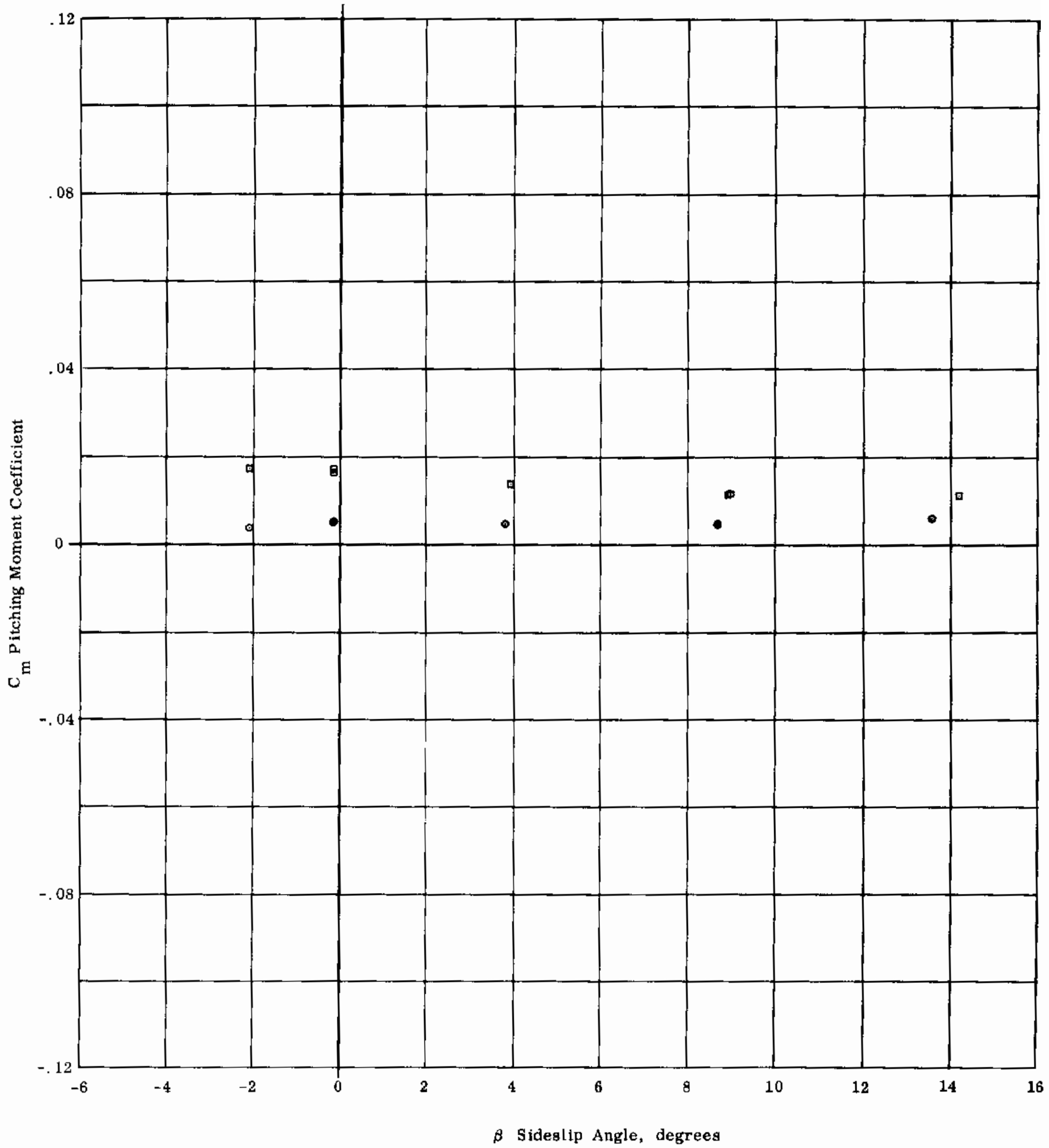

b) α = 0 and δ_{fin} = +15°

Fig. 5.8 Mach 5 Sideslip Polars for Basic Configuration with Ventral Fin and Upper Surface Port Flap Deflections (sheet 5 of 12)

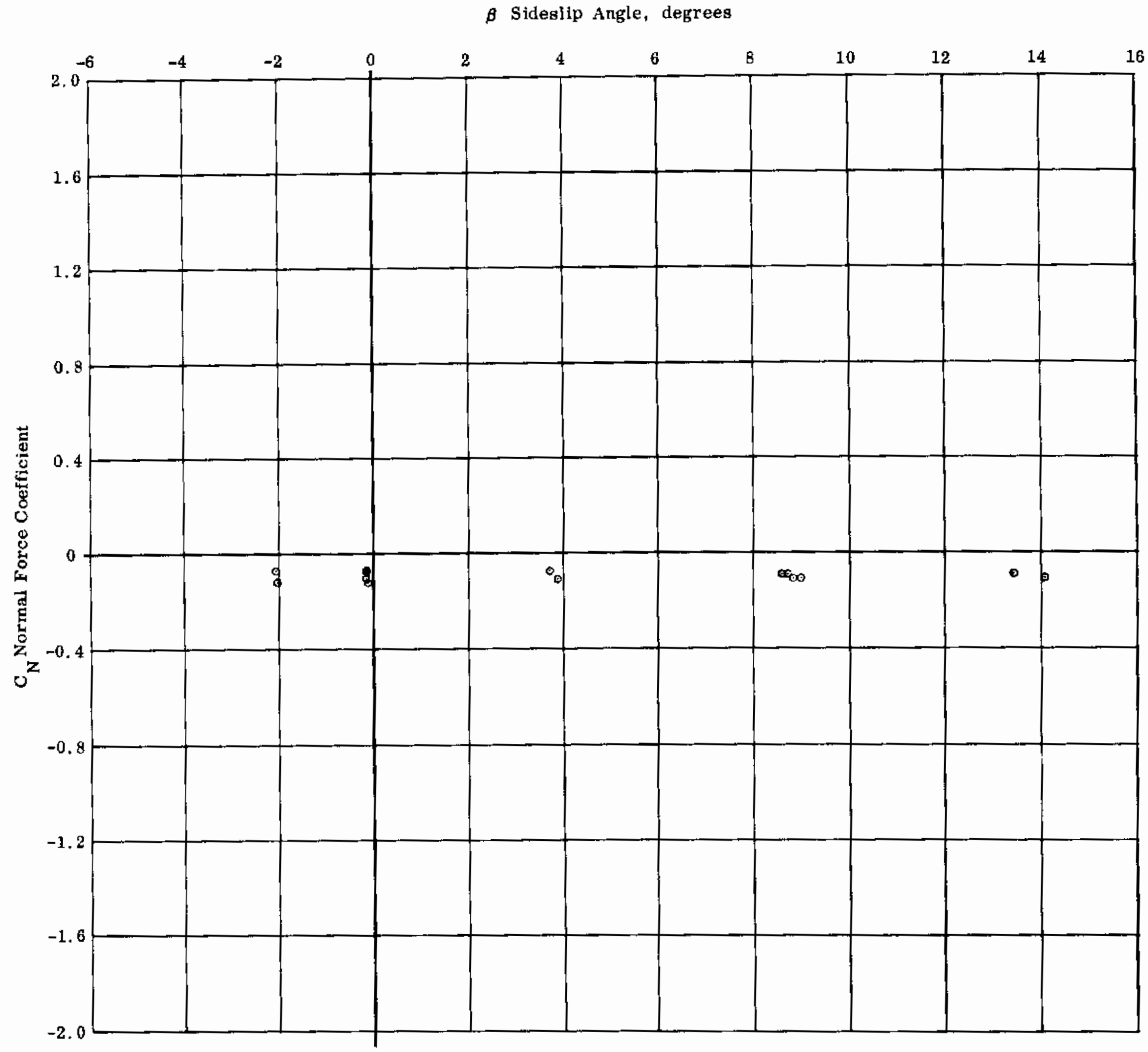

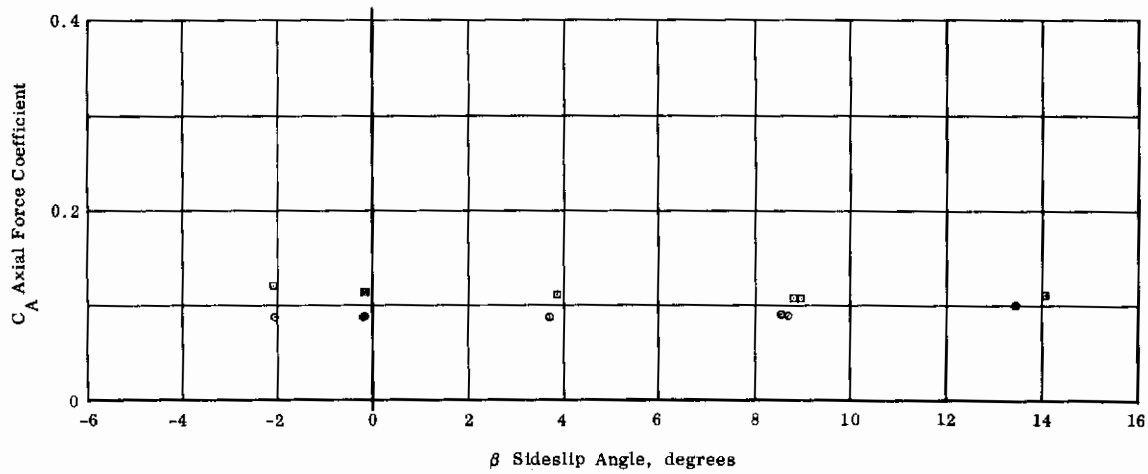

b) $\alpha = 0$ and $\delta_{fin} = +15°$

Fig. 5.8 Mach 5 Sideslip Polars for Basic Configuration with Ventral Fin and Upper Surface Port Flap Deflections (sheet 6 of 12)

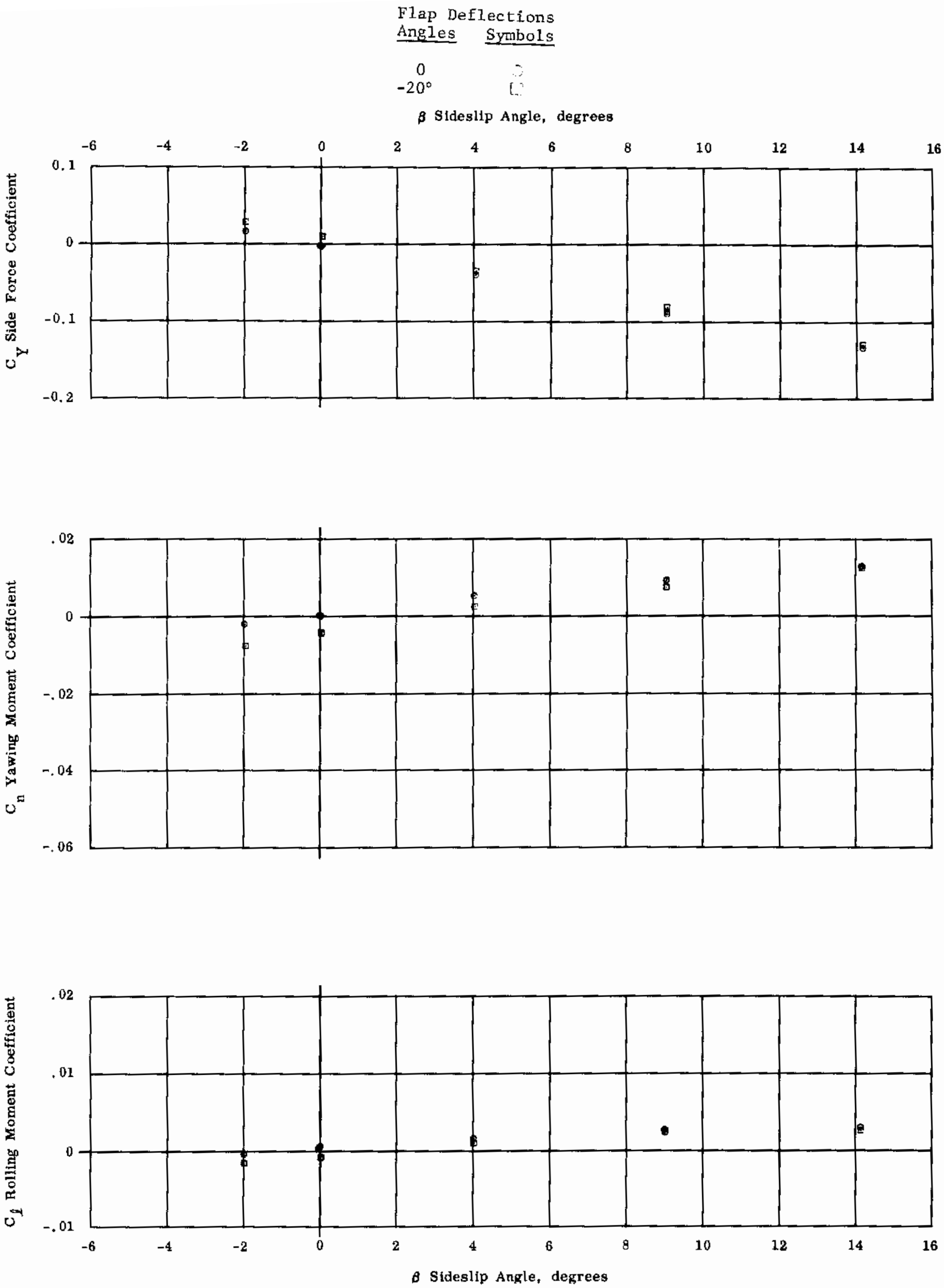

c) $\alpha = +14.3°$ and $\delta_{fin} = 0$

Fig. 5.8 Mach 5 Sideslip Polars for Basic Configuration with Ventral Fin and Upper Surface Port Flap Deflections (sheet 7 of 12)

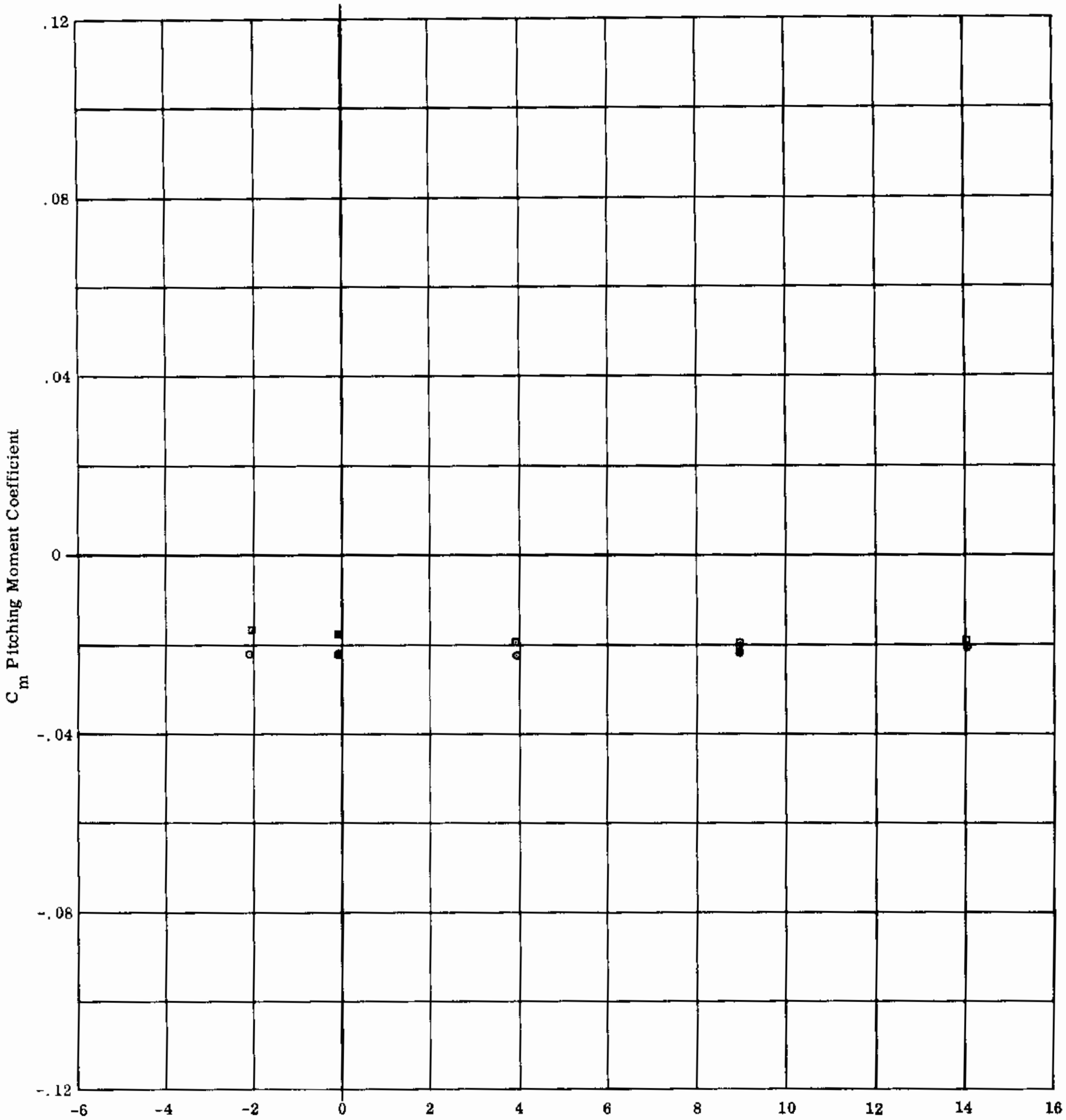

c) $\alpha = +14.3°$ and $\delta_{fin} = 0$

Fig. 5.8 Mach 5 Sideslip Polars for Basic Configuration with Ventral Fin and Upper Surface Port Flap Deflections (sheet 8 of 12)

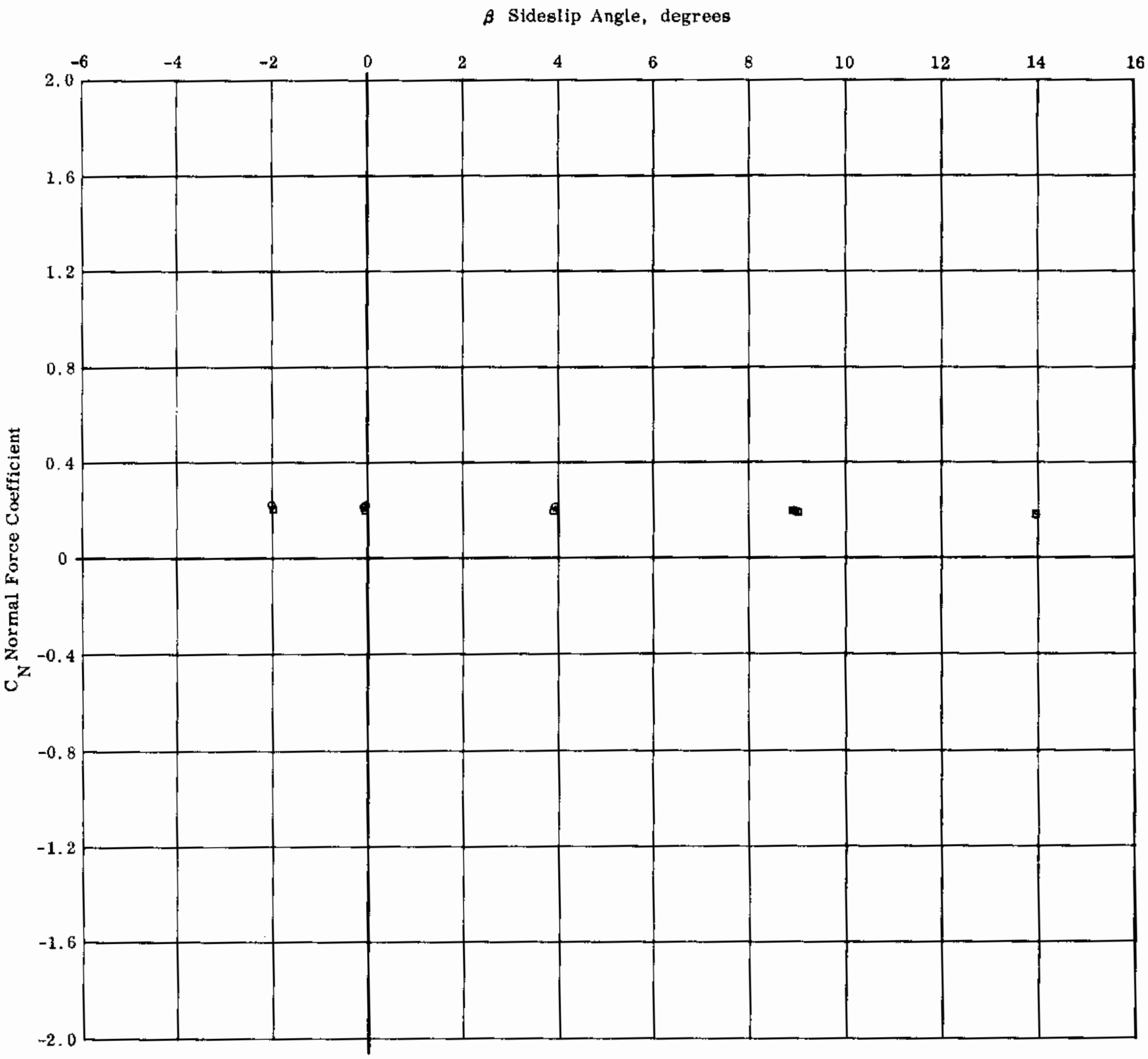

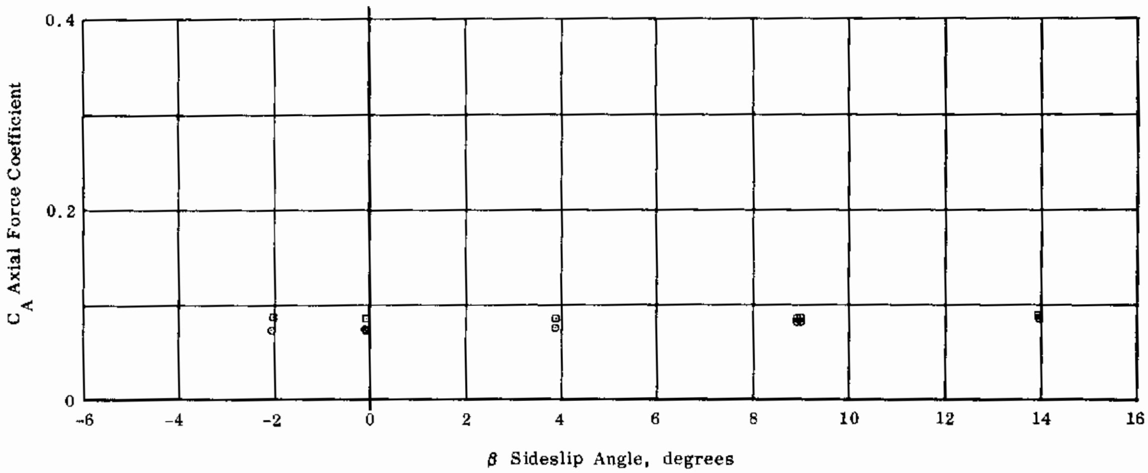

c) $\alpha = +14.3°$ and $\delta_{fin} = 0$

Fig. 5.8 Mach 5 Sideslip Polars for Basic Configuration with Ventral Fin and Upper Surface Port Flap Deflections (sheet 9 of 12)

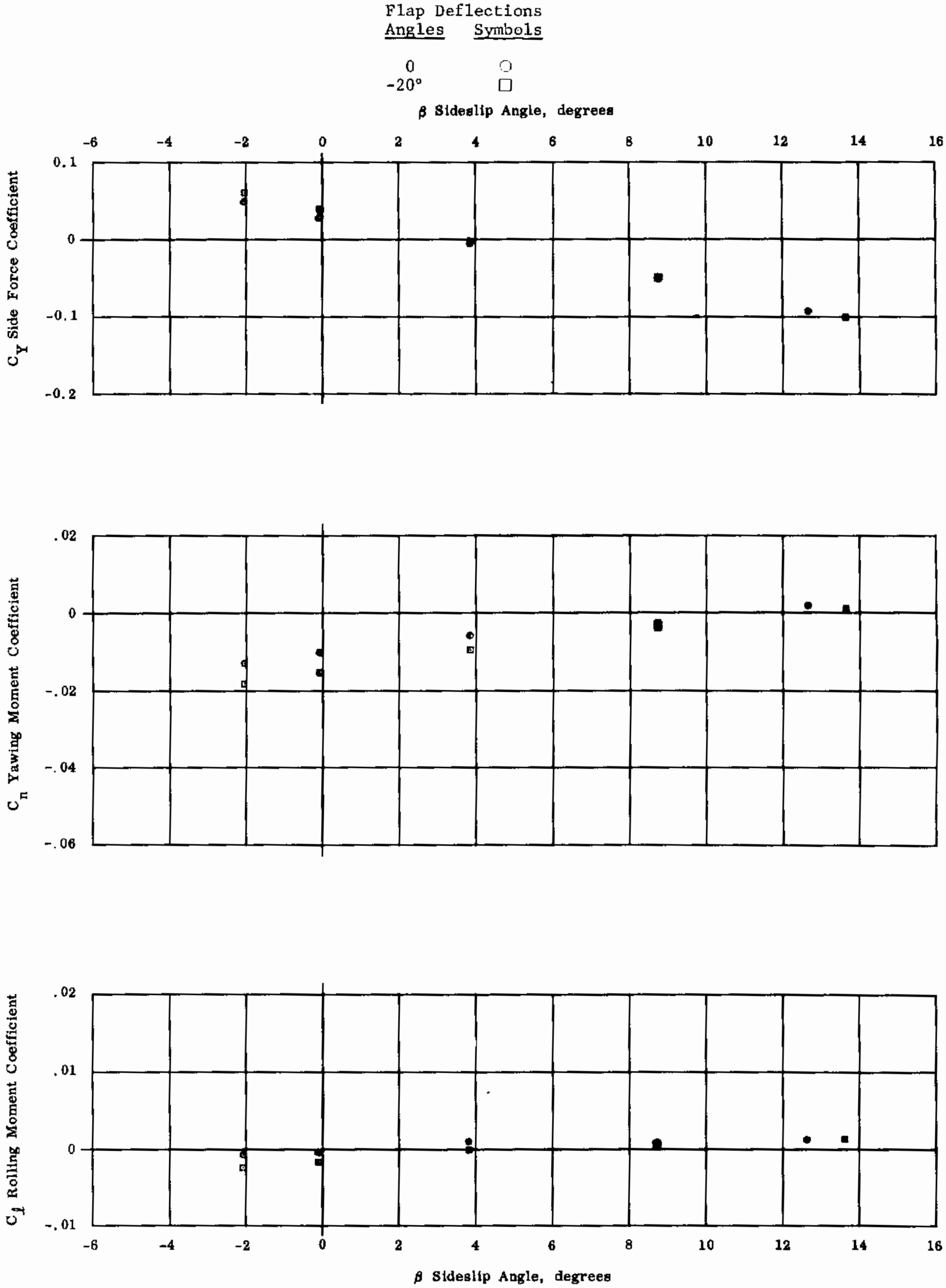

d) $\alpha = +14.3°$ and $\delta_{fin} = +15°$

Fig. 5.8 Mach 5 Sideslip Polars for Basic Configuration with Ventral Fin and Upper Surface Port Flap Deflections (sheet 10 of 12)

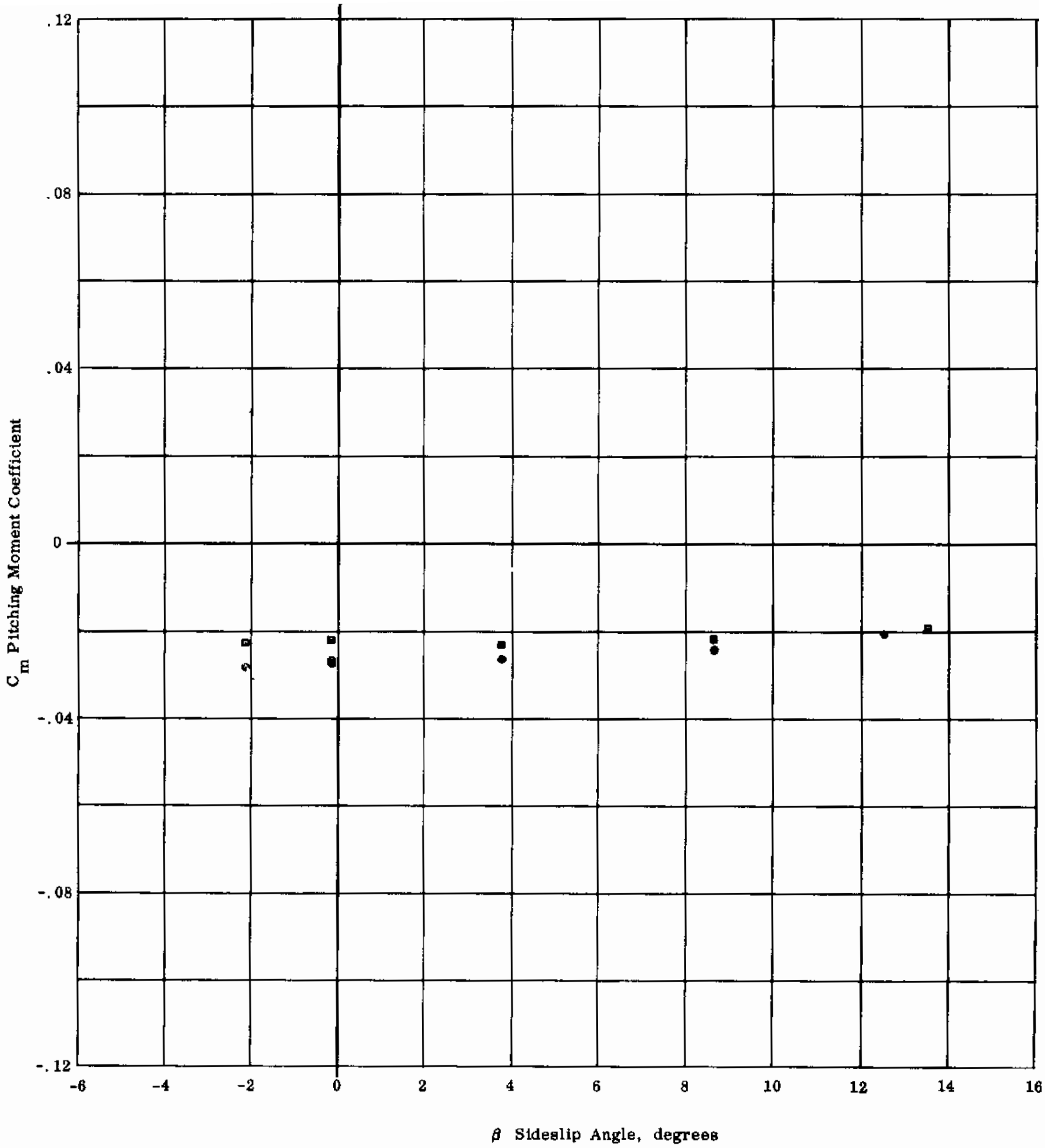

d) $\alpha = +14.3°$ and $\delta_{fin} = +15°$

Fig. 5.8 Mach 5 Sideslip Polars for Basic Configuration with Ventral Fin and Upper Surface Port Flap Deflections (sheet 11 of 12)

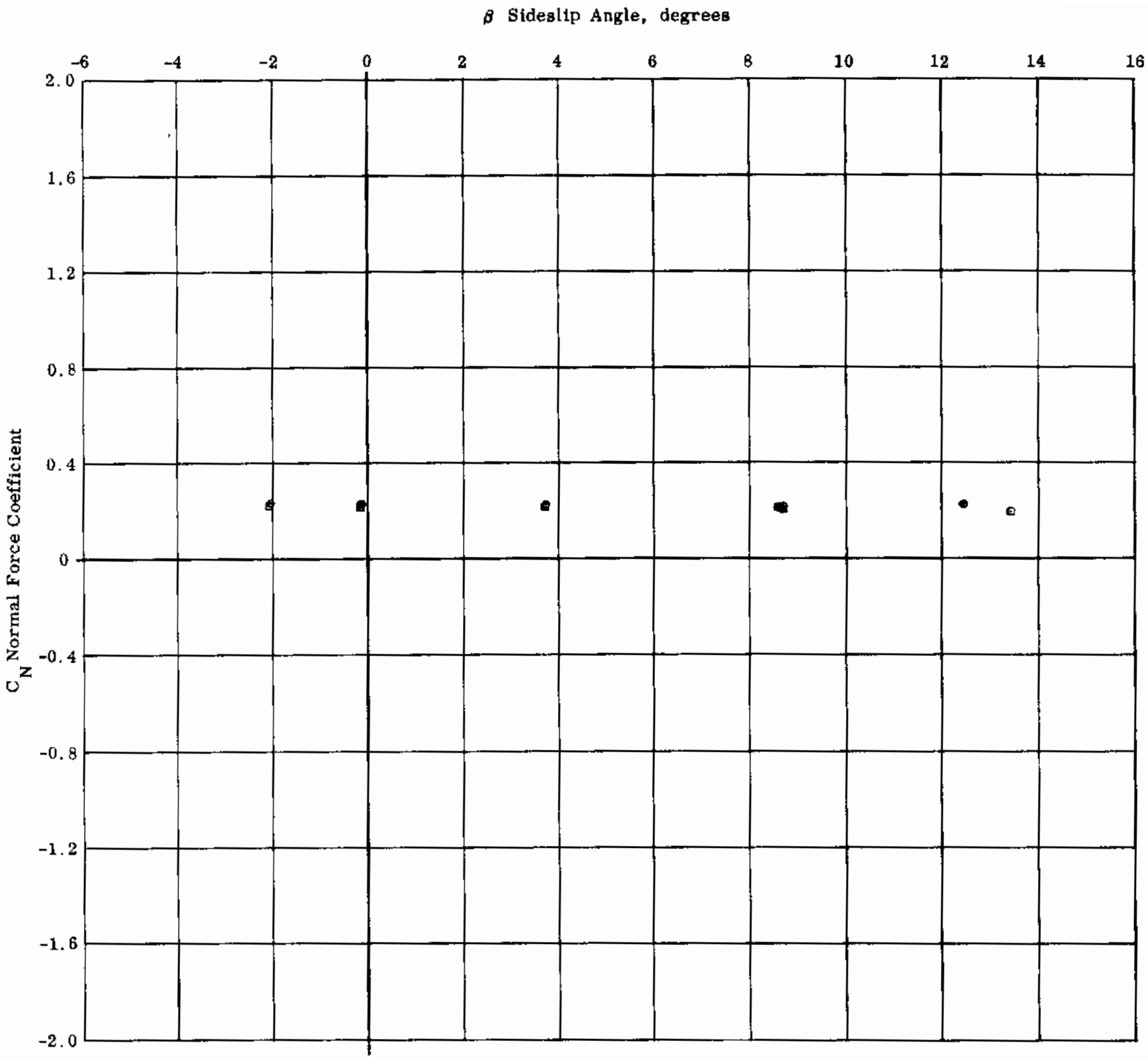

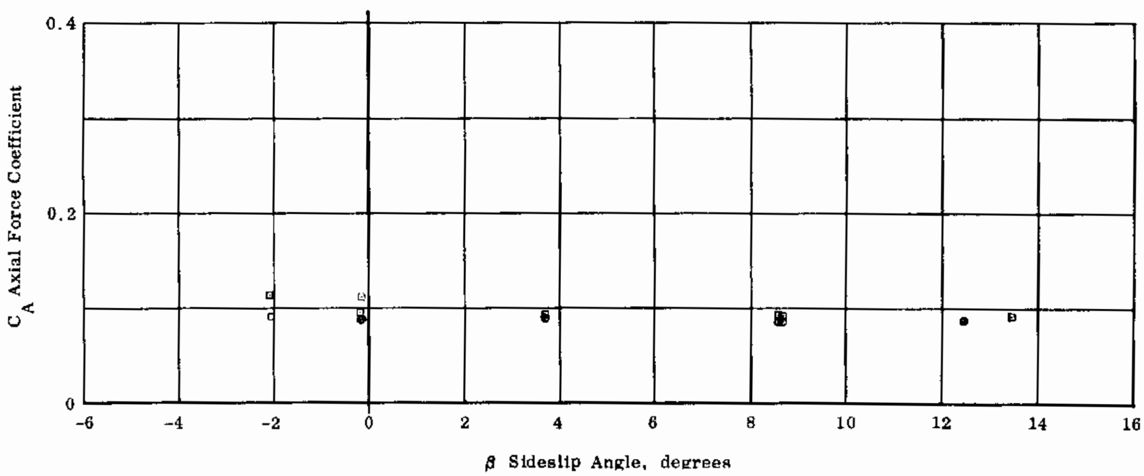

d) α = +14.3° and δ_{fin} = +15°

Fig. 5.8 Mach 5 Sideslip Polars for Basic Configuration with Ventral Fin and Upper Surface Port Flap Deflections (sheet 12 of 12)

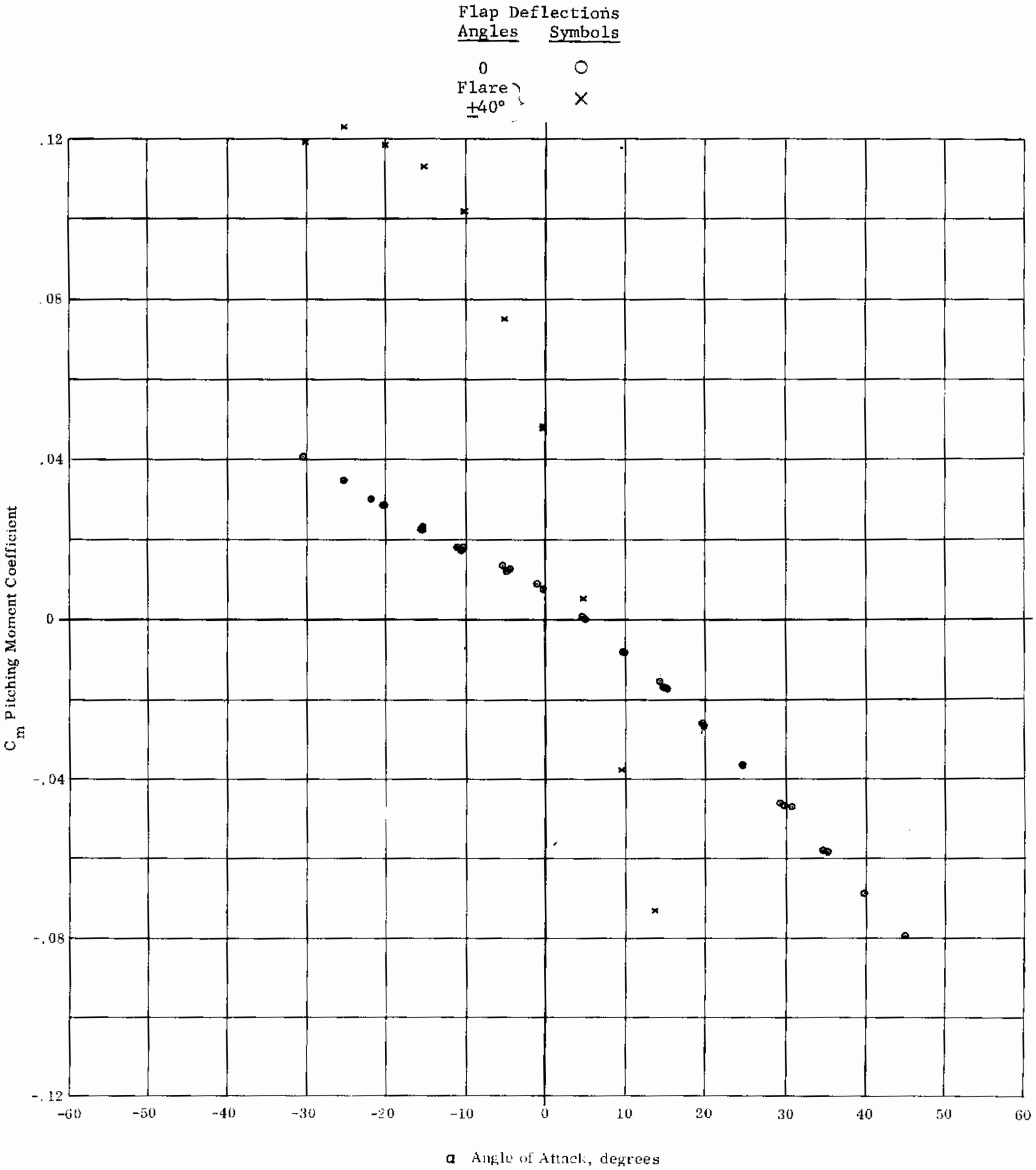

Fig. 5.9 Mach 5 Pitch Polars for Basic Configuration with All Flaps Deflected (sheet 1 of 2)

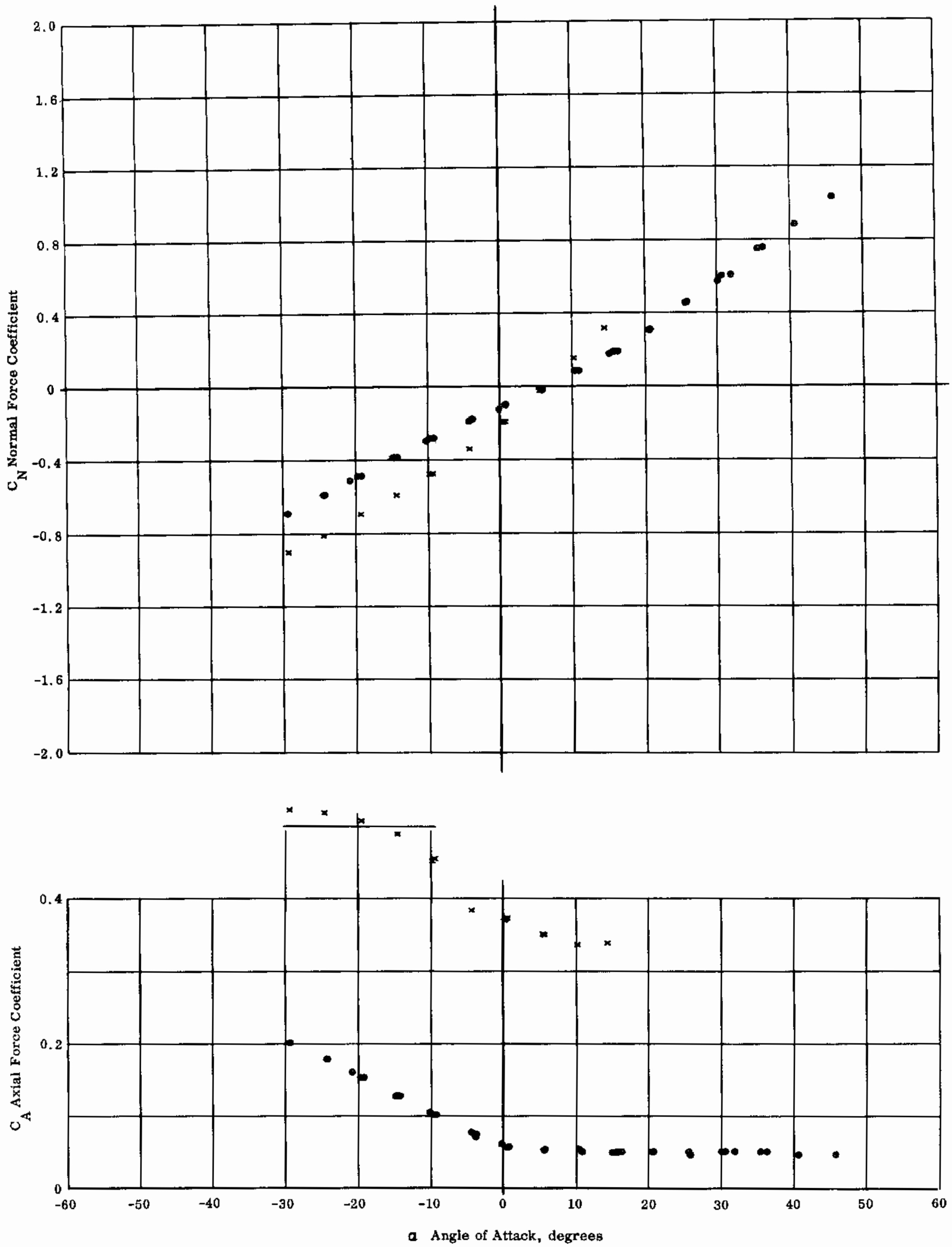

Fig. 5.9 Mach 5 Pitch Polars for Basic Configuration with All Flaps Deflected (sheet 2 of 2)

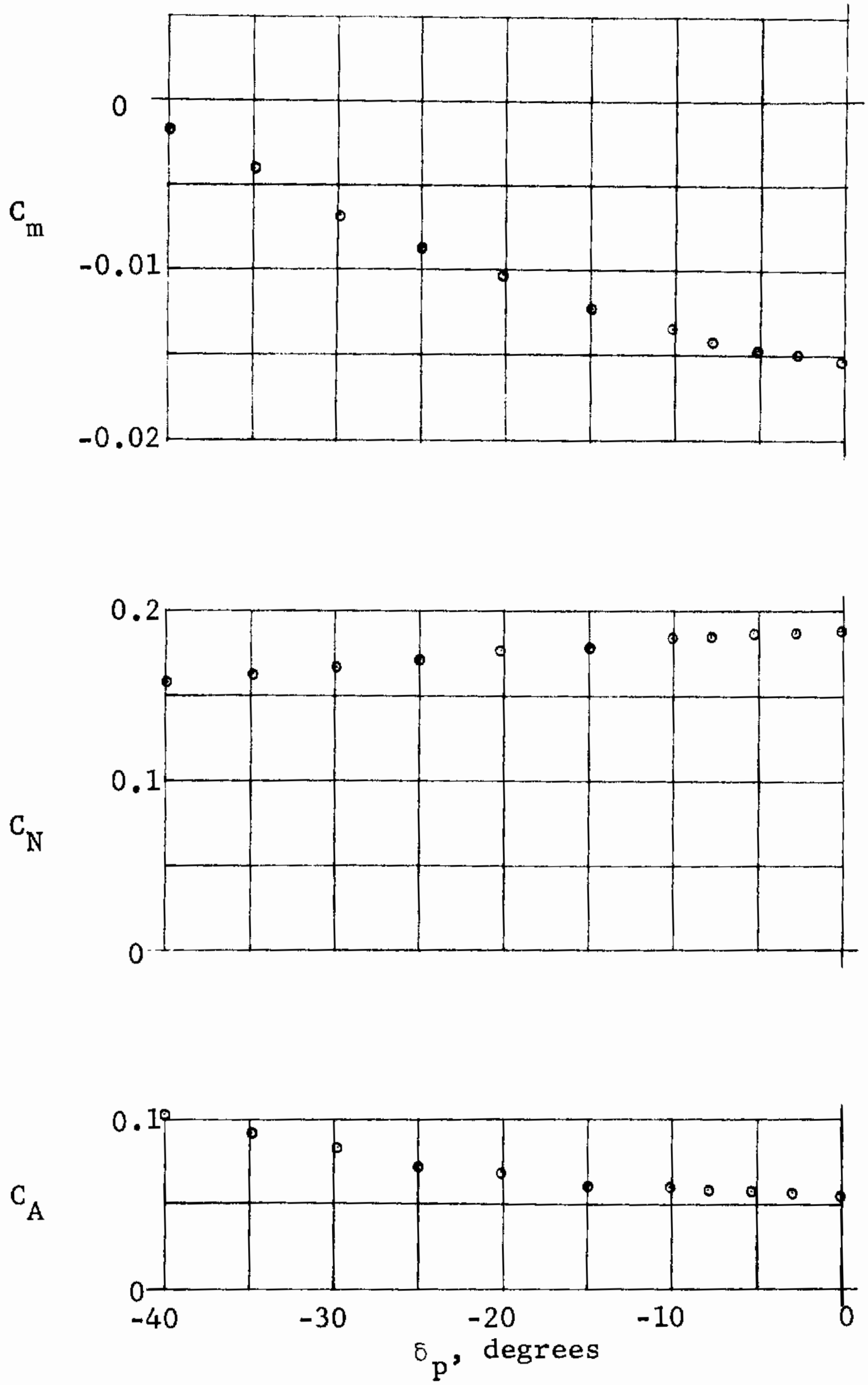

Fig. 5.10 Effects of Upper Surface Port Flap Deflections on Mach 5 Force and Moment Coefficients for $\alpha = +14.3°$ and $\beta = 0$ (sheet 1 of 2)

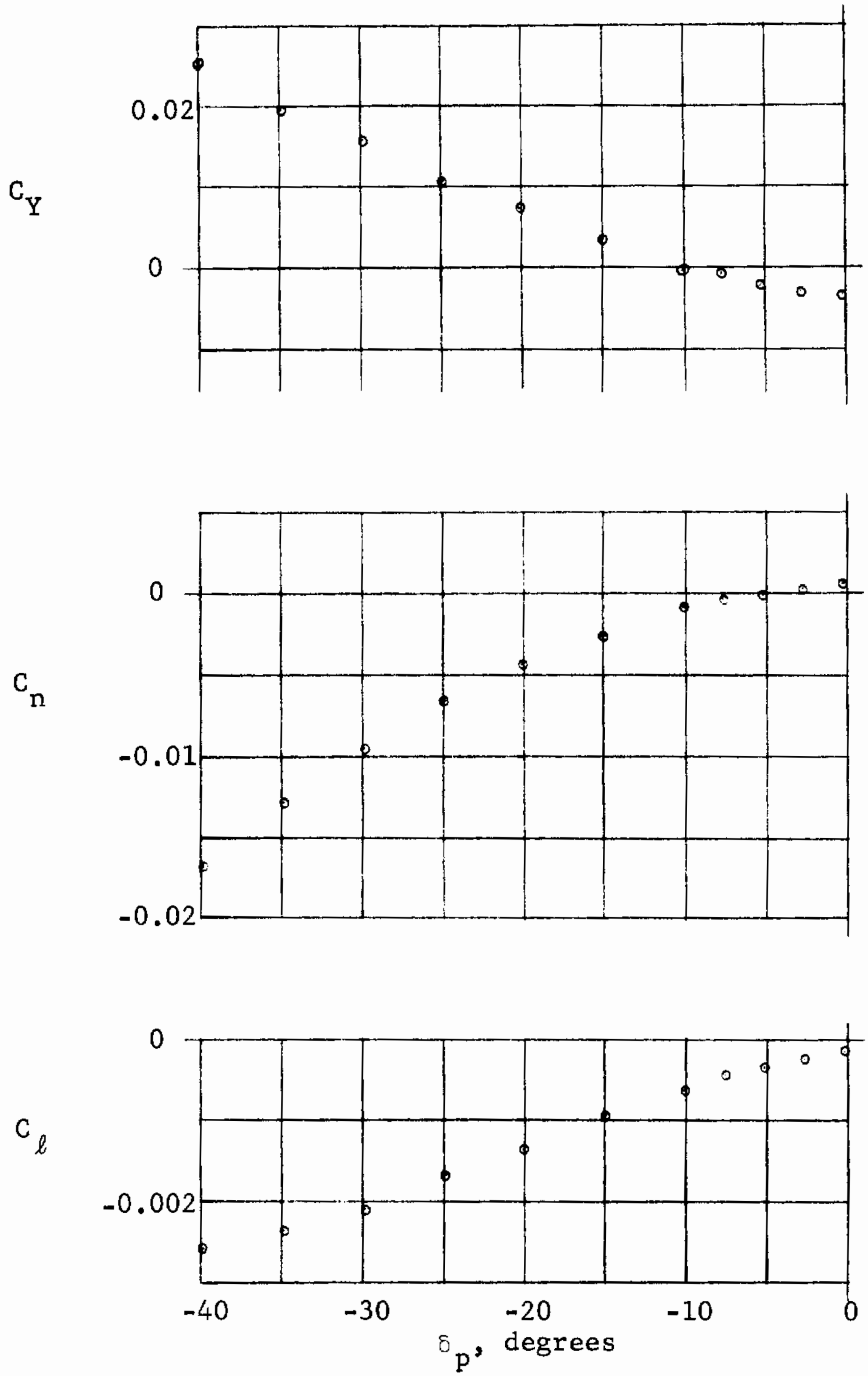

Fig. 5.10 Effects of Upper Surface Port Flap Deflections on Mach 5 Force and Moment Coefficients for $\alpha = +14.3°$ and $\beta = 0$ (sheet 2 of 2)

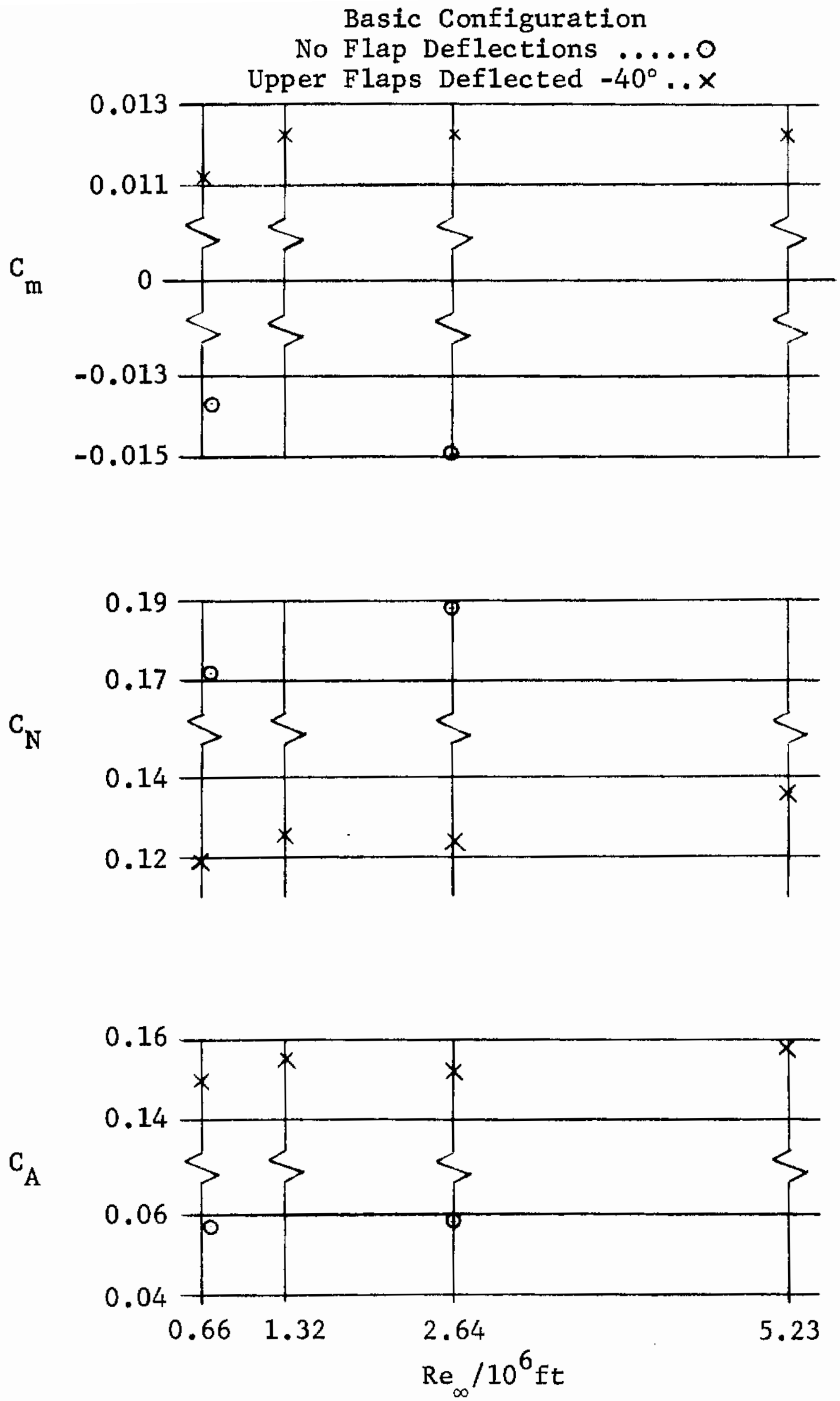

Fig. 5.11 Reynolds Number Effects on Mach 5 Force and Moment Coefficients for $\alpha = +14.3°$ and $\beta = 0$

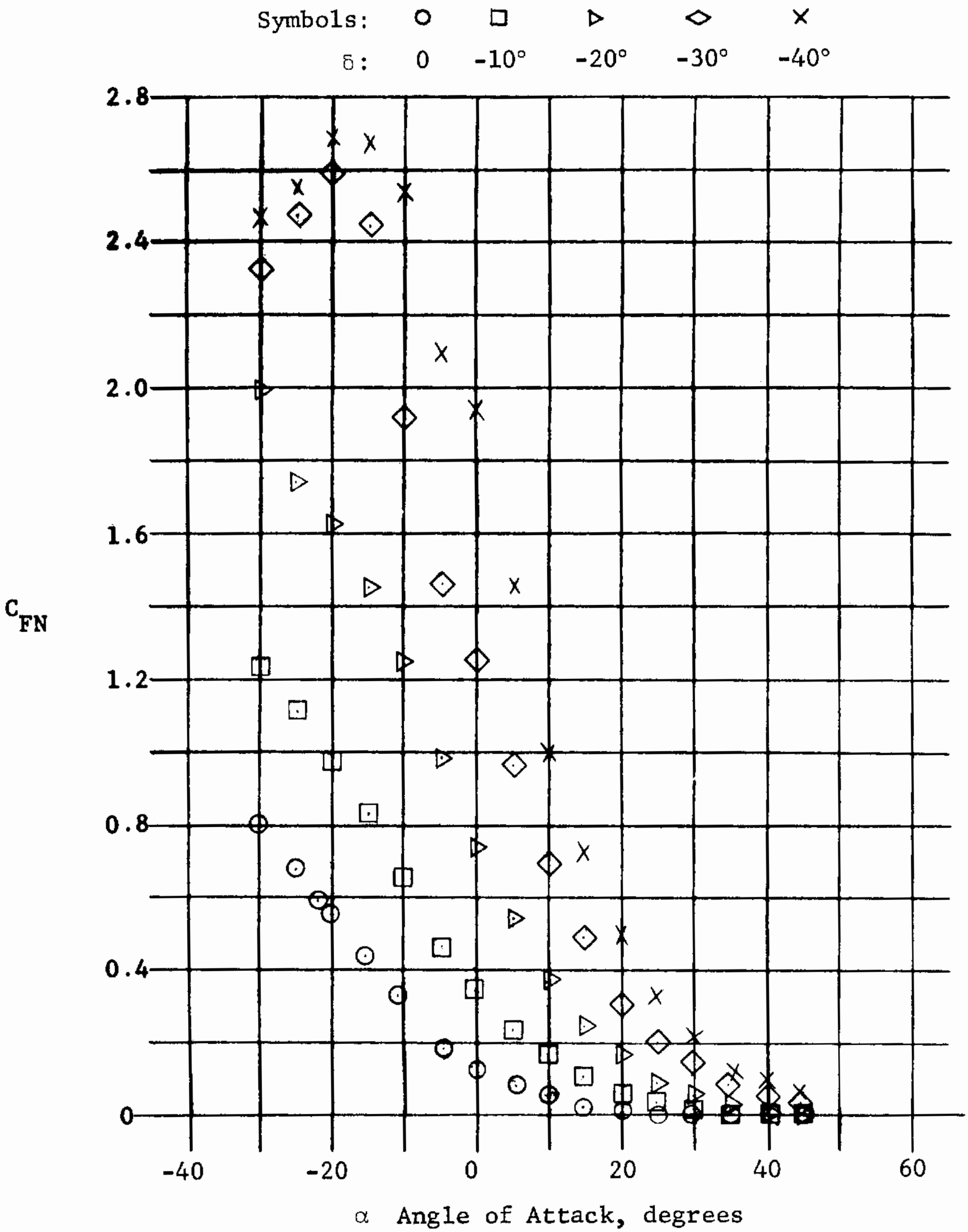

Fig. 6.1 Mach 5 Flap Loadings versus α for Basic Configuration with Symmetric Flap Settings (sheet 1 of 2)

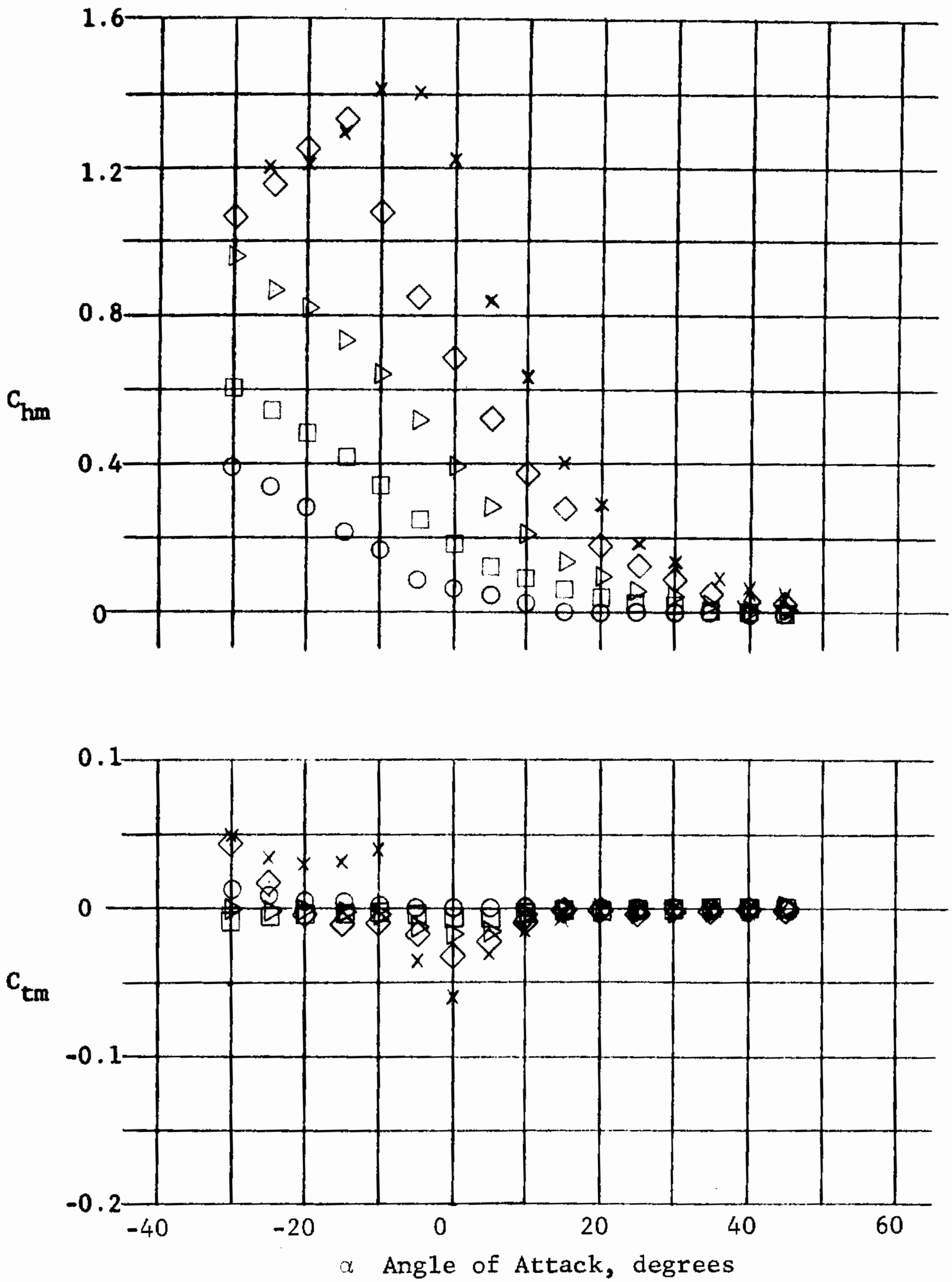

Fig. 6.1 Mach 5 Flap Loadings versus α for Basic Configuration with Symmetric Flap Settings (sheet 2 of 2)

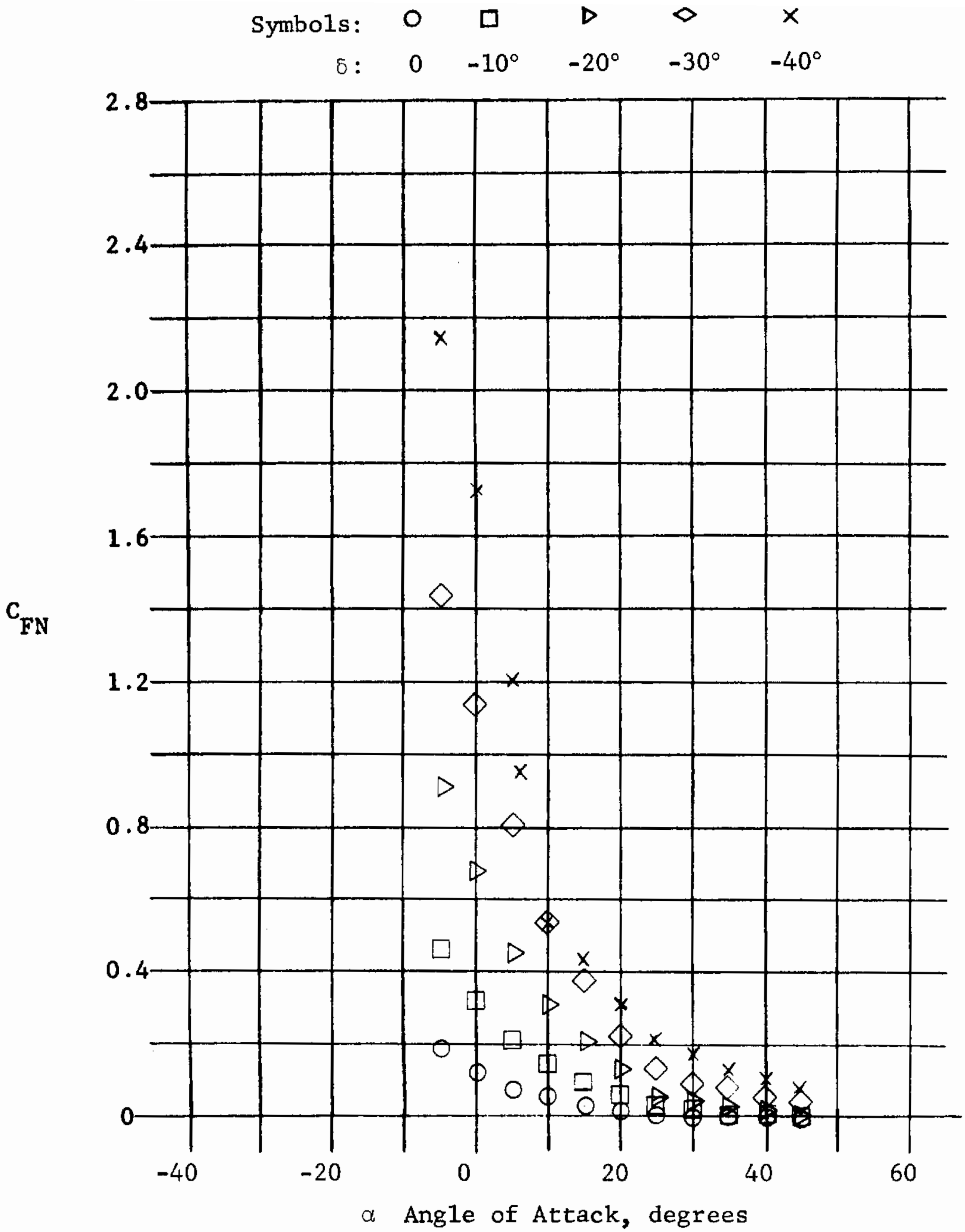

Fig. 6.2 Mach 5 Flap Loadings versus α for Basic Configuration with Canards and Symmetric Flap Settings (sheet 1 of 2)

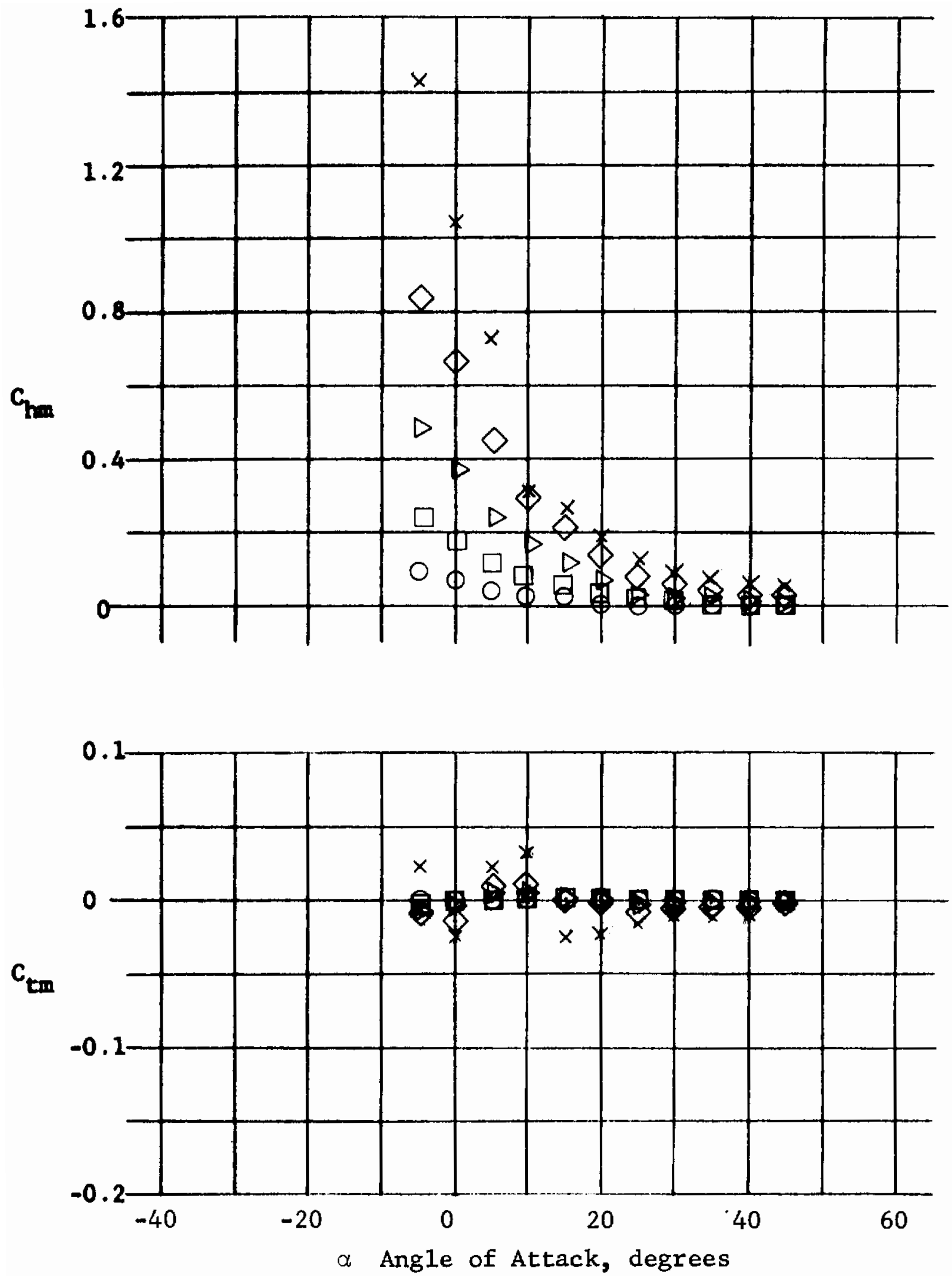

Fig. 6.2 Mach 5 Flap Loadings versus α for Basic Configuration with Canards and Symmetric Flap Settings (sheet 2 of 2)

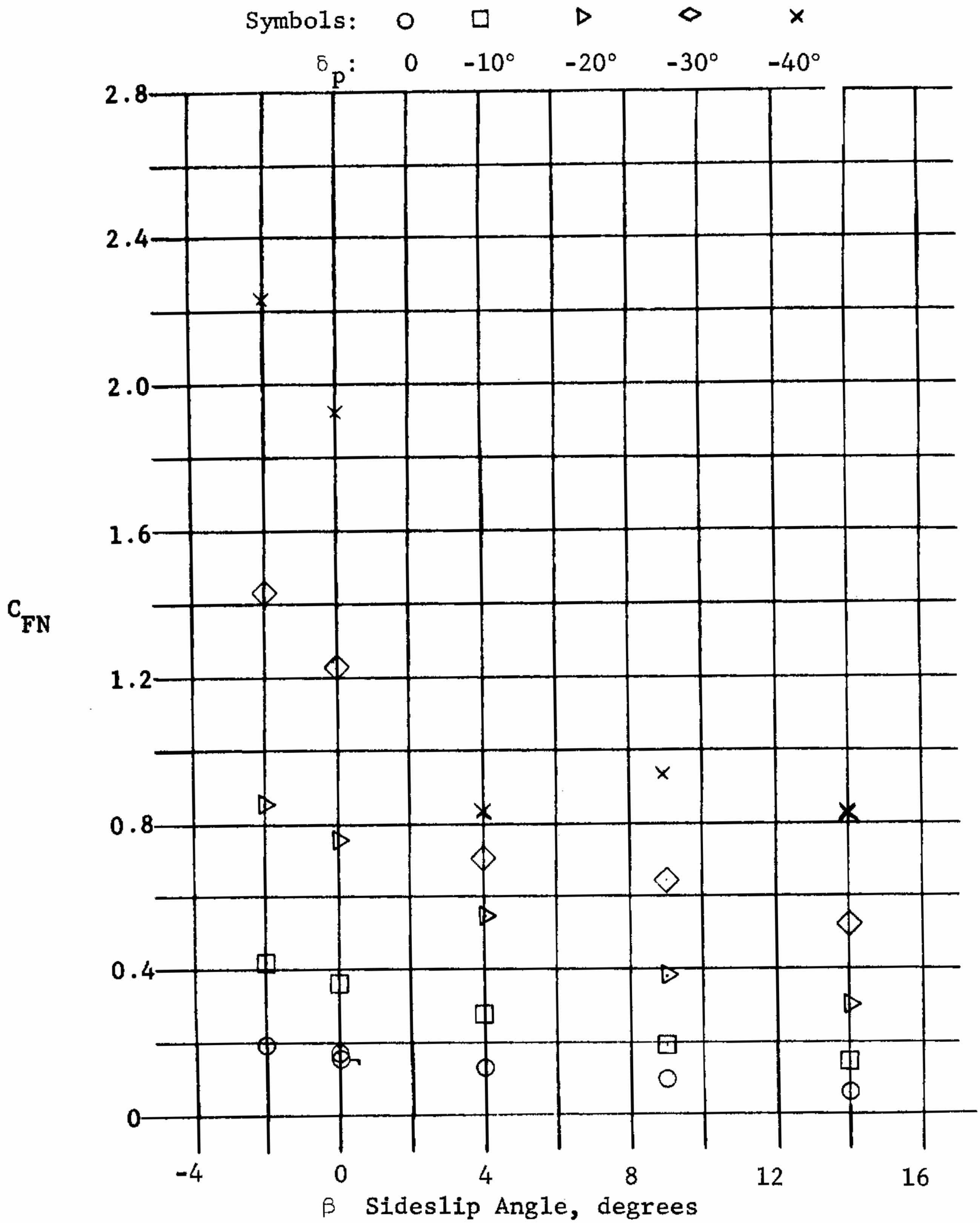

a) α = 0

Fig. 6.3 Mach 5 Flap Loadings versus β for Basic Configuration with Upper Surface Port Flap Deflections (sheet 1 of 6)

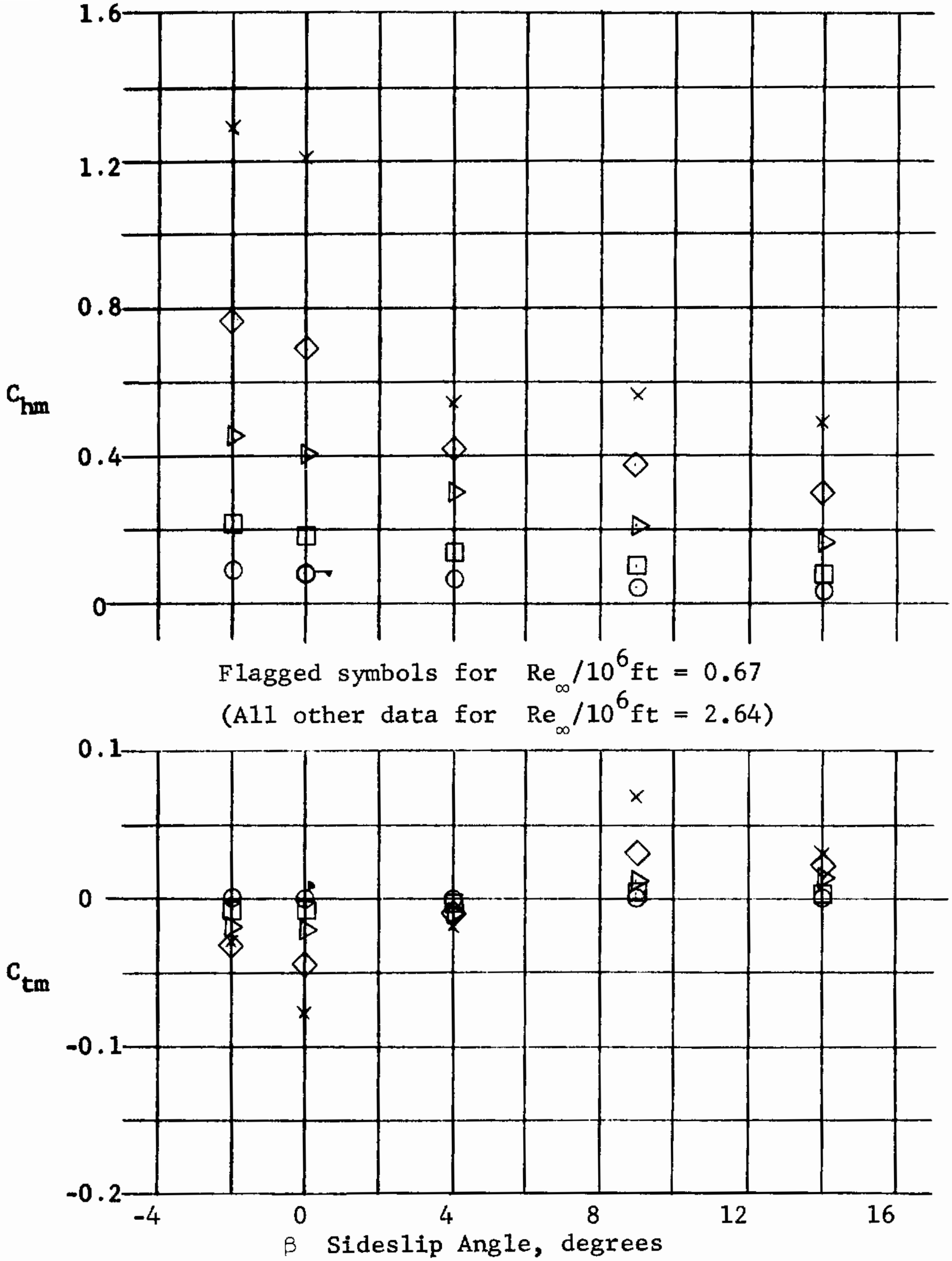

a) α = 0

Fig. 6.3 Mach 5 Flap Loadings versus β for Basic Configuration with Upper Surface Port Flap Deflections (sheet 2 of 6)

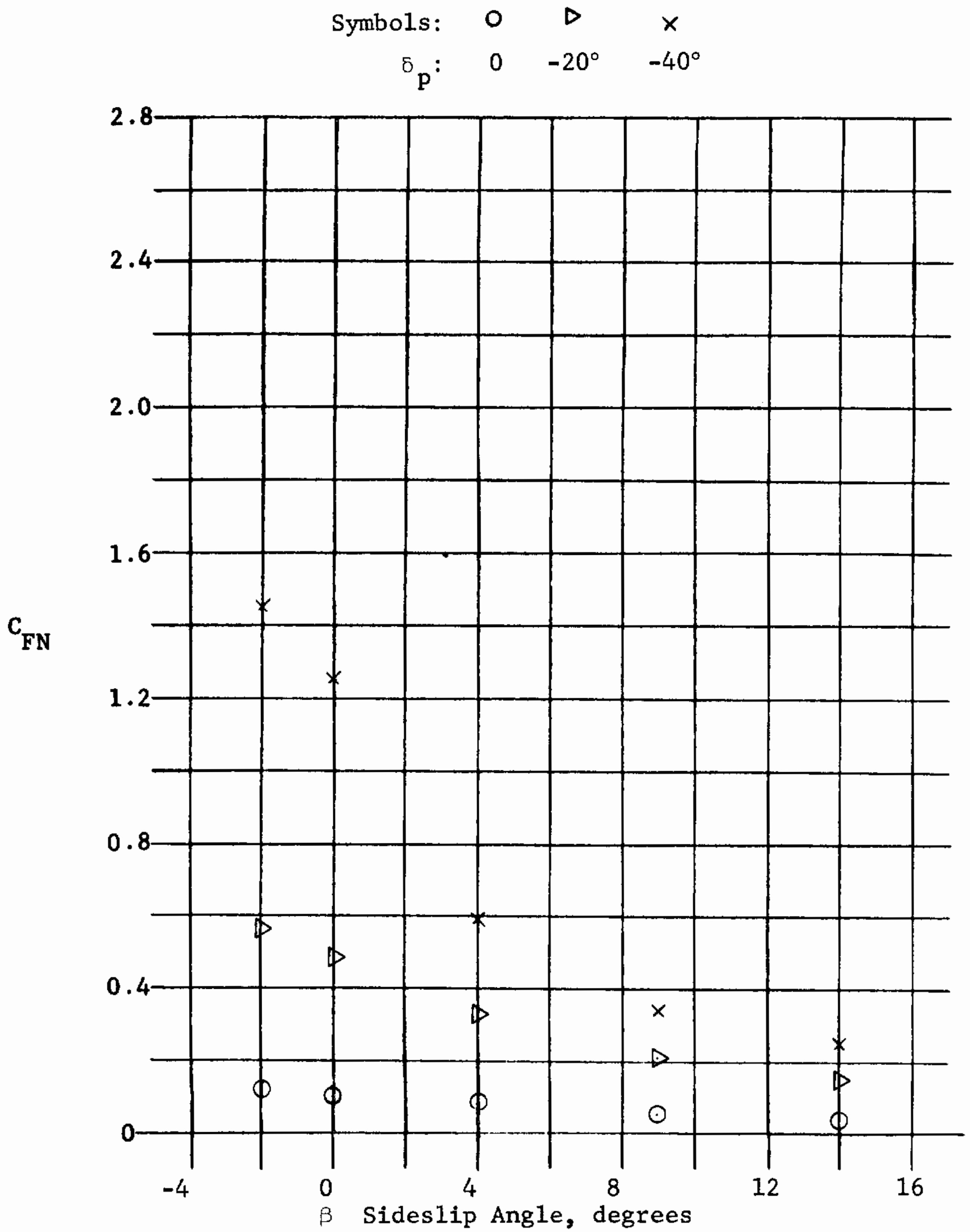

b) $\alpha = +7°$

Fig. 6.3 Mach 5 Flap Loadings versus β for Basic Configuration with Upper Surface Port Flap Deflections (sheet 3 of 6)

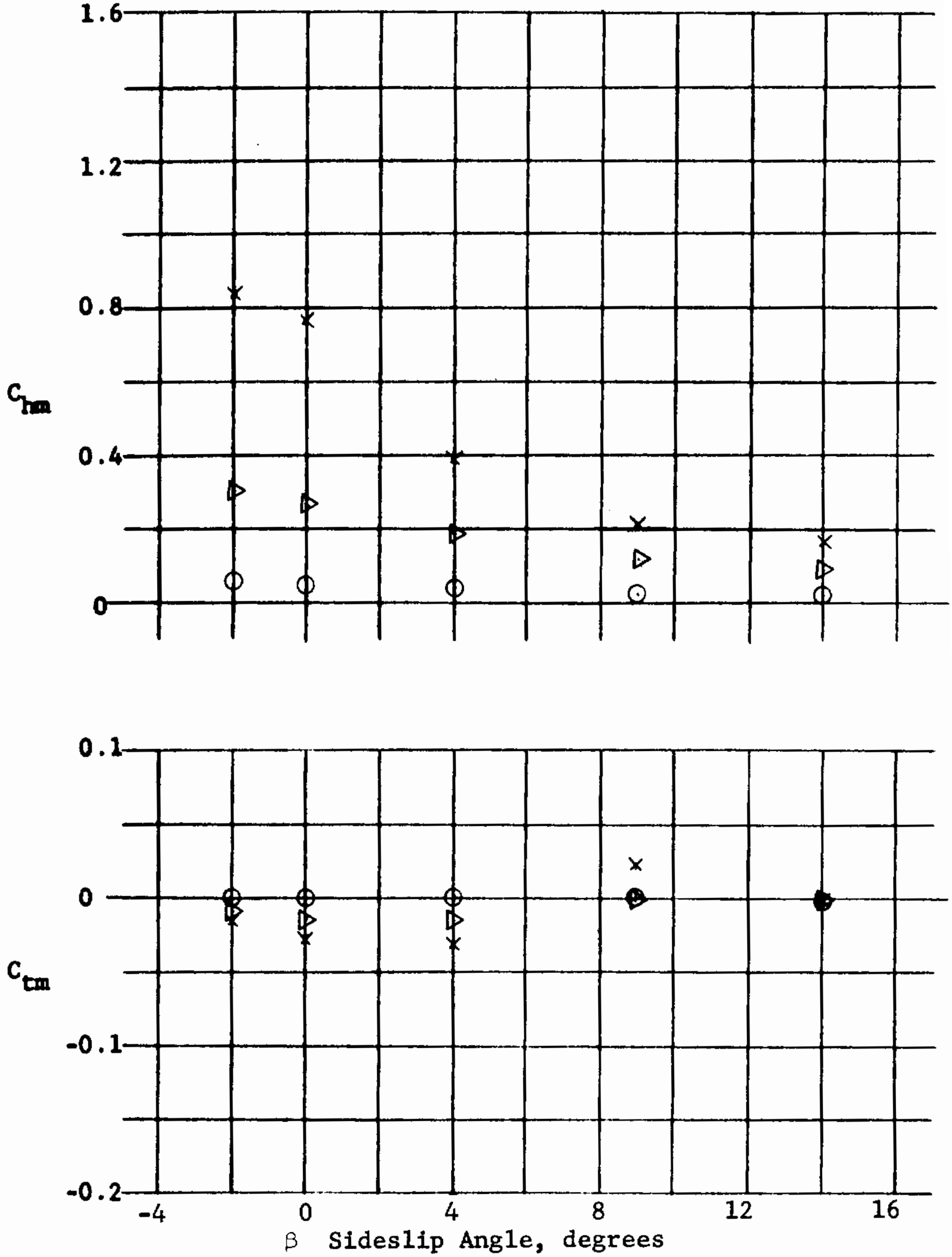

b) α = +7°

Fig. 6.3 Mach 5 Flap Loadings versus β for Basic Configuration with Upper Surface Port Flap Deflections (sheet 4 of 6)

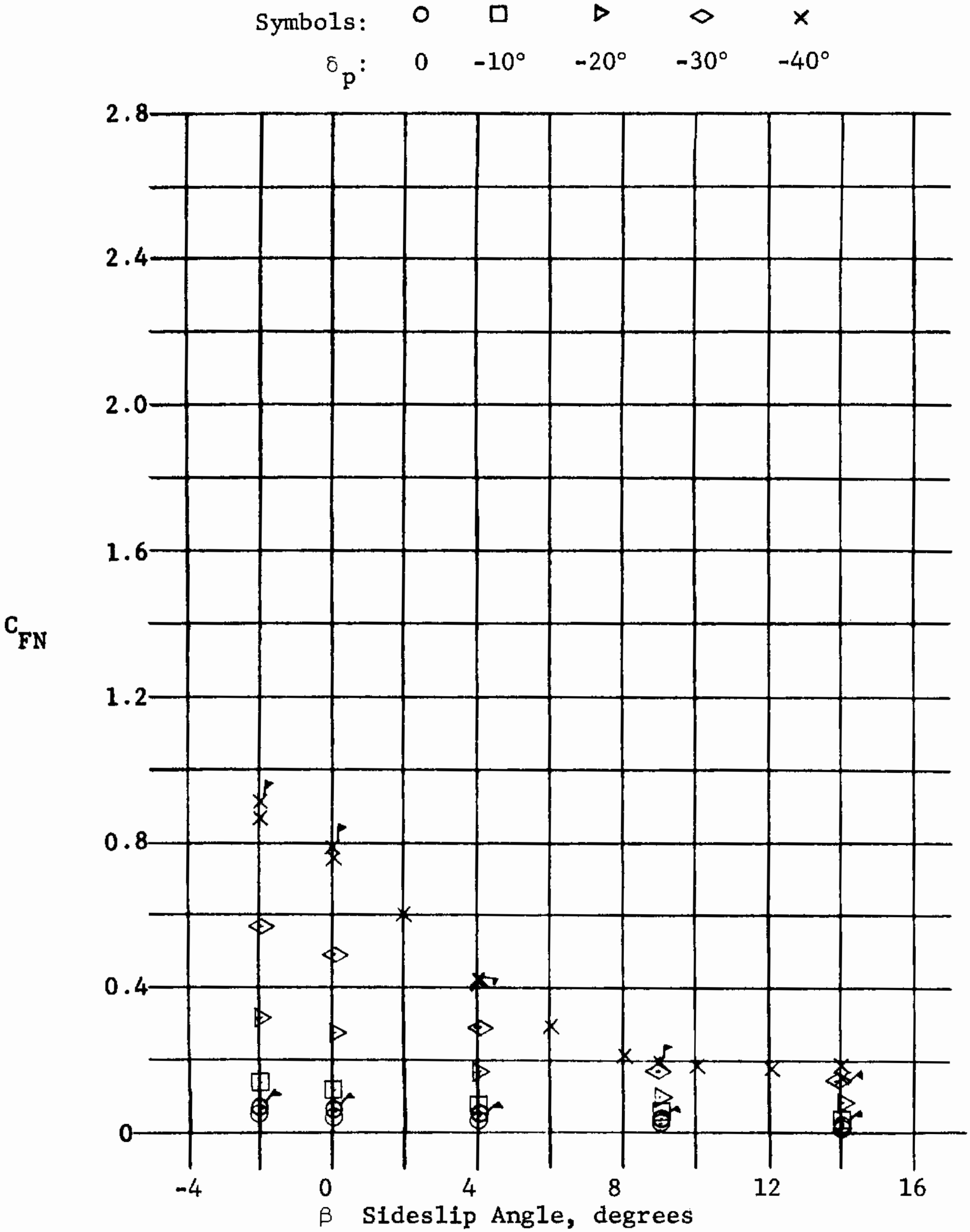

c) $\alpha = +14.3°$

Fig. 6.3 Mach 5 Flap Loadings versus β for Basic Configuration with Upper Surface Port Flap Deflections (sheet 5 of 6)

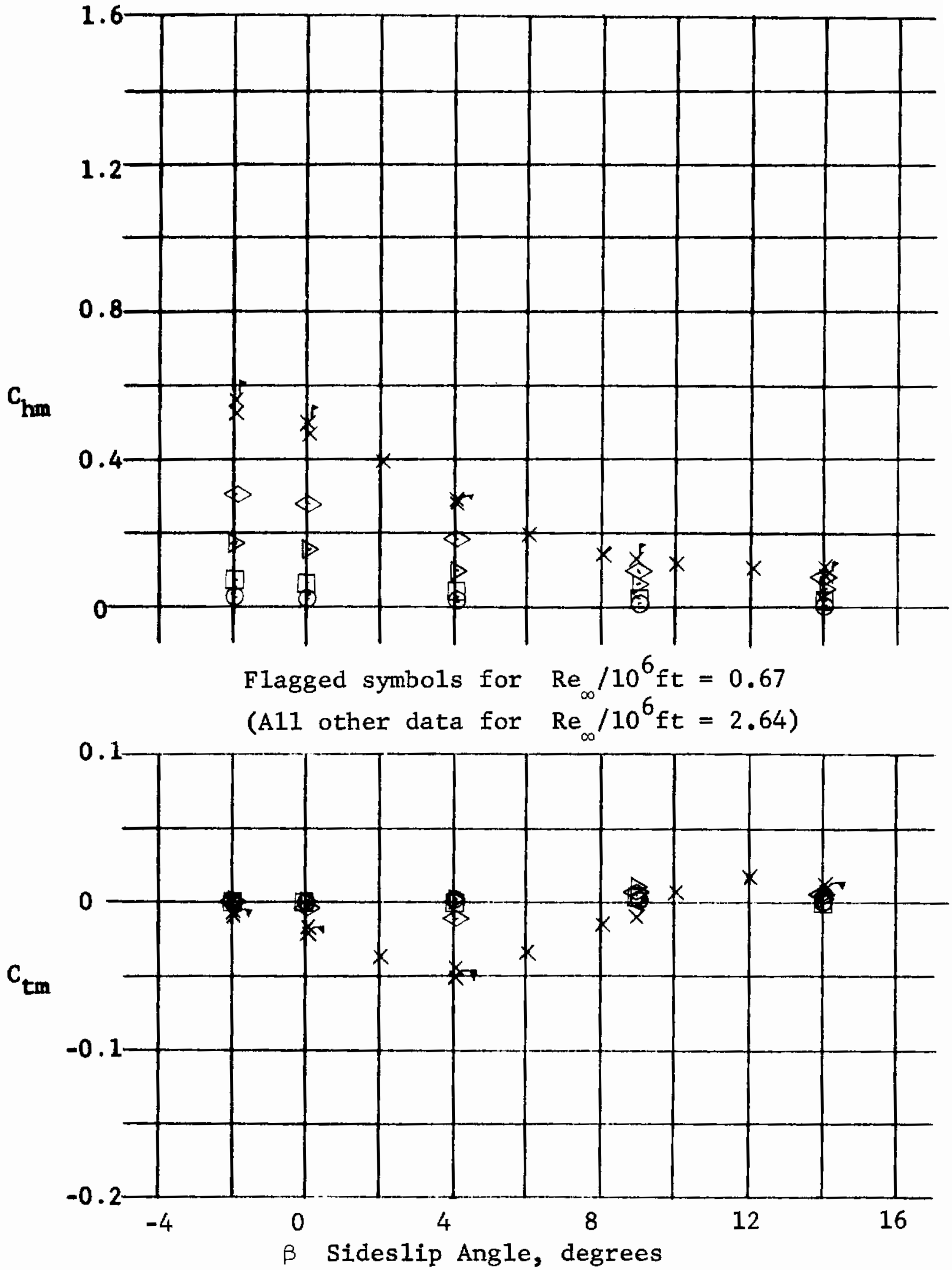

c) α = +14.3°

Fig. 6.3 Mach 5 Flap Loadings versus β for Basic Configuration with Upper Surface Port Flap Deflections (sheet 6 of 6)

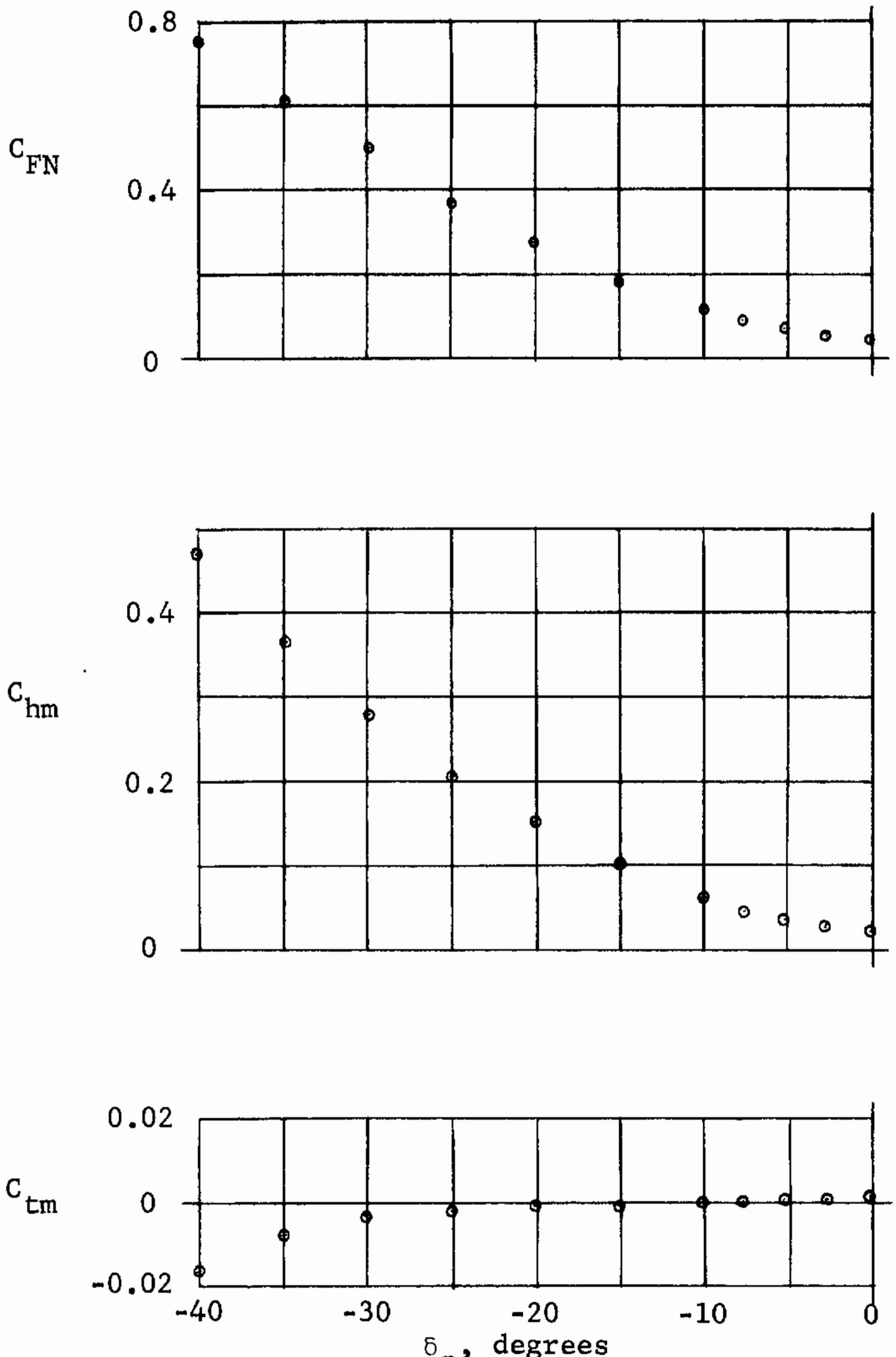

Fig. 6.4 Effects of Upper Surface Port Flap Deflections on Flap Loadings for Mach 5, $\alpha = +14.3°$ and $\beta = 0$

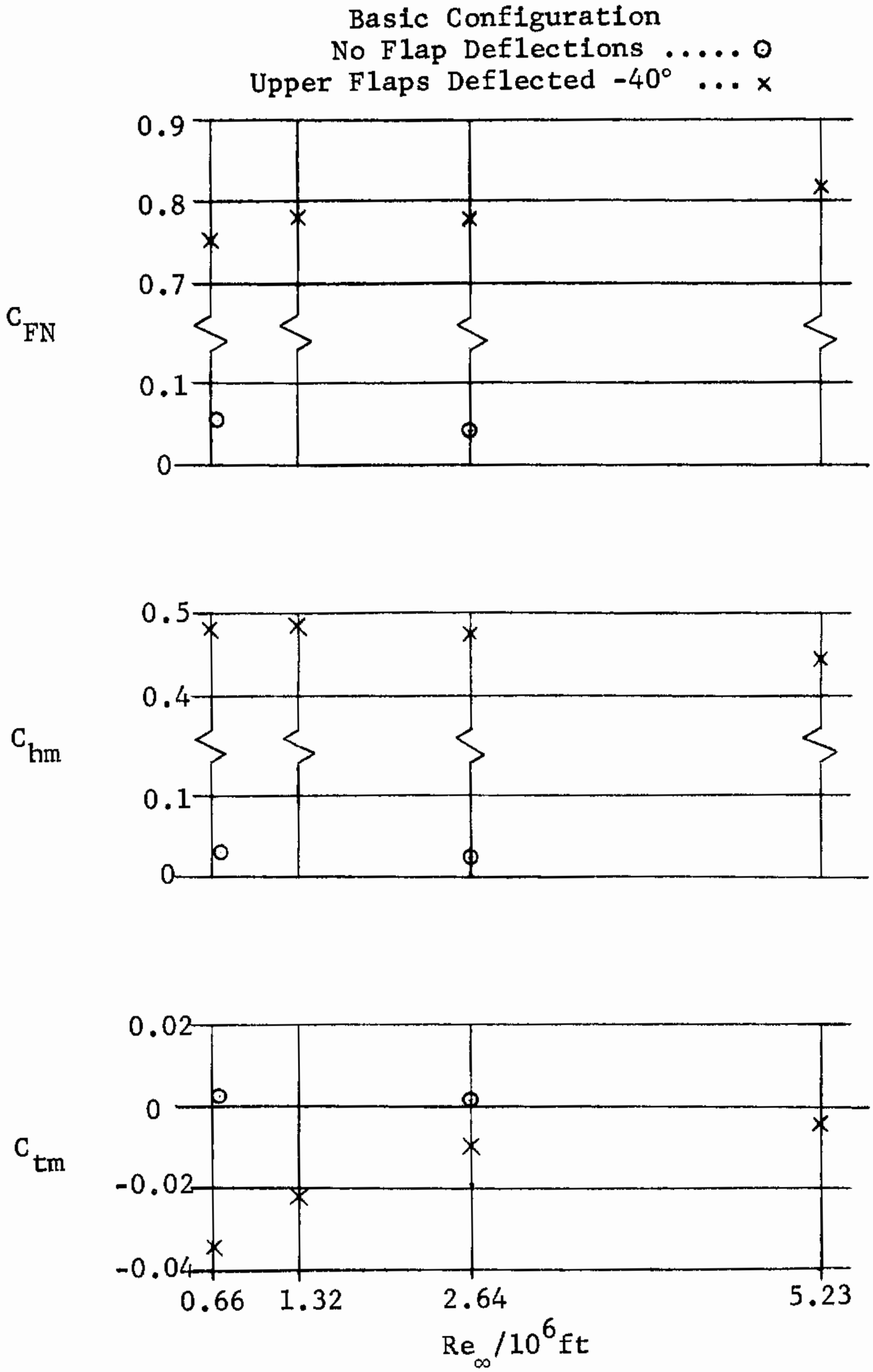

Fig. 6.5 Reynolds Number Effects on Flap Loadings for Mach 5, $\alpha = +14.3°$ and $\beta = 0$

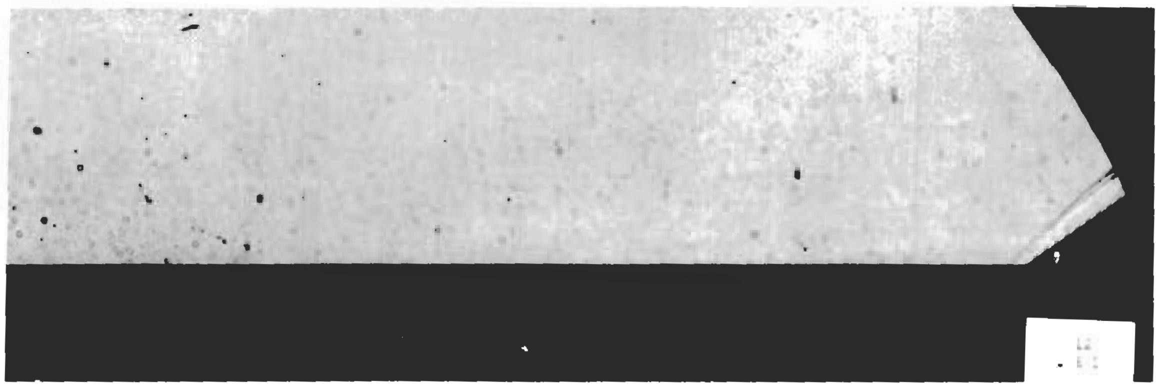

a) Basic Configuration at $\alpha = +14.3°$

b) Basic Configuration with Canards at $\alpha = +14.3°$

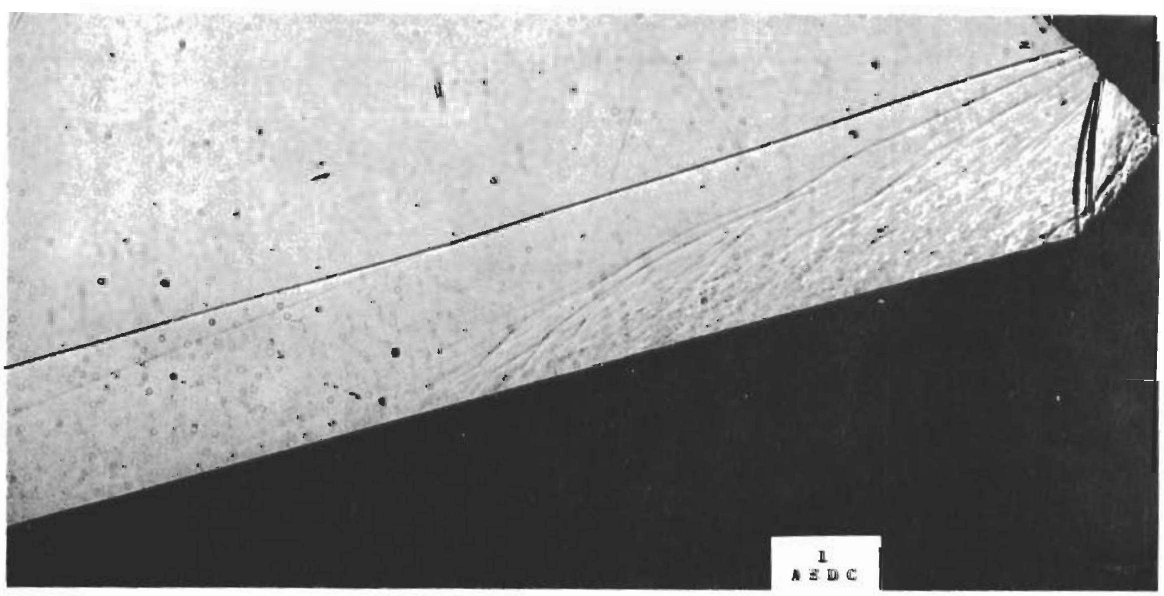

c) Basic Configuration with Canards at $\alpha = 0$

Fig. 7.1 Shadowgraphs of Mach 8 Flows Ahead of Upper Flaps Deflected -40°

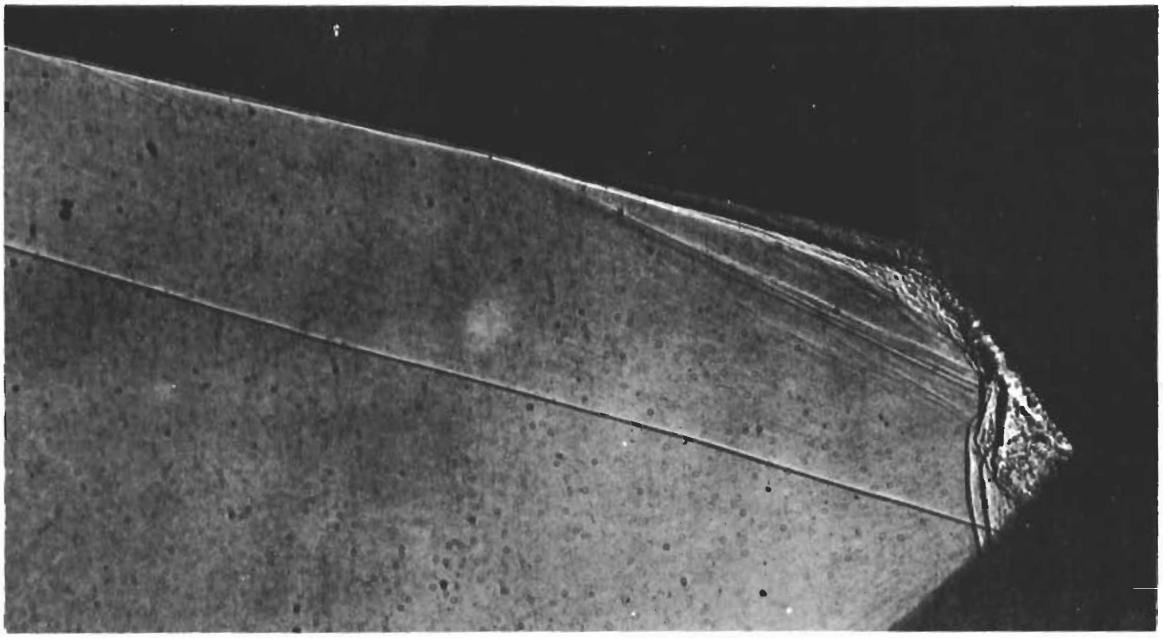

a) Both Lower Flaps Deflected +40°; α = +12°

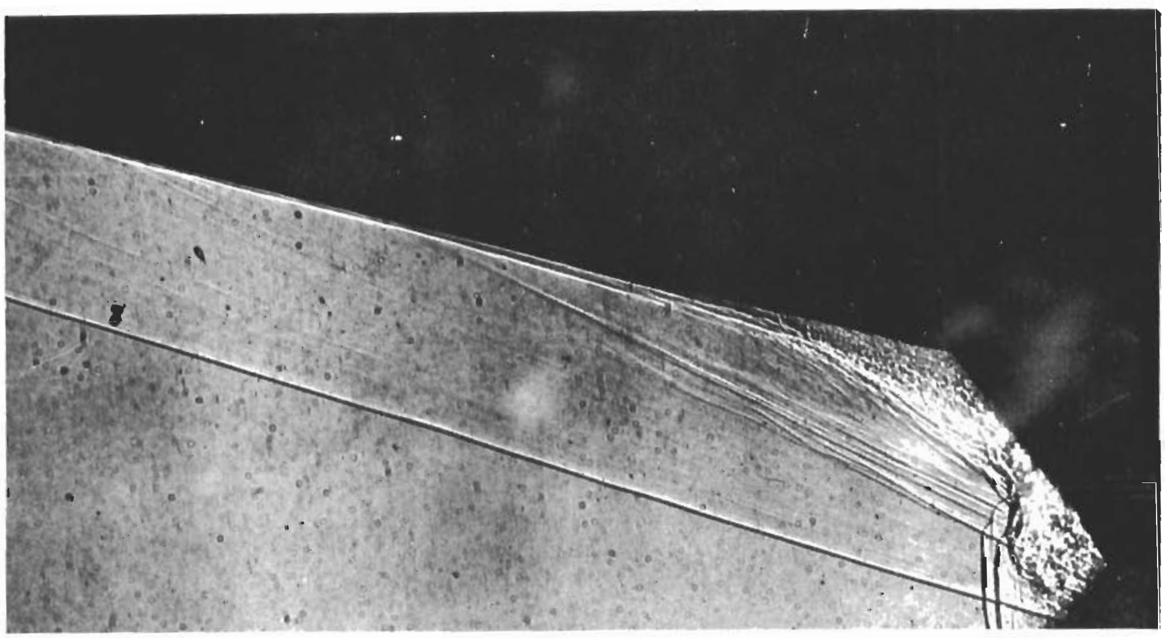

b) Both Lower Flaps Deflected +40°; α = +14.3°

Fig. 7.2 Shadowgraphs of Mach 8 Flows Ahead of Flaps on Lower Surface of Basic Configuration (sheet 1 of 2)

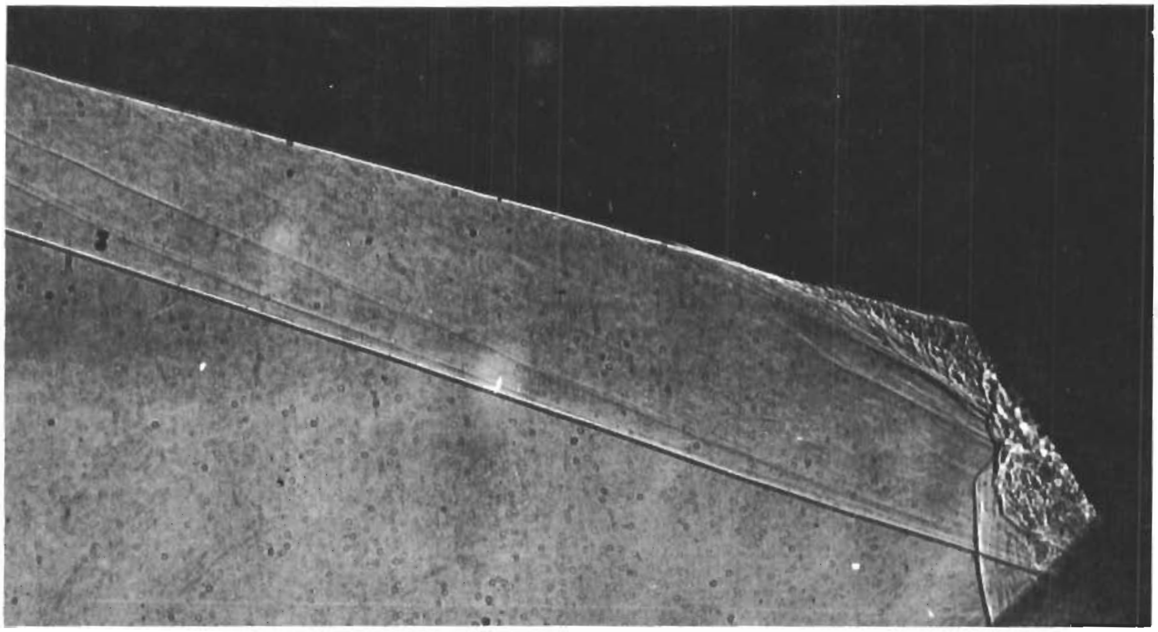

c) Port Lower Flap Deflected +40°; α = +14.3°

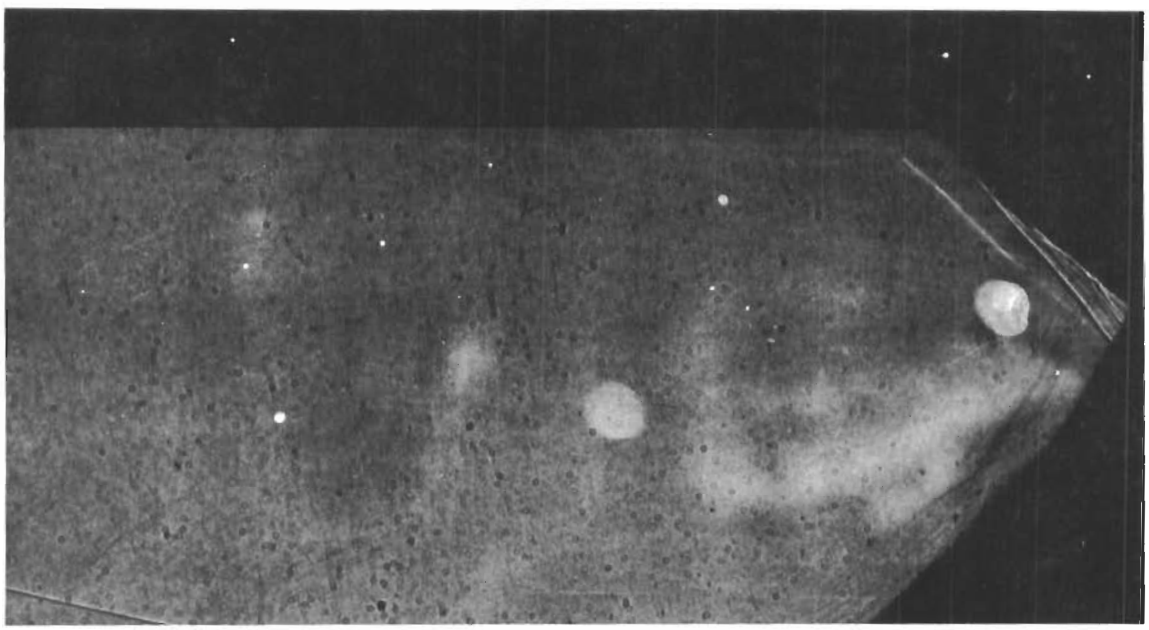

d) Port Lower Flap Deflected +40°; α = 0

Fig. 7.2 Shadowgraphs of Mach 8 Flows Ahead of Flaps on Lower Surface of Basic Configuration (sheet 2 of 2)

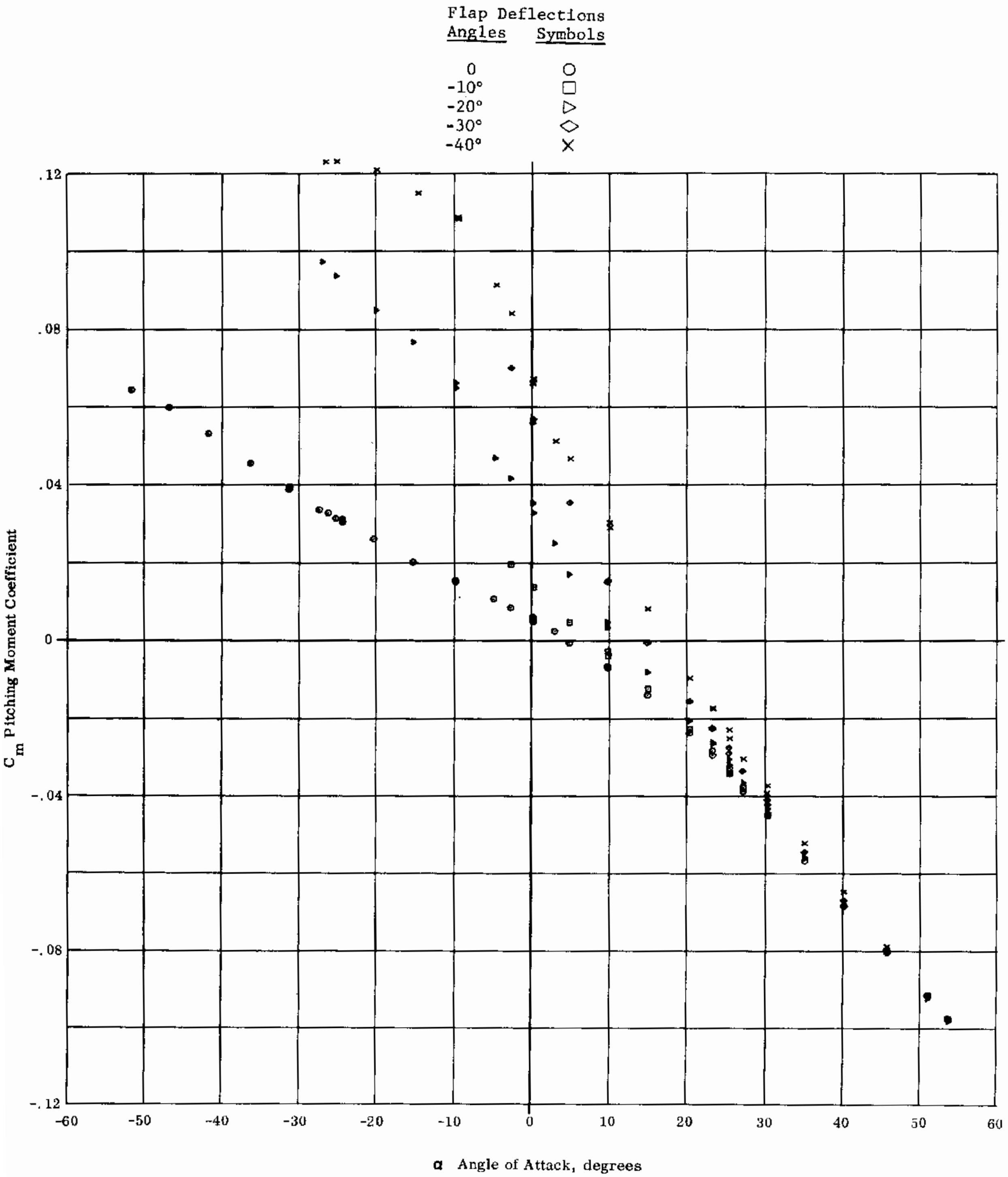

a) Upper Flaps Deflected

Fig. 8.1 Mach 8 Pitch Polars for Basic Configuration (sheet 1 of 4)

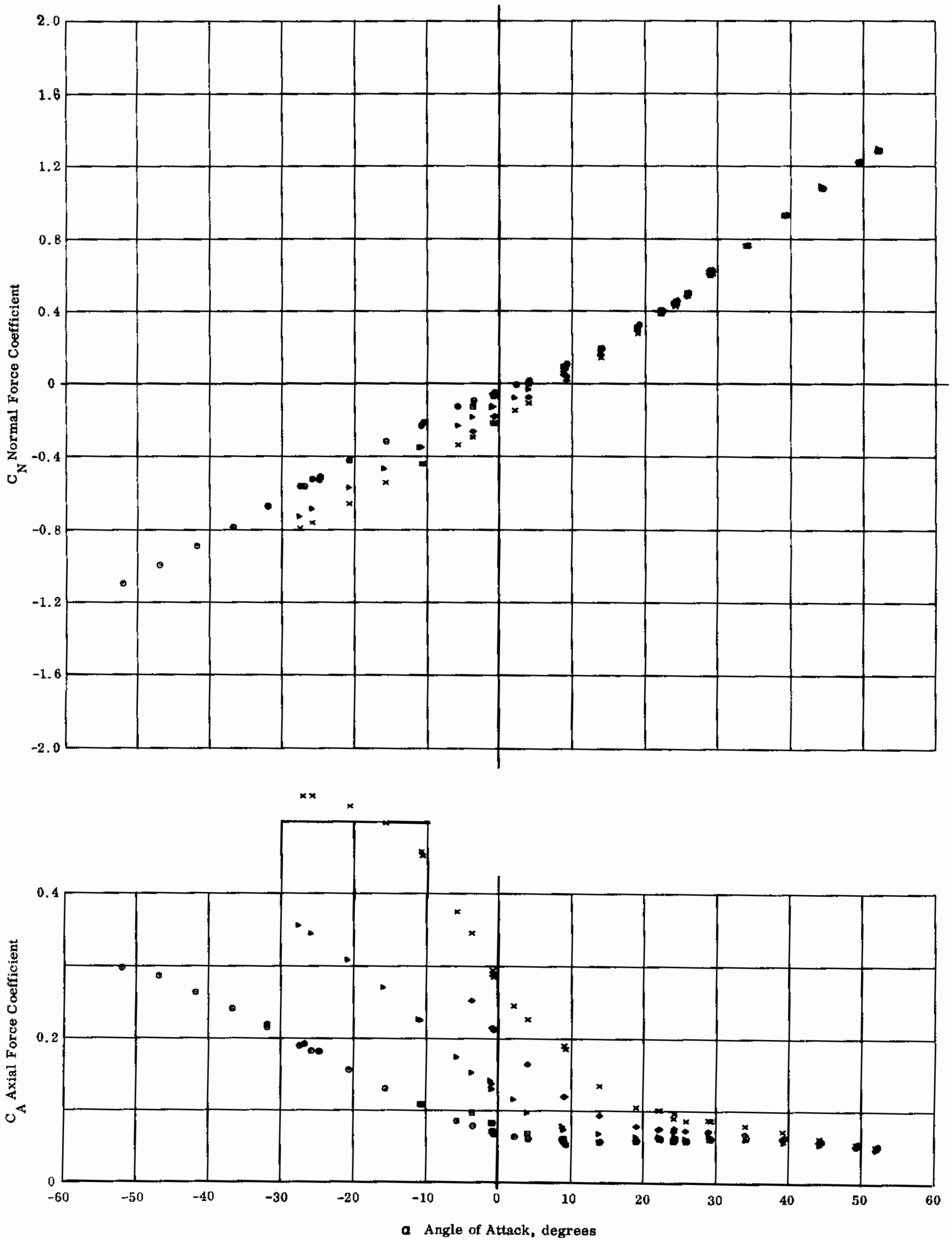

a) Upper Flaps Deflected

Fig. 8.1 Mach 8 Pitch Polars for Basic Configuration (sheet 2 of 4)

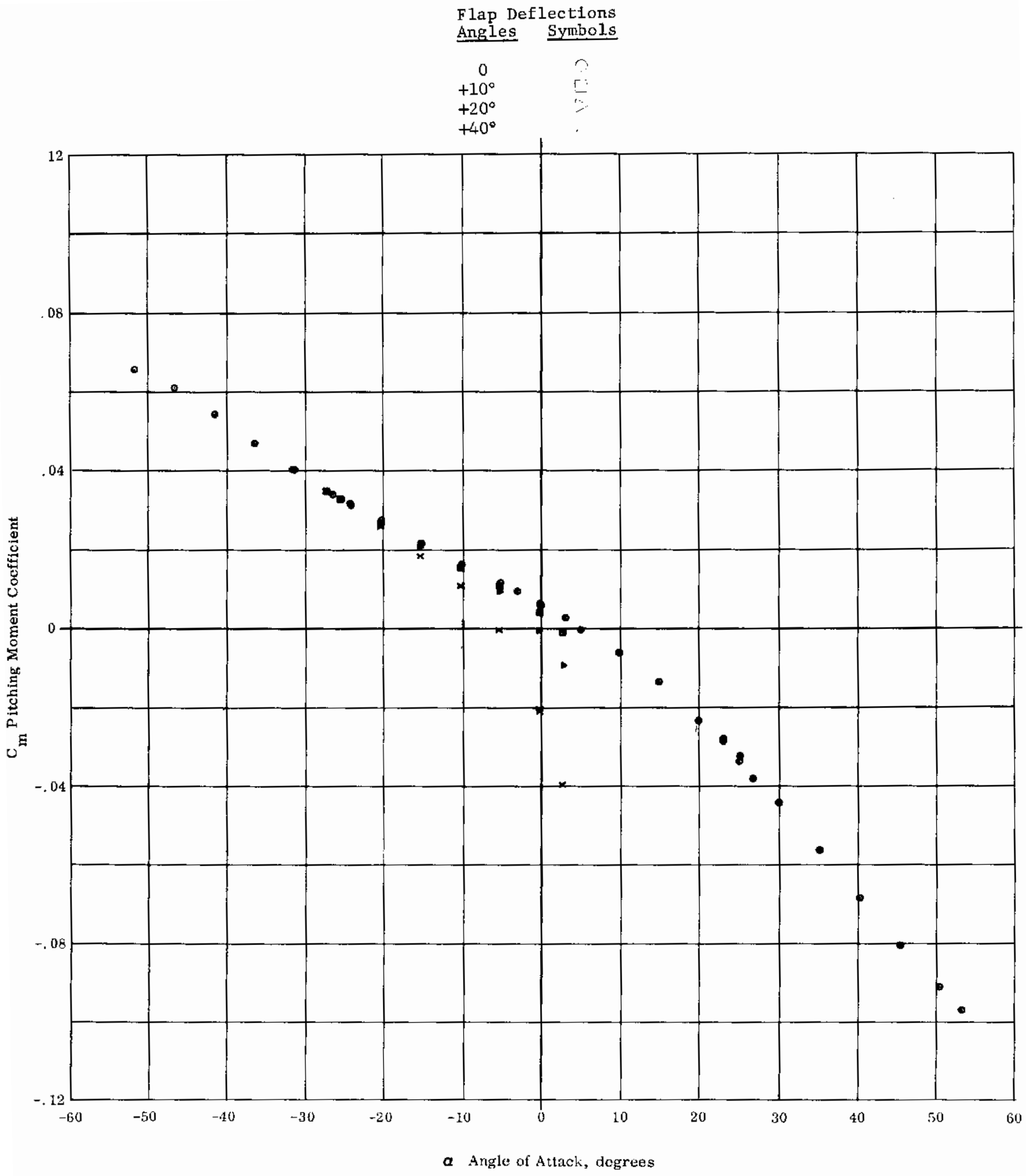

b) Lower Flaps Deflected

Fig. 8.1 Mach 8 Pitch Polars for Basic Configuration (sheet 3 of 4)

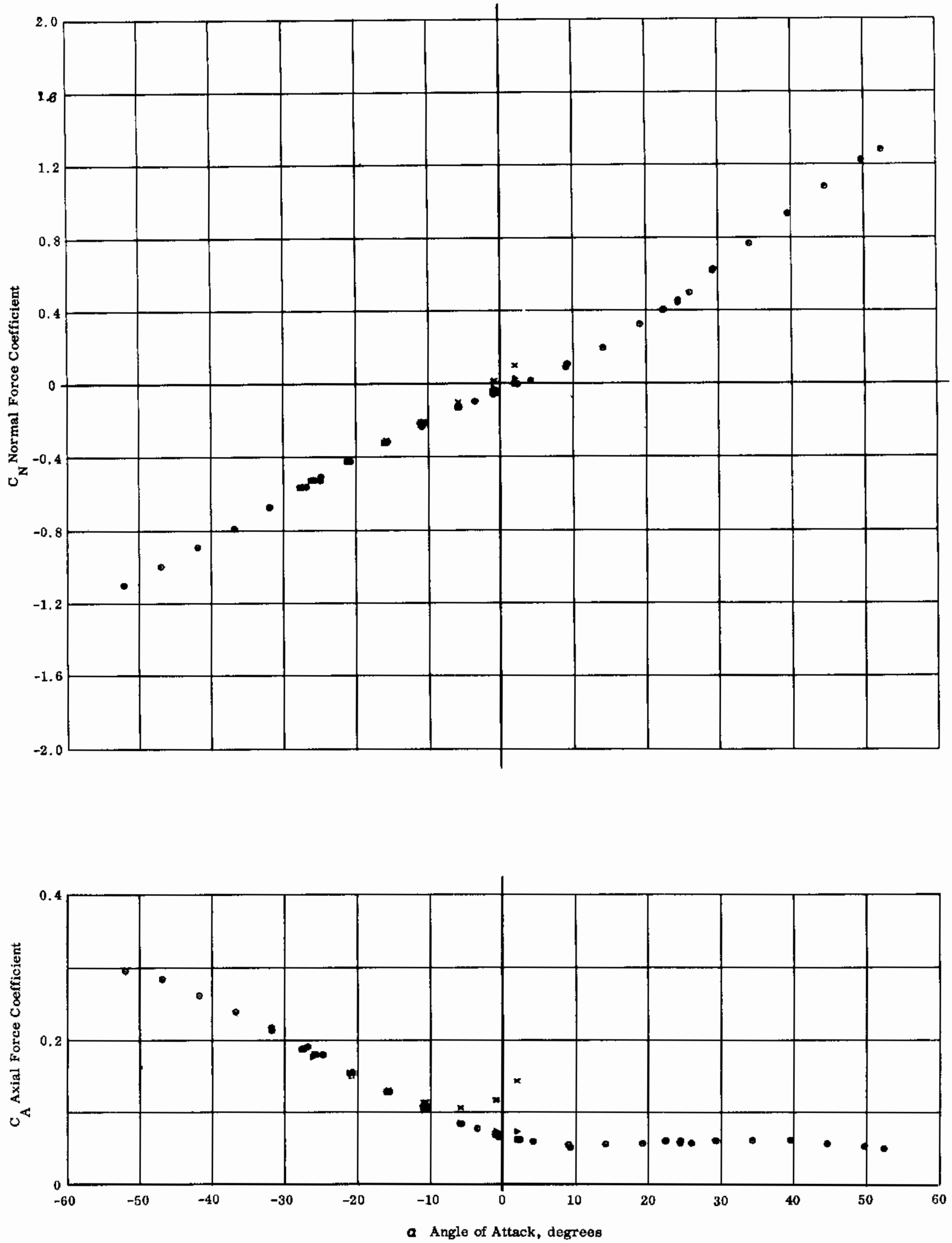

b) Lower Flaps Deflected

Fig. 8.1 Mach 8 Pitch Polars for Basic Configuration (sheet 4 of 4)

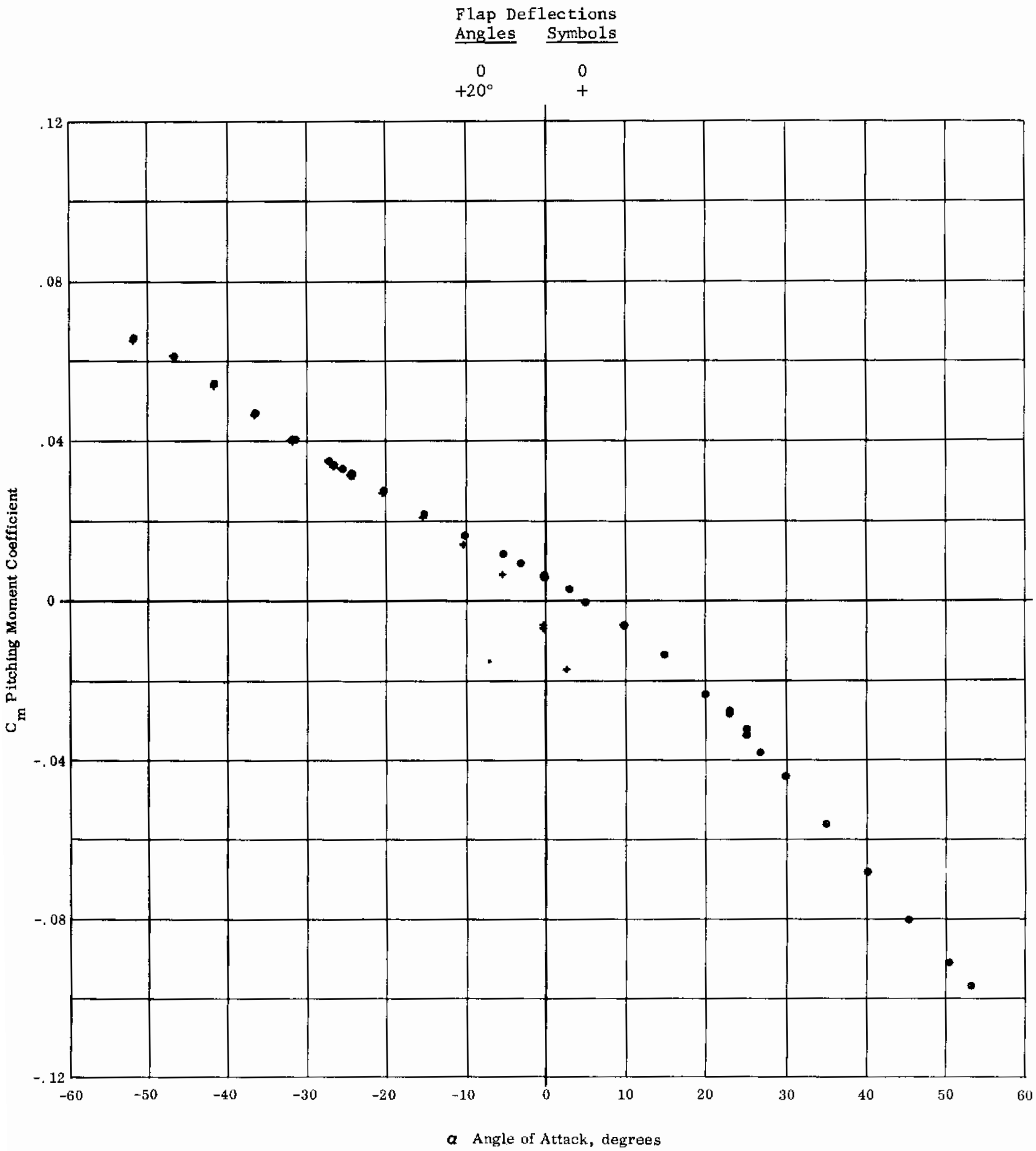

Fig. 8.2 Mach 8 Pitch Polars for Basic Configuration with Longer Chord Flaps on Lower Surface (sheet 1 of 2)

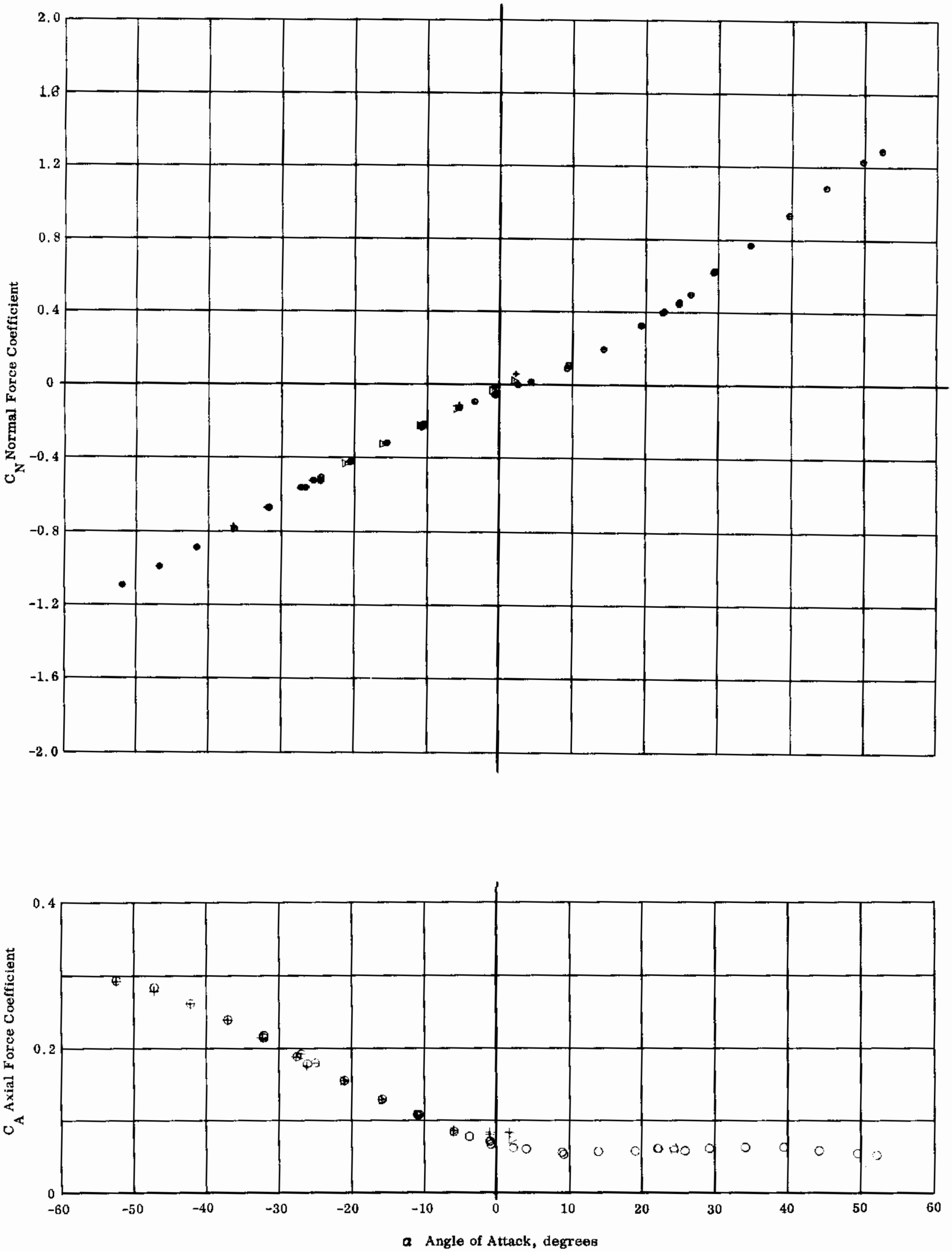

Fig. 8.2 Mach 8 Pitch Polars for Basic Configuration with Longer Chord Flaps on Lower Surface (sheet 2 of 2)

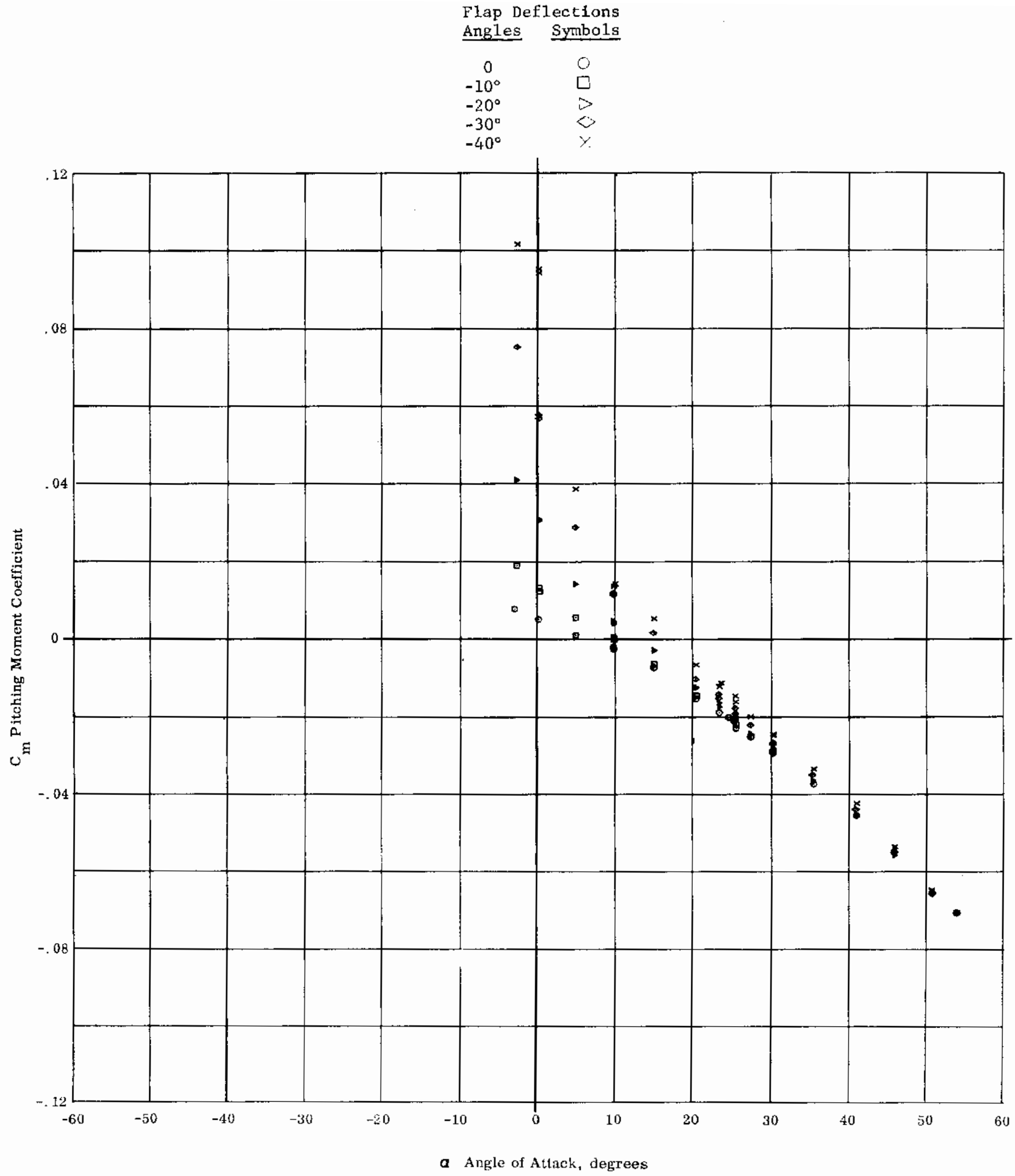

Fig. 8.3 Mach 8 Pitch Polars for Basic Configuration with Canards (sheet 1 of 2)

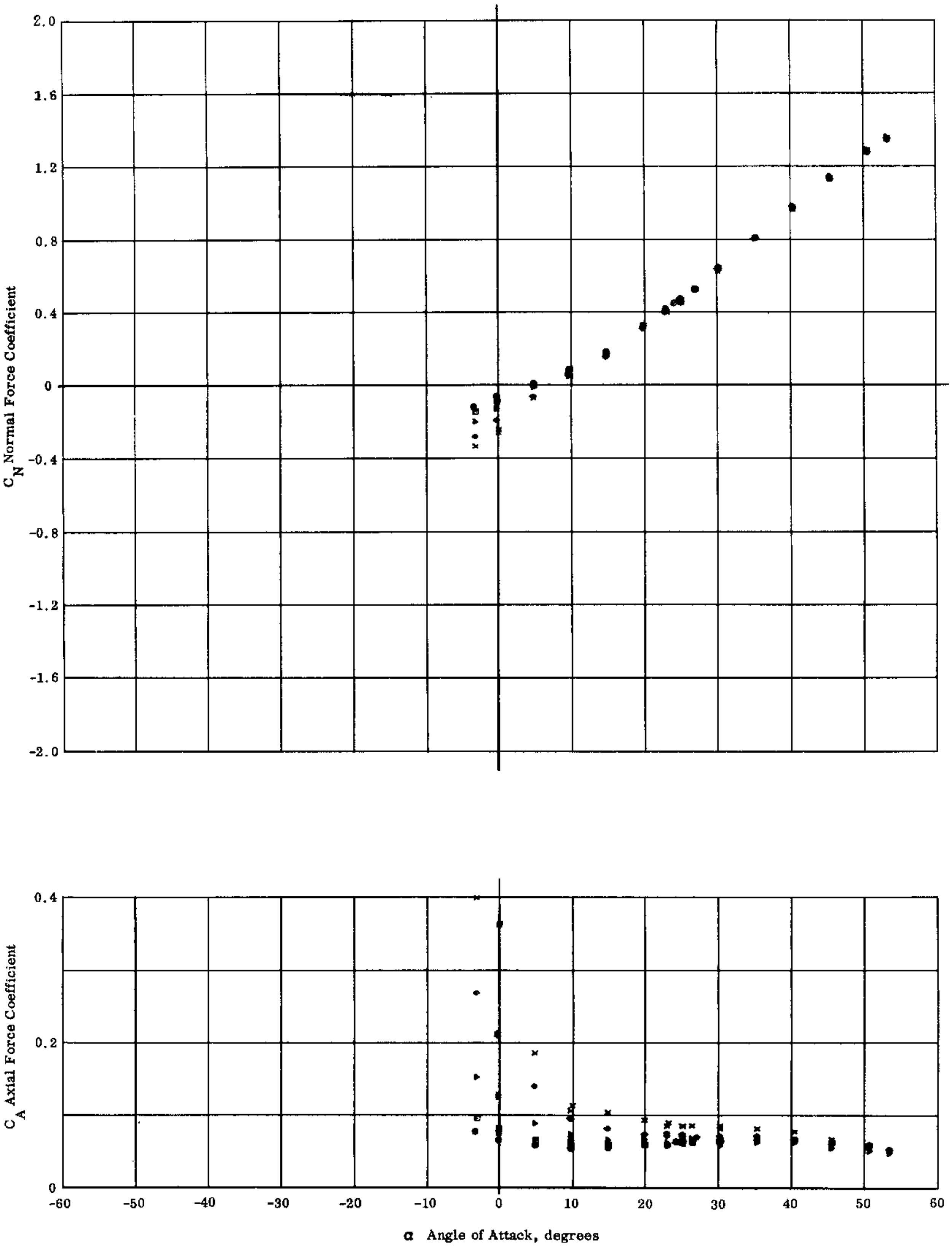

Fig. 8.3 Mach 8 Pitch Polars for Basic Configuration with Canards (sheet 2 of 2)

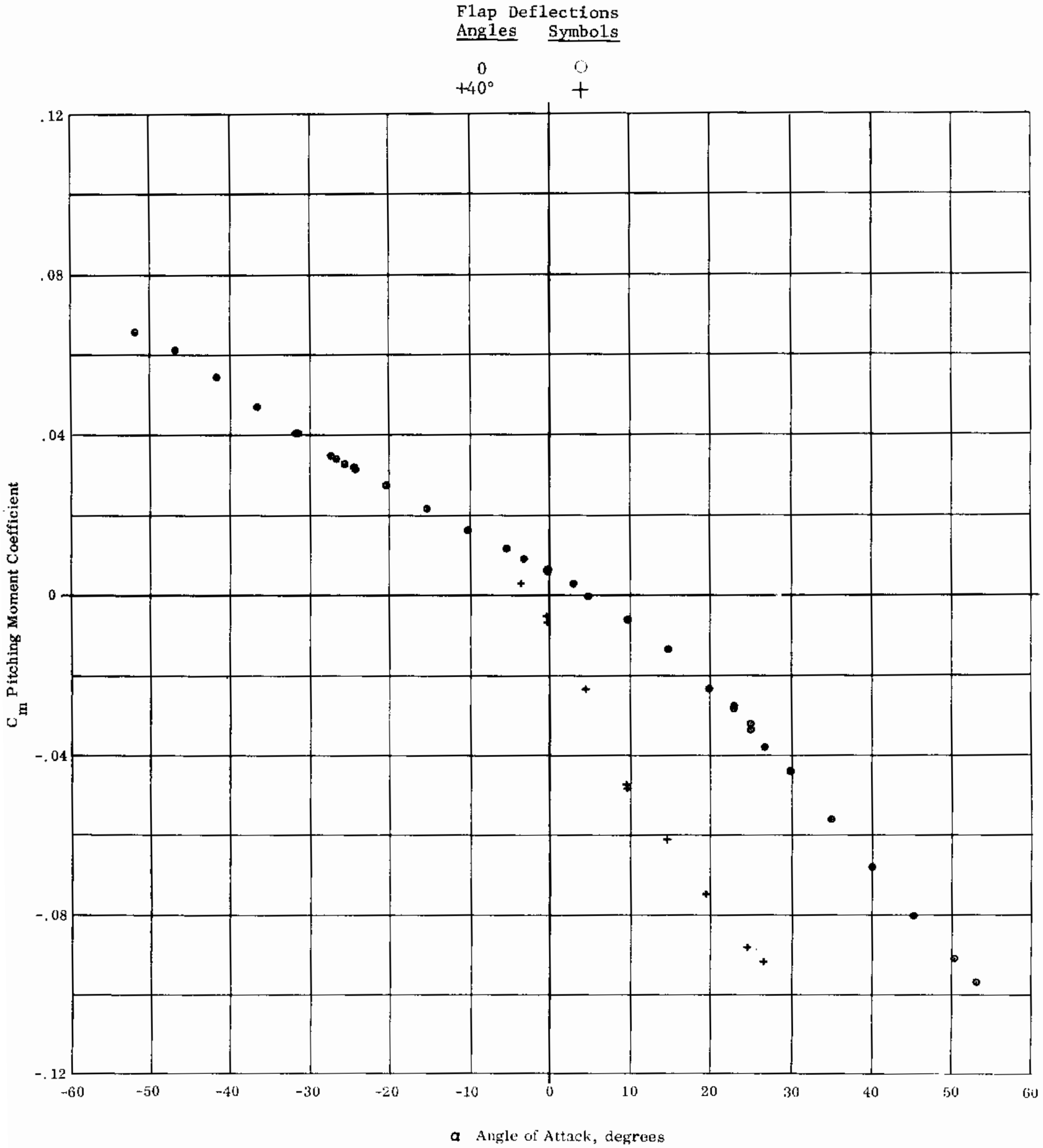

Fig. 8.4 Mach 8 Pitch Polars for Basic Configuration with Port Flap on Lower Surface (sheet 1 of 3)

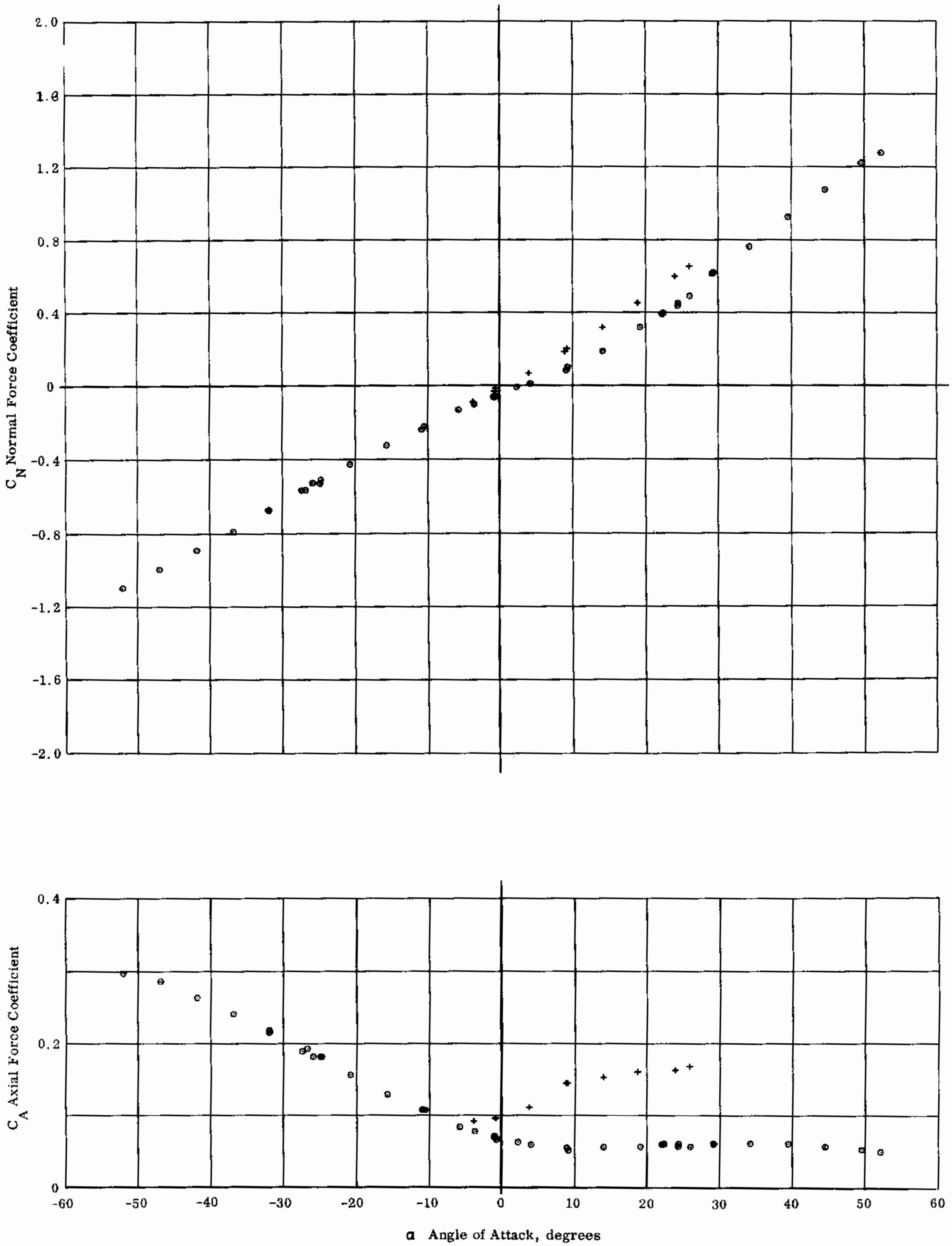

Fig. 8.4 Mach 8 Pitch Polars for Basic Configuration with Port Flap on Lower Surface (sheet 2 of 3)

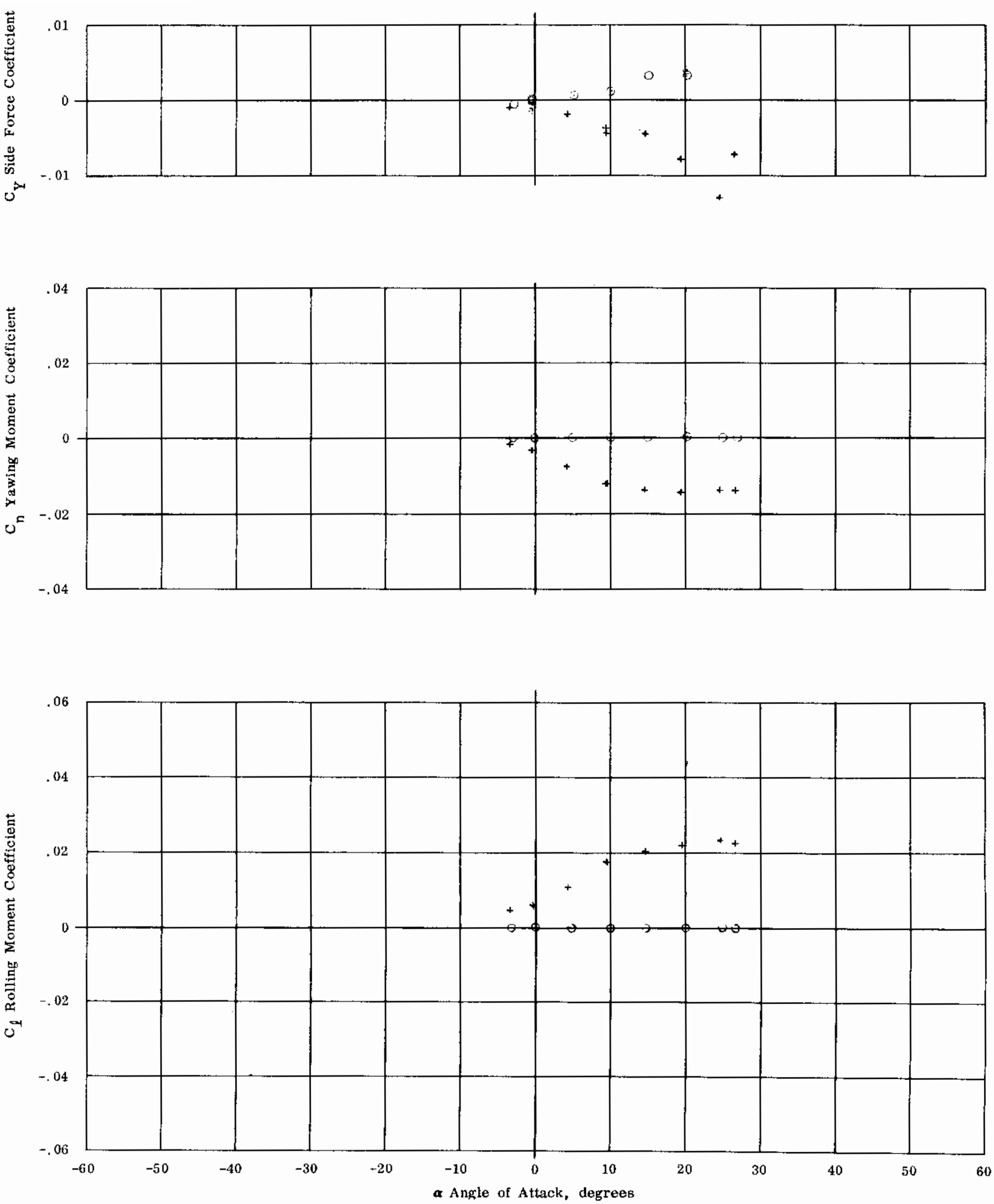

Fig. 8.4 Mach 8 Pitch Polars for Basic Configuration with Port Flap on Lower Surface (sheet 3 of 3)

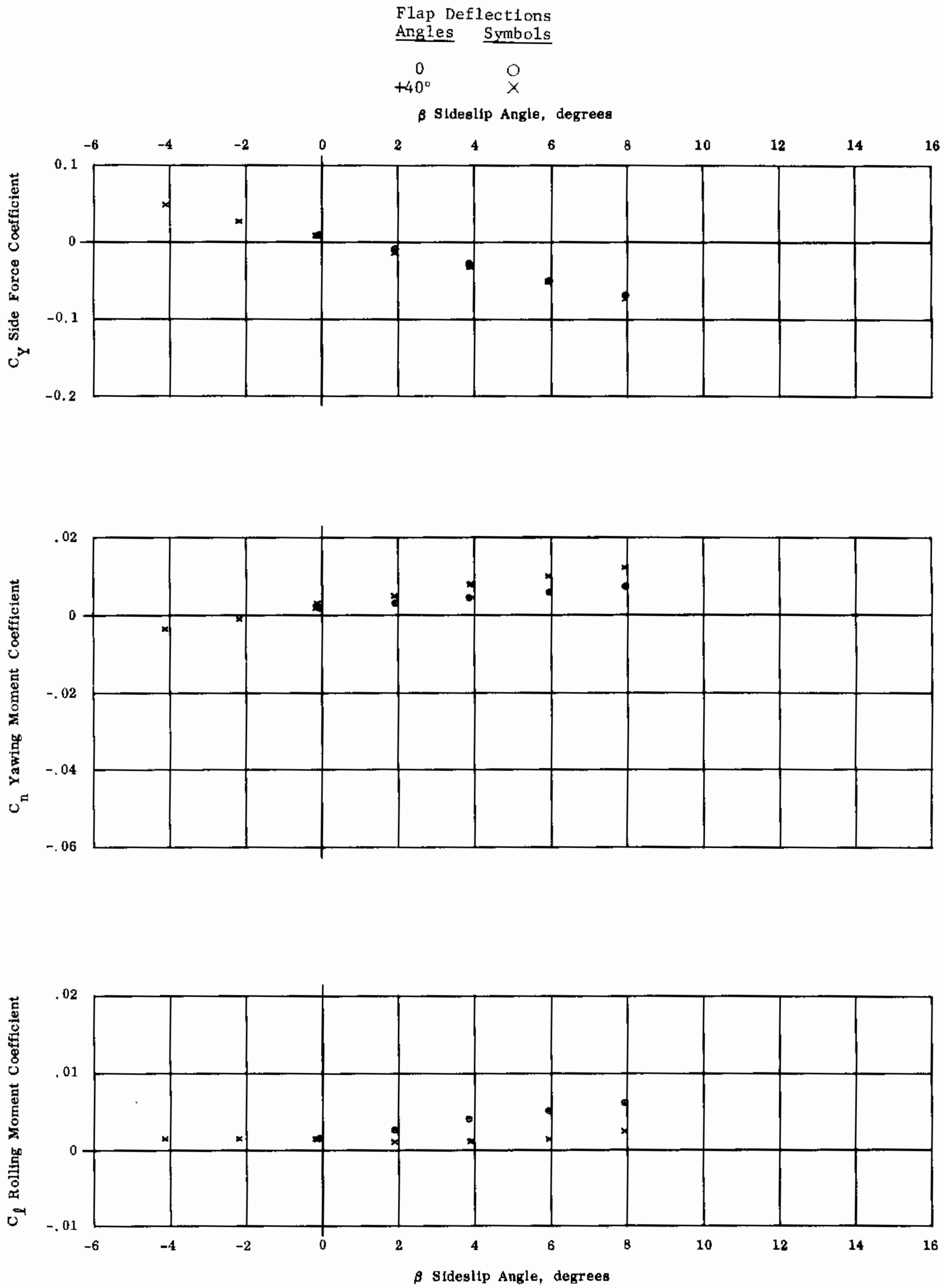

a) $\alpha = 0$

Fig. 8.5 Mach 8 Sideslip Polars for Basic Configuration (sheet 1 of 9)

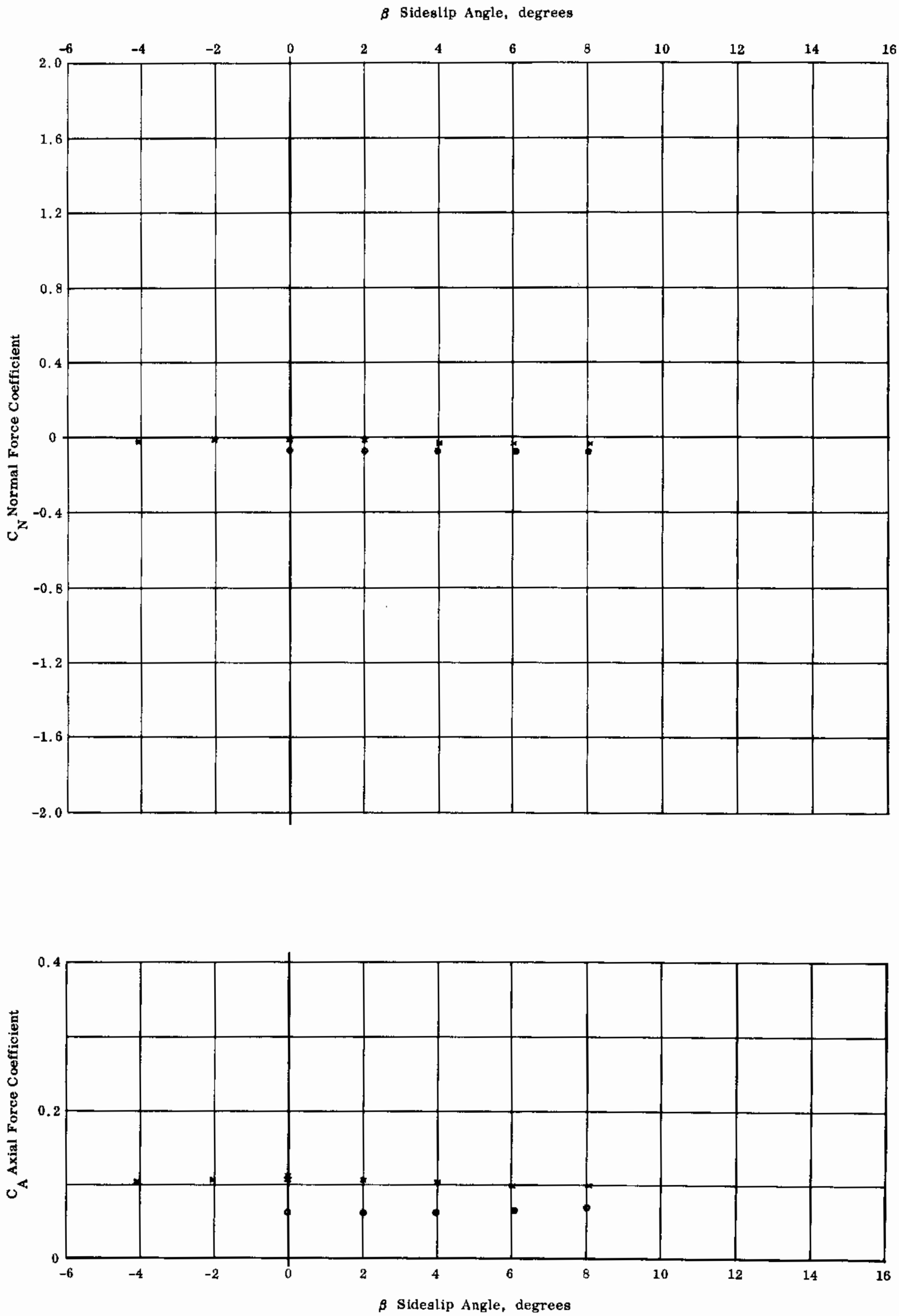

a) α = 0

Fig. 8.5 Mach 8 Sideslip Polars for Basic Configuration (sheet 2 of 9)

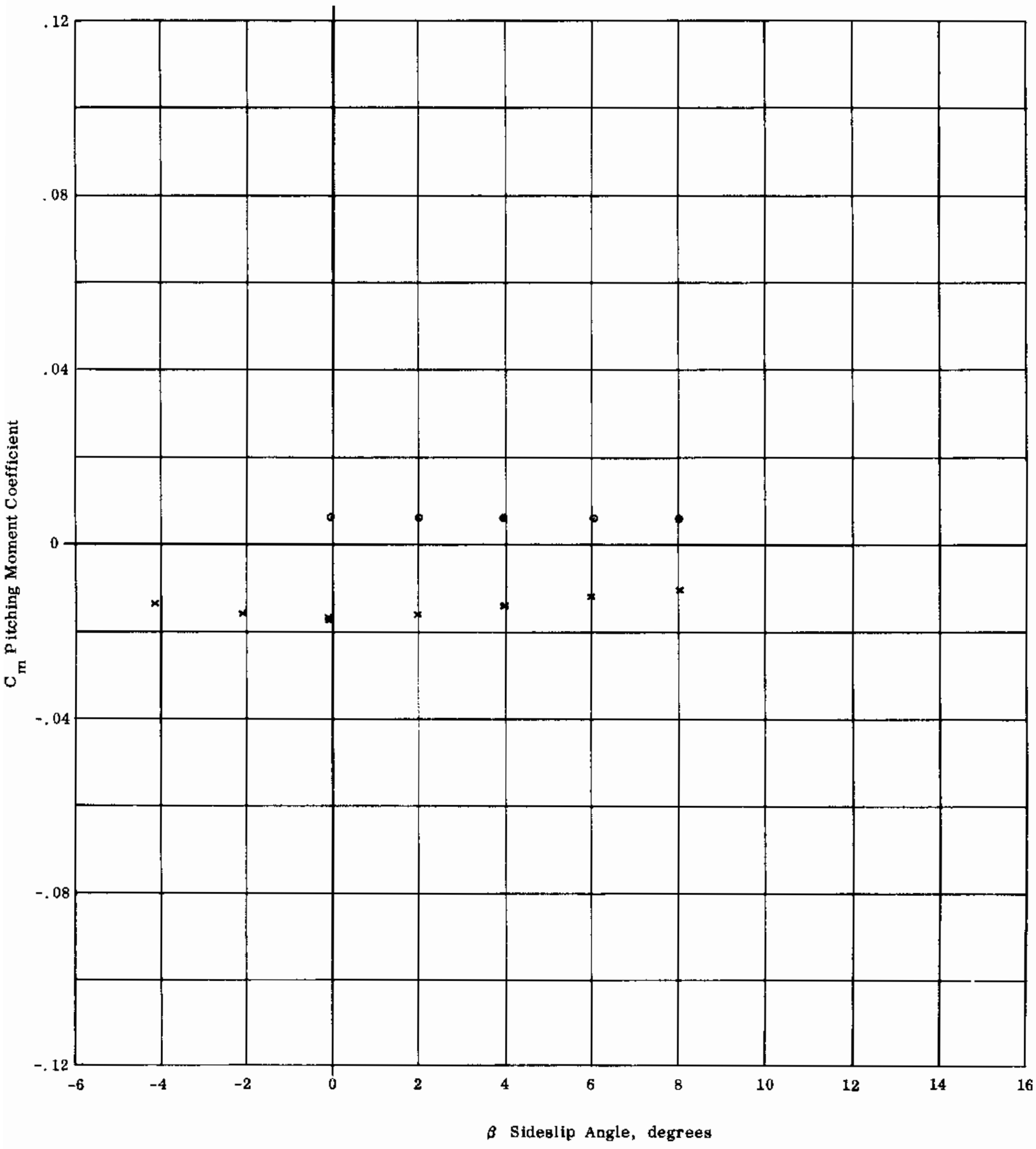

a) $\alpha = 0$

Fig. 8.5 Mach 8 Sideslip Polars for Basic Configuration (sheet 3 of 9)

No Flap Deflections

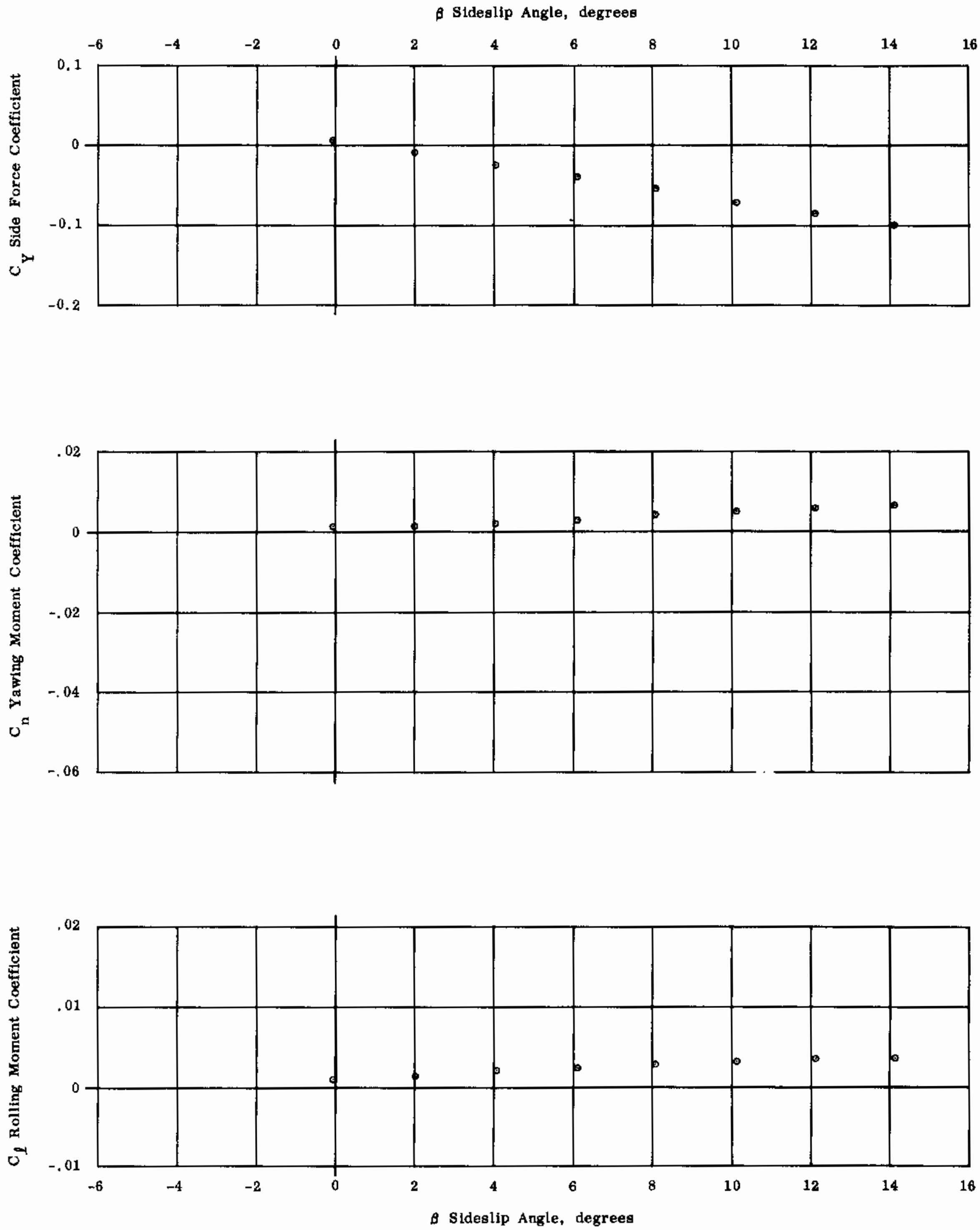

b) $\alpha = +7°$

Fig. 8.5 Mach 8 Sideslip Polars for Basic Configuration (sheet 4 of 9)

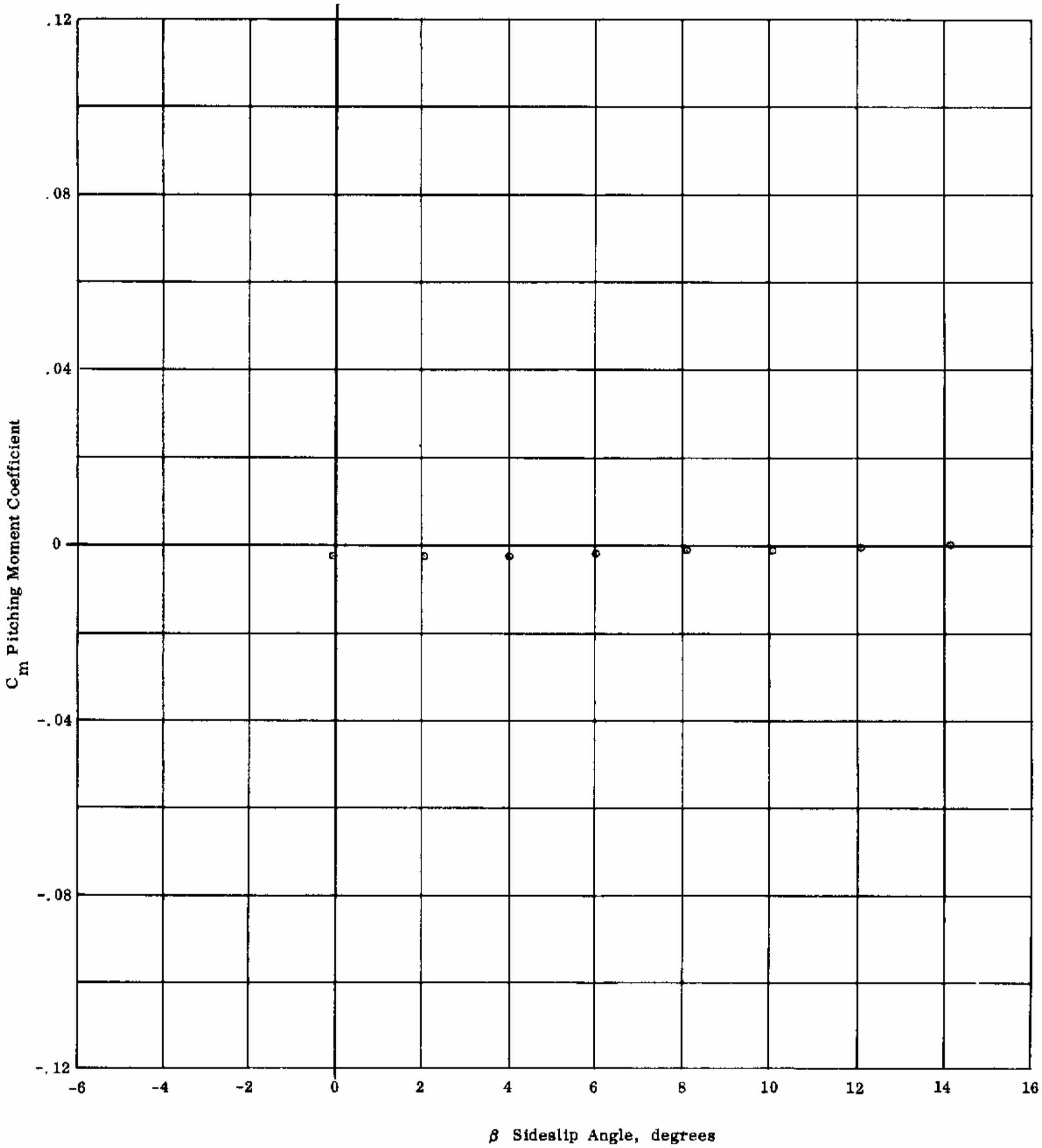

b) α = + 7°

Fig. 8.5 Mach 8 Sideslip Polars for Basic Configuration (sheet 5 of 9)

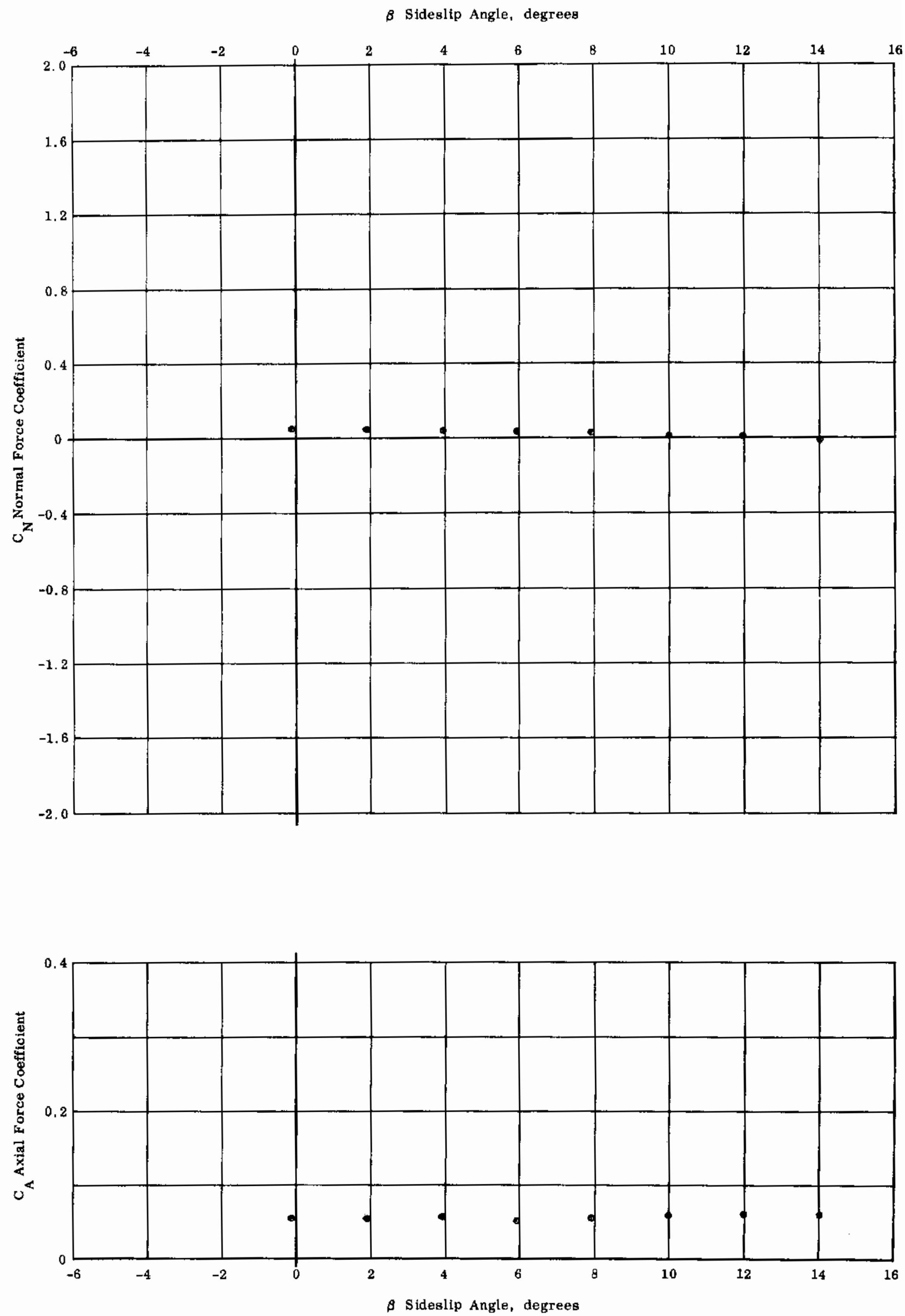

b) $\alpha = +7°$

Fig. 8.5 Mach 8 Sideslip Polars for Basic Configuration (sheet 6 of 9)

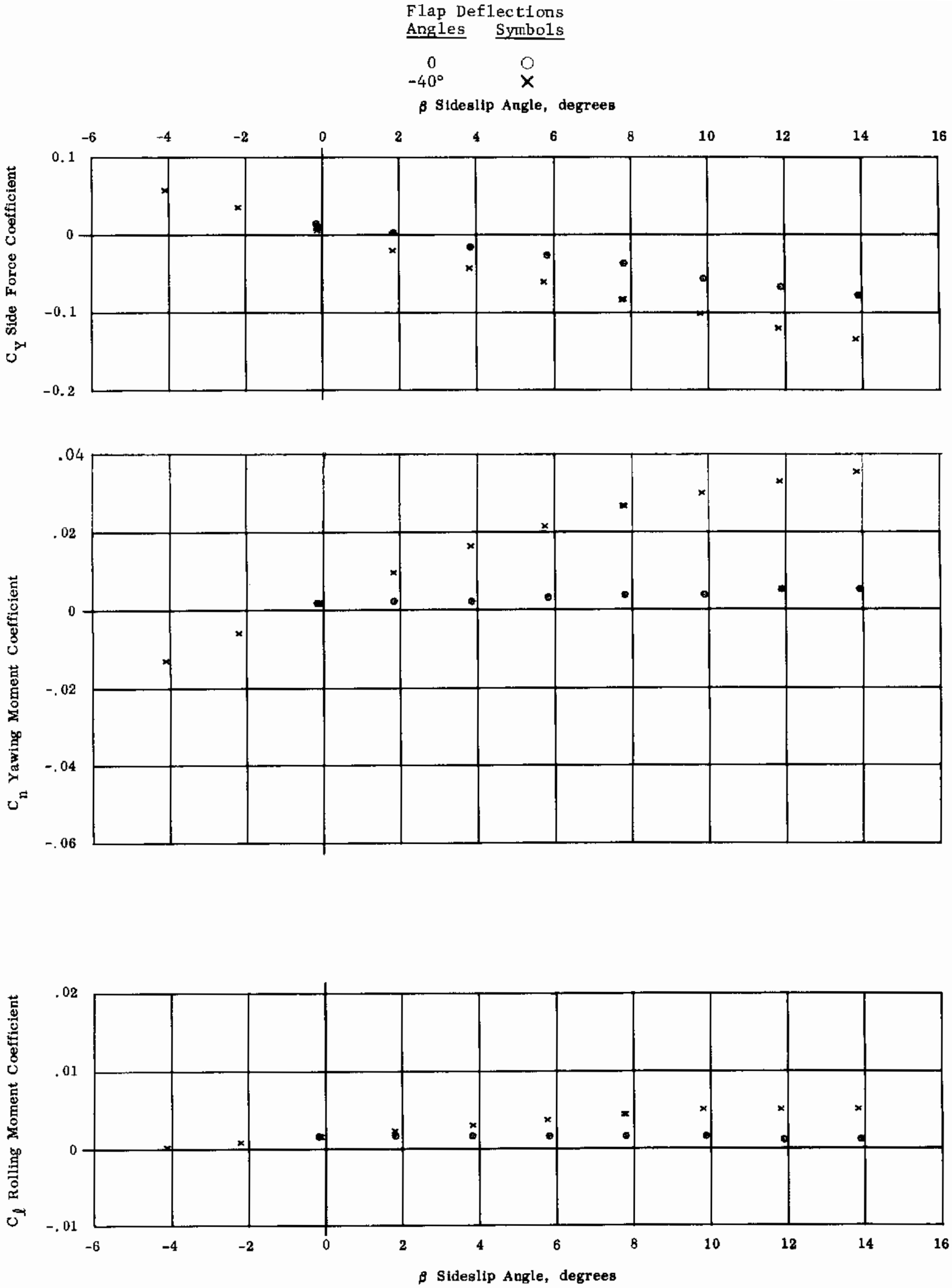

c) α = + 14.3°

Fig. 8.5 Mach 8 Sideslip Polars for Basic Configuration (sheet 7 of 9)

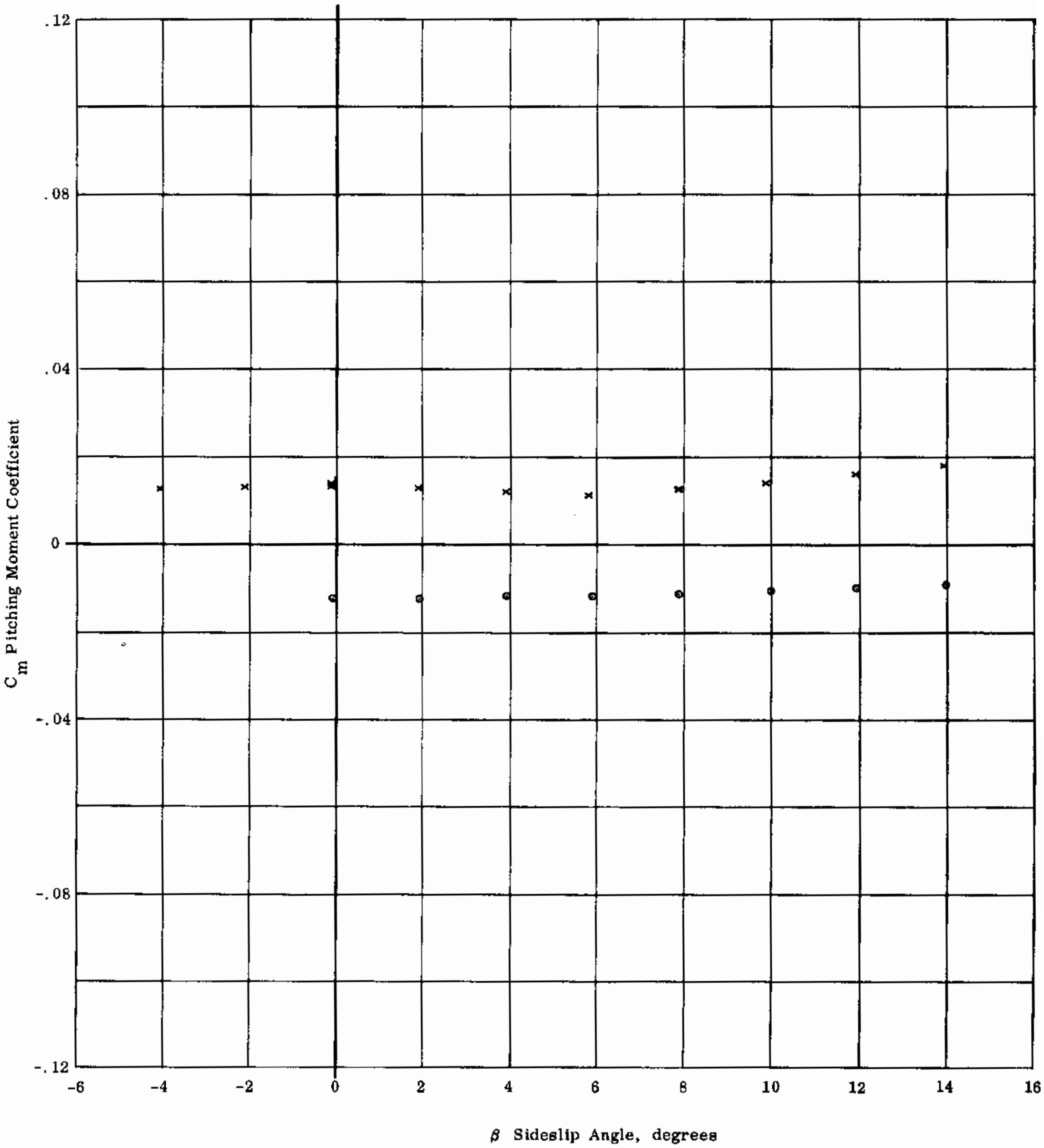

c) α = + 14.3°

Fig. 8.5 Mach 8 Sideslip Polars for Basic Configuration (sheet 8 of 9)

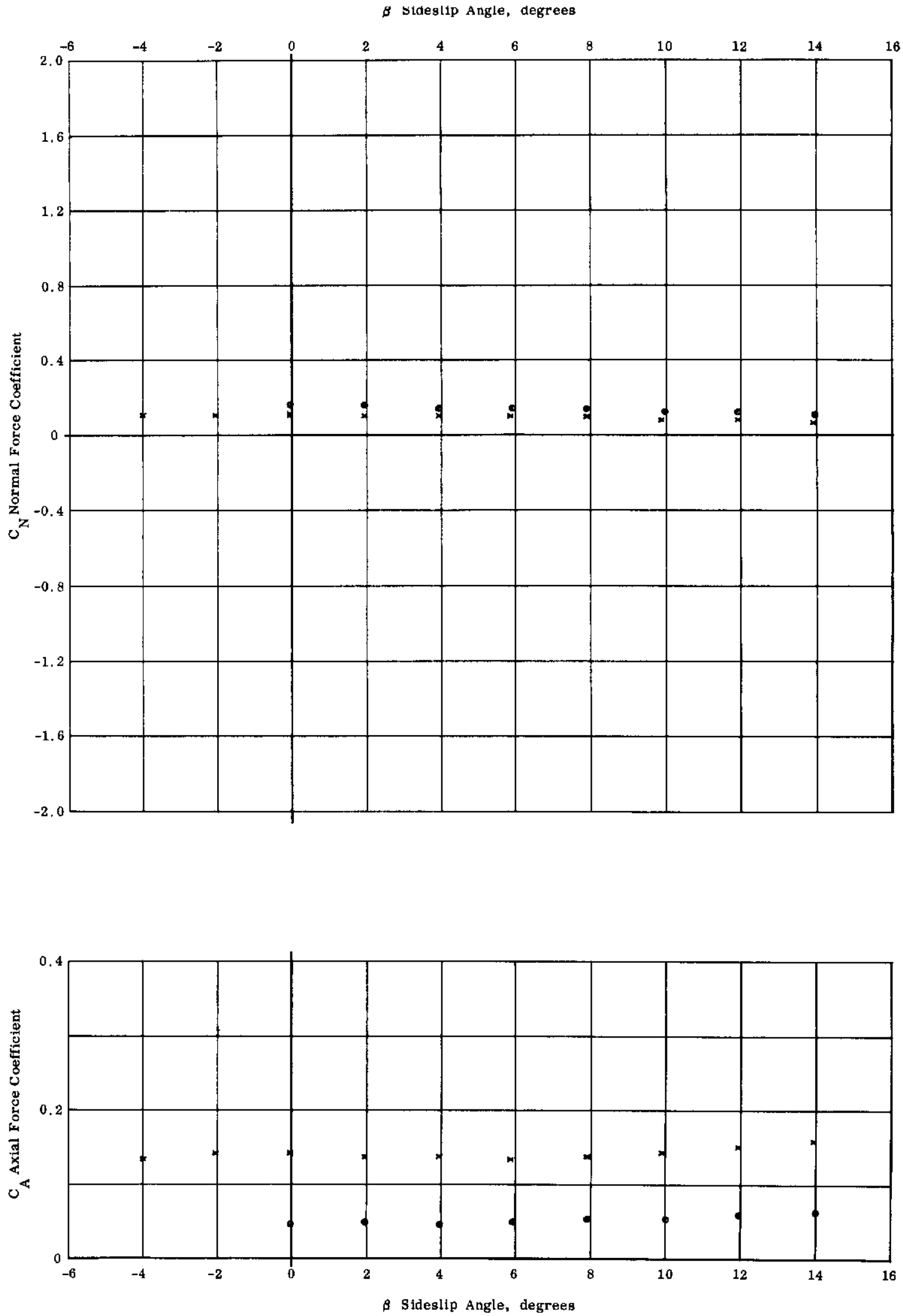

c) α = + 14.3°

Fig. 8.5 Mach 8 Sideslip Polars for Basic Configuration (sheet 9 of 9)

Flap Deflections

Angles	Symbols
0	○
-10°	□
-20°	▷
-30°	◇
-40°	×

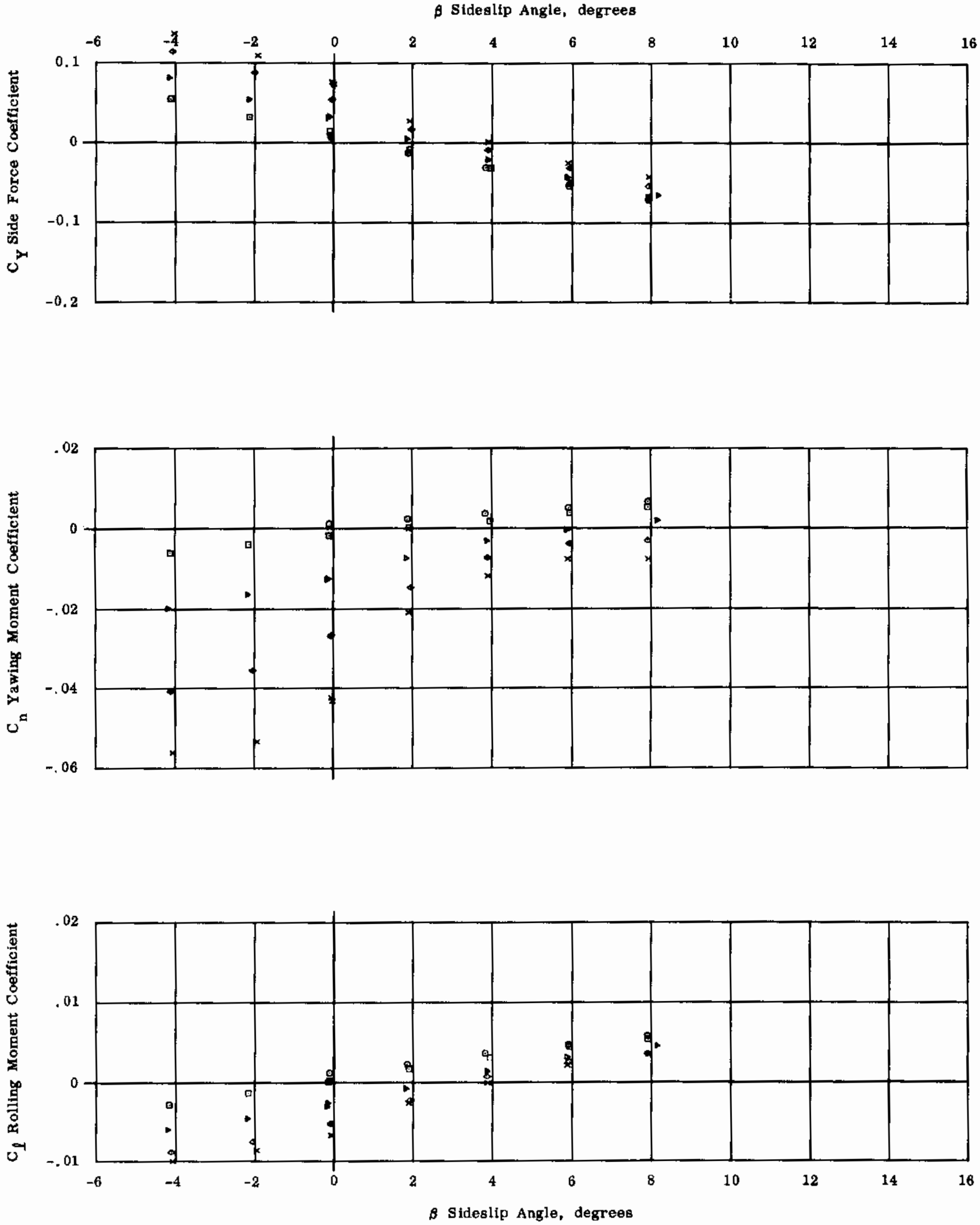

a) α = 0

Fig. 8.6 Mach 8 Sideslip Polars for Basic Configuration with Upper Surface Port Flap Deflections (sheet 1 of 9)

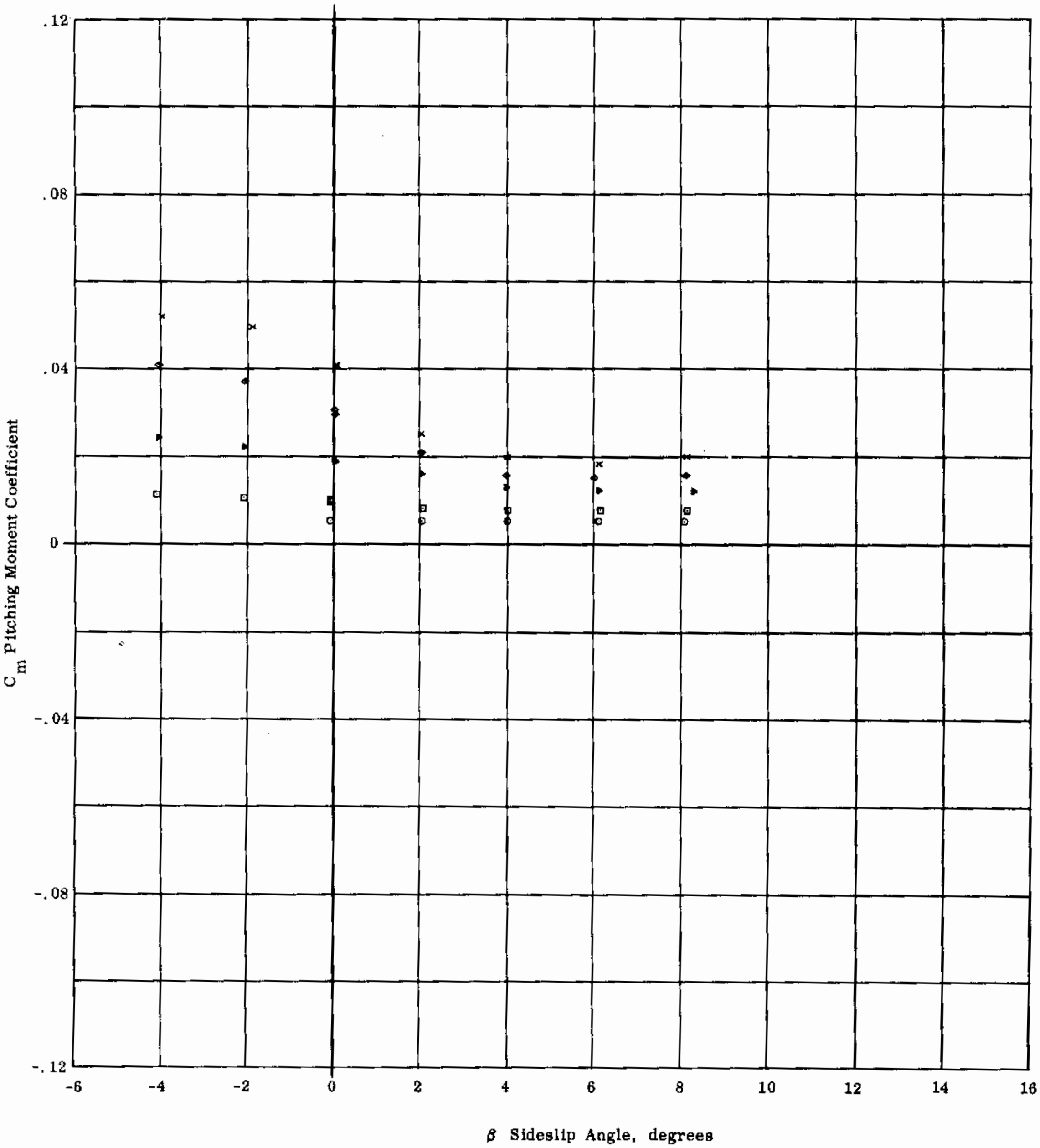

a) α = 0

Fig. 8.6 Mach 8 Sideslip Polars for Basic Configuration with Upper Surface Port Flap Deflections (sheet 2 of 9)

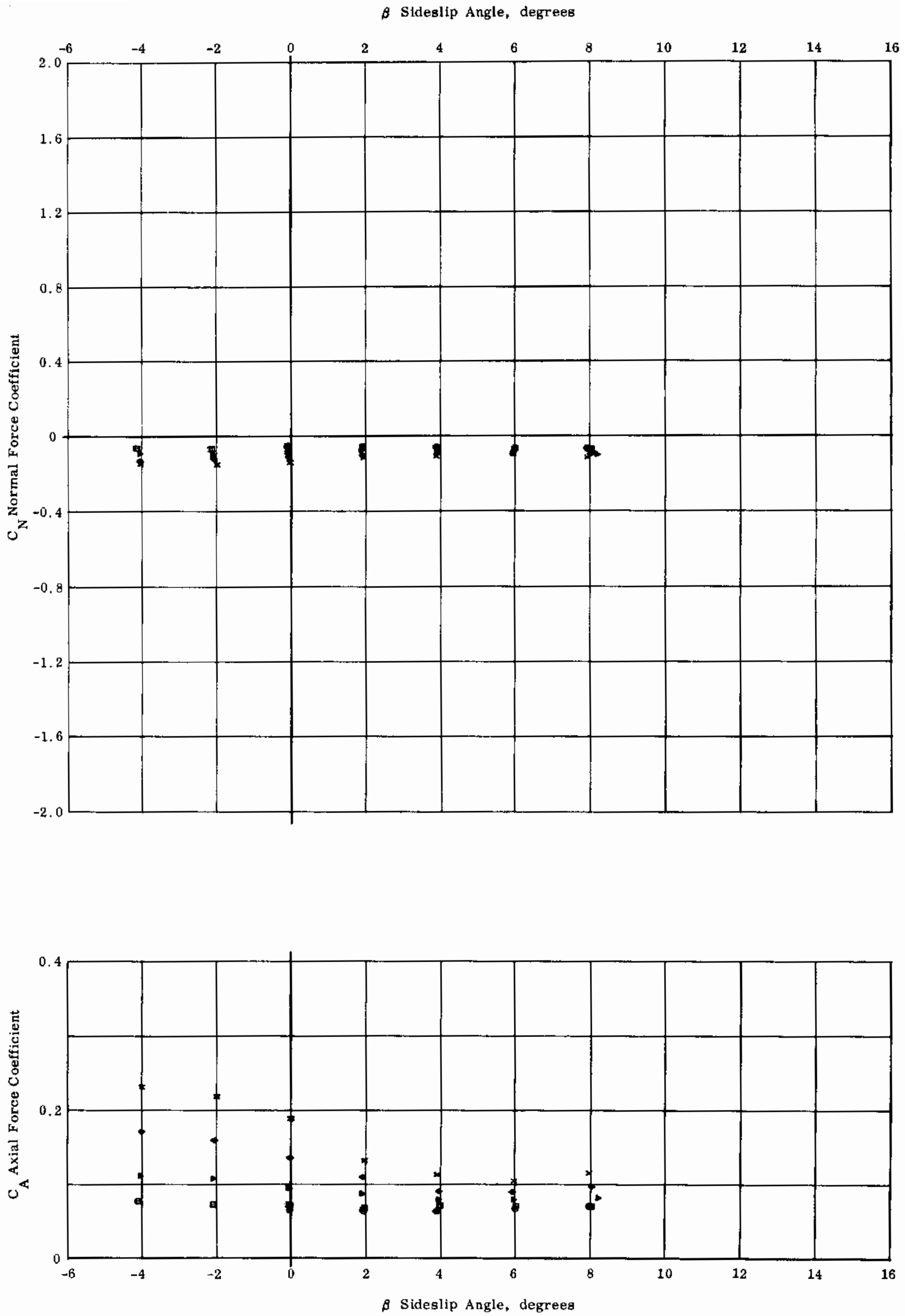

a) α = 0

Fig. 8.6 Mach 8 Sideslip Polars for Basic Configuration with Upper Surface Port Flap Deflections (sheet 3 of 9)

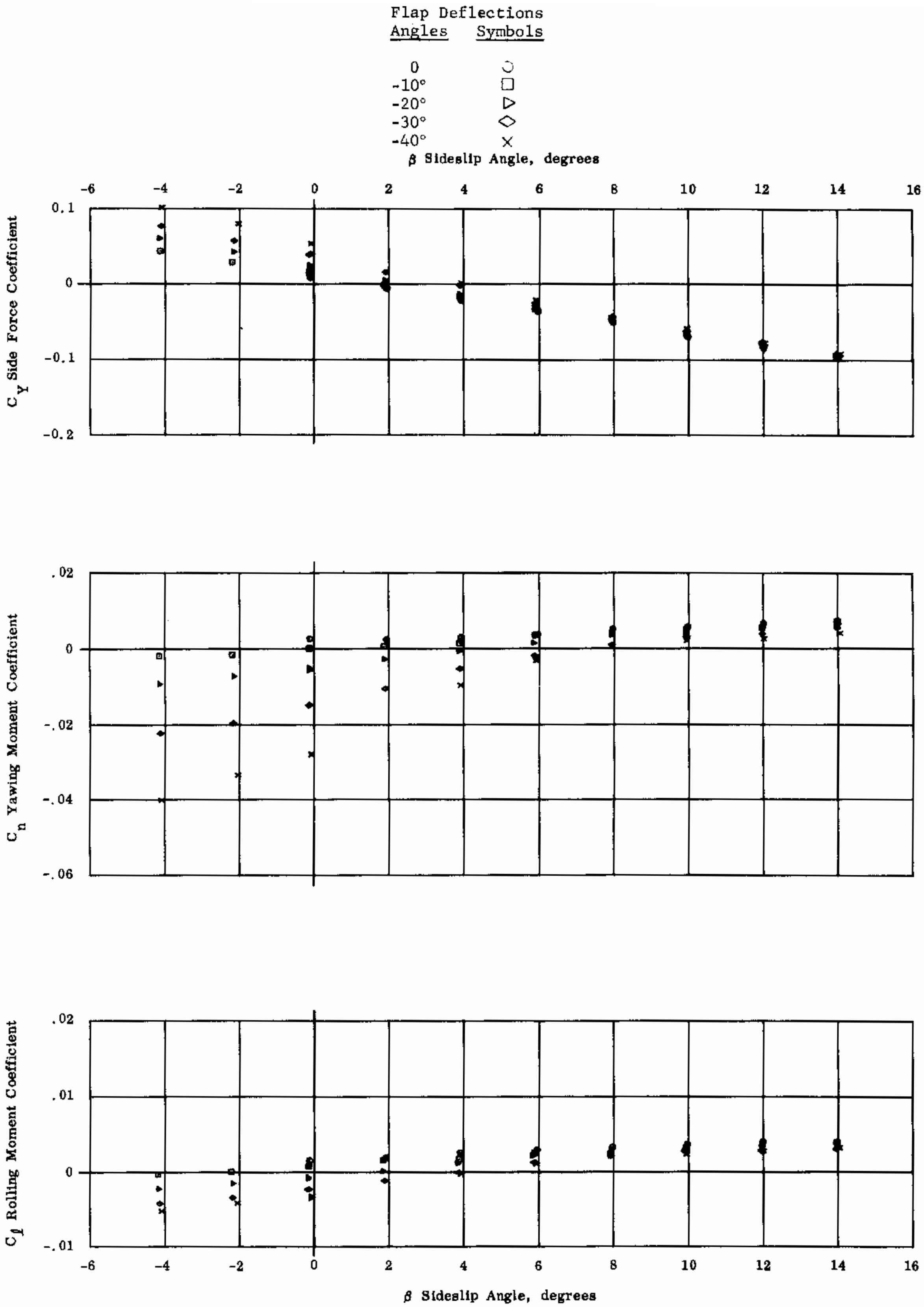

b) α = + 7°

Fig. 8.6 Mach 8 Sideslip Polars for Basic Configuration with Upper Surface Port Flap Deflections (sheet 4 of 9)

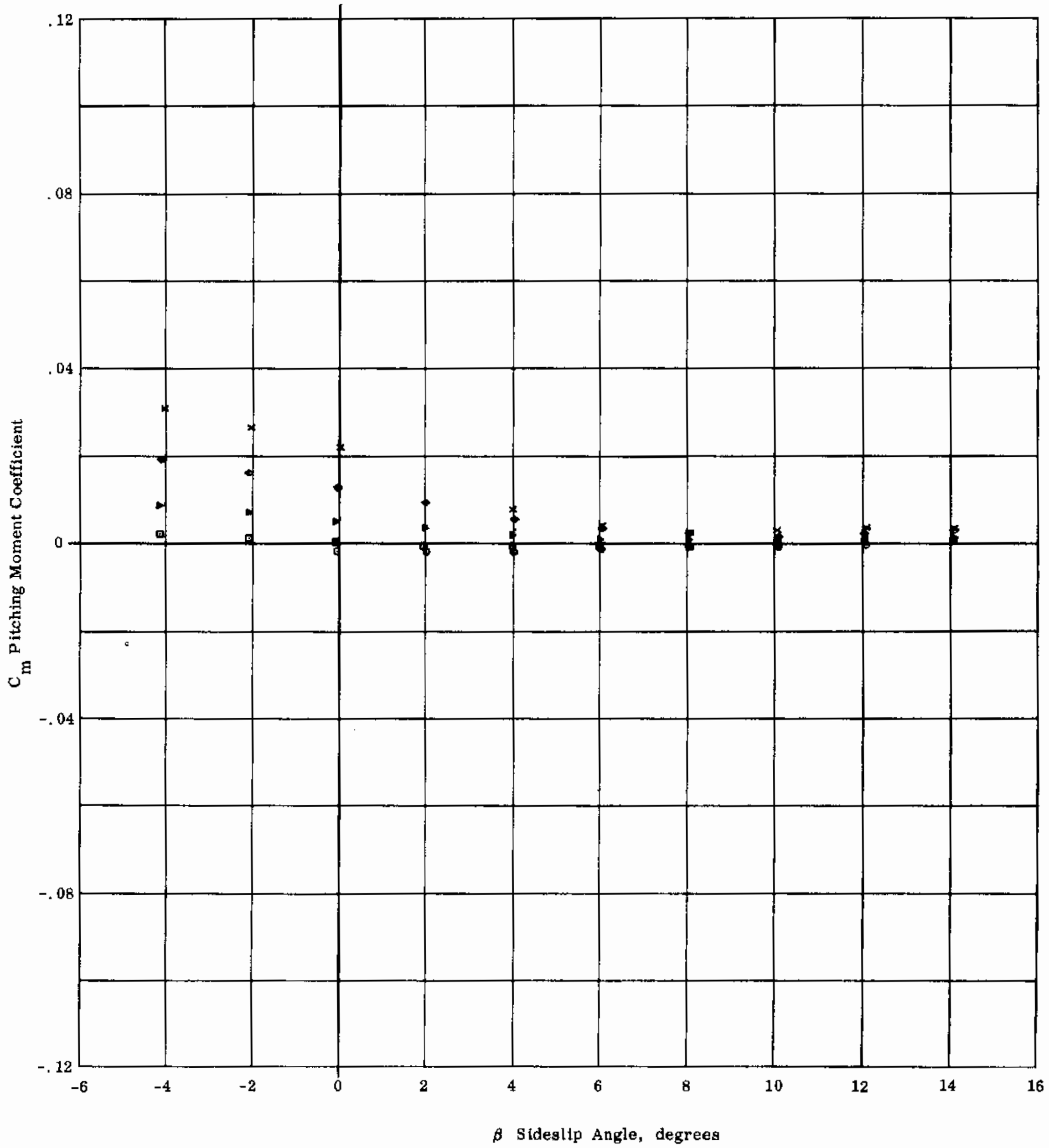

b) $\alpha = + 7°$

Fig. 8.6 Mach 8 Sideslip Polars for Basic Configuration with Upper Surface Port Flap Deflections (sheet 5 of 9)

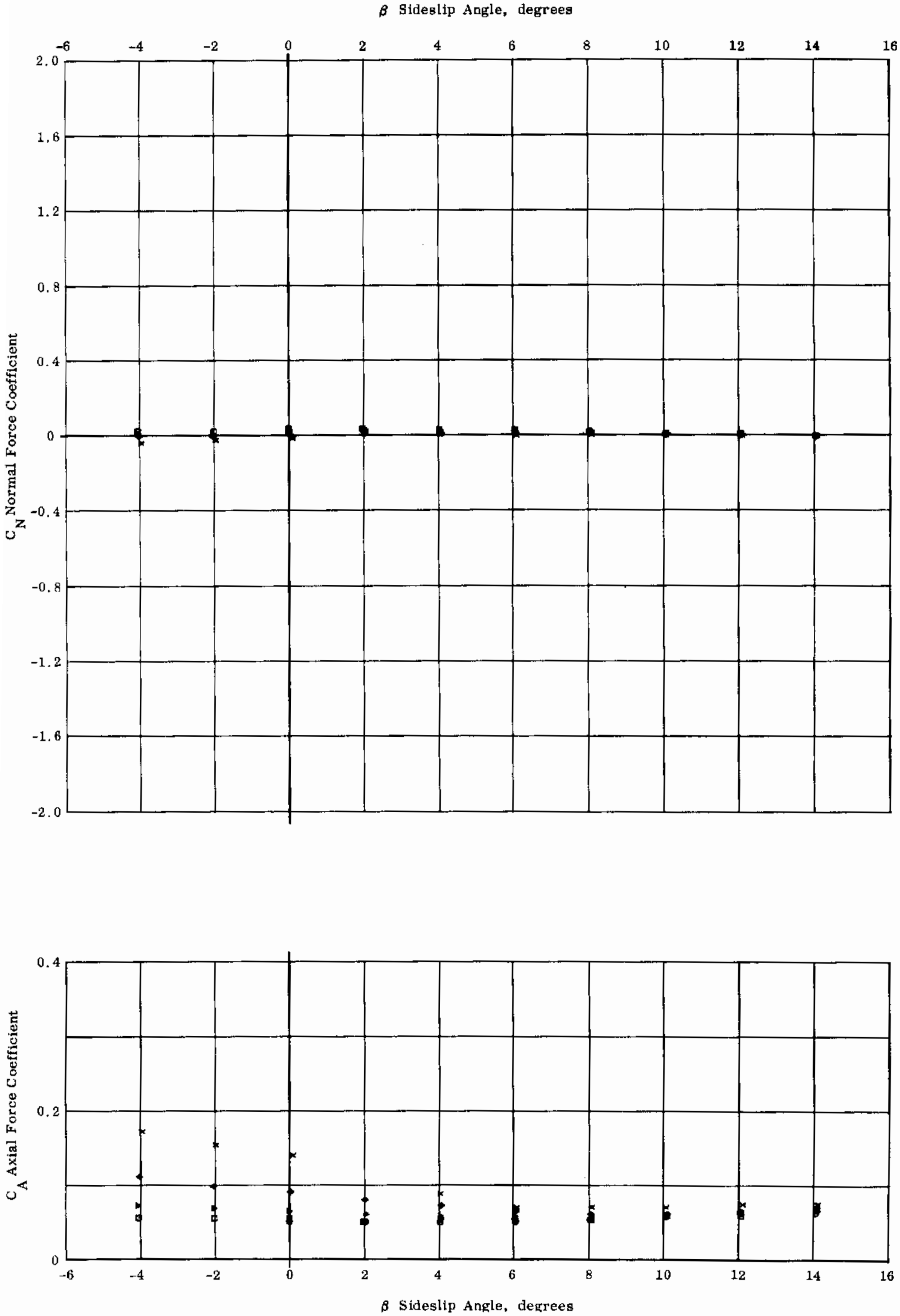

b) α = + 7°

Fig. 8.6 Mach 8 Sideslip Polars for Basic Configuration with Upper Surface Port Flap Deflections (sheet 6 of 9)

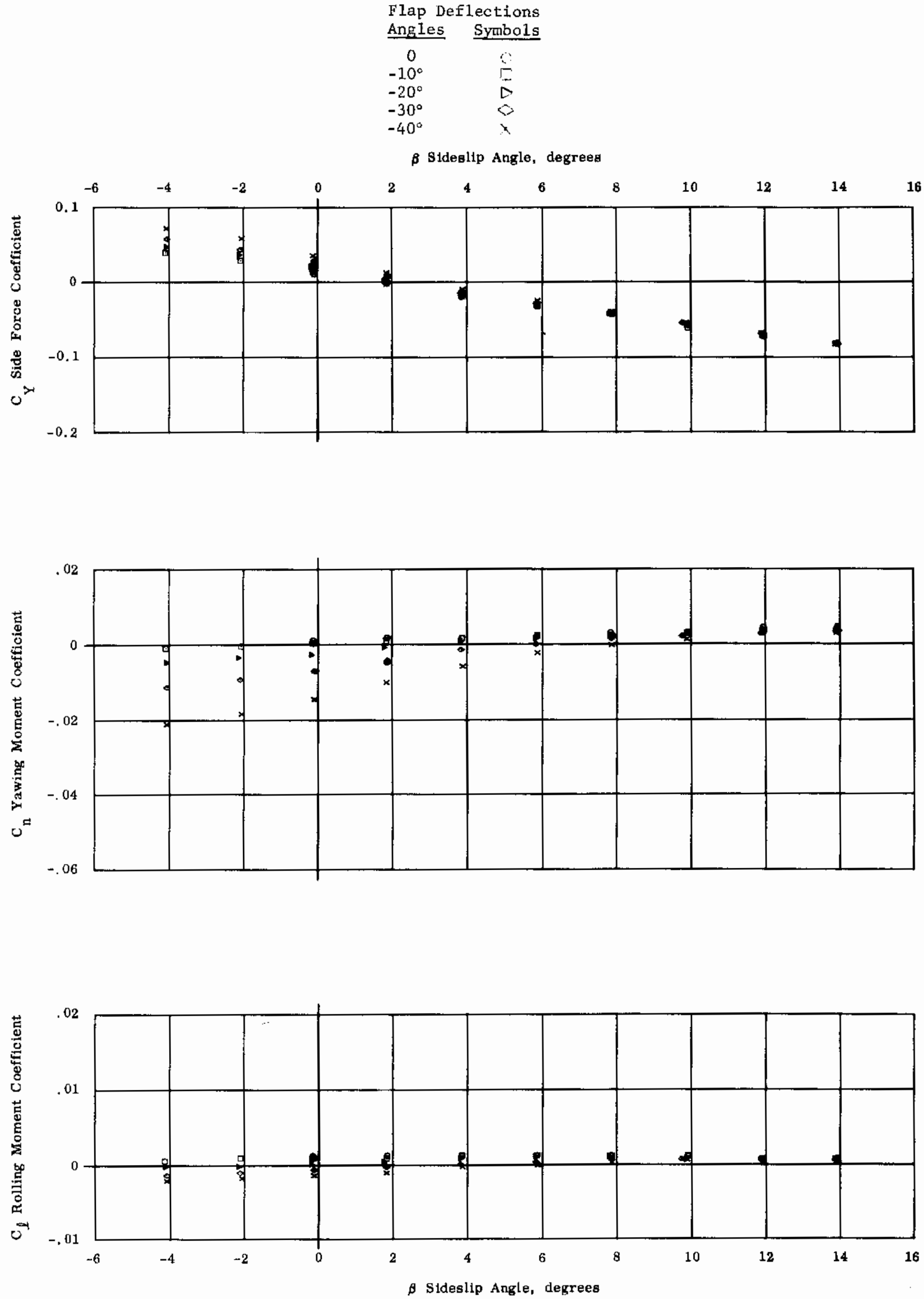

c) $\alpha = +14.3°$

Fig. 8.6 Mach 8 Sideslip Polars for Basic Configuration with Upper Surface Port Flap Deflections (sheet 7 of 9)

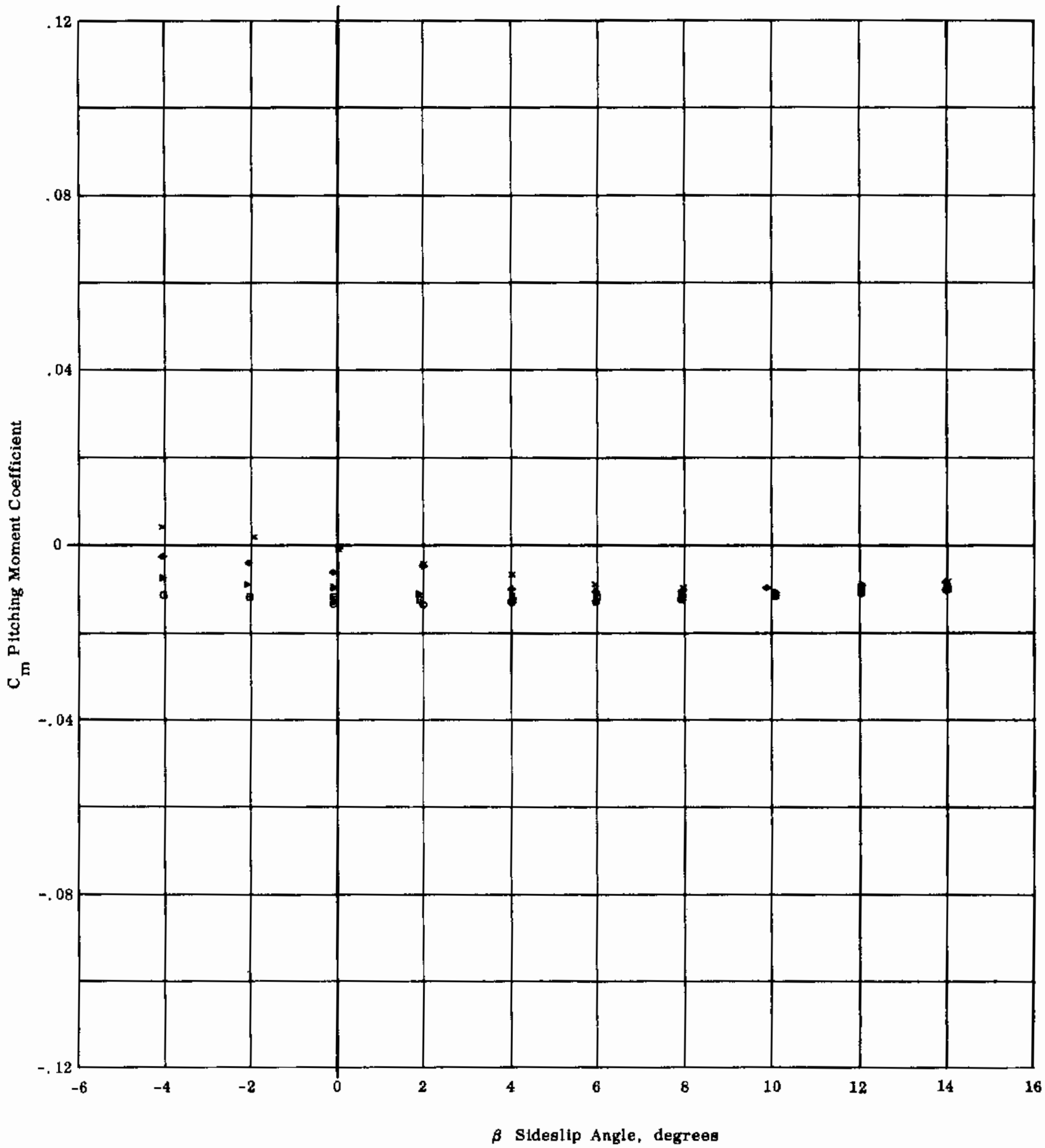

c) α = + 14.3°

Fig. 8.6 Mach 8 Sideslip Polars for Basic Configuration with Upper Surface Port Flap Deflections (sheet 8 of 9)

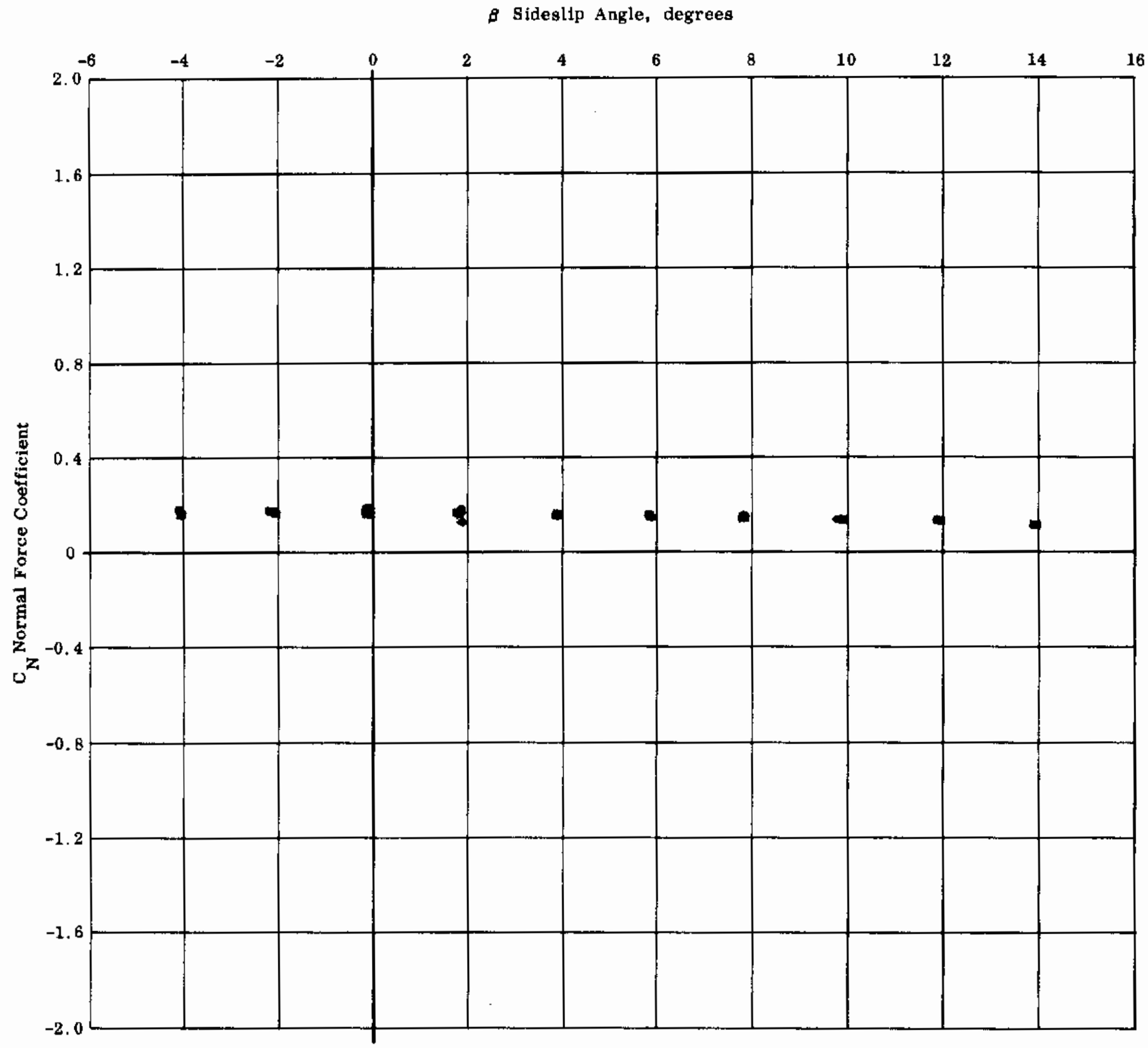

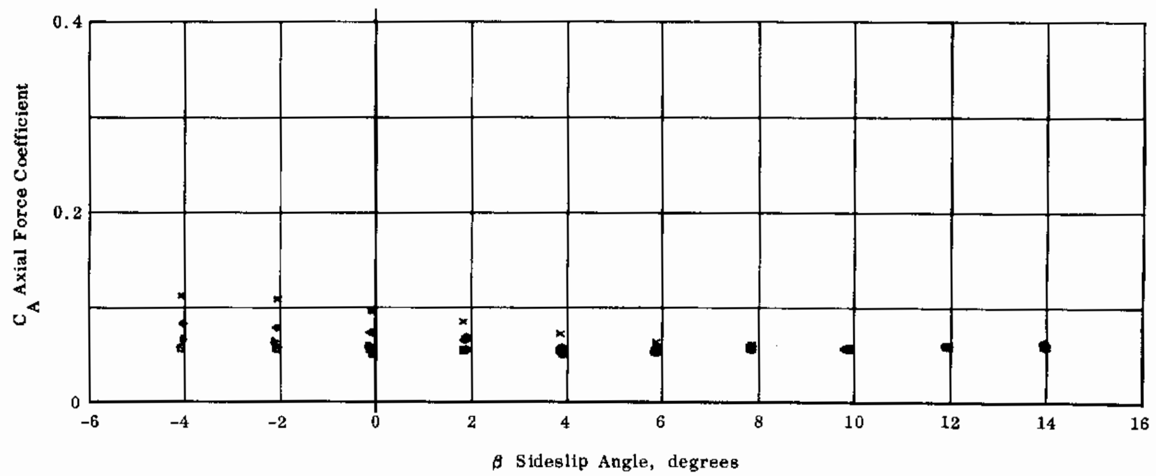

c) $\alpha = +14.3°$

Fig. 8.6 Mach 8 Sideslip Polars for Basic Configuration with Upper Surface Port Flap Deflections (sheet 9 of 9)

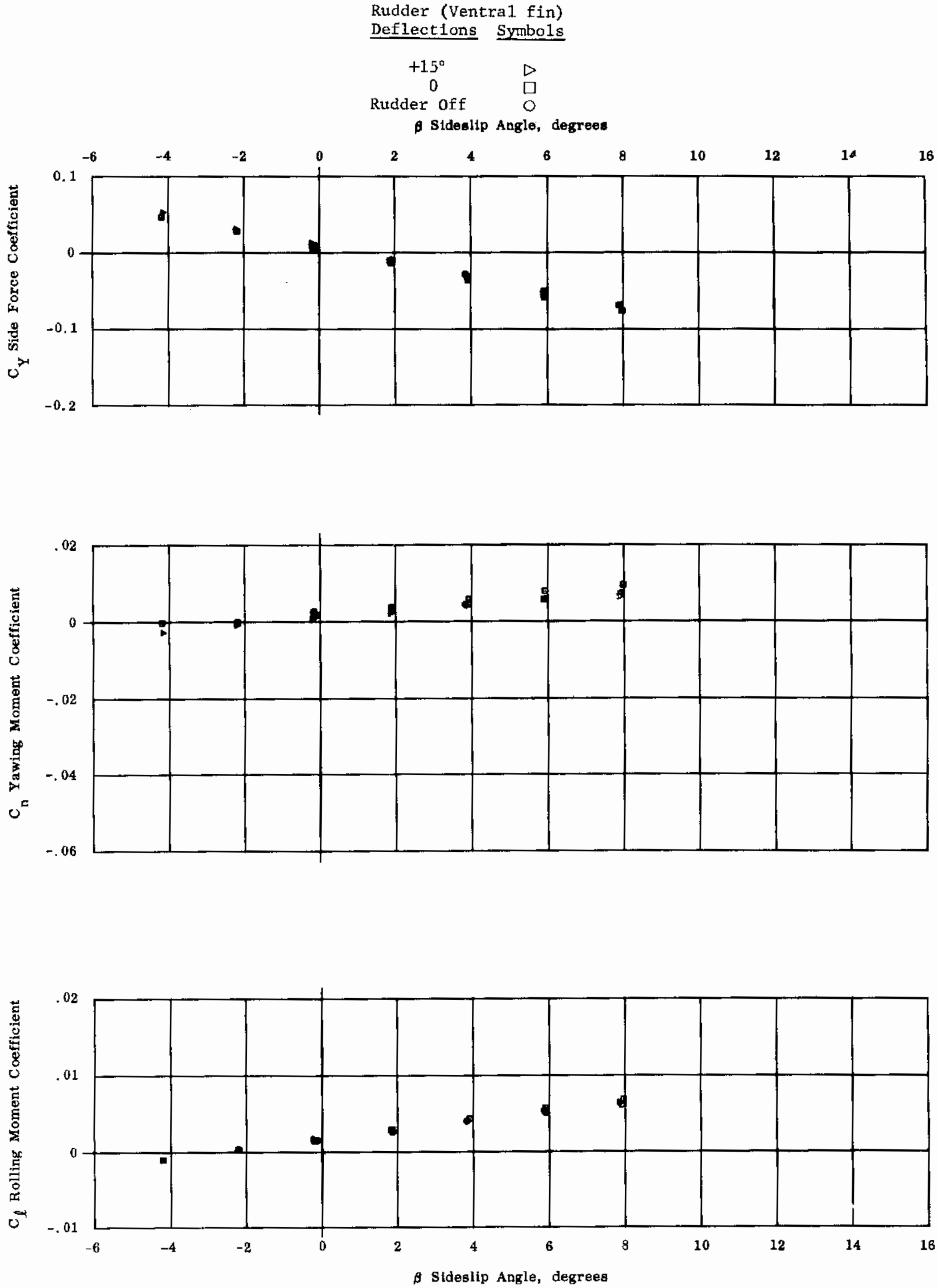

a) α = 0

Fig. 8.7 Mach 8 Sideslip Polars for Basic Configuration with Ventral Fin (sheet 1 of 9)

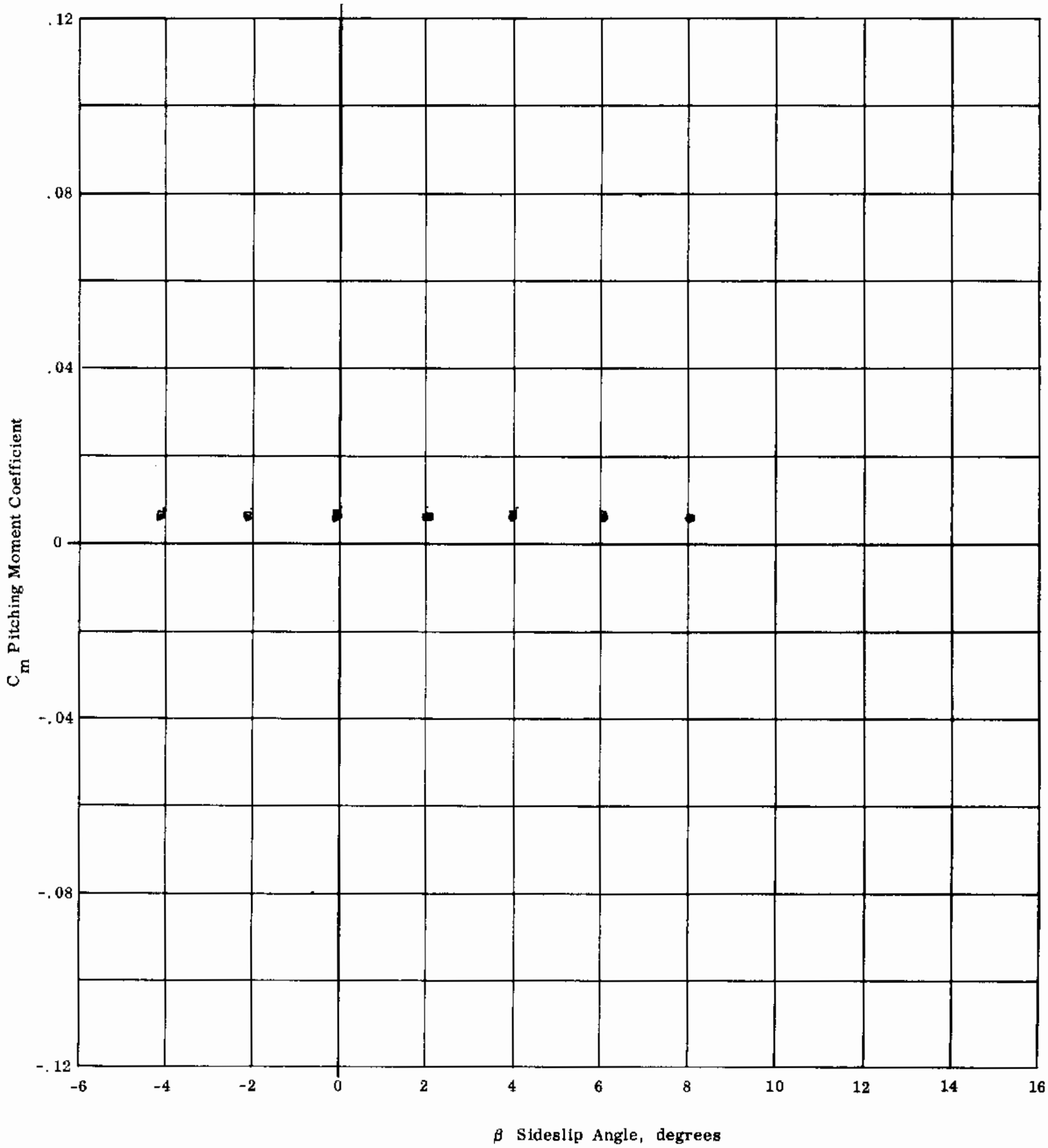

a) α = 0

Fig. 8.7 Mach 8 Sideslip Polars for Basic Configuration with Ventral Fin (sheet 2 of 9)

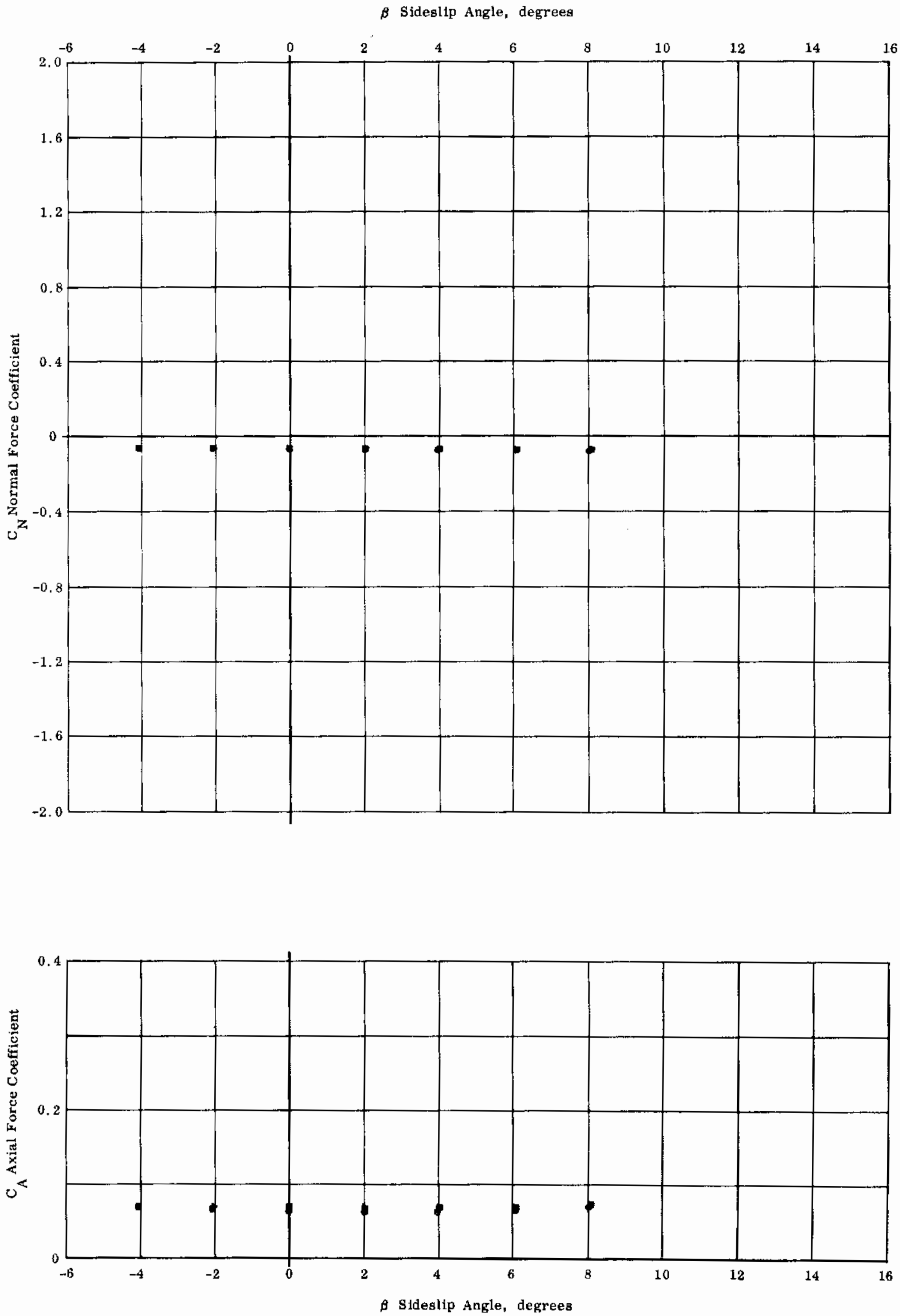

a) α = 0

Fig. 8.7 Mach 8 Sideslip Polars for Basic Configuration with Ventral Fin (sheet 3 of 9)

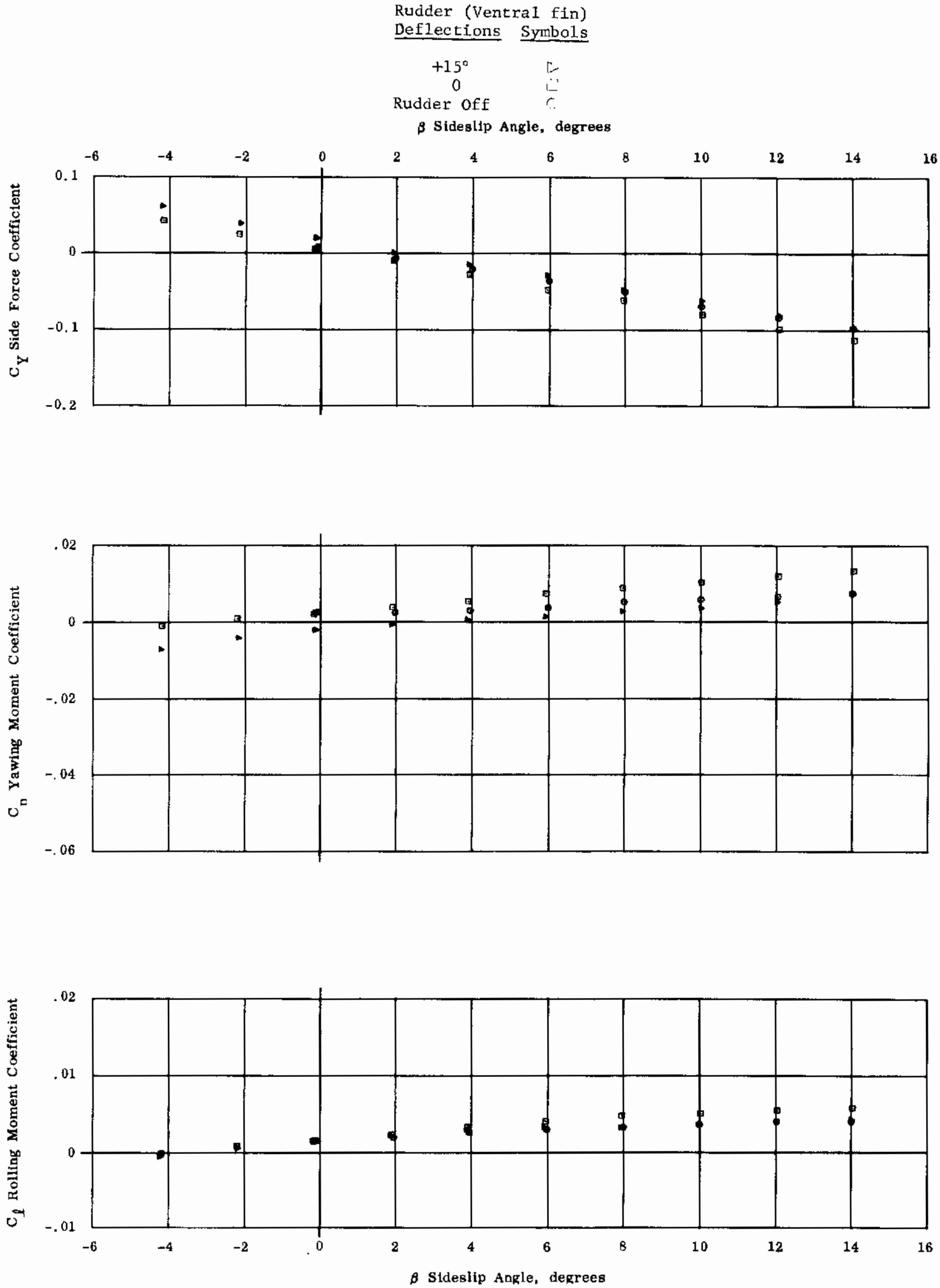

b) $\alpha = +7°$

Fig. 8.7 Mach 8 Sideslip Polars for Basic Configuration with Ventral Fin (sheet 4 of 9)

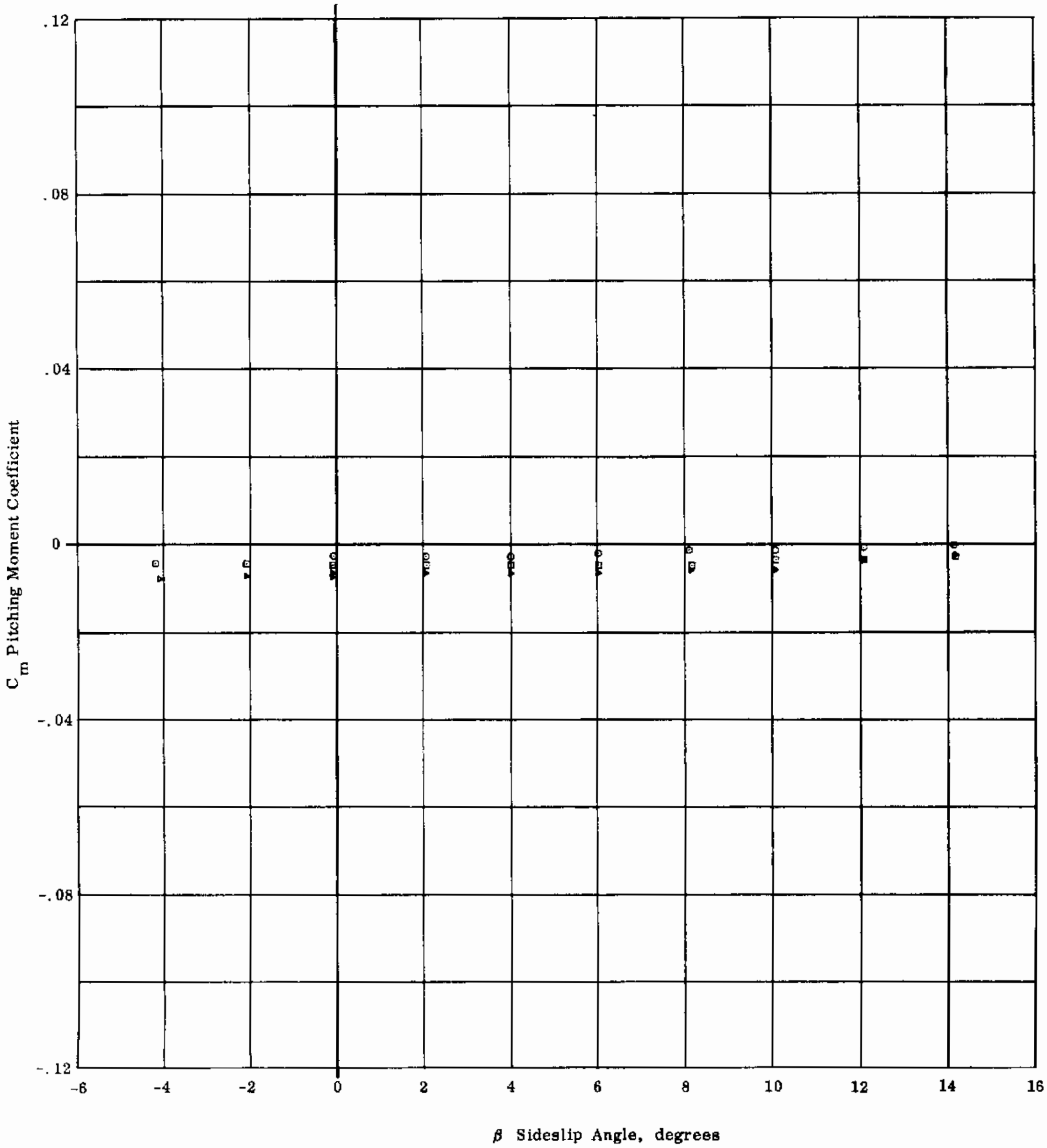

b) α = + 7°

Fig. 8.7 Mach 8 Sideslip Polars for Basic Configuration with Ventral Fin (sheet 5 of 9)

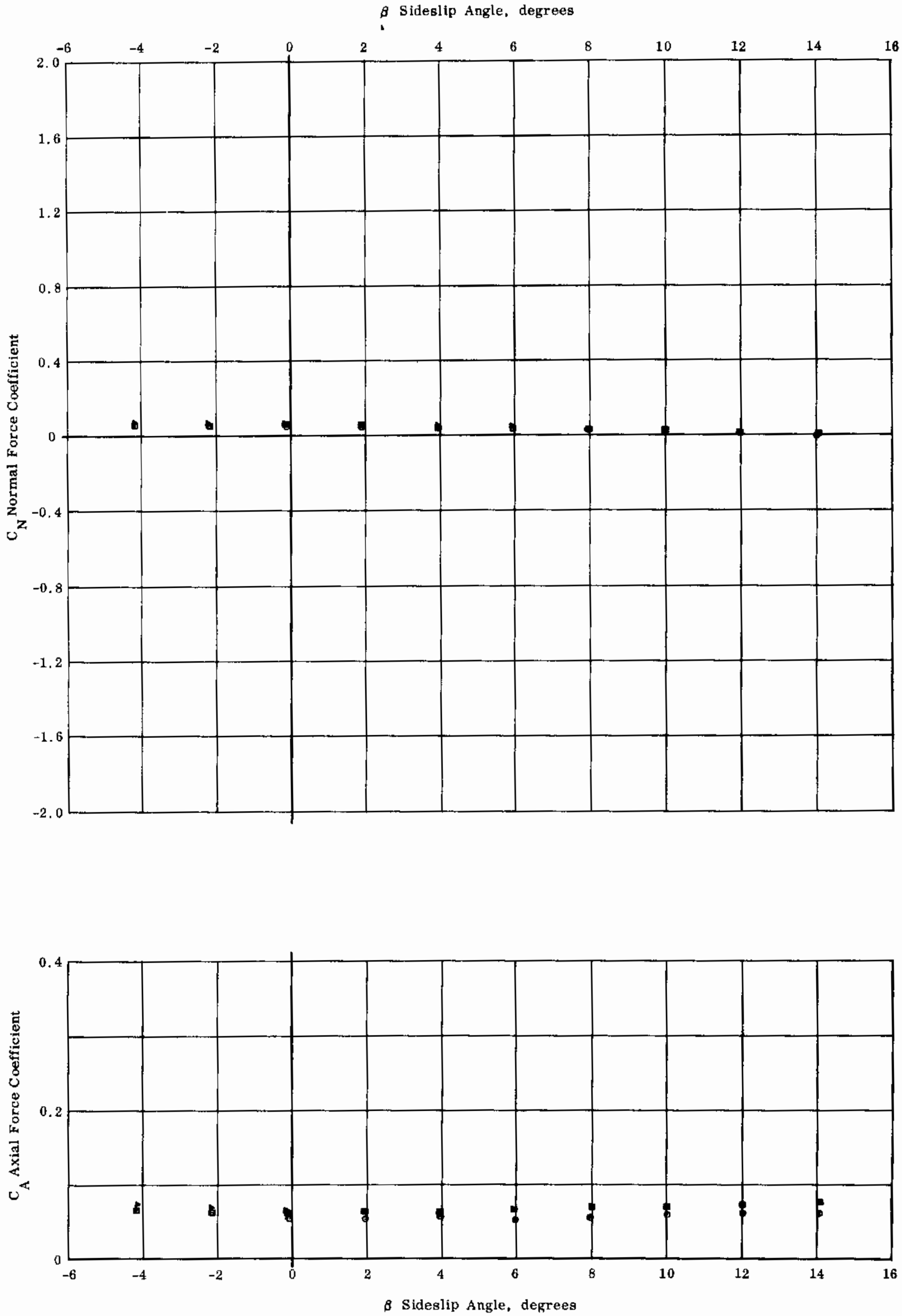

b) α = + 7°

Fig. 8.7 Mach 8 Sideslip Polars for Basic Configuration with Ventral Fin (sheet 6 of 9)

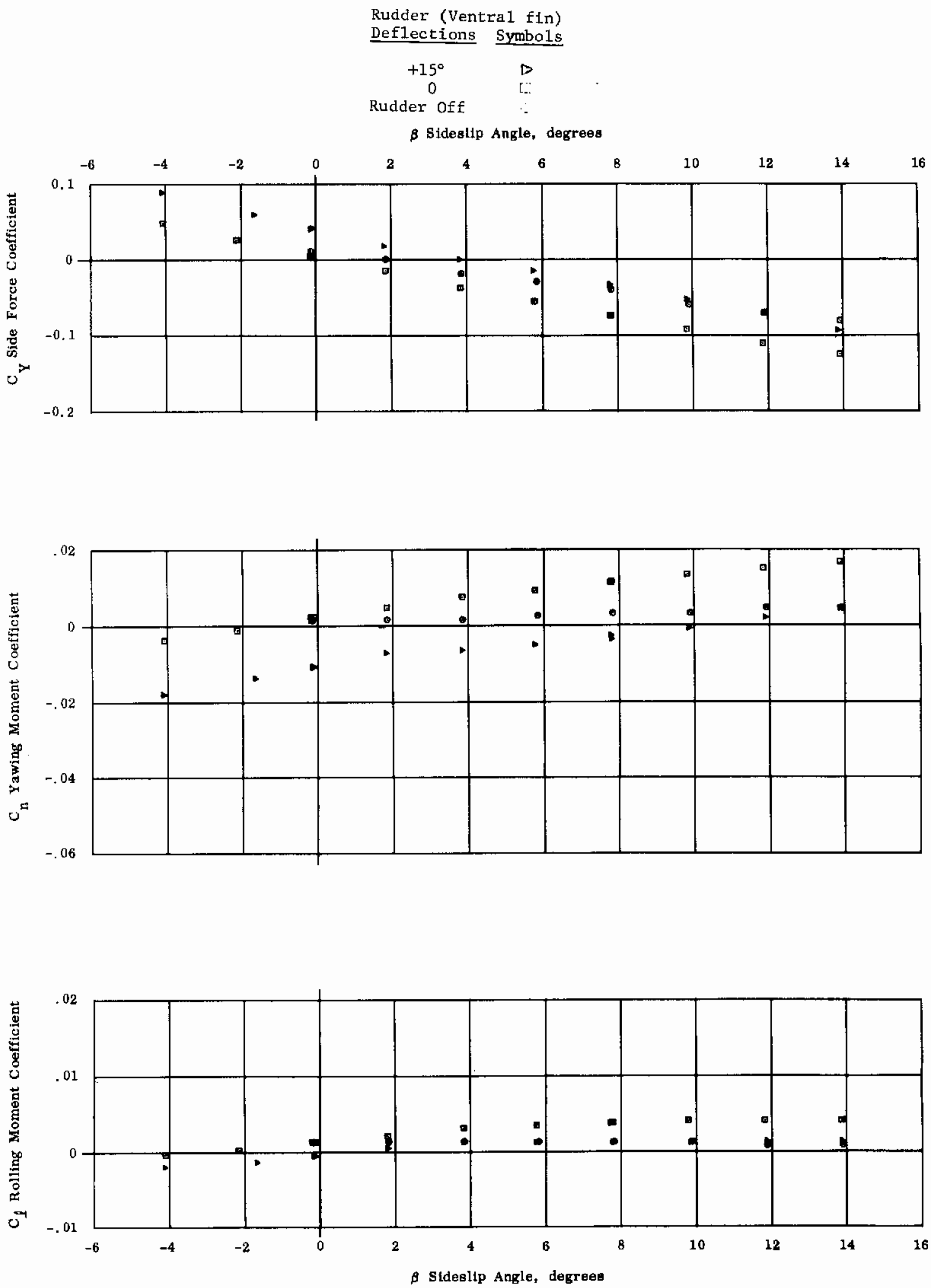

c) α = + 14.3°

Fig. 8.7 Mach 8 Sideslip Polars for Basic Configuration with Ventral Fin (sheet 7 of 9)

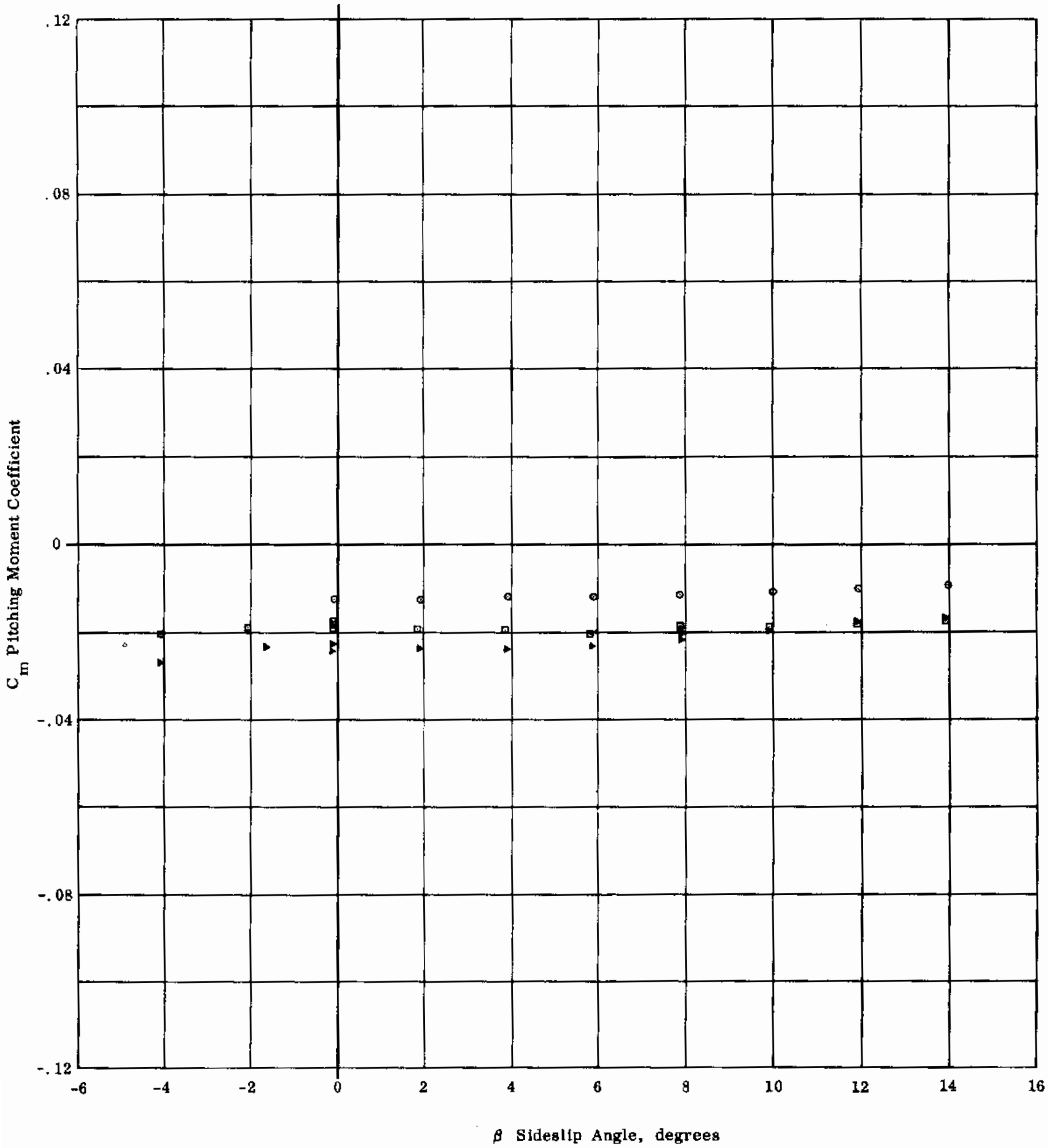

c) α = 14.3°

Fig. 8.7 Mach 8 Sideslip Polars for Basic Configuration with Ventral Fin (sheet 8 of 9)

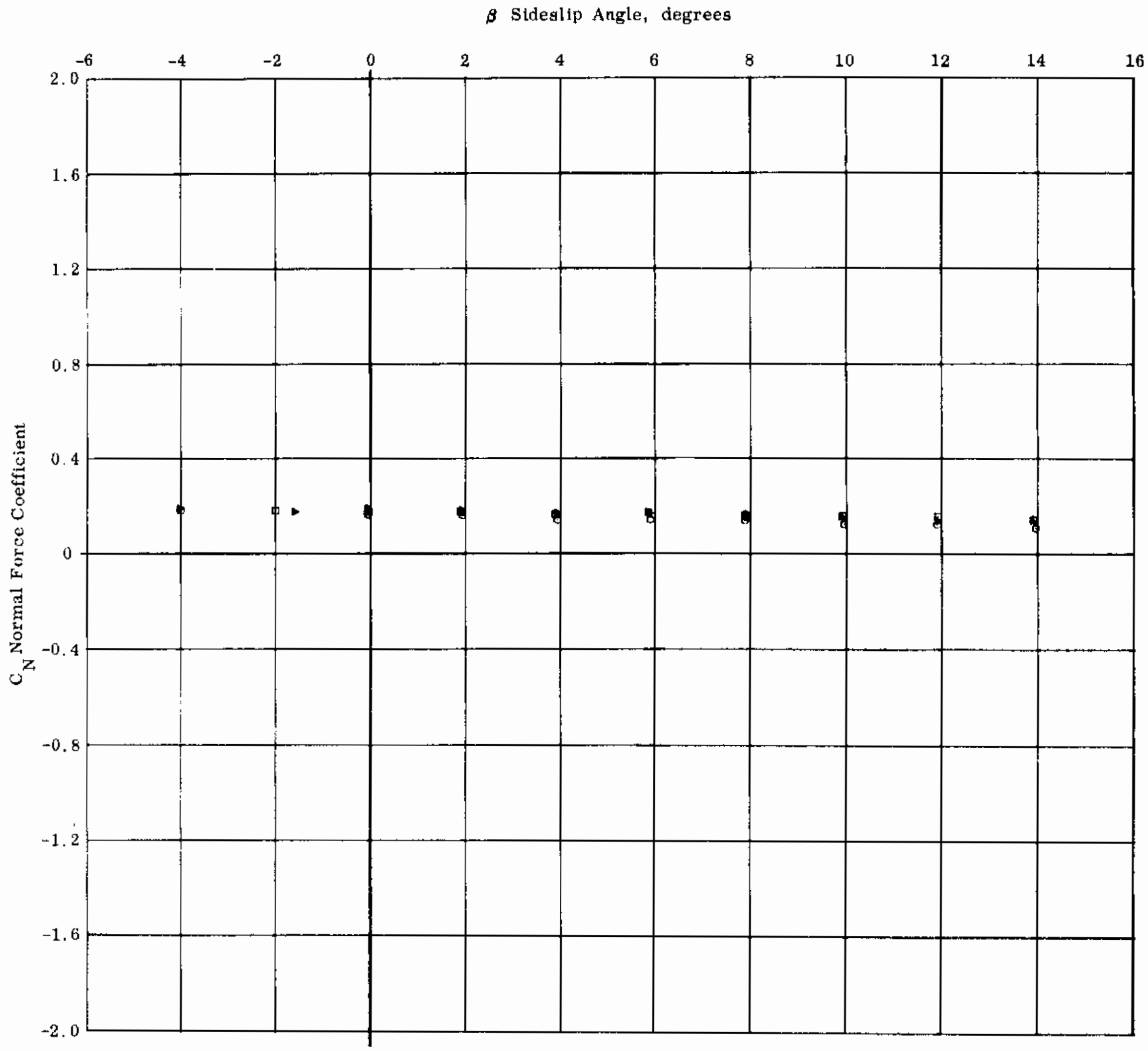

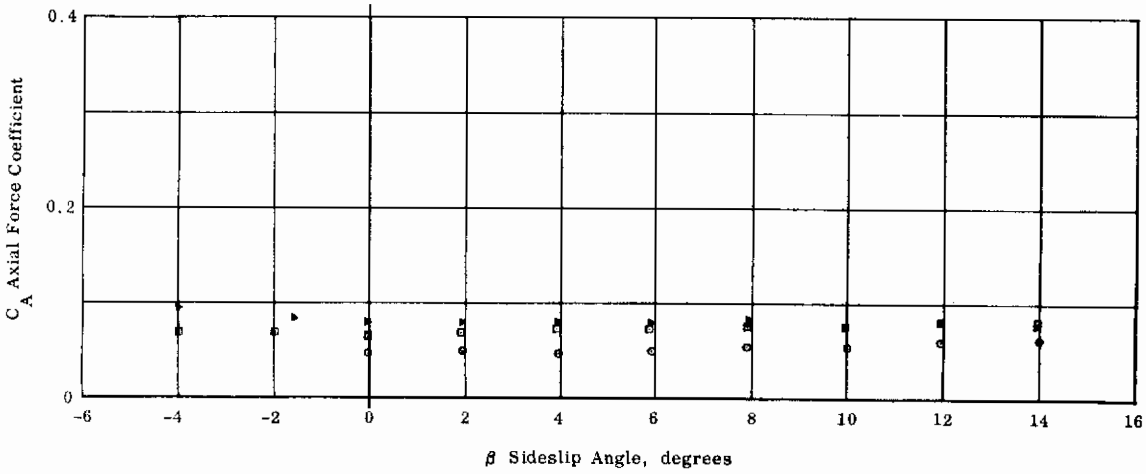

c) $\alpha = +14.3°$

Fig. 8.7 Mach 8 Sideslip Polars for Basic Configuration with Ventral Fin (sheet 9 of 9)

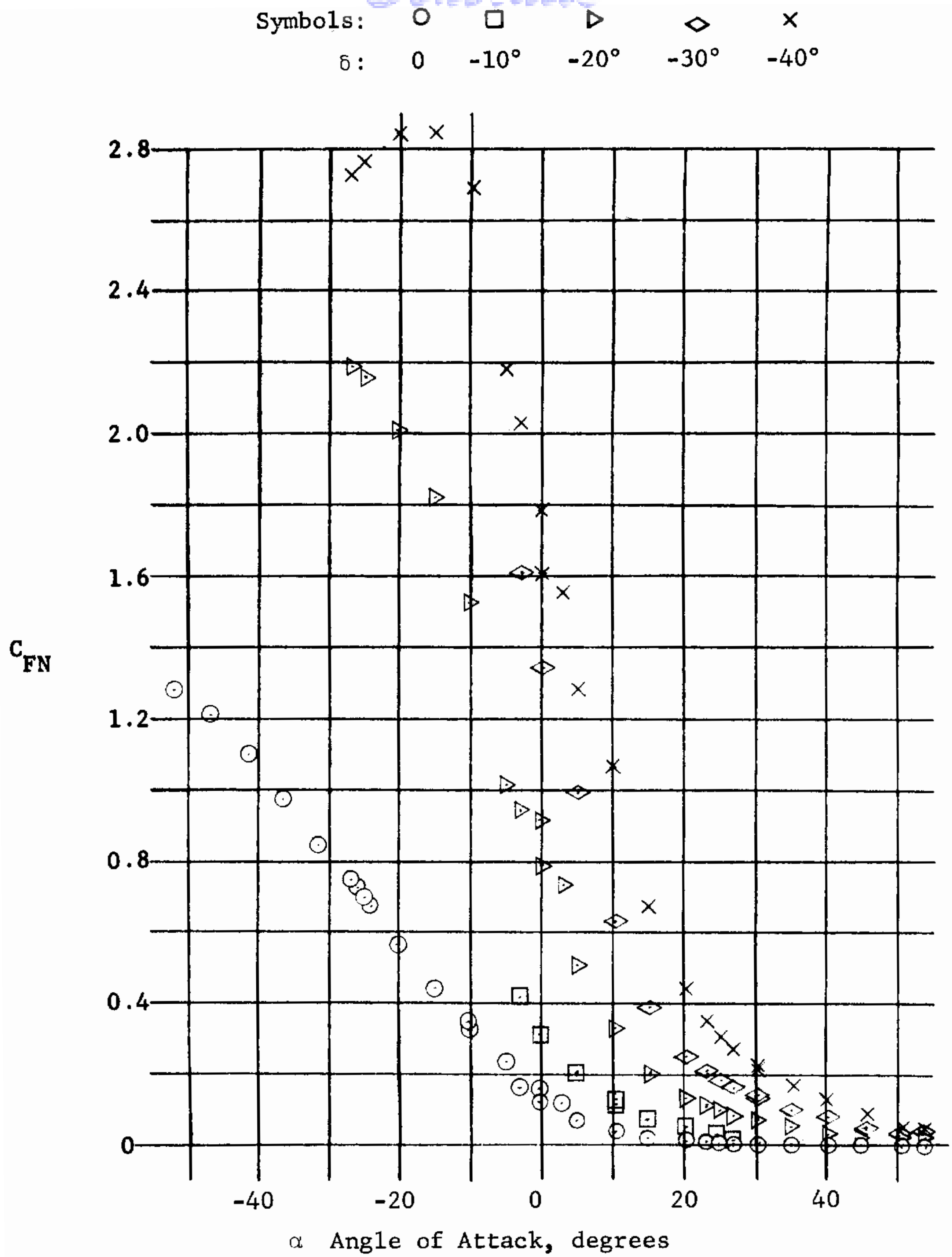

Fig. 9.1 Mach 8 Flap Loadings versus α for Basic Configuration with Symmetric Flap Settings (sheet 1 of 2)

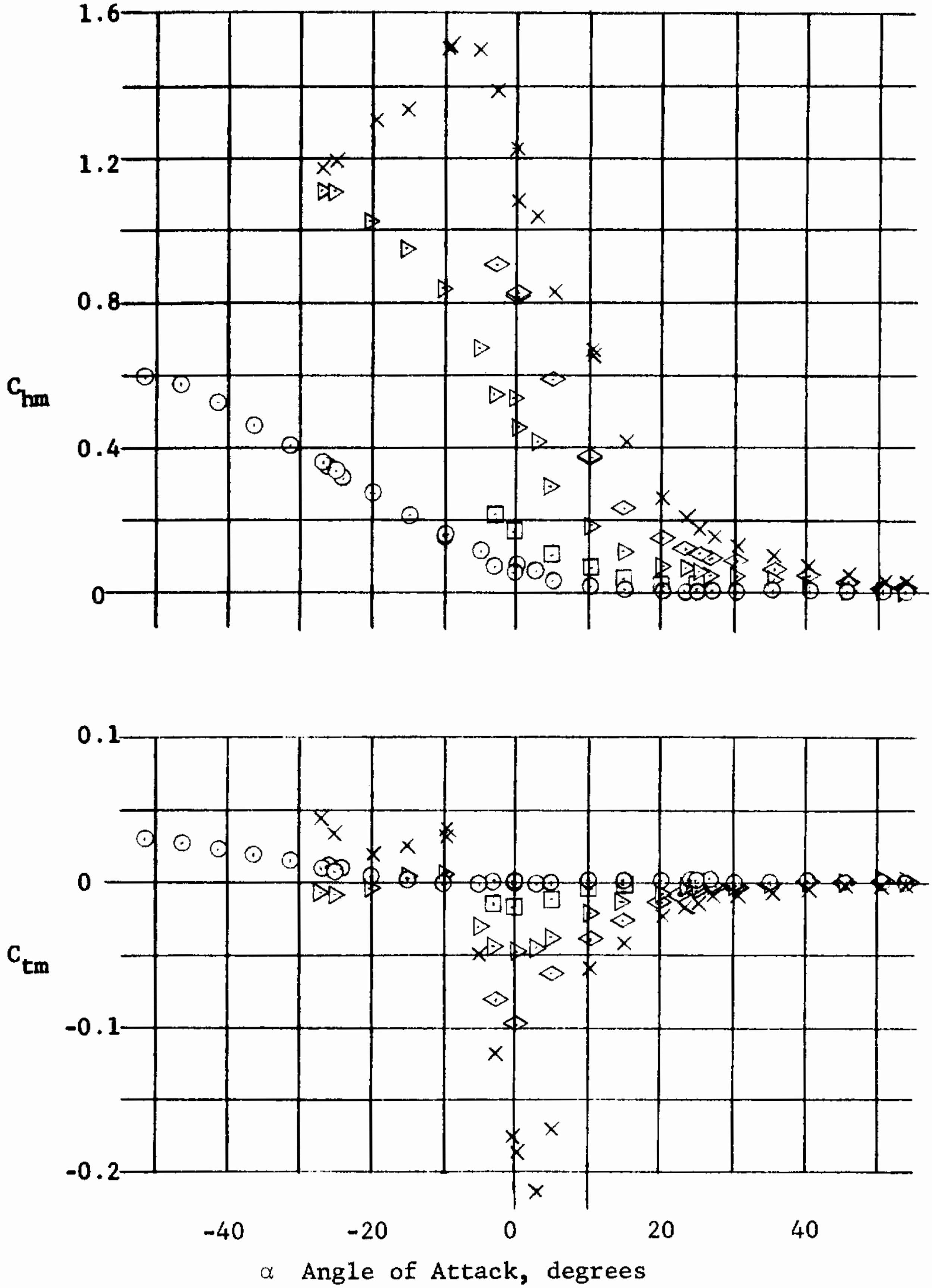

Fig. 9.1 Mach 8 Flap Loadings versus α for Basic Configuration with Symmetric Flap Settings (sheet 2 of 2)

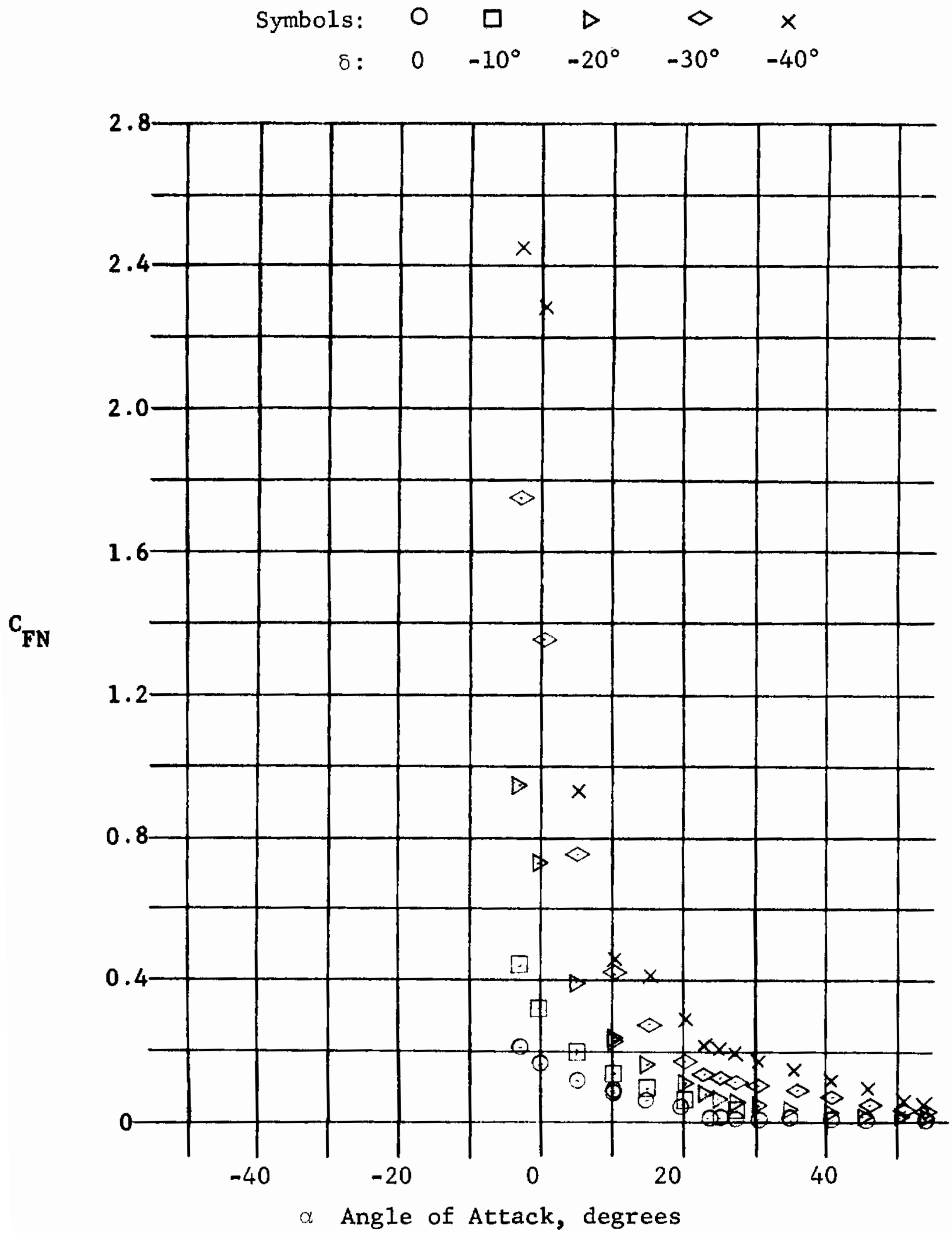

Fig. 9.2 Mach 8 Flap Loadings versus α for Basic Configuration with Canards and Symmetric Flap Settings (sheet 1 of 2)

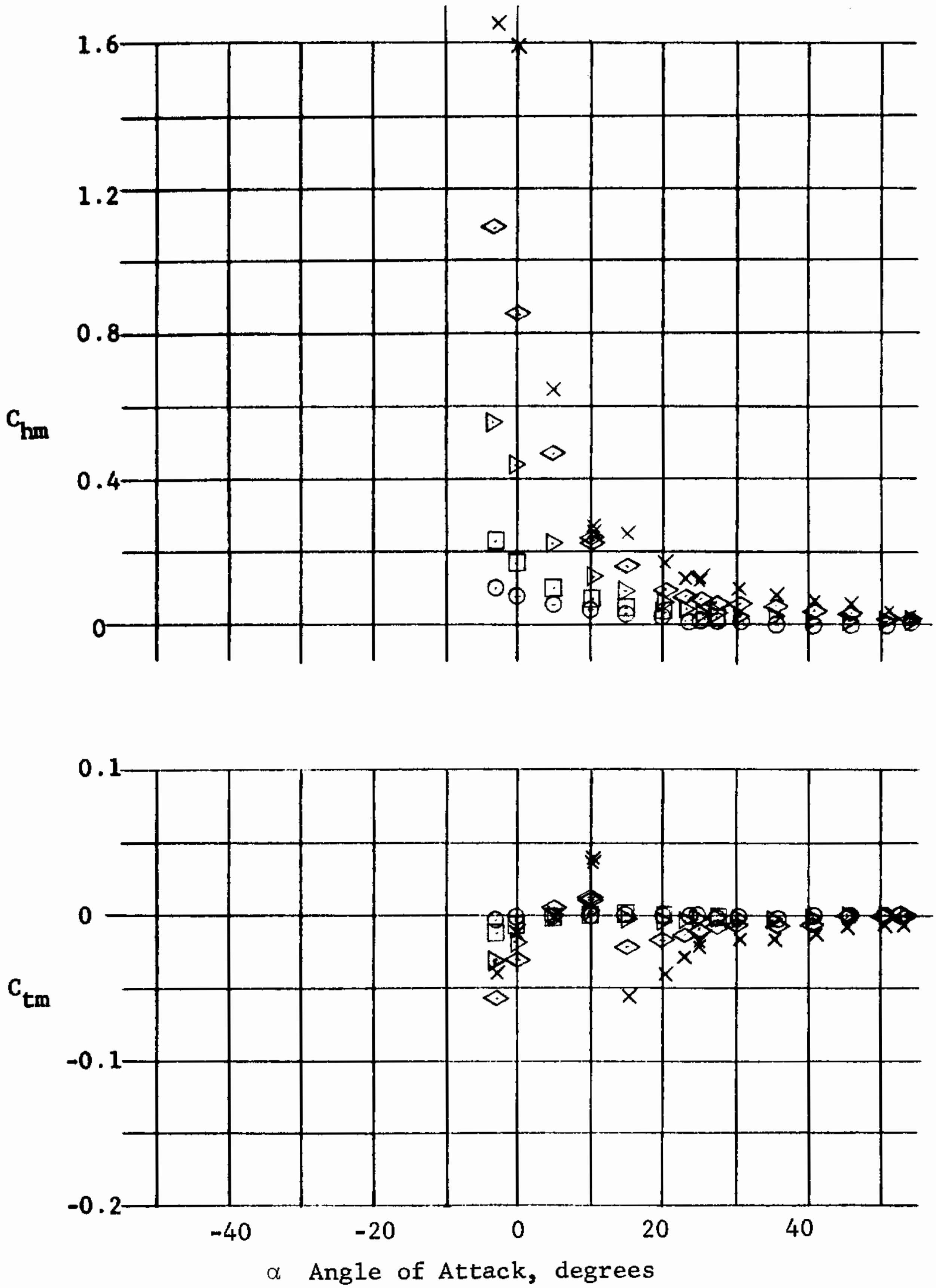

Fig. 9.2 Mach 8 Flap Loadings versus α for Basic Configuration with Canards and Symmetric Flap Settings (sheet 2 of 2)

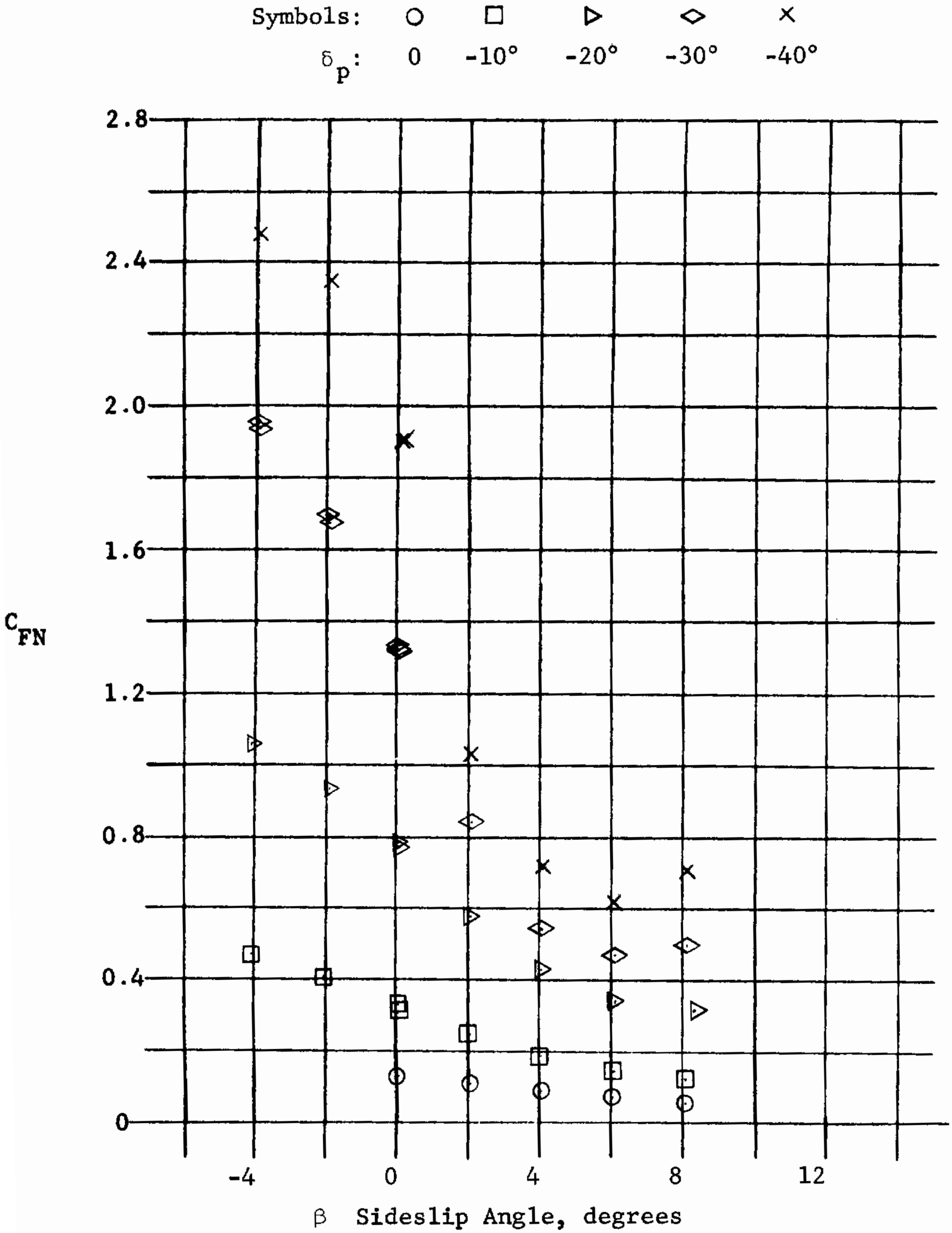

a) $\alpha = 0$

Fig. 9.3 Mach 8 Flap Loadings versus β for Basic Configuration with Upper Surface Port Flap Deflections (sheet 1 of 6)

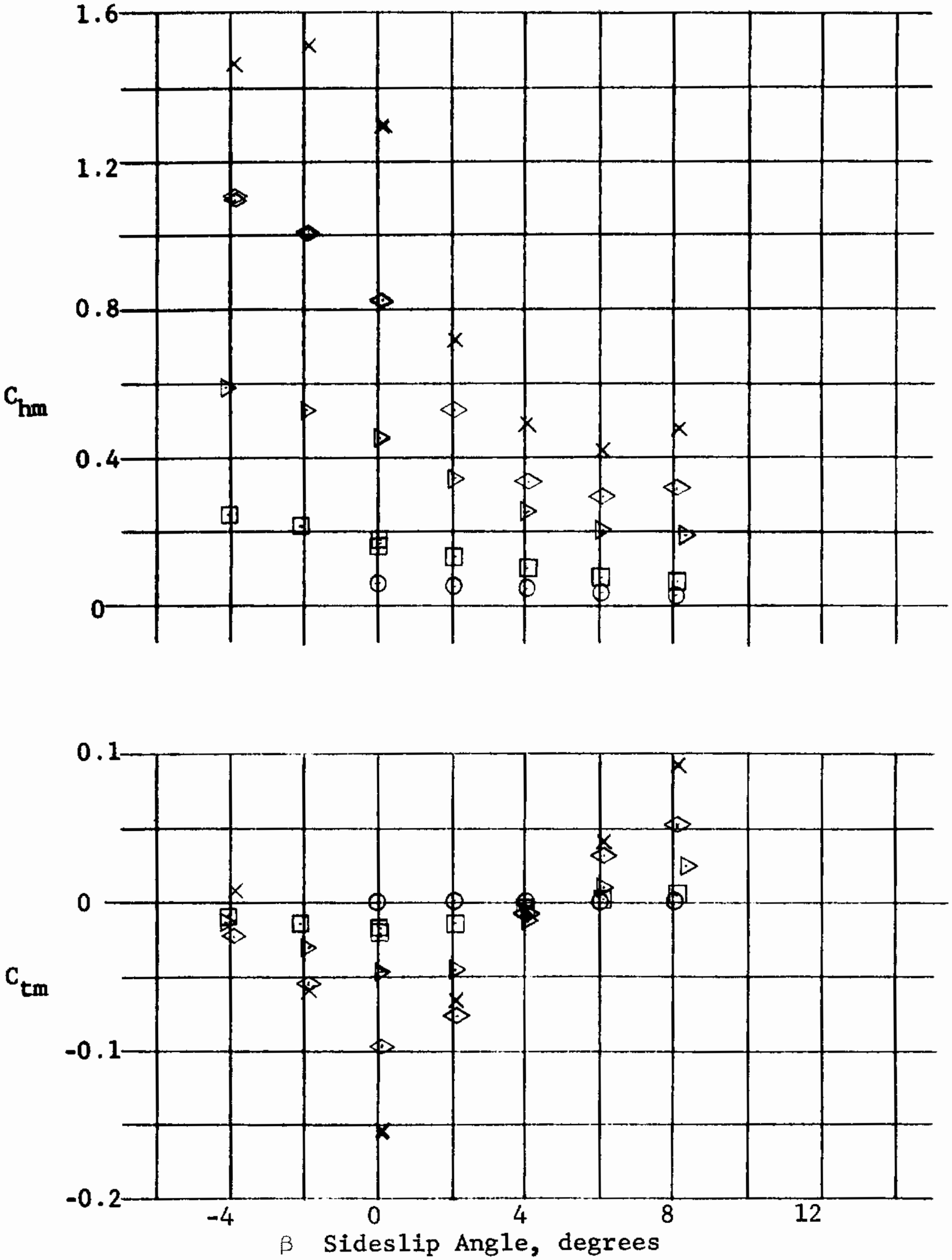

a) α = 0

Fig. 9.3 Mach 8 Flap Loadings versus β for Basic Configuration with Upper Surface Port Flap Deflections (sheet 2 of 6)

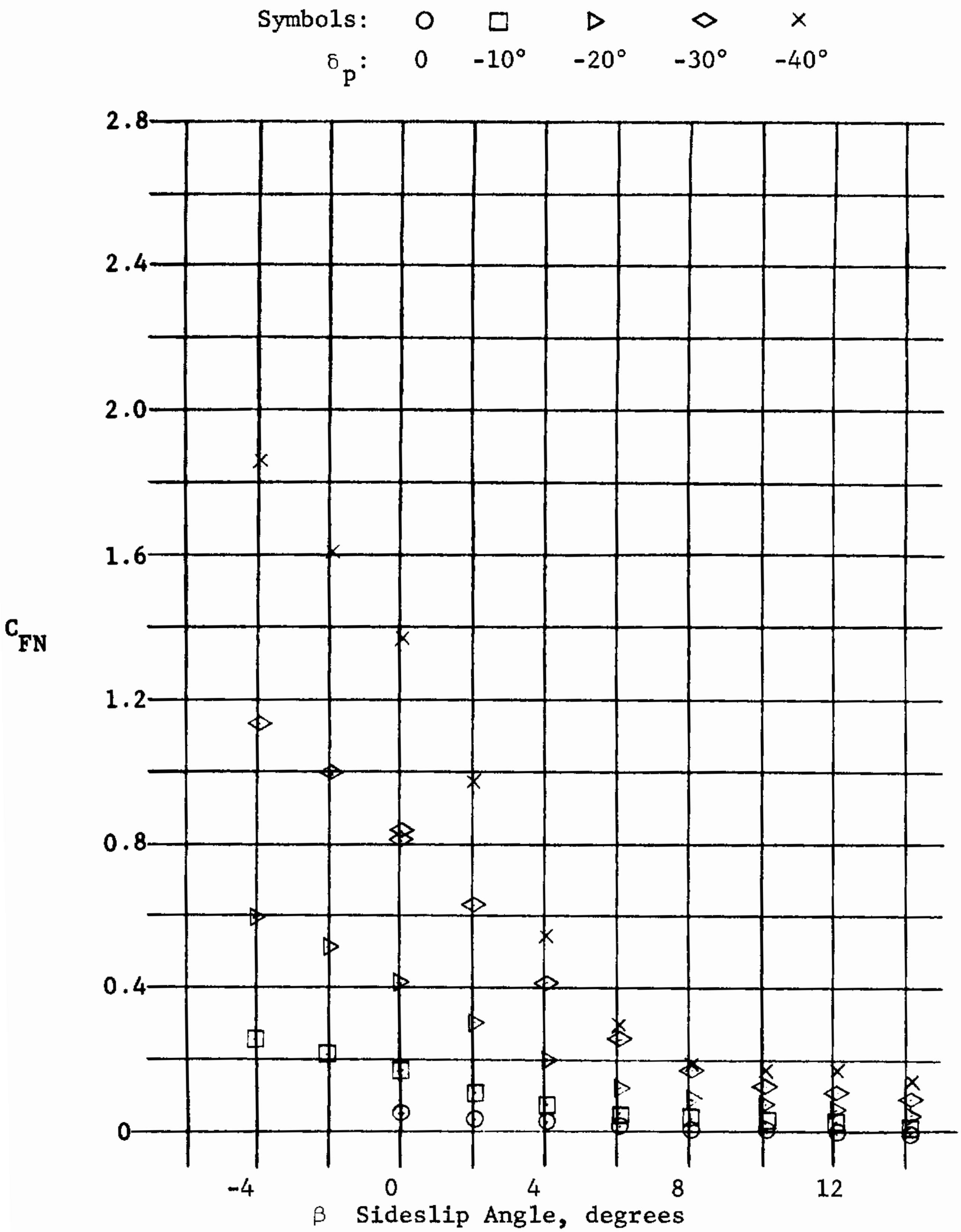

b) α = +7°

Fig. 9.3 Mach 8 Flap Loadings versus β for Basic Configuration with Upper Surface Port Flap Deflections (sheet 3 of 6)

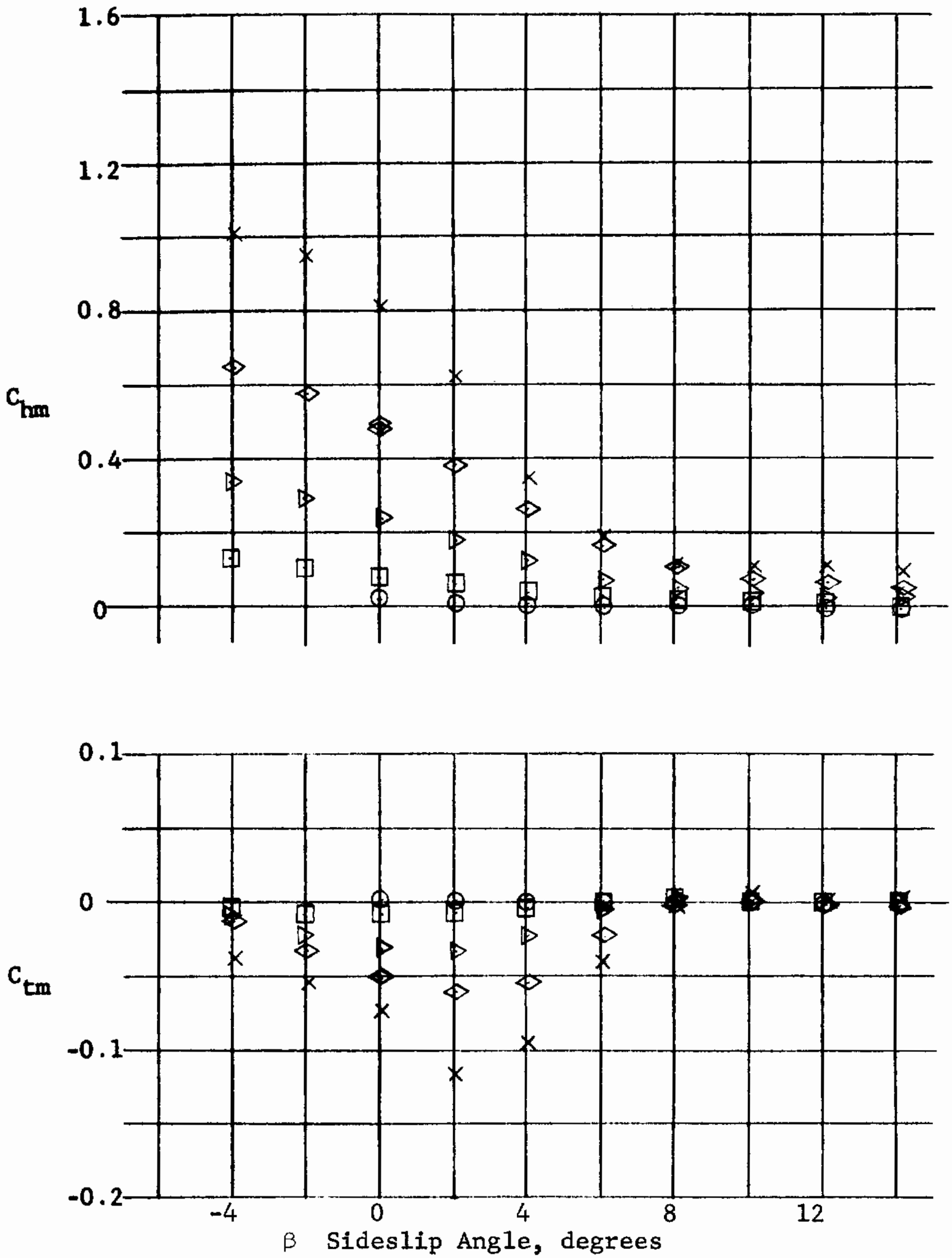

b) α = +7°

Fig. 9.3 Mach 8 Flap Loadings versus β for Basic Configuration with Upper Surface Port Flap Deflections (sheet 4 of 6)

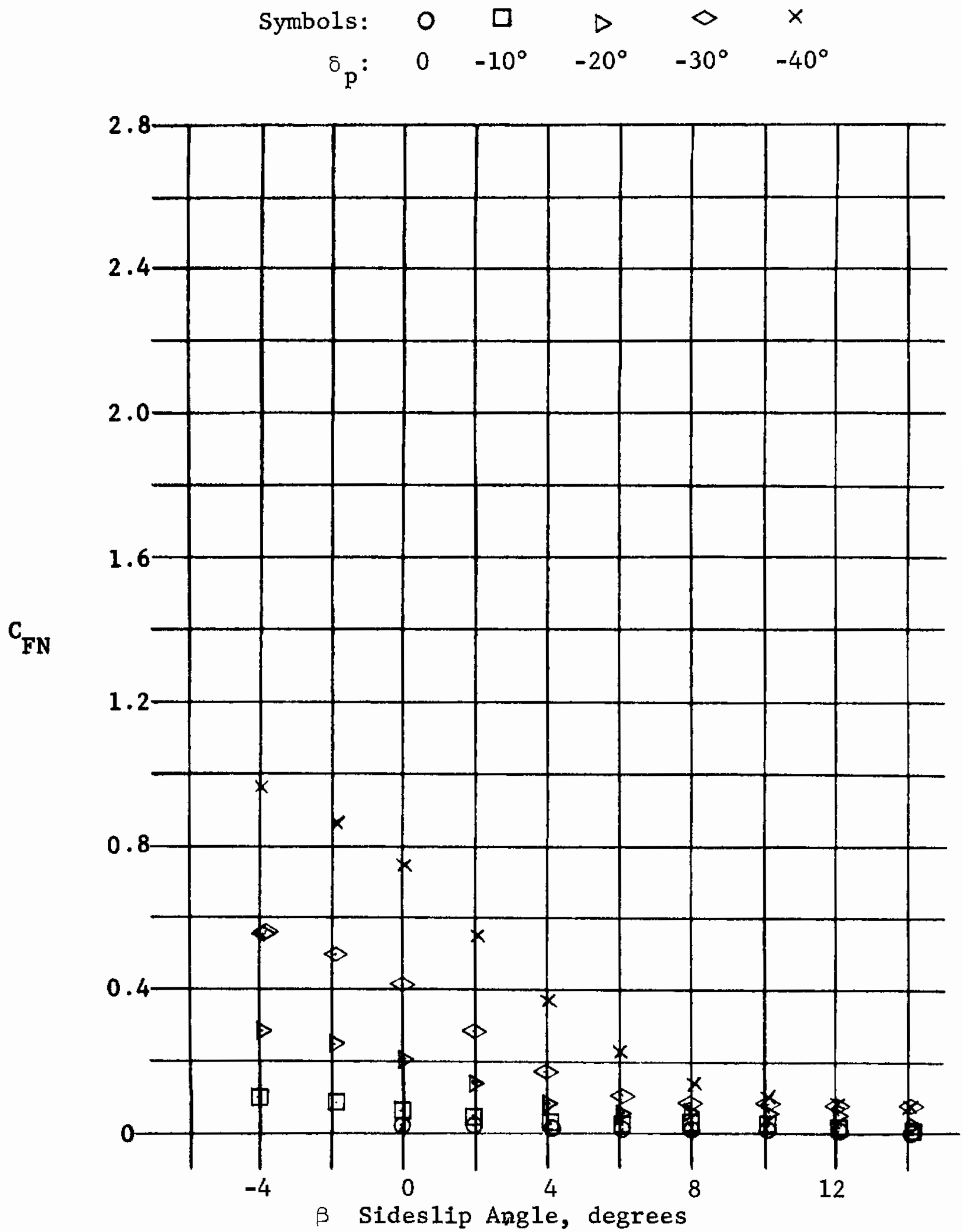

c) $\alpha = +14.3°$

Fig. 9.3 Mach 8 Flap Loadings versus β for Basic Configuration with Upper Surface Port Flap Deflections (sheet 5 of 6)

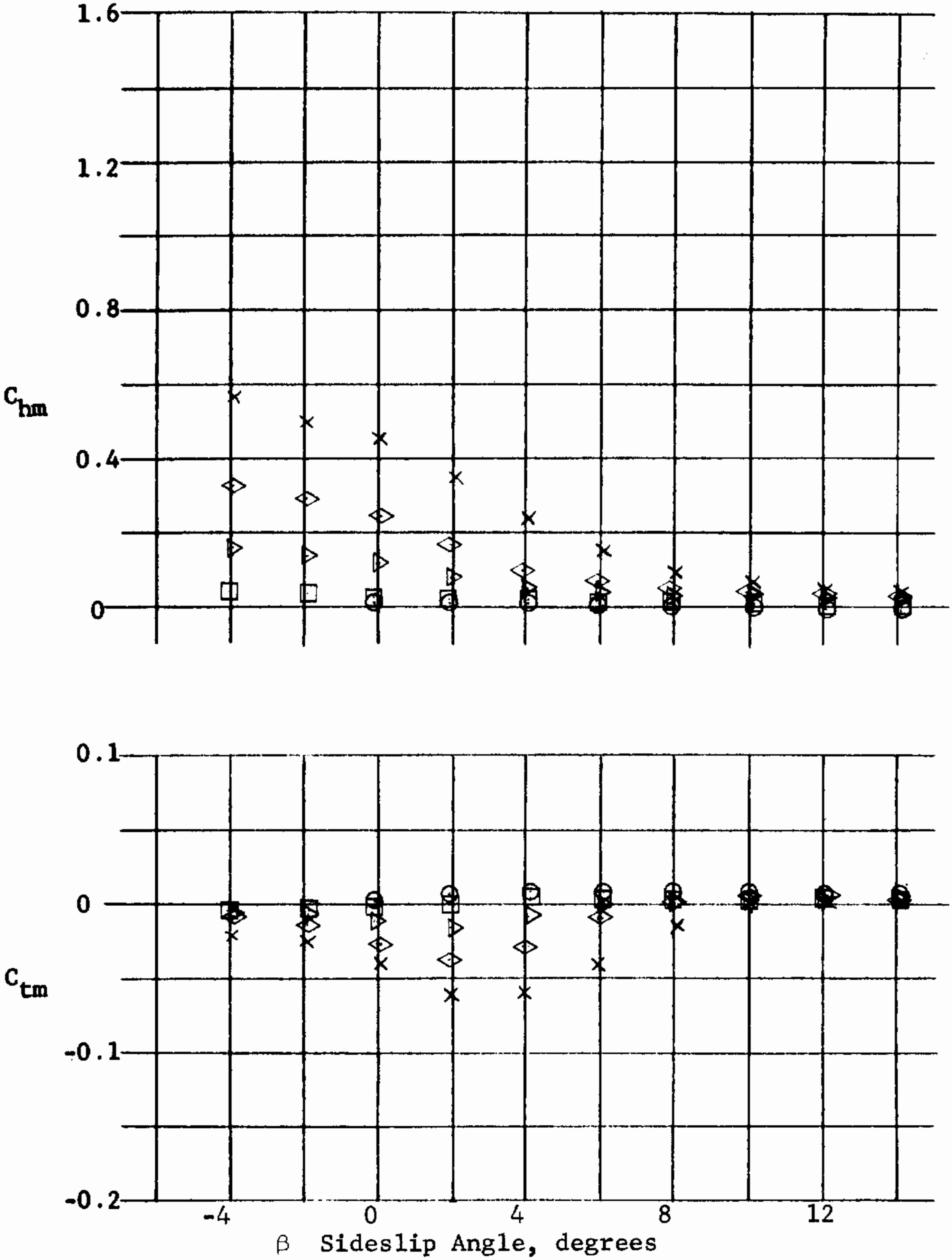

c) α = +14.3°

Fig. 9.3 Mach 8 Flap Loadings versus β for Basic Configuration with Upper Surface Port Flap Deflections (sheet 6 of 6)